UNIVERSITÀ DEGLI STUDI DI MILANO

Scuola di Dottorato in Scienze Biomediche Cliniche e Sperimentali

Dipartimento di Scienze Cliniche e di Comunità

Corso di Dottorato in Biotecnologie Applicate alle Scienze Mediche

BIO/10 - BIO/13 - BIO/14 - BIO/19 - MED/06 - MED/09 - MED/13 - MED/43

Ciclo XXVI

Basic and translational aspects of cell-based approaches for early and late stage osteoarthritis

Dottorando:

Silvia Lopa

Tutor:

Prof. Diego Fornasari

Dr. Matteo Moretti

Coordinatore:

Prof. Alessandro Gianni

A.A. 2012/2013

Table of contents

Chapter 1

Abstract

Abstract

Osteoarthritis (OA) is a highly disabling pathology which is worldwide investigated by the scientific community due to its increasing diffusion. The incidence of this age-related disease is increasing with population ageing and worldwide estimates indicate that 9.6% of men and 18% of women with more than 60 years present OA-related symptoms.

Osteoarthritis induces the progressive damage of articular cartilage and subchondral bone and can eventually lead to the complete loss of joint functionality. Nowadays, the management of OA includes non-pharmacological, pharmacological, and surgical treatments. Non pharmacological approaches include exercise, weight loss, and physiotherapy and are used in conjunction with pharmacological treatments. The pharmacological management of OA patients is mainly based on the use of anti-inflammatory drugs for pain control. Hence, the pharmacological approach to OA patients is synptomatic, but not resolutive, since it is not able to alter the progression of the disease. These therapeutical options are not suitable for late stage OA patients, whereby the severe pain and the functional limitations caused by advanced OA degeneration are currently resolved by joint replacement.

Due to the low self-repair ability of articular cartilage, untreated cartilage lesions can easily degenerate into OA. Different strategies have been developed to treat promptly chondral lesions, comprising cell-based therapies, such as autologous chondrocyte implantation (ACI). These cell-based therapies have been recently proposed also for the treatment of early OA patients in order to overcome or at least delay the need for a more invasive intervention such as joint replacement.

However, major issues associated to the clinical use of autologous articular chondrocytes (ACs) are the limited number of cell harvestable from a small cartilage biopsy and the de-differentiation process occurring during the expansion phase required to achieve a clinically relevant number of cells. Furthermore, advanced age and pathological state of joints negatively affect the chondrogenic potential of ACs, representing important factors to be considered when applying chondrocyte-based therapies in particular categories of patients. In view of a possible use of autologous cell-based therapies for OA patients, we analyzed specific features of ACs as cellular yield, cell doubling rates and the dependence between these parameters and patient-related data in a set of 211 OA patients undergoing total joint replacement (***Chapter 3***). The patient age was not statistically correlated to the cellular yield, but was negatively correlated with the proliferation rate. No significant correlation was observed between the level of cartilage degeneration (ICRS score) and cellular yield and proliferation rates. However, in samples with the highest degree of cartilage degeneration (ICRS score 4) the cellular yield was lower compared to the other three groups (ICRS scores 1-3). In conclusion, we found that age and degenerative state of cartilage affect some basic parameter of articular chondrocytes and should be considered when evaluating the quality of the cell source to be used in clinical applications.

To overcome some of the limitations related to the use of ACs, mesenchymal stem cells (MSCs) present in several tissues, such as bone marrow and fat, have been proposed as cell candidate for cartilage treatment thanks to their demonstrated chondrogenic ability. When developing treatments for knee chondral lesions, infrapatellar fat pad and knee subcutaneous adipose tissue, two fat depots easily accessible during knee surgery, can be considered appealing sources for MSCs harvesting. We performed a donor-matched comparison between infrapatellar fat pad MSCs (IFP-MSCs) and knee subcutaneous adipose tissue stem cells (ASCs) obtained from OA patients undergoing total knee replacement, analyzing their immunophenotype and multi-differentiative ability, with a focus on their osteogenic and chondrogenic potential (***Chapter 4***). We found that these cell populations share common features at the undifferentiated state, such as immunophenotype and clonogenic potential, but display a specific commitment towards the osteogenic and chondrogenic lineage. Indeed, significantly higher levels of osteogenic markers, as calcified matrix deposition and alkaline phosphatase activity, were found in ASCs, highlighting the superior osteogenic commitment of this cell population in comparison with IFP-MSCs. Conversely, IFP-MSCs differentiated towards the chondrogenic lineage by 3D pellet culture showed greater glycosaminoglycans (GAGs) deposition and higher expression of chondrogenic genes as aggrecan (*ACAN)* and type II collagen (*COL2A1*) compared to ASCs pellets, revealing a superior chondrogenic potential. This result was supported by lower expression of hyperthrophic and fibrotic markers, as type X (*COL10A1*) and type I (*COL1A1*) collagen, in IFP-MSCs pellets compared to ASCs. The observed dissimilarities indicate that populations of adipose-derived MSCs harvested from different anatomical sites have specific features that suggest their preferential use for specific cell-based applications.

In the last decade, the co-culture of ACs and MSCs has gained growing interest to investigate the cross-talk between these cell types and to evaluate the possibility of replacing a fraction of ACs with MSCs, in order to reduce the *in vitro* expansion phase of ACs and subsequently limit their de-differentiation. Controversial results have been reported on the possibility to generate cartilage-like matrix by co-culturing ACs and MSCs, indicating a prominent role for the origin and de-differentiation state of chondrocytes as determinants of the outcomes. We evaluated whether the co-culture of IFP-MSCs and ASCs with a small fraction of ACs was able to lead to cartilage-like matrix generation and to the expression of chondrogenic markers comparable to ACs (***Chapter 5***). To better resemble a possible clinical application of this strategy we performed autologous co-cultures combining IFP-MSCs and ASCs with expanded and cryo-preserved donor-matched ACs and we used cells derived from OA patients so as not to neglect the impact of the pathological and de-differentiated state of ACs on the outcome of the co-cultures. Chondrogenic genes SRY (sex determining region Y)-box 9 (*SOX9*), *COL2A1*, and *ACAN* were less expressed in co-cultures compared to ACs mono-cultures. No significant differences were

observed for GAGs/DNA in mono-cultures, demonstrating the reduced chondrogenic potential of ACs, probably deriving by both their pathological origin and their de-differentiated state. Total GAGs content in co-cultures did not differ significantly from values predicted as the sum of each cell type contribution corrected for the co-culture ratio, as confirmed by histology. Therefore, a small percentage of expanded and cryopreserved ACs did not lead to IFP-MSCs and ASCs chondro-induction. Our results suggest that chondrogenic potential and origin of chondrocytes play a relevant role in the outcome of co-cultures, indicating the need for further investigations to demonstrate their clinical relevance in the treatment of aged osteoarthritic patients.

As aforementioned, chondrogenic differentiation of both ACs and MSCs is usually performed in 3D culture models that partially mimic the 3D environment of cartilagineous matrix such as culture in pellets and in 3D scaffolds. Pellet culture is widely used in the field of cartilage tissue engineering to test and optimize differentiation protocols. These experiments normally require to prepare replicates from a relevant number of donors to investigate different culture conditions. Unfortunately, handling a high number of samples in 3D pellet culture is extremely time consuming and is a major issue in experiments with many different conditions. To overcome these limitations, we exploited low-cost rapid prototyping techniques, such as laser ablation and replica molding, to generate multi-well chips in polydimethylsiloxane (PDMS) for the formation and culture of cell aggregates (***Chapter 6***). Each PDMS chip allowed the simultaneous culture of several pellets leading to a significant reduction in the time required for pellet seeding and medium refresh operations. Proliferation and metabolic activity were comparable between pellets of ACs cultured in PDMS chips and pellets cultured in polypropylene tubes, whereas type II collagen deposition was increased in pellets cultured in the PDMS chips. The same rapid prototyping approach was applied to generate a patterned scaffold. As a proof of concept, we biofabricated a multi-well implantable constructs using clinically approved fibrin glue. We demonstrated that regions with different cell densities can be generated within the construct and that cells can be distributed in a spatially controlled way. These multi-well implantable scaffolds can be seeded with multiple cell types allowing the precise distribution of different cell populations, thus representing a useful tool to investigate *in vitro* and *in vivo* cell interactions in a 3D environment.

The introduction of engineered tissue into the clinical practice implies the achievement of high quality and safety standards. The use of automated bioreactor-based manufacturing can significantly increase the reproducibility of the results, being minimally affected by operator variability. Furthermore dynamic culture systems, such as perfusion bioreactors, represent a smart approach to overcome the limitations encountered in the static culture of 3D constructs having clinically relevant dimensions. Indeed, perfusion bioreactors have been shown to increase the homogeneity of cell distribution within the scaffold compared to static cell seeding. Perfusion culture provides a continuous and homogeneous

influx of fresh medium throughout the construct, improving the quality and homogeneity of the extracellular matrix. The use of optimized protocols for the expansion and re-differentiation of ACs employing clinically approved growth factors is another key step to achieve a successful outcome and to grant the clinical translability of the results. Thus, in collaboration with the group supervised by Prof. Frédéric Mallein-Gerin (Institut de Biologie et Chimie des Proteines, Lyon, France) we tested the combination of a specific cocktail of clinically approved growth factors with a bi-directional perfusion bioreactor (OPB, Oscillating Perfusion Bioreactor) with the aim of improving cartilage matrix production (***Chapter 7***). We established a perfusion program including phases of high and low perfusion speeds to alternate sequences of cell stimulation and matrix deposition and we compared collagen sponges seeded and cultured in dynamic conditions with sponges seeded and cultured in standard static conditions. We found that perfusion improved cartilage matrix deposition within the sponges, in comparison with static conditions. More precisely, in the sponges cultured in the bioreactor a cartilaginous matrix rich in type II and type IX collagen and GAGs, with no signs of hypertrophy, was produced. Furthermore, a lower amount of type I collagen was produced in the sponges cultured in dynamic conditions, indicating that perfusion limits the risk of fibrocartilage formation. In conclusions, the dynamic culture by means of a perfusion bioreactor combined with the use of a cocktail of clinically approved growth factors proved to be effective for the generation of engineered cartilagineous grafts, improving the homogeneity and quality of the extracellular matrix generated by articular chondrocytes seeded within collagen sponges.

Aged patients with late stage OA involving an extensive erosion of articular cartilage and exposure of the underlying subchondral bone cannot be treated with cell-based therapies or standard surgical approaches aiming at cartilage restoration. In these patients, joint replacement is currently the only clinical option to restore the articular function. The insufficient implant stability is an important determinant in the failure of cementless prostheses, leading to an increase in the risk of implant mobilization and in the number of revision procedures, with major drawbacks for patients and for National Health Systems. With the aim of increasing implant osseointegration, porous metallic materials have been developed and applied to cementless implant technology to maximize bone ingrowth and bone-implant contact. More recently, the enrichment of porous titanium with growth factors has been proposed as a novel strategy to further improve implant osseointegration. We combined a macroporous titanium (Trabecular Titanium™, TT), currently used in the clinical practice, with a biocompatible hydrogel (amidated carboxymethylcellulose, CMCA) able to encapsulate osteoinductive factors and osteoprogenitor cells (***Chapter 8***). In particular, we chose strontium as osteoinductive factor and bone-marrow derived MSCs (BMSCs) as osteogenic progenitor cells for implant enrichment. We tested different concentrations of $SrCl_2$ to select the optimal concentration to induce BMSCs differentiation.

We found that $SrCl_2$ at 5 µg/ml significantly increased calcified matrix deposition, type I collagen (*COL1A1*) expression and alkaline phosphatase activity, being the most effective concentration among the ones tested. The enrichment of TT with CMCA (TT+CMCA) significantly increased cell retention within the implant, representing an important improvement in view of a future clinical application of the bioactive implant. Furthermore, we found that BMSCs cultured in TT+CMCA in the presence of $SrCl_2$ underwent a more efficient osteogenic differentiation, as demonstrated by higher alkaline phosphatase activity and calcium levels. Based on these *in vitro* results, we performed an *in vivo* study to evaluate the performance of the bioactive implant generated combining the macroporous titanium with strontium-enriched CMCA and BMSCs (***Chapter 9***). To mimic implant-bone interaction, an ectopic model was developed grafting TT implants into decellularized bone seeded with human BMSCs. TT was loaded or not with strontium-enriched CMCA and/or BMSCs and constructs were implanted subcutaneously in athymic mice. Osteodeposition at the bone-implant interface was investigated with fluorescence imaging, micro-CT, scanning electron microscopy (SEM), histology and biomechanical testing at different time points. Micro-CT analysis demonstrated the homogeneity of the engineered bone in all groups, supporting the reproducibility of the ectopic model. Fluorescence imaging, histology, SEM and pull-out mechanical testing showed superior tissue ingrowth in TT implants loaded with both strontium-enriched CMCA and BMSCs. In our model, the synergic action of the bioactive hydrogel and BMSCs increased both bone deposition and TT integration, indicating that the generation of bioactive implants able to promote bone deposition is a promising strategy for the improvement of implant osseointegration.

Joint inflammation is an important trait of osteoarthritis, indeed synovitis is observed in various degrees in OA patients, with OA synovium showing a mixed inflammatory infiltrate mainly consisting of macrophages. The central role of macrophages in OA evolution supports the interest in investigating their response to signals typical of OA joints, such as the ones contained in the synovial fluid (SF) of OA patients. In collaboration with the Connective Tissue Cells and Repair group supervised by Prof. Gerjo J.V.M. van Osch (Erasmus MC, Rotterdam, The Netherlands), we investigated the effect of SF from OA patients on the transcriptional expression of anti-inflammatory and pro-inflammatory mediators in monocyte-derived macrophages (***Chapter 10***). SF from donors without any joint pathology was used as control, and the effect of the different types of SF was tested on non-activated macrophages (M0) and on macrophages activated by IFNγ and TNFα (M1 activation) or IL4 (M2 activation). We found that *IL10* and *IL1ra* were modulated by the treatment with OA SF in M0 and M2 conditions. The effect on *IL10* was lost in M1 conditions probably due to the high up-regulation induced by the treatment with IFNγ and TNFα. Our results support the idea that arthritic SF is for macrophages a less pro-inflammatory environment compared to control SF. This may mimic the macrophage situation in the joint, where feedback mechanisms are induced to counteract the ongoing pro-inflammatory processes.

Altogether our findings highlight the complexity and multiplicity of factors that should be considered for the development of successful cell based treatments for early and late OA patients. We found that basic features of articular chondrocytes were affected by donors age and cartilage degeneration. We also found that expanded OA ACs did not exert a significant chondroinductive effect on co-cultured MSCs, suggesting that the evaluation of the clinical relevance of this approach in OA patients should strongly consider the impact of the de-differentiation state and pathological origin of ACs. Further investigations in this field are needed to verify whether it is possible to replicate the results obtained using non-expanded healthy ACs to co-cultures using expanded ACs from aged patients affected by osteoarthritis. These investigations may require the optimization of clinically approved protocols for expansion and re-differentiation of OA chondrocytes as well as the implementation of three-dimensional and dynamic culture systems. We demonstrated that low-cost rapid prototyping techniques are a useful tool to develop high-throughput systems for the culture of 3D cell aggregates and to generate patterned scaffolds that allow the controlled spatial disposition of different cell types. We also showed that the use of perfusion bioreactors for the dynamic culture of 3D constructs can improve the quality of the engineered tissue, granting a more homogeneous and efficient distribution of nutrients and cells throughout the construct. In order to overcome the limitations related to the use of ACs, MSCs can be considered as promising alternative cell candidates. Here, the identification of specific subsets of MSCs displaying a peculiar commitment should drive the selection of the most suitable cell source. Indeed, as we demonstrated for IFP-MSCs and ASCs, despite common features, specific populations of MSCs harvested from different anatomical sites have intrinsic features that make them more or less suitable for a specific application.

Cell-based therapies aiming at cartilage restoration cannot be currently applied to late stage OA patients. However, in this category of patients cell-based approaches can be developed to face issues that are critical in implant technology, such as poor osseointegration. As we proposed here, osteoprogenitor cells, osteoinductive factors, and macroporous metals can be combined to generate a bioactive implant with improved osseointegration ability. This approach could be used to generate “off-the-shelf” implants pre-loaded with osteoinductive factors that can be seeded with autologous BMSCs with a fully intra-operative approach.

Finally, when developing cell-based approaches for OA patients, the inflammatory state of the OA joint cannot be neglected. We found that macrophage transcriptional expression was affected by OA synovial fluid. This suggests that OA environments may also induce alterations in the re-implanted cells and highlights the need for better *in vitro* models to evaluate the response of cells and engineered tissues to a diseased environment.

In conclusion, to develop novel cell-based approaches for the treatment of OA basic and translational

studies should take into account multiple factors that may affect the clinical outcome, such as the impaired phenotype of OA chondrocytes, the peculiar commitment of specific populations of MSCs, and the impact of inflammatory environment of OA joints.

Chapter 2

Introduction

Introduction

Osteoarthritis (OA) is the most common type of arthritis worldwide and its diffusion is rapidly increasing with ageing populations (1). Worldwide estimates report that 9.6% of men and 18.0% of women with more than 60 years have symptomatic osteoarthritis, indicating that this pathology is not only a major source of pain and disability for patients, but represents also a consistent economic burden for National Health Systems (2).

Osteoarthritis is a highly invalidating disease. Indeed, progressive degradation of articular cartilage and subchondral bone often leads to the complete loss of joint functionality, compromising patients quality of life (3,4). Ideally, the diagnosis of OA should occur at a very early stage allowing a prompt intervention to restore the damaged articular cartilage and to limit the progression of joint degeneration and the development of joint inflammation. Nowadays, OA is no longer considered an exclusively degenerative joint disorder, being related to changes in the synovial membrane such as the increased infiltration of immune cells, in particular macrophages, which secrete pro-inflammatory mediators and participate to cartilage degradation (5,6).

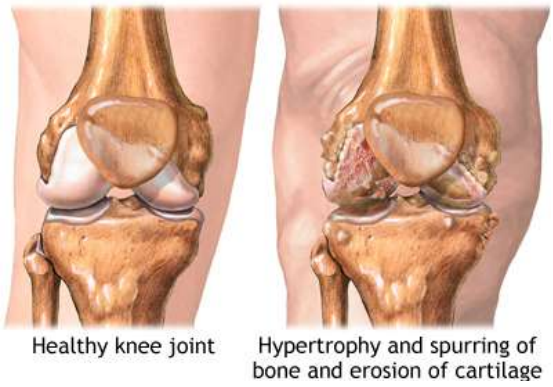

Fig. 1. Comparison of healthy and osteoarthritic knee joint. (*Source: http://umm.edu*)

Age, obsesity, excessive or unbalanced joint load are risk factors for OA development, however articular cartilage damage due to excessive "wear and tear" or traumatic events is one of the main determinants of OA. In damaged cartilage, a shift in equilibrium between anabolic and catabolic activities occurs, compromising the integrity of extracellular matrix (ECM) and subsequently the biomechanical properties of articular cartilage. As a result, an unbalanced load is transferred to the underlying bone during joint movement, inducing pathological changes in the subchondral bone. Bone overgrowth, leading to osteophyte formation, is indeed one of the main features of OA together with joint swelling induced by osteophyte formation and/or synovial fluid accumulation.

A prompt intervention in the early phase of OA is critical to delay the need for joint replacement, which so far is the only clinical option available to treat late stage OA. Joint replacement, despite being a successful treatment for older patients, is not suitable for young or middle-aged patients who have a more active life, as demonstrated by the poorer outcomes of joint replacement procedures in this category of patients (7).

The involvement of articular cartilage damage in the early phase of OA insurgence highlights the fundamental role of this tissue for a proper function of joints. Articular cartilage has a highly anisotropic

structure composed by multiple layers that differ in terms of matrix composition and organization (Fig. 2) (8-12). Type-II collagen and proteoglycans are the main components of cartilage ECM. Thanks to their negative charges, proteoglycans are able to retain water molecules within the tissue, allowing the load-dependent deformation (8). Lack of vascularisation, low cellularity and the limited metabolic activity of chondrocytes, which are the only resident cell type, are key features of this tissue and are related to its low self-repair ability.

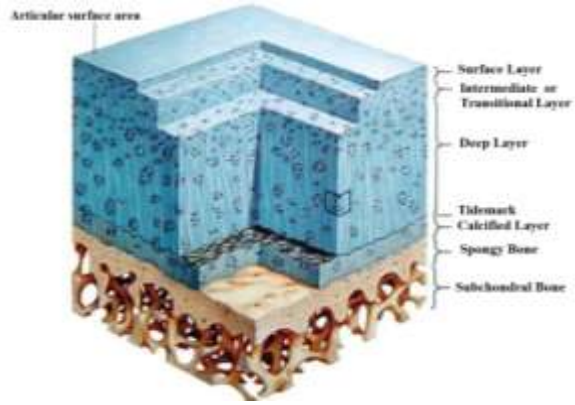

Fig. 2. Anisotropic structure of articular cartilage. (*Source: http://www.intechopen.com/)*

Treatment options for the management of articular cartilage lesions include different surgical approaches. A first group of approaches can be defined as "marrow-stimulation techniques" and include subchondral bone drilling and microfracture technique (Fig. 3). These approaches are based on the recruitment of mesenchymal stem cells from bone marrow to the damaged tissue and on their participation to the healing process. However, these techniques fail to yield long-term solutions, leading to the development of fibrocartilage that lacks many of the mechanical properties of the hyaline cartilage that covers articular surfaces (13,14). In a second group of surgical approaches, the chondral defect is reshaped to a standard cylindrical defect and is replaced with osteochondral autografts or allografts (Fig. 4). The limited availability of autologous osteochondral grafts and the morbidity of the donor site are the main limitations of this approach, whereas osteochondral allografts are associated with a high risk of disease transmission. Furthermore, the implantation of osteochondral grafts requires the conversion of a chondral lesion into an osteochondral injury to perform the surgical procedure, which may negatively affect the functionality of the entire bone-cartilage unit (13,15).

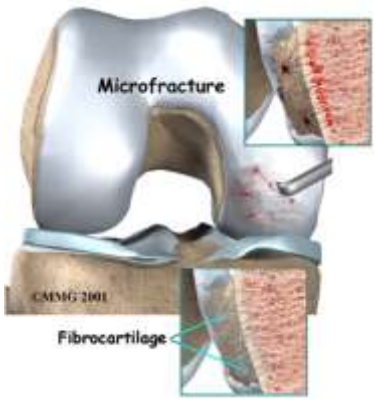

Fig. 3. Microfracture technique. (*Source: http://www.eorthopod.com*)

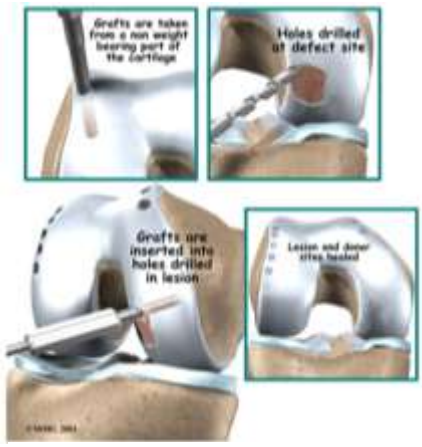

Fig. 4. Osteochondral autograft. (*Source: http://www.eorthopod.com/*)

In order to overcome the limitations of the aforementioned approaches, cell-based therapies have been proposed for the treatment of cartilage lesions. According to the EMA definition (Regulation (EC) No 1394/2007), cell-based therapies are

advanced-therapy medicinal products (ATMPs) defined as “medicines for human use that are based on gene therapy, somatic-cell therapy or tissue engineering. They offer groundbreaking new opportunities for the treatment of disease and injury”. Articular cartilage has long been considered one of the most promising tissues for the application of cell-based approaches since it contains only one cell type, the articular chondrocytes (ACs), responsible for the production and deposition of highly specific extracellular matrix. Articular chondrocytes were the first cell type used in autologous cell-based therapies aiming at cartilage repair. Autologous chondrocyte implantation (ACI), proposed by Brittberg *et al.* for the treatment of knee chondral lesions (16), is a two-stage procedure (Fig. 5). During the preliminary surgery, a biopsy of articular cartilage is harvested from non-bearing areas and autologous chondrocytes are isolated and expanded *in vitro*. During the second surgery, expanded chondrocytes are implanted back in the damaged area. More recently, other approaches based on the use of autologous articular chondrocytes have been developed, such as matrix-induced autologous chondrocyte implantation (MACI), where a three-dimensional matrix is used instead of the periostal flap, and co.don chondrosphere®, where 3D spheroids of chondrocytes are implanted in the chondral defect. The clinical applicability of these approaches depends on the lesion size since the amount of harvestable tissue, and consequently the number of autologous chondrocytes that can be isolated, is limited to reduce the risk of generating secondary lesions and to minimize donor site morbidity. However, even for the treatment of small focal defects, chondrocytes need to undergo *in vitro* expansion prior to re-implantation to obtain a clinically relevant number of cells, which is related to major drawbacks such as chondrocyte de-differentiation (17). This limitation is even more relevant when considering the treatment of osteoarthritic patients who present extensive cartilage lesions and require a significantly higher number of cells, implying a longer phase of *in vitro* expansion and a deeper impact of the de-differentiation process on chondrocyte phenotype. Furthermore, the application of cell-based therapies involving the use of autologous chondrocytes in OA patients has to take into consideration that cells derived from aged and/or diseased patients display peculiar features that differentiate them from chondrocytes obtained from young and/or healthy patients. Indeed, increasing age negatively affects the proliferative and differentiative potential of ACs, as shown by the reduced proliferative and chondrogenic potential observed in chondrocytes harvested from middle-age and aged patients (18). Different studies have indicated OA chondrocytes as possible

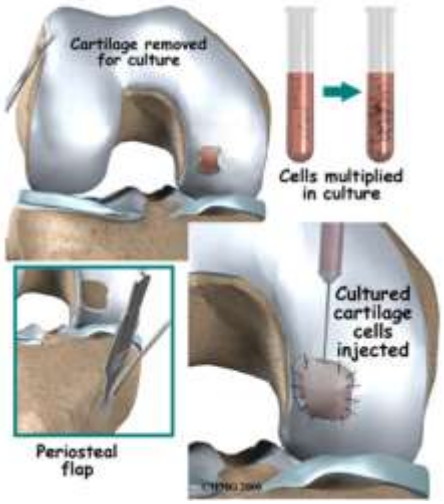

Fig. 5. Autologous chondrocyte implantation. (*Source: http://www.eorthopod.com/*)

candidates for chondral cell-based therapies (19-21), but more recent data have shown that these cells show a peculiar form of age- and stress-induced cell senescence, progressing over time due to the accumulation of DNA damage and impairing the ability of chondrocytes to participate to tissue homeostasis (22). Furthermore, the increased methylation of the promoter of *SOX9* found in OA cartilage in comparison with healthy cartilage suggests that the cascade of chondrogenic genes induced by this transcriptional factor may be down-regulated in OA cartilage (23), thus at least partially explaining the differences in cartilage ECM observed between healthy and OA joints.

To overcome the limitations in the use of articular chondrocytes, mesenchymal stem cells (MSCs) have been proposed as an alternative cell source for cartilage cell-based therapies. The presence in the bone marrow of non-hematopoietic stem cells was suggested by Friedenstein in 1968 (24). These cells were then named "mesenchymal stem cells" for their ability to undergo the mesengenic process differentiating into osteoblasts, chondrocytes, adipocytes, and myoblasts (Fig. 6) (25,26).

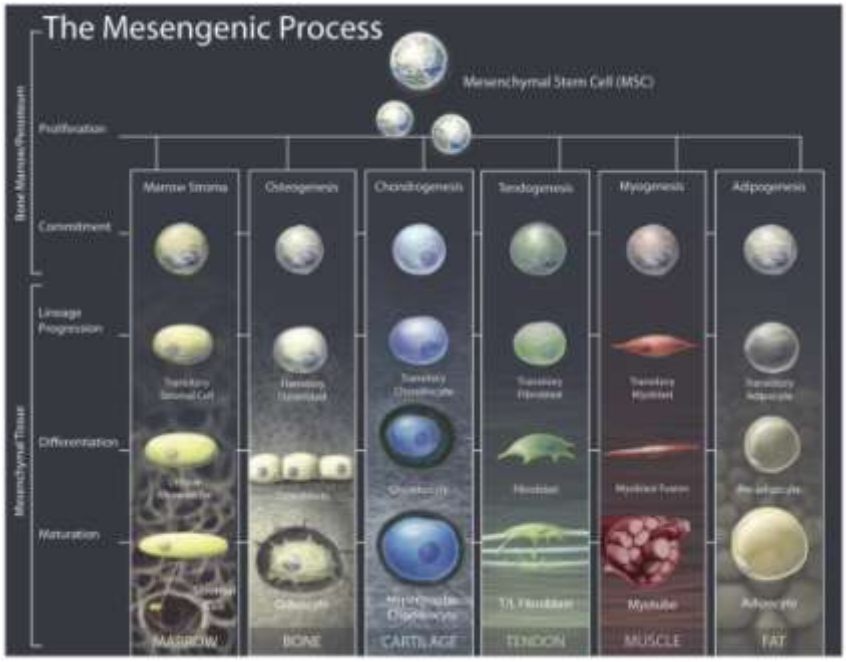

Fig. 6. The mesengenic process. Multi-differentiative potential of mesenchymal stem cells. (*Source: http://stemcellgurus.wordpress.com/*)

Thanks to their proliferative and multi-lineage potential, MSCs represent nowadays an exceptional tool to design cell-based therapies aiming at the reconstruction of mesenchymal tissues. The bone marrow is still the main and most investigated source of MSCs, but MSCs have been identified in other adult tissues such as adipose tissue. Subcutaneous fat was the first source of adipose-derived MSCs (27,28), since this tissue is readily available as waste material after liposuction surgery. More recently, the presence of ASCs has been shown in other adipose depots such as visceral adipose tissue (29), buccal fat pad (30), and orbital fat tissue (31). Adipose-derived MSCs have been successfully used in bone and cartilage applications (32-36), proving to be a relevant cell source for the development of musculo-skeletal cell-based therapies. Considering the development of cell-based approaches for the treatment of knee chondral defects, the infrapatellar fat pad and the knee subcutaneous adipose tissue can be considered appealing cell sources since they can be easily harvested during orthopaedic surgery without need to harvest bone marrow from the iliac crest. Despite several studies have demonstrated

the multi-differentiative potential of MSCs from infrapatellar fat pad (37-41) and subcutaneous adipose tissue (27,42,43), an extensive and quantitative comparison of their potential as cell candidates for bone and cartilage application has not been reported yet. Indeed, in the few studies performing a comparison of IFP-MSCs and ASCs (44-46) gene expression data are not present (44,45) and the comparison is restricted to very few donors (46), therefore limiting the clinical relevance of the findings and indicating the need for a deeper insight in the features of these MSCs populations.

In the last decade, several groups have focused on the co-culture of ACs and MSCs in order to investigate the mutual influences between these cell types and to evaluate the possibility of replacing a fraction of ACs with MSCs, in the attempt of reducing the *in vitro* expansion phase of ACs and its impact on the phenotype of ACs. Results from studies evaluating the co-culture of ACs with bone marrow-derived (47-53) and adipose-derived MSCs (47,48,54,55) have highlighted the potential of this approach demonstrating that through the combination of these cell types it is possible to generate cartilagineous matrix. However, the studies displaying the most promising results employ either animal chondrocytes (50,51,55) or non expanded healthy chondrocytes (48,49), suggesting that the outcome of the co-culture approach is strongly dependent on the origin and de-differentiation state of articular chondrocytes. Considering the application of a co-culture approach to aged OA patients, it is clear that the impact of origin and pathological features of chondrocytes cannot be neglected and needs further investigation. Indeed, the combination of pathological origin and de-differentiation state of ACs deriving from their *in vitro* expansion has been indicated as a determinant in the outcome of co-cultures between OA chondrocytes and BMSCs (53). Furthermore, to resemble the clinical use of autologous co-cultures, *in vitro* and *in vivo* experiments should be performed with donor-matched MSCs and ACs, facing practical issues, such as the different proliferation rate and cellular yield of these cell types and inter-donor variability, issues that may greatly affect the final outcome and that are only partially considered in the current literature.

According to one of the paradigms of Tissue Engineering, defined in 1993 as "the application of principles and methods of engineering and life sciences for the development of biological substitutes, to restore, maintain or improve tissue function", the *in vitro* development of engineered tissues is usually achieved by

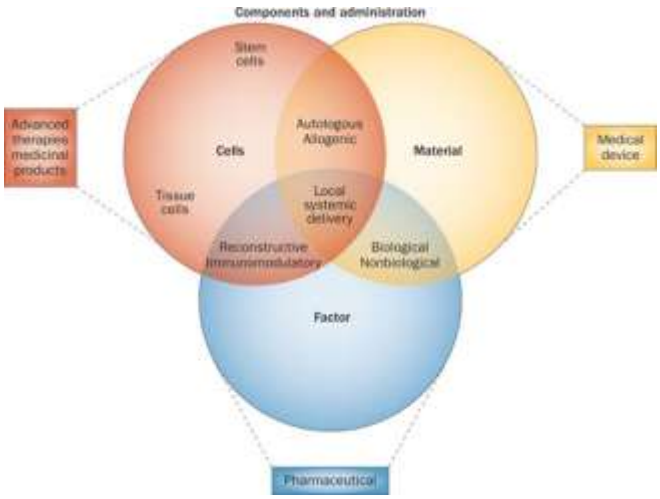

Fig. 7. The Tissue Engineering paradigm. (*Source: Ringe et al., Nat Rev Rheumatol. 2012)*

the combination of a suitable cell source, growth factors able to promote cell proliferation and/or differentiation, and a 3D scaffold that provides the template for tissue development (Fig. 7) (56). This paradigm implies the need for efficient three-dimensional (3D) models to investigate cellular cross-talks in co-cultured cells and to optimize protocols for cell differentiation. In the field of cartilage tissue engineering, 3D culture systems are widely used in basic and translational studies. Indeed, chodrogenic differentiation of ACs and MSCs is usually performed by pellet culture (57-61) or by cell culture within suitable 3D scaffolds (62,63). Pellet culture, which is traditionally obtained from cell centrifugation in polypropylene conical tubes (59), offers a favorable 3D structure for cells, enabling cell-to-cell interactions and enhancing the expression of a chondrogenic phenotype (64,65). Articular chondrocytes pellets are widely used in this field to test and optimize differentiation protocols. These experiments require to prepare replicates from a relevant number of donors to investigate simultaneously different culture conditions (66). Unfortunately, handling a high number of samples in 3D pellet culture is extremely time consuming and is a major issue in experiments with many different conditions. To overcome this limitation, in the last years, attention has been focused on the possibility to develop devices able to support the generation and the culture of multiple cell aggregates, which have a broad range of applications in the areas of tissue engineering, stem cells research and cancer models (67-70).

Low-cost rapid prototyping approaches, widely used in the fabrication of microfluidics devices (71-75), can be exploited to generate these devices. Biofabrication technologies can also be applied to the generation of implantable scaffolds with a controlled architecture can be used as screening devices (Fig. 8) (76,77) as well as to mimic anatomical structures (78), with a broad range of applications in basic and translational research.

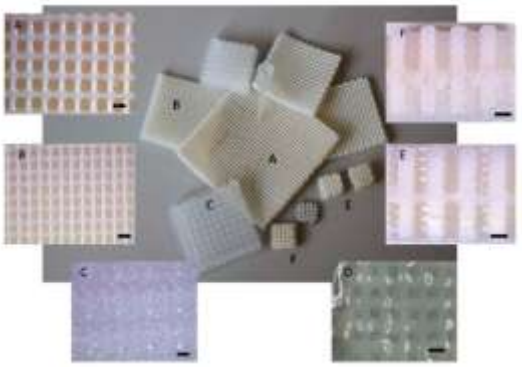

Fig. 8. Multi-well implantable scaffolds (*Source: Higuera et al., Integr Biol (Camb). 2013)*

The introduction of engineered tissues into the clinical practice implies high quality standards of the product to satisfy safety and efficacy requirements. The use of automated bioreactor-based manufacturing (Fig. 8) has been proposed as a way to increase the reproducibility of the result, being only minimally affected by operator variability, which has instead a big impact on the outcomes of standard cell culture procedures (79). Besides considerations on quality and safety requirements of engineered grafts, dynamic culture systems, such as perfusion bioreactors, represent a smart approach to overcome the limitations encountered in the static culture of 3D constructs (80-82). A specific advantage of direct perfusion bioreactors is the continuous influx of fresh medium and waste removal from the construct. Furthermore, the use of perfusion bioreactors increases the homogeneity of cell

distribution within the scaffold compared to static cell seeding, favoring the generation of homogeneous matrix throughout the scaffold (83).

As aforementioned, the optimization of protocols for cell expansion and re-differentiation is a key step in the generation of engineered tissues. In the last years, different protocols have been tested in order to reduce the negative impact of the *in vitro* expansion on the phenotype of articular chondrocytes and to improve their re-differentiation (59,84,85). These protocols include the use of soluble growth factors such as transforming growth factor beta (TGF-β), basic fibroblast growth factor (bFGF), insulin growth factor (IGF) and members of the bone morphogenetic proteins (BMPs) family. If the definition of the optimal combination of growth factors for cell expansion and chondrogenic differentiation is complex due to multiple variables in the experimental set-up of published studies (i.e. duration of expansion phase, origin of articular chondrocytes, source of MSCs, growth factors concentration, basal medium composition), a more general consideration is related to the possibility to translate the results obtained *in vitro* into the clinical practice. Indeed, the re-implantation of cells and cell-based products in human beings in naturally correlated to safety concerns, that imply the need to use clinically approved growth factors during cell expansion and differentiation.

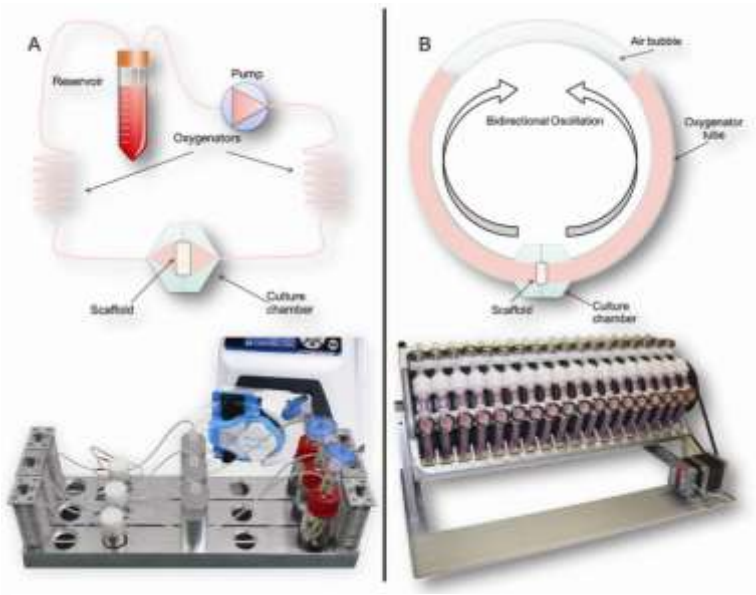

Fig. 9. (A) Schematic of a standard perfusion bioreactor system with its implementation. (B) Schematic and photograph of an oscillating perfusion bioreactor exploiting a pump-less perfusion method (*Source: Courtesy of Ske s.r.l.*)

Promising cocktails of clinically-approved growth factors have been optimized for the expansion (FGF-2 and Insulin, FI) and re-differentiation of ACs (BMP-2, Insulin and T3, BIT) (86). The sequential addition of these growth factors has been shown to induce the production of cartilagineous matrix when ACs were re-differentiated within collagen sponges. Nevertheless, matrix deposition was confined in the peripheral region of the scaffold, indicating the inefficient perfusion of nutrients and growth factors in the scaffold core (86). To overcome the limitations of static culture, combining dynamic culture systems with clinically approved protocols for cell expansion and differentiation appears as a promising approach to engineer *in vitro* clinically relevant grafts. Indeed, the use of automated bioreactors may allow to overcome major limitations encountered in the static culture of 3D constructs, that are directly

correlated with the increasing size of the engineered graft, and would increase the clinical translability of the results thank to improved compliance to quality and safety standards.

Despite the great potential of cell-based therapies and tissue engineering approaches in the treatment of articular cartilage defects, currently these approaches are not clinically relevant when considering late stage OA joints, characterized by an extensive erosion of articular cartilage and exposure of the underlying subchondral bone. Cartilage erosion causes the unprotected bone to rub directly on the opposing bone, a condition associated with high morbidity and impaired articular functionailty. So far, in late stage OA patients joint replacement (Fig. 10) is the only option to restore the articular function and to improve patients quality of life. Implant technology, however, is not free from drawbacks and critical issues. In particular, poor osseointegration is a key factor in the mobilization of cementless implants, often leading to prosthetic failure and to the need for re-intervention. Hence, the improvement of osseointegration can lead to a reduction in the risk of implant mobilization and, consequently, in the number of revision procedures (87-89), which have major drawbacks such as patients morbidity and relevant costs for National Health Systems. Porous metallic materials, such as macroporous titanium, have been introduced in cementless implant technology to maximize bone ingrowth and bone-implant contact (90-93) and are used to produce prosthetic components (Fig. 11) and to fill cavitary and segmental bone defects. Besides surface and structure modifications, the implant enrichment with progenitor cells (94,95) and bioactive factors (96-103) is a fascinating approach to convert metallic implants from bioinert to bioactive. Autologous bone marrow concentrate, obtained with an intra-operative approach, improves bone healing (104). Indeed, a recent study has shown that the enrichment of acetabular components with autologous BMSCs is able to improve bone formation and bone-implant contact in a caprine animal model (94). Since aging and age-related diseases negatively affect bone healing (105), the enrichment of the

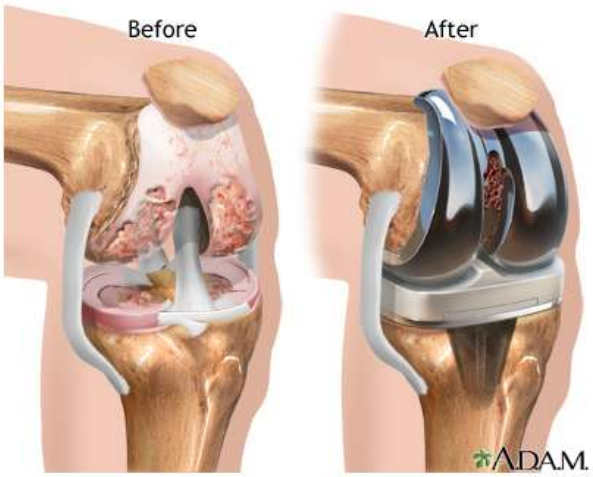

Fig. 10. Representation of OA knee before and after total joint replacement (*Source: http://physioworks.com.au*)

Fig. 11. Acetabular cup realized in macroporous titanium (*Source: Limacorporate s.p.a.)*

population of osteoprogenitor cells at the implant site may be particularly useful. Considering the clinical application of a prosthetic components enriched with autologous MSCs, cell retention into the implant may be critical due to the presence of body fluids. The use of biocompatible hydrogels in association with macroporous metals can be a promising strategy to overcome this limitation. Recent studies have demonstrated that bioactive hydrogels can be combined with metals to enrich implants with antibiotics (100,103), VEGF (101) and FGF-2 (102). Exploiting this approach for the simultaneous enrichment of progenitor cells and osteoinductive factors could represent a step further in the generation of bioactive prostheses with improved osseointegration potential.

In conclusion, cell-based therapies and tissue engineering strategies have a great potential for the treatment of patients affected by osteoarthritis either at early or late stage (106,107). However, when considering the re-implantation of autologous cells, being them autologous chondrocytes and/or mesenchymal stem cells, the impact of the inflammatory state of OA joints cannot be neglected. Nowaday, in contrast to the original view of OA as a simply "wear and tear" disease, it is recognized that pro-inflammatory cytokines and mediators play a key role in the onset and progression of this disease (Fig. 12) (108-110). This involves the recognition that implanted cell-based constructs may be subjected to the same inflammatory stimuli that contributed to the degradation of the original articular cartilage. In fact, inflammatory cytokines such as interleukin-1β (IL-1β) and transforming necrosis factor-α (TNFα), as well as conditioned medium from OA synovium or OA synovial fluid, can interfere with cartilagineous matrix deposition (111-113) and alter the phenotype of implanted cells (114,115).

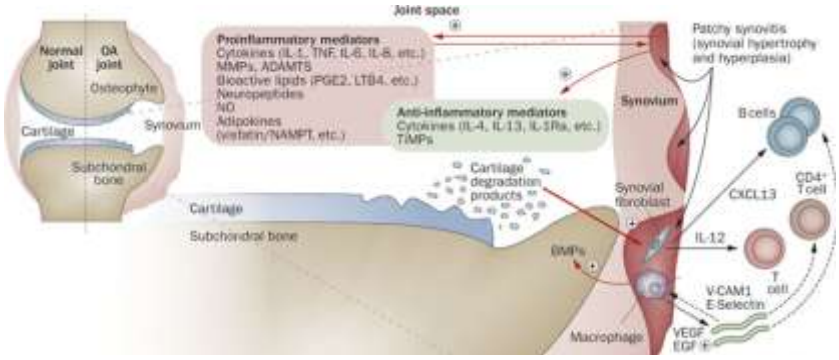

Fig. 12. Involvement of synovium in OA pathophisiology. Scheme showing the involvement of pro- and anti-inflammatory mediators and immune cells. (*Source: Sellam and Berembaum, Nat Rev Rheumatol. 2010*)

All these evidences highlight the need to develop *in vitro* models mimicking the environment of OA joint. These models can be exploited to test the performance of tissue engineered constructs in an inflammatory environment and should comprise the soluble factors as well as the cell types present in OA joints, such as macrophages. Activated macrophages secerning nitric oxide and proinflammatory cytokines like IL-1β and TNFα are accumulated in the synovium of early OA patients and drive the inflammatory process participating to synovitis (6). Furthermore, macrophages can directly participate to cartilage degradation thanks to the expression of catabolic enzymes such as matrix metallo-

proteinases (MMPs) (116,117). Conversely, macrophages also release factors that are important for tissue repair and suppression of inflammatory response to tissue damage (118). Hence, OA progression might induce and/or be induced by an inappropriate differentiation of resident tissue macrophages, and imbalance between functionally distinct phenotype. This suggests that further investigation on the influence of stimuli typical of diseased joints on macrophage phenotype is needed to understand their role in OA joint and to develop proper models to investigate the applicability of tissue engineered products in a diseased environment.

In order to evaluate basic and translational aspects related to potential cell-based approaches for early and late stage OA, in this thesis articular chondrocytes, adipose-derived mesenchymal stem cells, and their association were investigated in view of their potential use for the treatment of chondral defects. A multi-disciplinary approach was exploited to generate three-dimensional constructs and to develop novel strategies for the improvement of prosthetic implants. Finally, to better characterize the OA environment, the influence of stimuli typical of OA joint on macrophage phenotype was investigated.

References

1. Wenham CY, Conaghan PG. New horizons in osteoarthritis. Age Ageing.42:272-8. 2013.
2. Woolf AD, Pfleger B. Burden of major musculoskeletal conditions. B World Health Organ.81:646-56. 2003.
3. Aigner T, Rose J, Martin J, Buckwalter J. Aging theories of primary osteoarthritis: from epidemiology to molecular biology. Rejuvenation Res.7:134-45. 2004.
4. van der Kraan PM, van den Berg WB. Osteoarthritis in the context of ageing and evolution. Loss of chondrocyte differentiation block during ageing. Ageing Res Rev.7:106-13. 2008.
5. Hedbom E, Hauselmann HJ. Molecular aspects of pathogenesis in osteoarthritis: the role of inflammation. Cell Mol Life Sci.59:45-53. 2002.
6. Benito MJ, Veale DJ, FitzGerald O, van den Berg WB, Bresnihan B. Synovial tissue inflammation in early and late osteoarthritis. Ann Rheum Dis.64:1263-7. 2005.
7. Robertsson O, Dunbar M, Pehrsson T, Knutson K, Lidgren L. Patient satisfaction after knee arthroplasty: a report on 27,372 knees operated on between 1981 and 1995 in Sweden. Acta Orthop Scand.71:262-7. 2000.
8. Minas T. A primer in cartilage repair. J Bone Joint Surg Br.94:141-6. 2012.
9. Becerra J, Andrades JA, Guerado E, Zamora-Navas P, Lopez-Puertas JM, Reddi AH. Articular cartilage: structure and regeneration. Tissue Eng Part B Rev.16:617-27. 2010.
10. Wang F, Ying Z, Duan X, Tan H, Yang B, Guo L, Chen G, Dai G, Ma Z, Yang L. Histomorphometric analysis of adult articular calcified cartilage zone. J Struct Biol.168:359-65. 2009.
11. Hoemann CD, Lafantaisie-Favreau CH, Lascau-Coman V, Chen G, Guzman-Morales J. The cartilage-bone interface. J Knee Surg.25:85-97. 2012.
12. Huey DJ, Hu JC, Athanasiou KA. Unlike bone, cartilage regeneration remains elusive. Science.338:917-21. 2012.
13. Minas T, Nehrer S. Current concepts in the treatment of articular cartilage defects. Orthopedics.20:525-38. 1997.
14. Mithoefer K, McAdams T, Williams RJ, Kreuz PC, Mandelbaum BR. Clinical efficacy of the microfracture technique for articular cartilage repair in the knee: an evidence-based systematic analysis. Am J Sports Med.37:2053-63. 2009.
15. Minas T, Peterson L. Advanced techniques in autologous chondrocyte transplantation. Clin Sports Med.18:13-44, v-vi. 1999.
16. Brittberg M, Lindahl A, Nilsson A, Ohlsson C, Isaksson O, Peterson L. Treatment of deep cartilage defects in the knee with autologous chondrocyte transplantation. N Engl J Med.331:889-95. 1994.
17. Schnabel M, Marlovits S, Eckhoff G, Fichtel I, Gotzen L, Vecsei V, Schlegel J. Dedifferentiation-associated changes in morphology and gene expression in primary human articular chondrocytes in cell culture. Osteoarthritis Cartilage.10:62-70. 2002.
18. Barbero A, Grogan S, Schafer D, Heberer M, Mainil-Varlet P, Martin I. Age related changes in human articular chondrocyte yield, proliferation and post-expansion chondrogenic capacity. Osteoarthritis Cartilage.12:476-84. 2004.
19. Dehne T, Karlsson C, Ringe J, Sittinger M, Lindahl A. Chondrogenic differentiation potential of osteoarthritic chondrocytes and their possible use in matrix-associated autologous chondrocyte transplantation. Arthritis Res Ther.11:R133. 2009.
20. Tallheden T, Bengtsson C, Brantsing C, Sjogren-Jansson E, Carlsson L, Peterson L, Brittberg M, Lindahl A. Proliferation and differentiation potential of chondrocytes from osteoarthritic patients. Arthritis Res Ther.7:R560-8. 2005.
21. Cavallo C, Desando G, Facchini A, Grigolo B. Chondrocytes from patients with osteoarthritis express typical extracellular matrix molecules once grown onto a three-dimensional hyaluronan-based scaffold. J Biomed Mater Res A.93:86-95. 2010.
22. Rose J, Soder S, Skhirtladze C, Schmitz N, Gebhard PM, Sesselmann S, Aigner T. DNA damage, discoordinated gene expression and cellular senescence in osteoarthritic chondrocytes. Osteoarthritis Cartilage.20:1020-8. 2012.
23. Kim KI, Park YS, Im GI. Changes in the epigenetic status of the SOX-9 promoter in human osteoarthritic cartilage. J Bone Miner

Res.28:1050-60. 2013.
24. Friedenstein AJ, Petrakova KV, Kurolesova AI, Frolova GP. Heterotopic of bone marrow. Analysis of precursor cells for osteogenic and hematopoietic tissues. Transplantation.6:230-47. 1968.
25. Caplan AI. Mesenchymal stem cells. J Orthop Res.9:641-50. 1991.
26. Caplan AI. The mesengenic process. Clin Plast Surg.21:429-35. 1994.
27. Zuk PA, Zhu M, Ashjian P, De Ugarte DA, Huang JI, Mizuno H, Alfonso ZC, Fraser JK, Benhaim P, Hedrick MH. Human adipose tissue is a source of multipotent stem cells. Mol Biol Cell.13:4279-95. 2002.
28. Zuk PA, Zhu M, Mizuno H, Huang J, Futrell JW, Katz AJ, Benhaim P, Lorenz HP, Hedrick MH. Multilineage cells from human adipose tissue: implications for cell-based therapies. Tissue Eng.7:211-28. 2001.
29. Baglioni S, Cantini G, Poli G, Francalanci M, Squecco R, Di Franco A, Borgogni E, Frontera S, Nesi G, Liotta F, Lucchese M, Perigli G, Francini F, Forti G, Serio M, Luconi M. Functional differences in visceral and subcutaneous fat pads originate from differences in the adipose stem cell. PLoS One.7:e36569. 2012.
30. Niada S, Ferreira LM, Arrigoni E, Addis A, Campagnol M, Broccaioli E, Brini AT. Porcine adipose-derived stem cells from buccal fat pad and subcutaneous adipose tissue for future preclinical studies in oral surgery. Stem Cell Res Ther.4:148. 2013.
31. Korn BS, Kikkawa DO, Hicok KC. Identification and characterization of adult stem cells from human orbital adipose tissue. Ophthal Plast Reconstr Surg.25:27-32. 2009.
32. Rada T, Reis RL, Gomes ME. Adipose tissue-derived stem cells and their application in bone and cartilage tissue engineering. Tissue Eng Part B Rev.15:113-25. 2009.
33. Rhee SC, Ji YH, Gharibjanian NA, Dhong ES, Park SH, Yoon ES. In vivo evaluation of mixtures of uncultured freshly isolated adipose-derived stem cells and demineralized bone matrix for bone regeneration in a rat critically sized calvarial defect model. Stem Cells Dev.20:233-42. 2011.
34. Choi JW, Park EJ, Shin HS, Shin IS, Ra JC, Koh KS. In Vivo Differentiation of Undifferentiated Human Adipose Tissue-Derived Mesenchymal Stem Cells in Critical-Sized Calvarial Bone Defects. Ann Plast Surg. 2012.
35. Kang H, Peng J, Lu S, Liu S, Zhang L, Huang J, Sui X, Zhao B, Wang A, Xu W, Luo Z, Guo Q. In vivo cartilage repair using adipose-derived stem cell-loaded decellularized cartilage ECM scaffolds. J Tissue Eng Regen Med. 2012.
36. Jung SN, Rhie JW, Kwon H, Jun YJ, Seo JW, Yoo G, Oh DY, Ahn ST, Woo J, Oh J. In vivo cartilage formation using chondrogenic-differentiated human adipose-derived mesenchymal stem cells mixed with fibrin glue. J Craniofac Surg.21:468-72. 2010.
37. Wickham MQ, Erickson GR, Gimble JM, Vail TP, Guilak F. Multipotent stromal cells derived from the infrapatellar fat pad of the knee. Clin Orthop Relat Res.196-212. 2003.
38. Dragoo JL, Samimi B, Zhu M, Hame SL, Thomas BJ, Lieberman JR, Hedrick MH, Benhaim P. Tissue-engineered cartilage and bone using stem cells from human infrapatellar fat pads. J Bone Joint Surg Br.85:740-7. 2003.
39. English A, Jones EA, Corscadden D, Henshaw K, Chapman T, Emery P, McGonagle D. A comparative assessment of cartilage and joint fat pad as a potential source of cells for autologous therapy development in knee osteoarthritis. Rheumatology (Oxford).46:1676-83. 2007.
40. Liu Y, Buckley CT, Downey R, Mulhall KJ, Kelly DJ. The role of environmental factors in regulating the development of cartilaginous grafts engineered using osteoarthritic human infrapatellar fat pad-derived stem cells. Tissue Eng Part A.18:1531-41. 2012.
41. Khan WS, Adesida AB, Tew SR, Andrew JG, Hardingham TE. The epitope characterisation and the osteogenic differentiation potential of human fat pad-derived stem cells is maintained with ageing in later life. Injury.40:150-7. 2009.
42. Gimble JM, Guilak F. Differentiation potential of adipose derived adult stem (ADAS) cells. Curr Top Dev Biol.58:137-60. 2003.
43. Guilak F, Awad HA, Fermor B, Leddy HA, Gimble JM. Adipose-derived adult stem cells for cartilage tissue engineering. Biorheology.41:389-99. 2004.
44. Pires de Carvalho P, Hamel KM, Duarte R, King AG, Haque M, Dietrich MA, Wu X, Shah F, Burk D, Reis RL, Rood J, Zhang P, Lopez M, Gimble JM, Dasa V. Comparison of infrapatellar and subcutaneous adipose tissue stromal vascular fraction and stromal/stem cells in osteoarthritic subjects. J Tissue Eng Regen Med. 2012.
45. Alegre-Aguaron E, Desportes P, Garcia-Alvarez F, Castiella T, Larrad L, Martinez-Lorenzo MJ. Differences in surface marker expression and chondrogenic potential among various tissue-derived mesenchymal cells from elderly patients with osteoarthritis. Cells Tissues Organs.196:231-40. 2012.
46. Mochizuki T, Muneta T, Sakaguchi Y, Nimura A, Yokoyama A, Koga H, Sekiya I. Higher chondrogenic potential of fibrous synovium- and adipose synovium-derived cells compared with subcutaneous fat-derived cells: distinguishing properties of mesenchymal stem cells in humans. Arthritis Rheum.54:843-53. 2006.
47. Lee JS, Im GI. Influence of chondrocytes on the chondrogenic differentiation of adipose stem cells. Tissue Eng Part A.16:3569-77. 2010.
48. Acharya C, Adesida A, Zajac P, Mumme M, Riesle J, Martin I, Barbero A. Enhanced chondrocyte proliferation and mesenchymal stromal cells chondrogenesis in coculture pellets mediate improved cartilage formation. J Cell Physiol.227:88-97. 2012.
49. Sabatino MA, Santoro R, Gueven S, Jaquiery C, Wendt DJ, Martin I, Moretti M, Barbero A. Cartilage graft engineering by co-culturing primary human articular chondrocytes with human bone marrow stromal cells. J Tissue Eng Regen Med. 2012.
50. Meretoja VV, Dahlin RL, Kasper FK, Mikos AG. Enhanced chondrogenesis in co-cultures with articular chondrocytes and mesenchymal stem cells. Biomaterials.33:6362-9. 2012.
51. Meretoja VV, Dahlin RL, Wright S, Kasper FK, Mikos AG. Articular Chondrocyte Redifferentiation in 3D Co-cultures with Mesenchymal Stem Cells. Tissue Eng Part C Methods. 2014.
52. Giovannini S, Diaz-Romero J, Aigner T, Heini P, Mainil-Varlet P, Nesic D. Micromass co-culture of human articular chondrocytes and human bone marrow mesenchymal stem cells to investigate stable neocartilage tissue formation in vitro. Eur Cell Mater.20:245-59. 2010.
53. Aung A, Gupta G, Majid G, Varghese S. Osteoarthritic chondrocyte-secreted morphogens induce chondrogenic differentiation of human mesenchymal stem cells. Arthritis Rheum.63:148-58. 2011.
54. Hildner F, Concaro S, Peterbauer A, Wolbank S, Danzer M, Lindahl A, Gatenholm P, Redl H, van Griensven M. Human adipose-derived stem cells contribute to chondrogenesis in coculture with human articular chondrocytes. Tissue Eng Part A.15:3961-9. 2009.
55. Hwang NS, Im SG, Wu PB, Bichara DA, Zhao X, Randolph MA, Langer R, Anderson DG. Chondrogenic priming adipose-mesenchymal stem cells for cartilage tissue regeneration. Pharm Res.28:1395-405. 2011.
56. Langer R, Vacanti JP. Tissue engineering. Science.260:920-6. 1993.
57. Dehne T, Schenk R, Perka C, Morawietz L, Pruss A, Sittinger M, Kaps C, Ringe J. Gene expression profiling of primary human articular chondrocytes in high-density micromasses reveals patterns of recovery, maintenance, re- and dedifferentiation. Gene.462:8-17. 2010.
58. Zhang Z, McCaffery JM, Spencer RG, Francomano CA. Hyaline cartilage engineered by chondrocytes in pellet culture: histological,

immunohistochemical and ultrastructural analysis in comparison with cartilage explants. J Anat.205:229-37. 2004.
59. Jakob M, Demarteau O, Schafer D, Hintermann B, Dick W, Heberer M, Martin I. Specific growth factors during the expansion and redifferentiation of adult human articular chondrocytes enhance chondrogenesis and cartilaginous tissue formation in vitro. J Cell Biochem.81:368-77. 2001.
60. Bernstein P, Dong M, Corbeil D, Gelinsky M, Gunther KP, Fickert S. Pellet culture elicits superior chondrogenic redifferentiation than alginate-based systems. Biotechnol Prog.25:1146-52. 2009.
61. Pelttari K, Steck E, Richter W. The use of mesenchymal stem cells for chondrogenesis. Injury.39 Suppl 1:S58-65. 2008.
62. Kosuge D, Khan WS, Haddad B, Marsh D. Biomaterials and scaffolds in bone and musculoskeletal engineering. Curr Stem Cell Res Ther.8:185-91. 2013.
63. Filardo G, Kon E, Roffi A, Di Martino A, Marcacci M. Scaffold-based repair for cartilage healing: a systematic review and technical note. Arthroscopy.29:174-86. 2013.
64. Denker AE, Haas AR, Nicoll SB, Tuan RS. Chondrogenic differentiation of murine C3H10T1/2 multipotential mesenchymal cells: I. Stimulation by bone morphogenetic protein-2 in high-density micromass cultures. Differentiation.64:67-76. 1999.
65. Grassel S, Ahmed N. Influence of cellular microenvironment and paracrine signals on chondrogenic differentiation. Front Biosci.12:4946-56. 2007.
66. Leijten JC, Georgi N, Wu L, van Blitterswijk CA, Karperien M. Cell sources for articular cartilage repair strategies: shifting from monocultures to cocultures. Tissue Eng Part B Rev.19:31-40. 2013.
67. Moreira Teixeira LS, Leijten JC, Sobral J, Jin R, van Apeldoorn AA, Feijen J, van Blitterswijk C, Dijkstra PJ, Karperien M. High throughput generated micro-aggregates of chondrocytes stimulate cartilage formation in vitro and in vivo. Eur Cell Mater.23:387-99. 2012.
68. Babur BK, Ghanavi P, Levett P, Lott WB, Klein T, Cooper-White JJ, Crawford R, Doran MR. The interplay between chondrocyte redifferentiation pellet size and oxygen concentration. PLoS One.8:e58865. 2013.
69. de Ridder L, Cornelissen M, de Ridder D. Autologous spheroid culture: a screening tool for human brain tumour invasion. Crit Rev Oncol Hematol.36:107-22. 2000.
70. Baraniak PR, McDevitt TC. Scaffold-free culture of mesenchymal stem cell spheroids in suspension preserves multilineage potential. Cell Tissue Res.347:701-11. 2012.
71. Mohammed MI, Desmulliez MP. Planar lens integrated capillary action microfluidic immunoassay device for the optical detection of troponin I. Biomicrofluidics.7:64112. 2013.
72. Yap YC, Guijt RM, Dickson TC, King AE, Breadmore MC. Stainless steel pinholes for fast fabrication of high-performance microchip electrophoresis devices by CO2 laser ablation. Anal Chem.85:10051-6. 2013.
73. Khan Malek CG. Laser processing for bio-microfluidics applications (part I). Anal Bioanal Chem.385:1351-61. 2006.
74. Khan Malek CG. Laser processing for bio-microfluidics applications (part II). Anal Bioanal Chem.385:1362-9. 2006.
75. Fiorini GS, Chiu DT. Disposable microfluidic devices: fabrication, function, and application. Biotechniques.38:429-46. 2005.
76. Higuera GA, Hendriks JA, van Dalum J, Wu L, Schotel R, Moreira-Teixeira L, van den Doel M, Leijten JC, Riesle J, Karperien M, van Blitterswijk CA, Moroni L. In vivo screening of extracellular matrix components produced under multiple experimental conditions implanted in one animal. Integr Biol (Camb).5:889-98. 2013.
77. Li X, Zhang X, Zhao S, Wang J, Liu G, Du Y. Micro-scaffold array chip for upgrading cell-based high-throughput drug testing to 3D using benchtop equipment. Lab Chip.14:471-81. 2014.
78. Koroleva A, Gittard S, Schlie S, Deiwick A, Jockenhoevel S, Chichkov B. Fabrication of fibrin scaffolds with controlled microscale architecture by a two-photon polymerization-micromolding technique. Biofabrication.4:015001. 2012.
79. Martin I, Smith T, Wendt D. Bioreactor-based roadmap for the translation of tissue engineering strategies into clinical products. Trends Biotechnol.27:495-502. 2009.
80. Mabvuure N, Hindocha S, Khan WS. The role of bioreactors in cartilage tissue engineering. Curr Stem Cell Res Ther.7:287-92. 2012.
81. Santoro R, Olivares AL, Brans G, Wirz D, Longinotti C, Lacroix D, Martin I, Wendt D. Bioreactor based engineering of large-scale human cartilage grafts for joint resurfacing. Biomaterials.31:8946-52. 2010.
82. Martin I, Wendt D, Heberer M. The role of bioreactors in tissue engineering. Trends Biotechnol.22:80-6. 2004.
83. Vunjak-Novakovic G, Obradovic B, Martin I, Bursac PM, Langer R, Freed LE. Dynamic cell seeding of polymer scaffolds for cartilage tissue engineering. Biotechnol Prog.14:193-202. 1998.
84. Shakibaei M, Seifarth C, John T, Rahmanzadeh M, Mobasheri A. Igf-I extends the chondrogenic potential of human articular chondrocytes in vitro: molecular association between Sox9 and Erk1/2. Biochem Pharmacol.72:1382-95. 2006.
85. Liu G, Kawaguchi H, Ogasawara T, Asawa Y, Kishimoto J, Takahashi T, Chung UI, Yamaoka H, Asato H, Nakamura K, Takato T, Hoshi K. Optimal combination of soluble factors for tissue engineering of permanent cartilage from cultured human chondrocytes. J Biol Chem.282:20407-15. 2007.
86. Claus S, Mayer N, Aubert-Foucher E, Chajra H, Perrier-Goult E, Lafont J, Piperno M, Damour O, Mallein-Gerin F. Cartilage-characteristic matrix reconstruction by sequential addition of soluble factors during expansion of human articular chondrocytes and their cultivation in collagen sponges. Tissue Eng Part C Methods.18:104-12. 2012.
87. Bobyn JD. Fixation and bearing surfaces for the next millennium. Orthopedics.22:810-2. 1999.
88. Albrektsson T, Branemark PI, Hansson HA, Lindstrom J. Osseointegrated titanium implants. Requirements for ensuring a long-lasting, direct bone-to-implant anchorage in man. Acta Orthop Scand.52:155-70. 1981.
89. Ochsner PE. Osteointegration of orthopaedic devices. Semin Immunopathol.33:245-56. 2011.
90. Chaudhari A, Braem A, Vleugels J, Martens JA, Naert I, Cardoso MV, Duyck J. Bone tissue response to porous and functionalized titanium and silica based coatings. PLoS One.6:e24186. 2011.
91. Shannon FJ, Cottrell JM, Deng XH, Crowder KN, Doty SB, Avaltroni MJ, Warren RF, Wright TM, Schwartz J. A novel surface treatment for porous metallic implants that improves the rate of bony ongrowth. J Biomed Mater Res A.86:857-64. 2008.
92. Spoerke ED, Murray NG, Li H, Brinson LC, Dunand DC, Stupp SI. Titanium with aligned, elongated pores for orthopedic tissue engineering applications. J Biomed Mater Res A.84:402-12. 2008.
93. Heinl P, Muller L, Korner C, Singer RF, Muller FA. Cellular Ti-6Al-4V structures with interconnected macro porosity for bone implants fabricated by selective electron beam melting. Acta Biomater.4:1536-44. 2008.
94. Kalia P, Coathup MJ, Oussedik S, Konan S, Dodd M, Haddad FS, Blunn GW. Augmentation of bone growth onto the acetabular cup surface using bone marrow stromal cells in total hip replacement surgery. Tissue Eng Part A.15:3689-96. 2009.
95. van den Dolder J, Farber E, Spauwen PH, Jansen JA. Bone tissue reconstruction using titanium fiber mesh combined with rat bone marrow stromal cells. Biomaterials.24:1745-50. 2003.

96. Daugaard H, Elmengaard B, Andreassen T, Bechtold J, Lamberg A, Soballe K. Parathyroid hormone treatment increases fixation of orthopedic implants with gap healing: a biomechanical and histomorphometric canine study of porous coated titanium alloy implants in cancellous bone. Calcif Tissue Int.88:294-303. 2011.
97. Petrie TA, Raynor JE, Reyes CD, Burns KL, Collard DM, Garcia AJ. The effect of integrin-specific bioactive coatings on tissue healing and implant osseointegration. Biomaterials.29:2849-57. 2008.
98. Clark PA, Moioli EK, Sumner DR, Mao JJ. Porous implants as drug delivery vehicles to augment host tissue integration. FASEB J.22:1684-93. 2008.
99. Vrana NE, Dupret-Bories A, Bach C, Chaubaroux C, Coraux C, Vautier D, Boulmedais F, Haikel Y, Debry C, Metz-Boutigue MH, Lavalle P. Modification of macroporous titanium tracheal implants with biodegradable structures: tracking in vivo integration for determination of optimal in situ epithelialization conditions. Biotechnol Bioeng.109:2134-46. 2012.
100. De Giglio E, Cometa S, Ricci MA, Cafagna D, Savino AM, Sabbatini L, Orciani M, Ceci E, Novello L, Tantillo GM, Mattioli-Belmonte M. Ciprofloxacin-modified electrosynthesized hydrogel coatings to prevent titanium-implant-associated infections. Acta Biomater.7:882-91. 2011.
101. De Giglio E, Cometa S, Ricci MA, Zizzi A, Cafagna D, Manzotti S, Sabbatini L, Mattioli-Belmonte M. Development and characterization of rhVEGF-loaded poly(HEMA-MOEP) coatings electrosynthesized on titanium to enhance bone mineralization and angiogenesis. Acta Biomater.6:282-90. 2010.
102. Ichinohe N, Kuboki Y, Tabata Y. Bone regeneration using titanium nonwoven fabrics combined with fgf-2 release from gelatin hydrogel microspheres in rabbit skull defects. Tissue Eng Part A.14:1663-71. 2008.
103. Pitarresi G, Palumbo FS, Calascibetta F, Fiorica C, Di Stefano M, Giammona G. Medicated hydrogels of hyaluronic acid derivatives for use in orthopedic field. Int J Pharm.449:84-94. 2013.
104. Jager M, Herten M, Fochtmann U, Fischer J, Hernigou P, Zilkens C, Hendrich C, Krauspe R. Bridging the gap: bone marrow aspiration concentrate reduces autologous bone grafting in osseous defects. J Orthop Res.29:173-80. 2011.
105. Mehta M, Strube P, Peters A, Perka C, Hutmacher D, Fratzl P, Duda GN. Influences of age and mechanical stability on volume, microstructure, and mineralization of the fracture callus during bone healing: is osteoclast activity the key to age-related impaired healing? Bone.47:219-28. 2010.
106. Diekman BO, Guilak F. Stem cell-based therapies for osteoarthritis: challenges and opportunities. Curr Opin Rheumatol.25:119-26. 2013.
107. O'Connell GD, Lima EG, Bian L, Chahine NO, Albro MB, Cook JL, Ateshian GA, Hung CT. Toward engineering a biological joint replacement. J Knee Surg.25:187-96. 2012.
108. Beekhuizen M, Gierman LM, van Spil WE, Van Osch GJ, Huizinga TW, Saris DB, Creemers LB, Zuurmond AM. An explorative study comparing levels of soluble mediators in control and osteoarthritic synovial fluid. Osteoarthritis Cartilage.21:918-22. 2013.
109. Scanzello CR, Goldring SR. The role of synovitis in osteoarthritis pathogenesis. Bone.51:249-57. 2012.
110. Sellam J, Berenbaum F. The role of synovitis in pathophysiology and clinical symptoms of osteoarthritis. Nat Rev Rheumatol.6:625-35. 2010.
111. Heldens GT, Blaney Davidson EN, Vitters EL, Schreurs BW, Piek E, van den Berg WB, van der Kraan PM. Catabolic factors and osteoarthritis-conditioned medium inhibit chondrogenesis of human mesenchymal stem cells. Tissue Eng Part A.18:45-54. 2012.
112. Kruger JP, Endres M, Neumann K, Stuhlmuller B, Morawietz L, Haupl T, Kaps C. Chondrogenic differentiation of human subchondral progenitor cells is affected by synovial fluid from donors with osteoarthritis or rheumatoid arthritis. J Orthop Surg Res.7:10. 2012.
113. Boeuf S, Graf F, Fischer J, Moradi B, Little CB, Richter W. Regulation of aggrecanases from the ADAMTS family and aggrecan neoepitope formation during in vitro chondrogenesis of human mesenchymal stem cells. Eur Cell Mater.23:320-32. 2012.
114. Rohner E, Matziolis G, Perka C, Fuchtmeier B, Gaber T, Burmester GR, Buttgereit F, Hoff P. Inflammatory synovial fluid microenvironment drives primary human chondrocytes to actively take part in inflammatory joint diseases. Immunol Res.52:169-75. 2012.
115. Hoff P, Buttgereit F, Burmester GR, Jakstadt M, Gaber T, Andreas K, Matziolis G, Perka C, Rohner E. Osteoarthritis synovial fluid activates pro-inflammatory cytokines in primary human chondrocytes. Int Orthop.37:145-51. 2013.
116. Blom AB, van Lent PL, Libregts S, Holthuysen AE, van der Kraan PM, van Rooijen N, van den Berg WB. Crucial role of macrophages in matrix metalloproteinase-mediated cartilage destruction during experimental osteoarthritis: involvement of matrix metalloproteinase 3. Arthritis Rheum.56:147-57. 2007.
117. Smeets TJ, Barg EC, Kraan MC, Smith MD, Breedveld FC, Tak PP. Analysis of the cell infiltrate and expression of proinflammatory cytokines and matrix metalloproteinases in arthroscopic synovial biopsies: comparison with synovial samples from patients with end stage, destructive rheumatoid arthritis. Ann Rheum Dis.62:635-8. 2003.
118. Novak ML, Koh TJ. Macrophage phenotypes during tissue repair. J Leukoc Biol.93:875-81. 2013.

Chapter 3

Characterization of articular chondrocytes isolated from 211 osteoarthritic patients

Abstract

We analyzed specific features of chondrocytes as cellular yield, cell doubling rates and the dependence between these parameters and patient-related data in a set of 211 osteoarthritic (OA) patients undergoing total joint replacement. For each patient the data available were joint type, age and gender. Knee samples chosen randomly among all biopsies were graded according to ICRS score. Patients' age ranged between 30 and 90 years with a mean age of 66 ± 9.7 years. Patients were divided into age classes and statistically significant differences in proliferation rate at passage 1 were found between chondrocytes derived from young and old donors, with the last ones characterized by a lower proliferation rate. A similar trend was observed for proliferation rate at passage 2. For all the samples, cellular yields ranged between 0.1 and 5.5 million cells/g of tissue. No significant correlation was observed between the level of cartilage degeneration (ICRS score) and cellular yield and proliferation rates. However, in samples with a high degree of cartilage degeneration (ICRS score 4) the cellular yield was lower compared to the other three groups (ICRS scores 1-3). In this study we performed a systematic characterization of basic parameters of chondrocytes originating from a wide group of OA patients. Considering the use of autologous chondrocytes in chondral treatments, the characterization of cell basic features may represent an important step to determine the quality of the cell source which is a major determinant in the outcome of cell-based therapies.

Introduction

Osteoarthritis (OA) is a highly disabling pathology which is worldwide investigated by the scientific community due to its increasing diffusion. This age-dependent degenerative disease induces the progressive damage of articular cartilage and subchondral bone and can eventually lead to the complete loss of joint functionality (1,2). The combination of pharmacological and non-pharmacological therapies has been proved to be useful for the treatment of early- and middle-stage OA patients, but a successful clinical outcome is not granted when treating late-stage OA patients (3). In this category of patients, the severe pain and the functional limitations caused by advanced OA degeneration are currently resolved mainly by joint replacement surgery.

In the last two decades, "advanced therapies" have been intensely investigated in developed countries, with the aim to find a biological solution to several degenerative pathologies. In cartilage tissue engineering, a possible strategy for an autologous approach would be to isolate cells chondrocytes from a cartilage biopsy, to expand the cells and possibly cryopreserve them for future re-intervention. Expanded chondrocytes are then seeded on a biomaterial and the cellularized construct is finally implanted back to the patient (4). Cartilage tissue engineering applied to OA patients appears to be in contrast with the controversial opinion that healthy autologous chondrocytes or mesenchymal stem cells are necessary to obtain healthy cartilage in vitro (2,5,6). Recent works, however, have demonstrated the possibility to use human OA chondrocytes to obtain autologous engineered cartilage with properties similar to those of the constructs obtained from non-OA chondrocytes (7-10). Moreover, a recent work (11) on human OA articular chondrocytes characterized their genetic stability during long term expansion and demonstrated the safety of this cell type for autologous advanced therapies. Since the quality of cells used to generate the engineered tissue greatly influences the outcome, a characterization of OA chondrocytes in a wide patient group can help in extending the validity of the reported results.

In this work we analyzed specific features of chondrocytes collected from 211 osteoarthritic patients undergoing total joint replacement. The characteristics investigated were cellular yield and cell doubling rates, and the dependence between these parameters and some patients-related data.

Materials and Methods

Chondrocyte isolation, expansion and data collection

Samples of adult human articular cartilage were harvested from subjects undergoing hip and knee routine arthroplasty procedures. With the patient's informed consent and in respect to the privacy law, the patient age, gender and joint type were recorded. Based on evaluation by orthopaedic surgeons,

random knee samples were also graded from score 1 to score 4 using the ICRS protocol (12), where higher scores indicate higher levels of cartilage degeneration. Minced cartilage fragments (2-3 mm^2) were weighted and chondrocyte isolation was carried out by cartilage digestion in 0.15% collagenase type II (Worthington) performed for 22 h at 37 °C, as previously described (13).

Viable cells were counted by trypan blue dye exclusion. Freshly isolated chondrocytes (P0) were plated for expansion at a density of 1*104 cells/cm2 for the first passage (P1) and cultured with complete proliferation medium (CM) containing Dulbecco's Modified Eagle Medium (DMEM) supplemented with 10% fetal bovine serum (FBS, Lonza), 1 mM sodium pyruvate, 100 mM HEPES buffer, 100 U/ml penicillin, 100 μg/ml streptomycin, 0.29 mg/ml L-glutamine, 1 ng/ml TGFb1, 5 ng/ml FGF-2 (PeproTech) (14). Where not otherwise specified, Invitrogen products were used. For the second passage (P2) cells were plated at a density of 0.5*104 cells/cm2. Cell doubling rate (d) was calculated as

$$d = \frac{log_2\left(\frac{N}{N_0}\right)}{t}$$

where N and N_0 are the final and initial cell number, respectively, and t is the expansion time. The cellular yield was calculated as the ratio between the viable cell number at P0, expressed in millions of cells, and the wet weight of the cartilage fragments, expressed in grams.

Data processing and statistical analysis

The software Graph Pad Prism® was used to order and process the data. For each patient, the available data were joint type, patient age, patient gender, ICRS grading, cellular yield, doubling rate at P1 and at P2. Mean and standard deviation were calculated for each parameter and relative normalized frequency (2) histograms were obtained. The normalized frequency was calculated as

$$nf = \frac{f}{S_c \times N_s}$$

where f is the frequency of the data inside the considered class, S_c is the spacing of the class and N_s is the sample size (132 patients for the hip group, 88 patients for the knee group). Relative normalized frequency histograms were also obtained for the scored knee cartilage samples. For all the relative normalized frequency histograms the Poisson distribution was calculated.

Non normal distribution of data was determined with a D'Agostino & Pearson normality test. Correlation between patients' age, cellular yield, and proliferation rate at P1 and at P2 was determined calculating the Spearman coefficient r and considered significant for $p<0.05$. To compare independent groups, Kruskal-Wallis test followed by Dunn's multiple comparison test was performed and differences were considered significant for $p<0.05$.

To better evaluate age-related differences in cellular yield and proliferation rate, patients were grouped in the following age classes: ≤60, 65-70, ≥75 years, composed of the same number of patients (n = 47).

Four years gaps between classes were left to avoid overlapping.

Box-plots were used for the visualization of the main parameters of the data statistical distribution both for age classes and for ICRS score groups (minimum, 25th percentile, 75th percentile, maximum).

Results

Patients' gender distribution showed that 42% of hip arthroplasties were performed on males and 58% on females (Fig. 1). For knee arthroplasties the percentage of male vs. female patients was 12% vs. 88%.

	Males [%]	Females [%]
Hip patients	42%	58%
Knee patients	12%	88%
Total patients	31%	69%

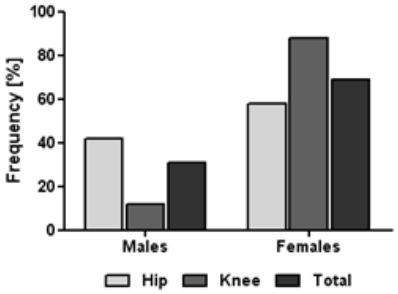

Fig. 1. Frequency distribution of patient gender. The patients, all affected by osteoarthritis, were subjected to total hip or knee replacement.

Considering both arthroplasty types together, female patients were 69% of the total. Patients' age ranged between 30 and 90 years and the frequency histograms showed a mean age of 66 years, both for knee and hip patients (Fig. 2 a-c). The ICRS grading system was applied to samples of knee cartilage randomly chosen among the donors, to classify the samples from score 1 (low damage) to score 4 (high damage). The mean age of patients did not differ significantly between scores and ranged from 65 to 69 years, as shown in frequency distribution graphs in Fig. 2d.

Cellular yield values ranged between 0.1 and 5.5 million cells/gram of tissue, with a mean of 1.85±1.37 and 1.62 ± 1.08 million cells/gram of tissue for hip and knee samples, respectively (Fig. 3 a-c). For the different ICRS scores, mean values of cellular yield were similar up to score 3 (about 1.4 million cells/gram of tissue), whereas it was lower for highly degenerated tissue (score 4, 0.9 million cells/gram of tissue).

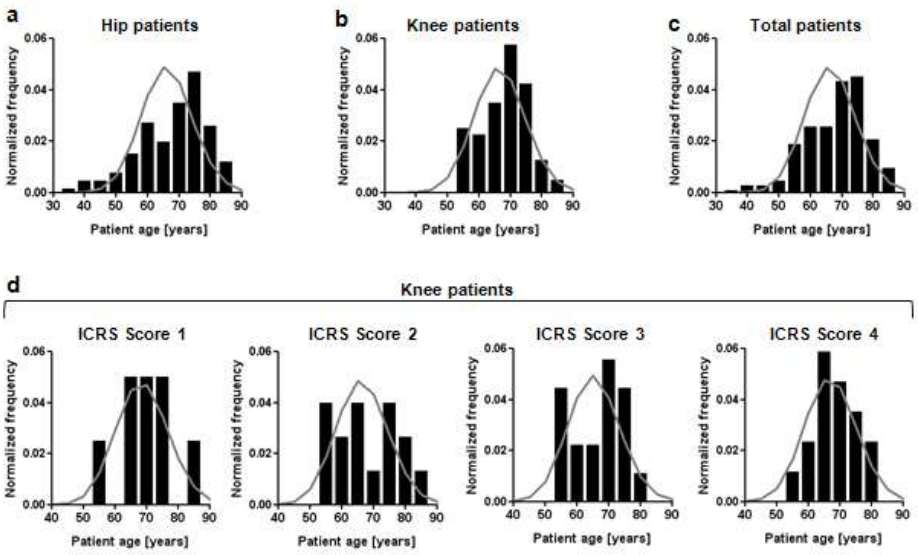

Fig. 2. Relative normalized frequency distribution obtained for increasing classes of patient age for the hip (a), knee (b), total (c) and increasing ICRS scores (d). The frequency histograms are approximated by Poisson's distribution

The analysis of the correlation between patients' age, cellular yield and proliferation rate at P1 and at P2 is reported in Fig. 4 with the corresponding correlation coefficients (Spearman r).

Significant correlations were observed between age and doubling rate at P1 (r = -0.223, p<0.01),

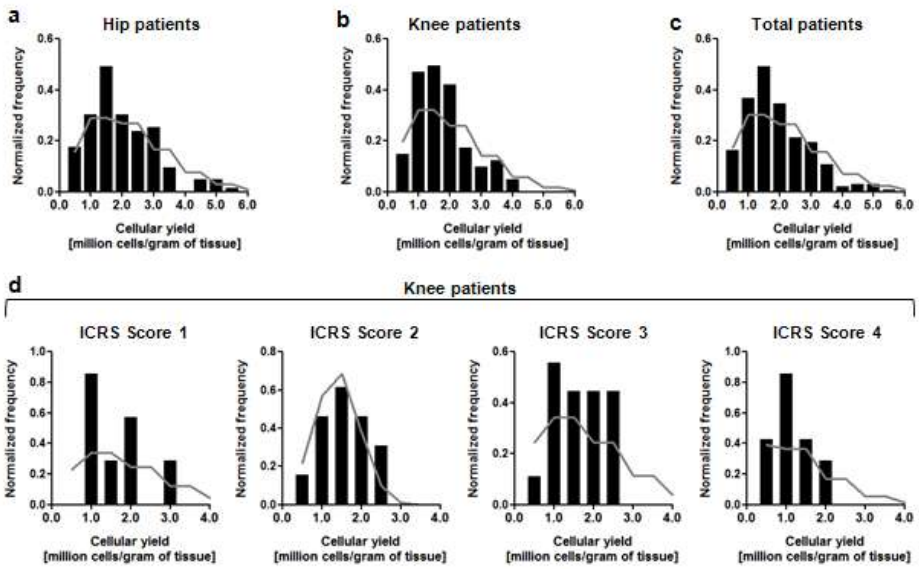

Fig. 3. Relative normalized frequency distribution obtained for increasing classes of cellular yield for the hip (a), knee (b), total (c) and increasing ICRS scores (d). The frequency histograms are approximated by Poisson's distribution

showing a decrease of doubling rate at P1 with increasing age, and between doubling rate at P2 and at P1 (r = 0.343, p<0.001), demonstrating a trend between cell growth at both passages. A significant correlation was found also between cellular yield and proliferation rate at P2 (r = 0.268, p<0.001), suggesting that cells deriving from samples with a higher cellular yield, retain a greater proliferation potential during expansion.

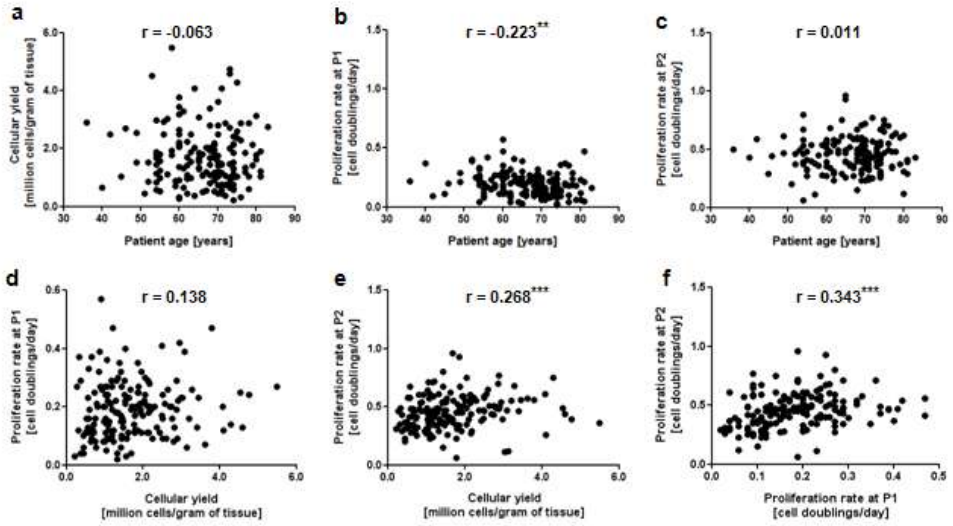

Fig. 4. Correlations among individual data groups. (a) cellular yield vs. patient age, (b) proliferation rate at P1 vs. patient age, (c) proliferation rate at P2 vs. patient age, (d) proliferation rate at P1 vs. cellular yield, (e) proliferation rate at P2 vs. cellular yield, and (f) proliferation rate at P2 vs. proliferation rate at P1. Correlation coefficients (Spearman r) are indicated in each graph. ** p<0.01, *** p<0.001.

Pair wise comparison of data, grouped on the basis of age classes, homogeneous in size, are shown in Fig. 5.

The average cellular yield did not significantly differ between age classes (Fig. 5a). We found statistically significant differences on proliferation rates at P1 between the age class ≤60 as compared to the ≥75, which was characterized by the lowest proliferation rate (Fig. 5b). Proliferation rates at P2 were higher than at P1, independently from the patient age (Fig. 5c).

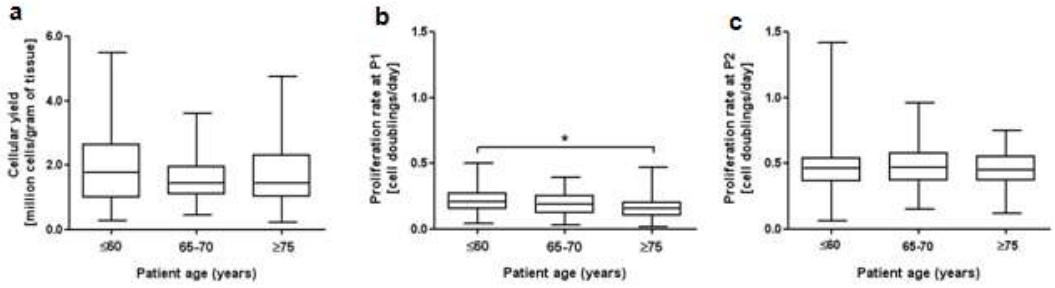

Fig. 5. Box plots showing pair-wise comparisons of grouped data pertaining to patient age and cellular yield classes homogeneous in size. (a) cellular yield vs. patient age, (b) proliferation rate at P1 vs. patient age, (c) proliferation rate at P2 vs. patient age. The values delimiting the box in the box plots are the 25th and 75th percentiles of the data distribution. * $p<0.05$.

No significant correlation was found among ICRS scores, cellular yields and proliferation rates at P1 and P2, as shown in Fig. 6. However, as the cartilage damage level increased, the mean cellular yield slightly decreased, whereas the proliferation rates did not differ with increasing scores. As already observed for data on hip and knee population, proliferation rates at P2 were higher than the rates at P1.

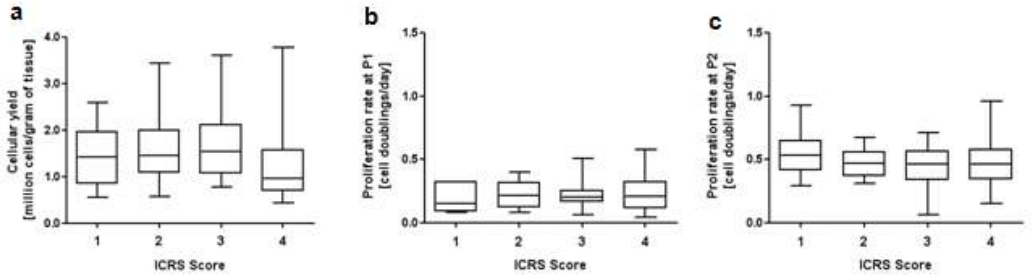

Fig. 6. Box plots (a-c) for the ICRS-scored knee cartilage samples. The values delimiting the box in the box plots are the 25th and 75th percentiles of the data distribution.

Discussion

OA is fully recognized as an age-dependent degenerative disease (15). Considering the high and increasing life expectancy in developed countries, osteoarthritis is assuming an important social effect. Coherently, countermeasures to OA such as cellular therapies are intensely investigated (16). In this study, adult human articular chondrocytes were isolated from anatomical specimens discarded during total joint replacement, with the aim to characterize them in view of their potential use as source for autologous cell therapy. More than two-hundred OA patients were included in this analysis, which required, for our institution, a period of four years for data collection. Accordingly with literature (17-19) we found that the majority of patients subjected to total joint replacement were postmenopausal women. The age of patients in our analysis ranged from 30 to 90 years old, but the frequency distributions showed that the highest amount of patients belonged to the range 65-70 years. The pair-wise analysis of data on cellular yield and proliferation rates showed that the patient age is not statistically correlated to the cellular yield, as in (20), but was negatively correlated with the proliferation rate at P1, which followed a trend analogue to the proliferation rate at P2. As already

reported in the literature (21) for healthy chondrocytes, the most relevant reduction in cellular yield is observed between patients younger than 40 years and older patients, then with increasing age this feature remains almost constant. 75% of our patients are older than 63 years: this could explain the lack of significant influence of patient age on cellular yield. In accordance with previously published data on healthy chondrocytes (22), cell proliferation significantly decreased with increasing age at P1, but this significant correlation was not found between age and doubling rate at P2. A possible explanation can be found in the use of TGFβ1 and FGF2, growth factors able to increase the proliferation rate and to maintain the chondrocyte phenotype during the expansion procedures. This property is particularly useful when large amounts of cells are needed requiring a long-term expansion (14). Thanks to the use of TGFβ1 and FGF-2, chondrocytes started soon to proliferate. The offset difference in cell proliferation rates that we found between P1 and P2 is in accordance with previous work (23,24) and can be attributed to an initial lag phase where cells recover from isolation procedure. Interestingly, however, a relationship between the proliferation rate at P1 and at P2 was found in our data suggesting that cells with the lowest proliferation rate at P1 were also less proliferative at P2 and that the cells with high proliferation rate at P1 maintained this feature at P2.

To correlate analyzed cellular parameters with the grade of cartilage degeneration, we evaluated random samples scored on the basis of ICRS scale. A lower cellular yield was observed in score 4 specimens. This result can be attributed to the higher degeneration level of this tissue whereby the inflammatory state of the tissue can affect cellularity. The proliferation rates for samples with different scores are in accordance with previously reported results (25): score has a slight influence only on the initial phase of in vitro expansion, whereas cell proliferation during the subsequent passages was independent from the degeneration of the excised cartilage.

In conclusion, our study allowed a systematic characterization of basic parameters as cellular yield and proliferation rates of chondrocytes originating from a wide group of OA patients. This characterization could be useful in view of a possible autologous cell therapy approach for osteoarthritis, as it is fundamental to determine the quality of the cell source, known to greatly influence the outcome of engineered tissue.

Acknowledgements

I would like to acknowledge all the co-authors: Laganà M, Arrigoni C, Sansone V, Zagra L, Moretti M, Raimondi MT. Furthermore, I would like to acknowledge Dr. A. Degrate for his support in statistical analysis of data. This study was supported by Italian Ministry of Health.

References

1. Aigner T, Rose J, Martin J, Buckwalter J. Aging theories of primary osteoarthritis: from epidemiology to molecular biology. Rejuvenation Res.7:134-45. 2004.
2. van der Kraan PM, van den Berg WB. Osteoarthritis in the context of ageing and evolution. Loss of chondrocyte differentiation block during ageing. Ageing Res Rev.7:106-13. 2008.
3. Zhang W, Moskowitz RW, Nuki G, Abramson S, Altman RD, Arden N, Bierma-Zeinstra S, Brandt KD, Croft P, Doherty M, Dougados M, Hochberg M, Hunter DJ, Kwoh K, Lohmander LS, Tugwell P. OARSI recommendations for the management of hip and knee osteoarthritis, Part II: OARSI evidence-based, expert consensus guidelines. Osteoarthritis Cartilage.16:137-62. 2008.
4. Roseti L, Bassi A, Grigolo B, Fornasari P. Development of Human Chondrocyte–Based Medicinal Products for Autologous Cell Therapy. In: Pignatello PR, ed. Biomaterials Science and Engineering: InTech; 2011. pp. 456.
5. Tran-Khanh N, Hoemann CD, McKee MD, Henderson JE, Buschmann MD. Aged bovine chondrocytes display a diminished capacity to produce a collagen-rich, mechanically functional cartilage extracellular matrix. J Orthop Res.23:1354-62. 2005.
6. Wang Y, Blasioli DJ, Kim HJ, Kim HS, Kaplan DL. Cartilage tissue engineering with silk scaffolds and human articular chondrocytes. Biomaterials.27:4434-42. 2006.
7. Carossino AM, Recenti R, Carossino R, Piscitelli E, Gozzini A, Martineti V, Mavilia C, Franchi A, Danielli D, Aglietti P, Ciardullo A, Galli G, Tognarini I, Moggi Pignone A, Cagnoni M, Brandi ML. Methodological models for in vitro amplification and maintenance of human articular chondrocytes from elderly patients. Biogerontology.8:483-98. 2007.
8. Cavallo C, Desando G, Facchini A, Grigolo B. Chondrocytes from patients with osteoarthritis express typical extracellular matrix molecules once grown onto a three-dimensional hyaluronan-based scaffold. J Biomed Mater Res A.93:86-95. 2010.
9. Dehne T, Karlsson C, Ringe J, Sittinger M, Lindahl A. Chondrogenic differentiation potential of osteoarthritic chondrocytes and their possible use in matrix-associated autologous chondrocyte transplantation. Arthritis Res Ther.11:R133. 2009.
10. Tallheden T, Bengtsson C, Brantsing C, Sjogren-Jansson E, Carlsson L, Peterson L, Brittberg M, Lindahl A. Proliferation and differentiation potential of chondrocytes from osteoarthritic patients. Arthritis Res Ther.7:R560-8. 2005.
11. Neri S, Mariani E, Cattini L, Facchini A. Long-term in vitro expansion of osteoarthritic human articular chondrocytes do not alter genetic stability: a microsatellite instability analysis. J Cell Physiol.226:2579-85. 2011.
12. Kleemann RU, Krocker D, Cedraro A, Tuischer J, Duda GN. Altered cartilage mechanics and histology in knee osteoarthritis: relation to clinical assessment (ICRS Grade). Osteoarthritis Cartilage.13:958-63. 2005.
13. Jakob M, Demarteau O, Schafer D, Stumm M, Heberer M, Martin I. Enzymatic digestion of adult human articular cartilage yields a small fraction of the total available cells. Connect Tissue Res.44:173-80. 2003.
14. Barbero A, Ploegert S, Heberer M, Martin I. Plasticity of clonal populations of dedifferentiated adult human articular chondrocytes. Arthritis Rheum.48:1315-25. 2003.
15. Loeser RF, Goldring SR, Scanzello CR, Goldring MB. Osteoarthritis: a disease of the joint as an organ. Arthritis Rheum.64:1697-707. 2012.
16. Goldring MB, Goldring SR. Osteoarthritis. J Cell Physiol.213:626-34. 2007.
17. Cicuttini FM, Wluka AE, Wang Y, Stuckey SL, Davis SR. Effect of estrogen replacement therapy on patella cartilage in healthy women. Clin Exp Rheumatol.21:79-82. 2003.
18. Musumeci G, Loreto C, Carnazza ML, Martinez G. Characterization of apoptosis in articular cartilage derived from the knee joints of patients with osteoarthritis. Knee Surg Sports Traumatol Arthrosc.19:307-13. 2011.
19. Wluka AE, Davis SR, Bailey M, Stuckey SL, Cicuttini FM. Users of oestrogen replacement therapy have more knee cartilage than non-users. Ann Rheum Dis.60:332-6. 2001.
20. Bobacz K, Erlacher L, Smolen J, Soleiman A, Graninger WB. Chondrocyte number and proteoglycan synthesis in the aging and osteoarthritic human articular cartilage. Ann Rheum Dis.63:1618-22. 2004.
21. Barbero A, Grogan S, Schafer D, Heberer M, Mainil-Varlet P, Martin I. Age related changes in human articular chondrocyte yield, proliferation and post-expansion chondrogenic capacity. Osteoarthritis Cartilage.12:476-84. 2004.
22. Dozin B, Malpeli M, Camardella L, Cancedda R, Pietrangelo A. Response of young, aged and osteoarthritic human articular chondrocytes to inflammatory cytokines: molecular and cellular aspects. Matrix Biol.21:449-59. 2002.
23. Barlic A, Drobnic M, Malicev E, Kregar-Velikonja N. Quantitative analysis of gene expression in human articular chondrocytes assigned for autologous implantation. J Orthop Res.26:847-53. 2008.
24. Lin Z, Willers C, Xu J, Zheng MH. The chondrocyte: biology and clinical application. Tissue Eng.12:1971-84. 2006.
25. Yin J, Yang Z, Cao YP, Ge ZG. Characterization of human primary chondrocytes of osteoarthritic cartilage at varying severity. Chin Med J (Engl).124:4245-53. 2011.

Chapter 4

Donor-matched mesenchymal stem cells from knee infrapatellar and subcutaneous adipose tissue of osteoarthritic donors display differential chondrogenic and osteogenic commitment

Abstract

Cell-based therapies have been recently proposed for the treatment of degenerative articular pathologies, such as early osteoarthritis, with an emphasis on autologous mesenchymal stem cells (MSCs), as an alternative to terminally differentiated cells. In this study we performed a donor-matched comparison between infrapatellar fat pad MSCs (IFP-MSCs) and knee subcutaneous adipose tissue stem cells (ASCs), as appealing candidates for cell-based therapies that are easily accessible during surgery.

IFP-MSCs and ASCs were obtained from 25 osteoarthritic patients undergoing total knee replacement and compared for their immunophenotype and differentiative potential.

Undifferentiated IFP-MSCs and ASCs displayed the same immunophenotype, typical of MSCs ($CD13^+/CD29^+/CD44^+/CD73^+/CD90^+/CD105^+/CD166^+/CD31^-/CD45^-$). IFP-MSCs and ASCs showed similar adipogenic potential, though undifferentiated ASCs had higher *LEP* expression compared to IFP-MSCs ($p<0.01$). Higher levels of calcified matrix ($p<0.05$) and alkaline phosphatase ($p<0.05$) in ASCs highlighted their superior osteogenic commitment compared to IFP-MSCs. Conversely, IFP-MSCs pellets showed greater amounts of glycosaminoglycans ($p<0.01$) and superior expression of *ACAN* ($p<0.001$), *SOX9*, *COMP* ($p<0.001$) and *COL2A1* ($p<0.05$) compared to ASCs pellets, revealing a superior chondrogenic potential. This was also supported by lower *COL10A1* ($p<0.05$) and *COL1A1* ($p<0.01$) expression and lower alkaline phosphatase release ($p<0.05$) by IFP-MSCs compared to ASCs.

The observed dissimilarities between IFP-MSCs and ASCs show that, despite expressing similar surface markers, MSCs deriving from different fat depots in the same surgical site possess specific features. Furthermore, the *in vitro* peculiar commitment of IFP-MSCs and ASCs from osteoarthritic donors towards the chondrogenic or osteogenic lineage may suggest a preferential use for cartilage and bone cell-based treatments, respectively.

Introduction

The low self-repair ability of articular cartilage and the lack of treatments that can reproducibly restore defects at the bone-cartilage interface provide a major reason for the development of cell-based therapies for bone and cartilage repair (1-3). Joint replacement, considered a successful and standard procedure in the treatment of elder patients affected by osteoarthritis (OA), is controversial in patients, considered too young or active for conventional arthroplasty, who experience higher implant failure rates and earlier revisions (4,5). Thus, cell-based therapies have been recently proposed also for the treatment of middle-aged early OA patients to alter the progression of degenerative disease, with the hope of obviating or at least delaying the need for joint replacement (6).

Mesenchymal stem cells (MSCs) have been investigated as an alternative to terminally differentiated cells to develop novel treatments for bone and cartilage defects, since they can be easily harvested from several adult tissues and are able to differentiate towards the osteogenic and chondrogenic lineages (7,8). Beside bone marrow MSCs (BMSCs), more recently adipose derived mesenchymal stem cells have been successfully used for bone and cartilage applications (9-13). In particular, MSCs resident in the infrapatellar fat pad (IFP-MSCs) and knee subcutaneous adipose tissue (ASCs) can be considered alternative appealing cell sources for articular cell-based therapies, thanks to their differentiative potential and ease of harvesting during knee surgery, which causes minimal additional morbidity to patients. Furthermore, the fast protocol employed in their isolation is advantageous in view of a future one-step surgical cell-based treatment.

Beneficial effects have been observed treating animals with induced OA with MSCs derived from different adipose depots, with cells playing a key role in the inhibition of OA progression and in the restoration of damaged cartilage (14-17). Moreover, it has been demonstrated that intra-articular injection of IFP-MSCs leads to relief in pain symptoms and to improvement of knee functions in patients suffering from knee OA (18).

Several studies have characterized the multi-lineage potential and immunophenotype of IFP-MSCs (19-24), but, to our knowledge, only few studies have reported a preliminary comparison of mesenchymal stem cells from infrapatellar fat pad and knee subcutaneous adipose tissue (25-27). Nevertheless, in these few comparative studies, the evaluation of osteogenic and chondrogenic potential has been performed mainly by qualitative histological stainings, without investigating gene expression profiles (25,26), and the comparison was restricted to very few donors (27), limiting the clinical relevance of the findings.

In the present study, to evaluate the different and specific relevance of IFP-MSCs and ASCs for orthopaedic cell-based therapies, we compared the features and the multi-differentiative potential of cells derived from 25 OA patients undergoing total knee replacement. To eliminate the common issue of

inter-donor variability, we performed a donor-matched evaluation, harvesting and comparing both IFP-MSCs and ASCs from the same patient and focusing on their osteogenic and chondrogenic potential through multiple, quantitative analyses, and evaluating also the expression of hypertrophic and fibrocatilagineous markers in chondrogenic differentiated cells.

Materials and Methods

Cell isolation and expansion

Infrapatellar fat pad and subcutaneous adipose tissue were harvested from the knee of 25 patients affected by OA (mean age 70±8 years, range 54-85 years) during total knee replacement, with patients' informed consent and with the approval of the Institutional Review Board.

Inclusion criteria were: male and female gender, age between 50 and 85 years, grade III and IV knee osteoarthritis according to Kellgren-Lawrence grading scale, indication for total knee replacement. Exclusion criteria were: rheumatoid arthritis, autoimmune diseases, systemic diseases, tumors, previous implant at the same knee and medical contraindication to elective surgery.

IFP-MSCs were isolated from infrapatellar fat pad (28). Briefly, adipose tissue was carefully separated from the synovium and were minced in small pieces. The sample was then enzymatically digested (37°C, 30 min) by 0.075% type I collagenase (Worthington Biochemical Co, Lakewood, New Jersey, USA). After digestion, the sample was centrifuged (1200 g, 10 min) and filtered through a cell strainer (100 µm pores) to remove undigested tissue. Cells were counted by Trypan blue exclusion and plated in control medium consisting of high glucose DMEM (HG-DMEM, Life Technologies, Carlsbad, California, USA) supplemented with 10% fetal bovine serum (FBS, Lonza, Basel, Switzerland), 0.029 mg/ml L-glutamine, 100 U/ml penicillin, 100 µg/ml streptomycin, 10 mM hepes, 1 mM sodium pyruvate (all from Life Technologies) at approximately 10^4 cells/cm^2 (37°C, 5% CO_2). The same protocol was used to isolate ASCs from knee subcutaneous adipose tissue. Non-adherent cells were removed with the first medium refresh. During culture, medium was changed twice a week. When IFP-MSCs and ASCs were about 90% confluent, they were detached using 0.05% trypsin/0.053 mM EDTA (Life Technologies) and plated at $3x10^3$ cells/cm^2 for the following passages.

Clonogenic ability assay

A colony-forming unit–fibroblast (CFU-F) assay was performed to assess the clonogenic ability of IFP-MSCs and ASCs (29). Cells were plated at different low densities (ranging from 48 cells/cm^2 to 1 cells/cm^2) and cultured in control medium with 20% FBS. After 10 days, cells were fixed with 10% neutral buffered formalin and stained with Gram's crystal violet (Sigma-Aldrich, St. Louis, Missouri, USA).

CFU-F frequency was established by scoring the individual colonies and expressing them as a percentage relative to the number of seeded cells.

Flow cytometry for the assessment of typical MSCs surface markers

At passage 4 (45-50 days of expansion) surface marker expression was evaluated by flow cytometry. IFP-MSCs and ASCs were detached using 0.05% trypsin/0.53 mM EDTA and washed twice in cold FACS Buffer (PBS w/o Ca^{2+}/Mg^{2+}containing 2% FBS and 0.1% NaN_3). For each sample, $2.5x10^5$ cells were incubated for 30 min with the following anti-human primary monoclonal antibodies: CD13-FITC, CD29-biotinylated, CD31-FITC, CD34-biotinylated, CD44-FITC, CD45-FITC, CD105-biotinylated, CD106-FITC, CD166-FITC (all from Ancell Corporation, Bayport, Minnesota, USA), CD90-FITC and CD73-PE (from Miltenyi Biotec, Bergisch Gladbach, Germany), and CD151 (R&D Systems Inc, Minneapolis, Minnesota, USA). After incubation, cells were washed with FACS buffer to remove the excess of primary antibody. Cells stained with biotinylated antibodies were incubated for 20 min with streptavidin-PE (Ancell Corporation), whereas samples stained with anti-CD151 primary antibody were incubated with a FITC-conjugated goat anti-mouse secondary antibody (Ancell Corporation). After incubation, cells were washed with FACS Buffer and suspended in 500 µl of FACS buffer for analysis. Background fluorescence was established by negative controls and data were acquired using a FACSCalibur flow cytometer (BD Biosciences, Franklin Lakes, New Jersey, USA) collecting a minimum of 10.000 events. Analysis was performed using CellQuest software (BD Biosciences).

Adipogenic differentiation

IFP-MSCs and ASCs at passage 4 were plated at $3x10^3$ cells/cm^2 and differentiated for 14 days in adipogenic medium using a repeated pulsed induction (30) with 3 days of induction in control medium supplemented with 1 µM dexamethasone, 10 µg/ml insulin, 500 µM 3-isobutyl-1-methylxanthine and 200 µM indomethacin (all from Sigma-Aldrich), followed by 3 days of maintenance in control medium supplemented with 10 µg/ml insulin.

The production of lipid vacuoles was quantified by Oil Red O staining. Cells were fixed in 10% neutral buffered formalin for 10 min, washed with 60% isopropanol, and stained with 8.5 mM Oil Red O (Sigma-Aldrich) for 15 min. After rinsing with ddH_2O, Oil Red O was unstained with 100% isopropanol and absorbance was read at 490 nm (Perkin Elmer Victor X3 microplate reader).

Osteogenic differentiation

IFP-MSCs and ASCs at passage 4 were plated at $3x10^3$ cells/cm^2 and differentiated for 14 or 21 days in osteogenic medium (30) consisting of control medium supplemented with 10 mM glicerol-2-phosphate,

10 nM dexamethasone, 150 µM L-ascorbic acid-2-phosphate and 10 nm cholecalciferol (all from Sigma-Aldrich).

Calcified matrix deposition was measured using Alizarin Red-S staining. Cells were rinsed with PBS, fixed with ice-cold 70% ethanol for 1 h and stained with 40 mM Alizarin Red-S (pH 4.1, Sigma-Aldrich) for 15 min. After washing with ddH_2O, samples were unstained for 30 min with 10% cetylpyridinium chloride monohydrate (CPC, Sigma-Aldrich) in 0.1 M phosphate buffer (pH 7.0). Absorbance was read at 570 nm (Perkin Elmer Victor X3 microplate reader).

Alkaline phosphatase activity (ALP) was quantified by enzymatic assay (31). Cells were rinsed with PBS and lysed in 0.1% Triton X-100 (Sigma-Aldrich). ALP was quantified by incubating cellular lysates at 37°C with 1 mM p-nitrophenylphosphate (Sigma-Aldrich) in alkaline buffer (100 mM diethanolamine and 0.5 mM $MgCl_2$, pH 10.5). The enzymatic reaction was stopped with 1 N NaOH and absorbance was read at 410 nm (Perkin Elmer Victor X3 microplate reader). ALP activity was normalized on total protein content, determined by BCA Protein Assay Kit (Pierce Biotechnology, Rockford, Illinois, USA), and expressed as ALP Units per mg of proteins.

Chondrogenic differentiation

Chondrogenic differentiation was performed by pellet culture. At passage 4, $4x10^5$ IFP-MSCs and ASCs were centrifuged (250 g, 5 min) to obtain cell pellets. Pellets were cultured for 14 days in chondrogenic medium (32) consisting of HG-DMEM supplemented with 0.029 mg/ml L-glutamine, 100 U/ml penicillin, 100 µg/ml streptomycin, 10 mM hepes, 1 mM sodium pyruvate, 1.25 mg/ml human serum albumin (all from Sigma-Aldrich), 1% ITS+1 (1.0 mg/ml insulin from bovine pancreas, 0.55 mg/ml human transferrin, 0.5 µg/ml sodium selenite, 50 mg/ml bovine serum albumin and 470 µg/ml linoleic acid, Sigma-Aldrich), 0.1 µM dexamethasone, 0.1 mM L-ascorbic acid-2-phosphate and 10 ng/ml TGF-β1 (Peprotech, Rocky Hill, New Jersey, USA).

For histological analysis, pellets were fixed for 24 h in 10% neutral buffered formalin, embedded in paraffin and sectioned at 4 µm. Sections were stained with haematoxylin-eosin (Sigma-Aldrich) and alcian blue (pH 2.5, Sigma-Aldrich) to evaluate extracellular matrix and glycosaminoglycans (GAGs) deposition.

For GAGs quantification, pellets were digested (16 h, 60°C) in 500 µl of PBE buffer (100 mM Na_2HPO_4, 10 mM NaEDTA, pH 6.8) containing 1.75 mg/ml L-cystein (Sigma-Aldrich) and 14.2 U/ml papain (Worthington). Samples were incubated with 16 mg/l dimethylmethylene blue (Sigma-Aldrich) and absorbance was read at 500 nm (Perkin Elmer Victor X3 microplate reader). The same samples were used for DNA quantification by CyQUANT Kit (Life Technologies).

Soluble ALP activity released in culture supernatants was measured by enzymatic assay. At the moment

of medium refresh, culture supernatant was collected from each pellet and 50 µl of medium were incubated with 1 mM p-nitrophenylphosphate. The release of ALP was determined at early phase (day 0 to day 3) and late phase (day 11 to day 14) of chondrogenic differentiation.

Gene expression analysis

After 14 days of adipogenic, osteogenic or chondrogenic differentiation, gene expression was evaluated by real time PCR (Rotor Gene RG3000 system, Qiagen). Total RNA was purified from cell lysates using the RNeasy Mini kit (Qiagen, Venlo, Netherlands) and reverse-transcribed to cDNA (5 min at 25°C, 30 minutes at 42°C and 5 min at 85°C) using iScript cDNA Synthesis Kit (Bio-Rad Laboratories, Hercules, California, USA). 20 ng of cDNA were incubated with a PCR mix (2 min at 50°C, 10 min at 95°C, followed by 40 cycles of 15 sec at 95°C and 1 min at 60°C) including TaqMan Universal PCR Master Mix and TaqMan® Assays-on-Demand™ Gene Expression probes (Life Technologies) using the following assays: glyceraldehyde-3-phosphate dehydrogenase (*GAPDH*, Hs99999905_m1), peroxisome proliferator-activated receptor gamma (*PPARG*, Hs01115513_m1), leptin (*LEP*, Hs00174877_m1), runt-related transcription factor 2 (*RUNX2*, Hs00231692_m1), collagen type I alpha 1(*COL1A1*, Hs01076777_m1), aggrecan (*ACAN*, Hs00153936_m1), SRY (Sex determining region Y)-box9 (*SOX9*, Hs00165814_m1), cartilage oligomeric matrix protein (*COMP*, Hs00164359_m1), collagen type II alpha I (*COL2A1*, Hs01060345_m1), collagen type X alpha 1 (COL10A1, Hs00166657_m1). The fold change in the expression of the different genes was normalized on the housekeeping *GAPDH*.

Statistical analysis

Data are expressed as mean±SEM. Normal distribution of values was assessed by Kolmogorov-Smirnov normality test. Statistical analysis was performed using Student's t-test and Wilcoxon test for paired data since IFP-MSCs and ASCs were obtained from the same donors; Student's t-test was used for data with a Gaussian distribution and Wilcoxon test for data with a non-Gaussian distribution. (GraphPad Prism v5.00, GraphPad Software). Level of significance was set at $p<0.05$ (* $p<0.05$, ** $p<0.01$, *** $p<0.001$). The number of data used for the statistical analyses, indicated in figure legends as "n", corresponds to independent experiments performed with IFP-MSCs and ASCs isolated from "n" individual donors, according to Ranstam (33).

Results

Undifferentiated IFP-MSCs and ASCs share common features and express a similar set of cell surface markers

IFP-MSCs and ASCs displayed a fibroblastoid shape, which was maintained throughout the entire culture period, without any difference between the two cell types (Fig. 1A). From passage 1 to 4, both cell populations displayed a high clonogenic ability (Fig. 1B,C), with a significantly higher clonogenic ability observed in IFP-MSCs compared to ASCs at passage 1 ($p<0.05$).

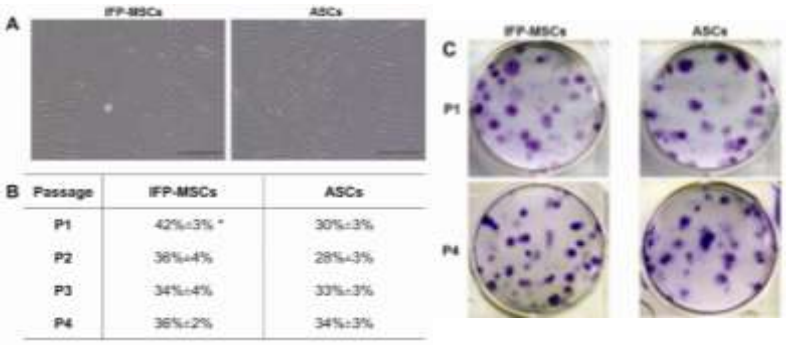

Passage	IFP-MSCs	ASCs
P1	42%±3% *	30%±3%
P2	36%±4%	28%±3%
P3	34%±4%	33%±3%
P4	36%±2%	34%±3%

Fig. 1. Morphology and clonogenic potential of IFP-MSCs and ASCs. (A) Cells in culture at passage 4 (scale bars 200 µm). (B) Percentage of clonogenic cells from passage 1 to passage 4 (scored colonies were normalized on number of seeded cells, n=7, $p<0.05$) (C) Representative pictures of stained CFU-F at P1 and P4.

As reported in Fig. 2A, both IFP-MSCs and ASCs analyzed at passage 4 showed a similar immunophenotype, being positive for CD13, CD29, CD44, CD73, CD90, CD105, CD166 and negative for CD31 and CD45. For all the tested markers no difference was observed between IFP-MSCs and ASCs (Fig. 2B). A variable expression of CD34 and CD106 was found for IFP-MSCs and ASCs depending on the donor (10-35% of positive cells). Both cell types expressed CD29, CD90, CD105, CD151 and CD166 (35-90% of positive cells). A very consistent expression of CD13, CD44 and CD73 was measured on IFP-MSCs and ASCs (90-100% of positive cells).

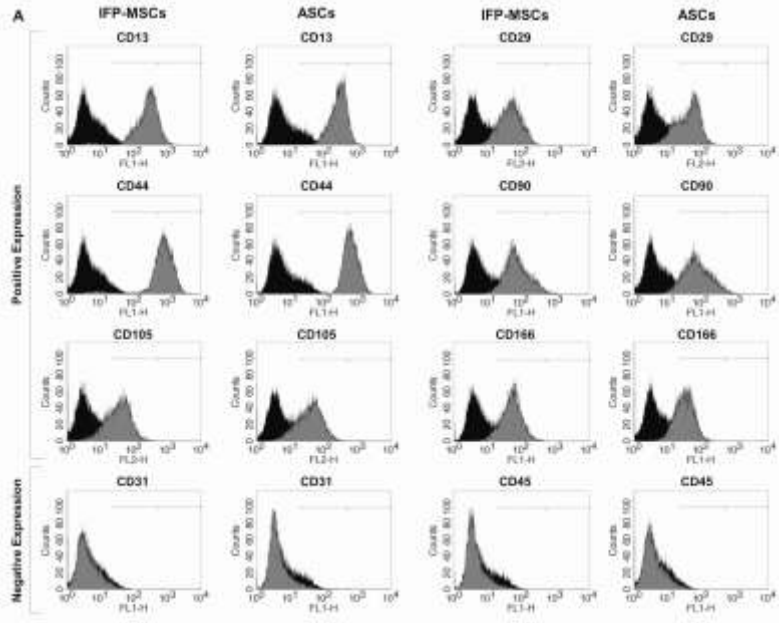

Surface Markers	IFP-MSCs		ASCs	
CD13	98.8%±0.2%	+++	96.2%±2.1%	+++
CD29	85.5%±3.1%	++	78.5%±11.9%	++
CD31	5.3%±1.1%	-	9.4%±2.4%	-
CD34	24.5%±9.2%	+/-	19.8%±3.6%	+/-
CD44	99.2%±0.5%	+++	98.4%±1.2%	+++
CD45	4.9%±1.2%	-	8.6%±2.2%	-

Surface Markers	IFP-MSCs		ASCs	
CD73	98.2%±1.2%	+++	91.2%±6.7%	+++
CD90	88.6%±4.6%	++	90.2%±3.8%	++
CD105	71.1%±11.4%	++	60.1%±8.7%	++
CD106	18.3%±8.0%	+/-	10.2%±2.5%	+/-
CD151	50.4%±6.9%	+	45.3%±7.9%	+
CD166	65.3%±3.1%	++	61.4%±14.3%	++

Fig. 2. Cell surface markers expression. (A) Expression of the typical MSCs surface markers pattern in IFP-MSCs and ASCs from the same donor at passage 4 (markers represented as grey histograms and isotype control antibodies represented as black histograms). (B) Percentage of positive cells for the whole panel of surface markers tested (n=6). Ranking was established as: - for 0-10%, +/- for 10-35%, + for 35-50%, ++ for 50-90%, and +++ for 90-100% positive cells.

Adipogenic differentiation of IFP-MSCs and ASCs induces a similar upregulation of adipogenic markers except for leptin gene expression

IFP-MSCs and ASCs cultured for 14 days in adipogenic medium showed the progressive loss of the fibroblastoid-like shape and the production of cytoplasmatic lipid vacuoles, as evidenced by Oil Red O staining (Fig. 3A, B). The dye extraction revealed a significant increase in lipid vacuoles content in differentiated cells in comparison with cells in control medium ($p<0.001$ for IFP-MSCs and $p<0.05$ for ASCs) (Fig. 3C). Gene expression analysis confirmed the ability of both cell types to respond to adipogenic induction. Indeed, a significant increase of *PPARG* expression was observed in IFP-MSCs ($p<0.05$) and ASCs ($p<0.01$) cultured in adipogenic medium in comparison with undifferentiated cells (Figure 3D). Differentiated IFP-MSCs and ASCs showed also a significant up-regulation of *LEP* expression, ($p<0.05$ and $p<0.01$, respectively) compared with undifferentiated cells. Finally, a significantly higher expression of *LEP* was observed in differentiated ASCs in comparison with differentiated IFP-MSCs (+295%, $p<0.01$).

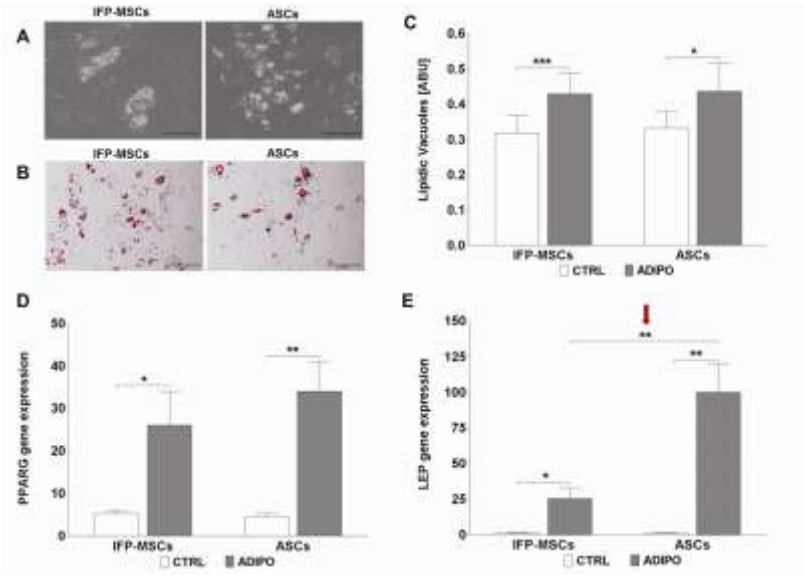

Fig. 3. Adipogenic differentiation. (A-B) Micrographs of IFP-MSCs and ASCs differentiated towards the adipogenic lineage during culture and after Oil Red O staining (scale bars 200 µm). (C) Quantification of lipid vacuoles in undifferentiated (CTRL) and adipogenic-differentiated (ADIPO) cells (n=13). (D-E) Gene expression of *PPARG* and *LEP* normalized to *GAPDH* (n=7). Red arrow indicates a significant difference between IFP-MSCs and ASCs.

ASCs respond more efficiently to osteogenic induction in respect to IFP-MSCs

Both IFP-MSCs and ASCs were able to differentiate towards the osteogenic lineage when cultured in osteo-inductive medium, as demonstrated by the upregulation of specific markers such as calcified matrix, ALP activity, and transcriptional expression of RUNX2 and COL1A1 (Fig. 4). Our results demonstrated that ASCs were more committed towards the osteogenic lineage in respect with IFP-MSCs. Indeed, after 14 days of culture in osteogenic medium the deposition of calcified matrix was more consistent in differentiated ASCs (Fig. 4A) and the quantification of calcified matrix revealed a significant difference between the two cell populations (+75% in ASCs, $p<0.05$, Fig. 4B). Furthermore, after 14 days of differentiation, ASCs produced significantly higher levels of ALP in comparison with IFP-MSCs (+66%, $p<0.05$, Fig. 4C). Comparing 14 and 21 days, we observed a significant increase of calcified matrix

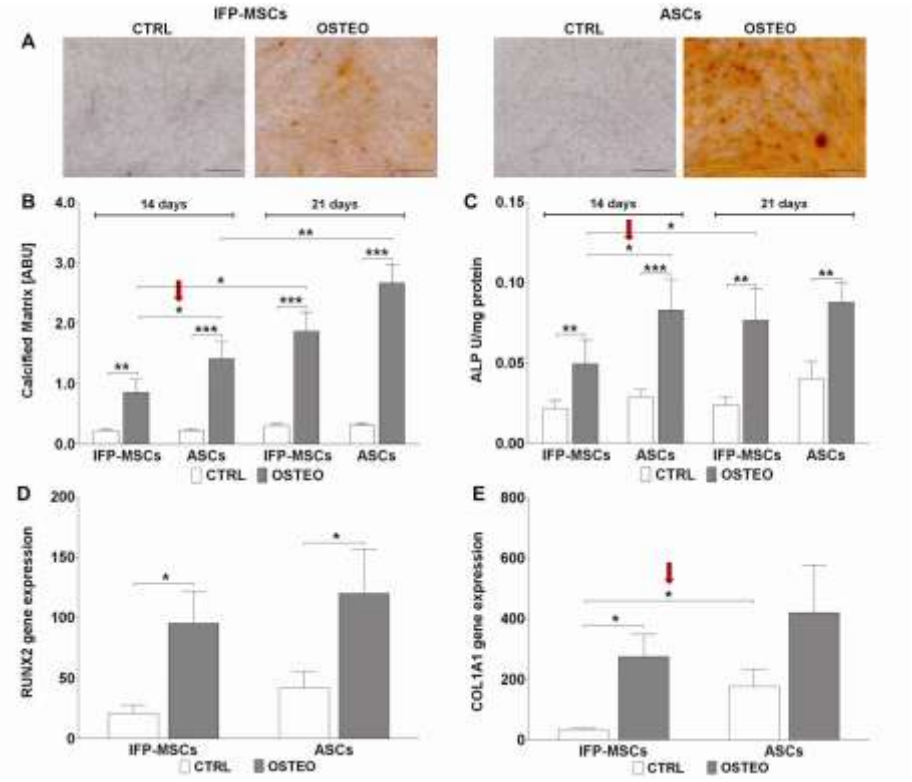

Fig. 4. Osteogenic differentiation. (A) Micrographs of IFP-MSCs and ASCs differentiated for 14 days and stained by AR-S (scale bars 500 µm). (B) Quantification of calcified matrix by AR-S staining and extraction in undifferentiated (CTRL) and osteogenic-differentiated (OSTEO) IFP-MSCs and ASCs (n=14). (C) ALP activity determined by enzymatic assay and normalized by protein content (n=9). (D-E) Gene expression of *RUNX2* and *COL1A1* normalized to *GAPDH* (n=7). Red arrows indicate significant differences between IFP-MSCs and ASCs.

deposition in IFP-MSCs ($p<0.05$) and ASCs ($p<0.01$) over time. ALP levels were increased from 14 to 21 days in differentiated IFP-MSCs ($p<0.05$), whereas this marker remained stable in ASCs. After 21 days of induction, we did not observe any significant difference between IFP-MSCs and ASCs in terms of calcified matrix deposition and ALP activity.

Higher expression of *RUNX2* and *COL1A1* was observed both in undifferentiated and differentiated ASCs in comparison to their IFP-MSCs counterparts (Fig. 4D, E), with a significant difference in the expression of *COL1A1* in undifferentiated cells (+53% in ASCs, $p<0.05$, Fig. 4E).

IFP-MSCs are more committed towards the chondrogenic lineage and express lower levels of hypertrophic and fibrocartilagineous markers as compared to ASCs

After 14 days of chondrogenic induction in pellet culture conditions, no significant difference was observed in terms of DNA content, related to cell proliferation, between IFP-MSCs and ASCs pellets, even if slightly higher values were measured in IFP-MSCs pellets (Fig. 5A).

A significantly higher amount of GAGs was observed in IFP-MSCs pellets as demonstrated both from histological analysis (Fig. 5B) and biochemical quantification of GAGs (+16%, $p<0.01$, Fig. 5C). In particular, histological sections revealed that IFP-MSCs produced a consistent amount of extracellular matrix which was positively stained by alcian blue, confirming the presence of GAGs. On the contrary, alcian blue staining was almost absent in ASCs pellets (Fig. 5B).

Accordingly with data obtained by histological and biochemical analyses, significantly higher levels of

ACAN gene expression were observed in IFP-MSCs pellets compared to ASCs pellets (+474%, p<0.001, Fig. 5D). Moreover, all the tested chondrogenic markers showed higher expression in IFP-MSCs, with significant differences for *COMP* (+127%, p<0.001) and *COL2A1* (+728%, p<0.05) in comparison with ASCs. The superior chondrogenic potential of IFP-MSCs compared to ASCs was confirmed also by data on hypertrophic and fibrocartilagineous markers (Fig. 5H, I): indeed, expression of *COL10A1* and *COL1A1* was significantly higher in ASCs in respect to IFP-MSCs (+132%, p<0.05 for *COL10A1*; +75%, p<0.01 for *COL1A1*).

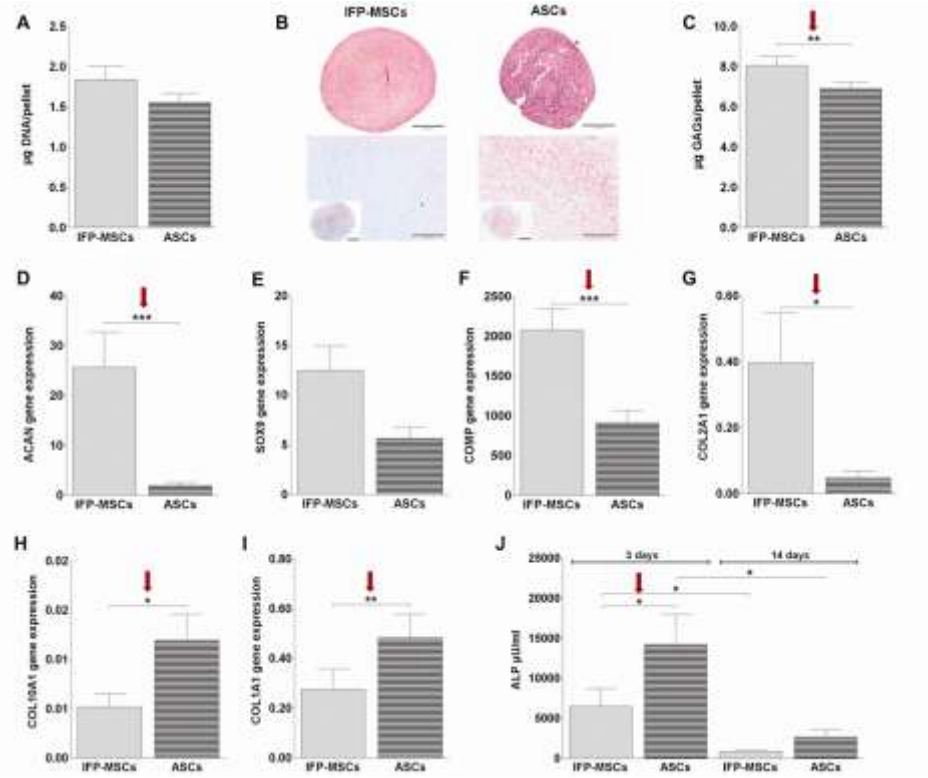

Fig. 5. Chondrogenic differentiation. (A) DNA content in IFP-MSCs and ASCs pellets (n=15). (B) Haematoxilin-eosin and alcian blue staining of representative pellet sections (C) Quantification of total GAGs in pellets (n=15). (D-I) Gene expression of *ACAN, SOX9, COMP, COL2A1, COL10A1* and *COL1A1* normalized to *GAPDH* (n=10). (J) Soluble ALP activity released in culture supernatants from day 0 to day 3 (indicated as 3 days) and from day 11 to day 14 (indicated as 14 days) (n=8). Red arrows indicate significant differences between IFP-MSCs and ASCs.

Furthermore, in the early phase of chondrogenic differentiation (day 0 to day 3) ALP released from ASCs pellets was significantly higher in comparison with IFP-MSCs pellets (+119%, p<0.05, Fig. 5J).

Discussion

The main finding of our study was the significantly different commitment of IFP-MSCs and ASCs in terms of differentiation ability; in particular, undifferentiated ASCs showed higher osteogenic potential in comparison with IFP-MSCs, whereas IFP-MSCs were characterized by a superior chondrogenic ability. In our study both cell populations were isolated from the same knee of each patient, thus eliminating the bias of inter-donor variability and allowing a strict comparison of cell features, giving more consistent results. Furthermore, all cells were derived from OA donors undergoing total knee replacement, to allow a more reliable prediction of the cell behavior in view of a future clinical application in early OA patients. Indeed, in the quest to identify cells able to regenerate bone and cartilage damages and to develop new

treatments for early OA patients, a major issue is to establish the ideal anatomical sites for autologous MSCs isolation. Both the fat depots investigated in this study are easily accessible during orthopaedic surgery and their harvesting causes a minimal discomfort and donor site morbidity, thus being ideal sources for the isolation of MSCs.

Undifferentiated IFP-MSCs and ASCs displayed similar features in terms of cell morphology, typically fibroblastoid. Both populations presented a high clonogenic ability, with percentage of clonogenic cells ranging between 30 and 40%, with IFP-MSCs forming a higher number of colonies compared to ASCs at passage 1, in accordance with previously published data (25).

After *in vitro* expansion, the immunophenotype was coherent with the one reported in previous studies for IFP-MSCs and ASCs (20,26,27,34,35) and, in accordance with literature, no difference was observed between the two populations (26,27).

Regarding the multilineage potential, both IFP-MSCs and ASCs were able to respond to the adipogenic stimuli, showing a similar induction of the characteristic adipogenic markers, but a significantly higher expression of *LEP* was observed in undifferentiated ASCs in comparison with undifferentiated IFP-MSCs. Leptin is an inflammatory mediator which is mainly produced and secreted by adipocytes (36,37). This adipokine stimulates IL-1β production, increases the effect of pro-inflammatory cytokines and induces the expression of matrix metalloproteinases which participate to cartilage matrix degradation in OA cartilage (38,39). The significantly superior basal expression of *LEP* in ASCs in respect to IFP-MSCs is coherent published data , reporting a significantly higher production and secretion of this adipokine in the subcutaneous adipose tissue of OA patients compared to their infrapatellar fat pad (40). However, the same study also reported a superior secretion of IL-6 and its soluble receptor in infrapatellar fat pad compared to subcutaneous adipose tissue. The inflammatory profile of MSCs derived from both adipose depots would hence need further investigations to better define how these cell populations could react to the inflammatory state of OA joints, in view of their possible application in a future cell-based therapy.

Several studies have demonstrated the osteogenic and chondrogenic potential of IFP-MSCs (19-22,24) and ASCs (41-43), but without comparing these cell populations.

In our study, the direct donor-matched comparison between IFP-MSCs and ASCs through quantitative analyses allowed to observe important differences in their osteogenic and chondrogenic commitment. Significantly higher levels of ALP and calcified matrix deposition in osteo-induced ASCs compared to IFP-MSCs, together with the superior expression of *COL1A1* in undifferentiated ASCs, demonstrated that ASCs are more committed towards the osteogenic lineage with respect to IFP-MSCs. These results differ from those described in previous studies whereby, on the basis of qualitative stainings, it has been reported that IFP-MSCs possess a similar (25) or higher (27) osteogenic potential compared to ASCs. We

believe that quantitative analyses and the inclusion of a more appropriate number of donors can determine a higher sensitivity compared to qualitative staining, that could have led us to such contrasting results compared to the current reported literature. Finally, differently from Mochizuki *et al.* (27) that used as tissue source a mixture of synovium and adipose subsynovium, we carefully selected only the adipose fraction of infrapatellar fat pad prior to cell isolation to evaluate solely the differentiation potential of IFP-MSCs, which could also partially explain the different results obtained in our study.

On the other hand, a more pronounced chondrogenic commitment was found in IFP-MSCs compared to ASCs, as revealed by the significantly higher transcriptional expression of chondrogenic markers such as *ACAN*, *COL2A1* and *COMP* in IFP-MSCs pellets. This result is in accordance with previously published results (26) where the histological evaluation of pellets revealed that ASCs were characterized by lower chondrogenic ability compared to IFP-MSCs that displayed a chondrogenic phenotype more similar to the one of BMSCs. A superior chondrogenic potential in IFP-MSCs was observed also described by Mochizuki *et al.* (27) who, however, analyzed expression of chondrogenic genes in pellets obtained from IFP-MSCs and ASCs from a single young non-OA donor. Our data, comprising GAGs quantification and gene expression analysis of cells derived from a larger number of old OA donors, support these literature data, providing an effective demonstration of the superior chondrogenic commitment of IFP-MSCs compared to ASCs, even when cells are obtained from osteoarthritic donors.

Furthermore, we investigated the expression of collagen X and alkaline phosphatase which are usually associated with the premature development of an hypertrophic phenotype during MSCs chondrogenesis (44-47). We found that, in the early phase of chondrogenic differentiation, release of ALP was significantly higher in ASCs pellets and that, after 14 days of chondrogenic differentiation, levels of *COL10A1* and *COL1A1* were significantly lower in IFP-MSCs compared to ASCs.

The dissimilarities found between IFP-MSCs and ASCs may depend on the different anatomical localization of infrapatellar fat pad and knee subcutaneous adipose tissue, considering that infrapatellar fat pad is in direct contact with synovial membrane and that the local tissue microenvironment could affect the commitment of MSCs. Differences in the expression of hypertrophic and fibrocartilagineous markers suggest that IFP-MSCs could be more suitable for cartilage applications aiming at the generation of specific cartilage-like matrix. However, further investigations after a longer period of chondrogenic differentiation are required to confirm the different trend between IFP-MSCs and ASCs in developing a hypertrophic phenotype.

Despite similar surface markers expression in the undifferentiated state, different populations of MSCs can display significantly different commitment towards specific cell lineages. This supports the importance of introducing more specific and predictive markers to identify which population of MSCs

could be more suitable for a specific clinical application. as proposed by recent studies that have investigated the differentiation potential of specific subsets of MSCs (48-50).

It should be highlighted that the differential commitment of IFP-MSCs and ASCs emerged from *in vitro* experiments and should be further confirmed through *in vivo* studies to better validate the clinical relevance of our data. However, our results contribute to show how quantitative analyses on larger donor populations are fundamental for a more reliable characterization of primary human cells, contributing to build a more consistent base for cell-based therapies.

Conclusions

To the best of our knowledge, this is the first study to compare donor-matched IFPs and ASCs from such a large number of OA donors, characterizing their osteogenic and chondrogenic potential through several quantitative analyses. This provided novel and interesting insights on their specific differentiation capabilities, opening to a more rational selection as preferential sources for regenerating cartilage and bone tissues or developing osteochondral treatments, aimed at future clinical cell-based treatments, also in OA patients.

Acknowledgements

I would like to thank all the co-authors: Colombini A., Stanco D., de Girolamo L., Sansone V., Moretti M. Furthermore, I would like to thank Turner L.J. and Bonora C. for their contribution in experiments and in harvesting of human biopsies. This study was financially supported by the Italian Ministry of Health.

References

1. Mohal JS, Tailor HD, Khan WS. Sources of adult mesenchymal stem cells and their applicability for musculoskeletal applications. Curr Stem Cell Res Ther.7:103-9. 2012.
2. Beane OS, Darling EM. Isolation, characterization, and differentiation of stem cells for cartilage regeneration. Ann Biomed Eng.40:2079-97. 2012.
3. Szpalski C, Barbaro M, Sagebin F, Warren SM. Bone tissue engineering: current strategies and techniques--part II: Cell types. Tissue Eng Part B Rev.18:258-69. 2012.
4. Julin J, Jamsen E, Puolakka T, Konttinen YT, Moilanen T. Younger age increases the risk of early prosthesis failure following primary total knee replacement for osteoarthritis. A follow-up study of 32,019 total knee replacements in the Finnish Arthroplasty Register. Acta Orthop.81:413-9. 2010.
5. Harrysson OL, Robertsson O, Nayfeh JF. Higher cumulative revision rate of knee arthroplasties in younger patients with osteoarthritis. Clin Orthop Relat Res.162-8. 2004.
6. Gomoll AH, Filardo G, Almqvist FK, Bugbee WD, Jelic M, Monllau JC, Puddu G, Rodkey WG, Verdonk P, Verdonk R, Zaffagnini S, Marcacci M. Surgical treatment for early osteoarthritis. Part II: allografts and concurrent procedures. Knee Surg Sports Traumatol Arthrosc.20:468-86. 2012.
7. Johnstone B, Hering TM, Caplan AI, Goldberg VM, Yoo JU. In vitro chondrogenesis of bone marrow-derived mesenchymal progenitor cells. Exp Cell Res.238:265-72. 1998.
8. Pittenger MF, Mackay AM, Beck SC, Jaiswal RK, Douglas R, Mosca JD, Moorman MA, Simonetti DW, Craig S, Marshak DR. Multilineage potential of adult human mesenchymal stem cells. Science.284:143-7. 1999.
9. Rada T, Reis RL, Gomes ME. Adipose tissue-derived stem cells and their application in bone and cartilage tissue engineering. Tissue Eng

Part B Rev.15:113-25. 2009.
10. Rhee SC, Ji YH, Gharibjanian NA, Dhong ES, Park SH, Yoon ES. In vivo evaluation of mixtures of uncultured freshly isolated adipose-derived stem cells and demineralized bone matrix for bone regeneration in a rat critically sized calvarial defect model. Stem Cells Dev.20:233-42. 2011.
11. Choi JW, Park EJ, Shin HS, Shin IS, Ra JC, Koh KS. In Vivo Differentiation of Undifferentiated Human Adipose Tissue-Derived Mesenchymal Stem Cells in Critical-Sized Calvarial Bone Defects. Ann Plast Surg. 2012.
12. Kang H, Peng J, Lu S, Liu S, Zhang L, Huang J, Sui X, Zhao B, Wang A, Xu W, Luo Z, Guo Q. In vivo cartilage repair using adipose-derived stem cell-loaded decellularized cartilage ECM scaffolds. J Tissue Eng Regen Med. 2012.
13. Jung SN, Rhie JW, Kwon H, Jun YJ, Seo JW, Yoo G, Oh DY, Ahn ST, Woo J, Oh J. In vivo cartilage formation using chondrogenic-differentiated human adipose-derived mesenchymal stem cells mixed with fibrin glue. J Craniofac Surg.21:468-72. 2010.
14. ter Huurne M, Schelbergen R, Blattes R, Blom A, de Munter W, Grevers LC, Jeanson J, Noel D, Casteilla L, Jorgensen C, van den Berg W, van Lent PL. Antiinflammatory and chondroprotective effects of intraarticular injection of adipose-derived stem cells in experimental osteoarthritis. Arthritis Rheum.64:3604-13. 2012.
15. Toghraie F, Razmkhah M, Gholipour MA, Faghih Z, Chenari N, Torabi Nezhad S, Nazhvani Dehghani S, Ghaderi A. Scaffold-free adipose-derived stem cells (ASCs) improve experimentally induced osteoarthritis in rabbits. Arch Iran Med.15:495-9. 2012.
16. Toghraie FS, Chenari N, Gholipour MA, Faghih Z, Torabinejad S, Dehghani S, Ghaderi A. Treatment of osteoarthritis with infrapatellar fat pad derived mesenchymal stem cells in Rabbit. Knee.18:71-5. 2011.
17. Desando G, Cavallo C, Sartoni F, Martini L, Parrilli A, Veronesi F, Fini M, Giardino R, Facchini A, Grigolo B. Intra-articular delivery of adipose derived stromal cells attenuates osteoarthritis progression in an experimental rabbit model. Arthritis Res Ther.15:R22. 2013.
18. Koh YG, Jo SB, Kwon OR, Suh DS, Lee SW, Park SH, Choi YJ. Mesenchymal stem cell injections improve symptoms of knee osteoarthritis. Arthroscopy.29:748-55. 2013.
19. Dragoo JL, Samimi B, Zhu M, Hame SL, Thomas BJ, Lieberman JR, Hedrick MH, Benhaim P. Tissue-engineered cartilage and bone using stem cells from human infrapatellar fat pads. J Bone Joint Surg Br.85:740-7. 2003.
20. English A, Jones EA, Corscadden D, Henshaw K, Chapman T, Emery P, McGonagle D. A comparative assessment of cartilage and joint fat pad as a potential source of cells for autologous therapy development in knee osteoarthritis. Rheumatology (Oxford).46:1676-83. 2007.
21. Liu Y, Buckley CT, Downey R, Mulhall KJ, Kelly DJ. The role of environmental factors in regulating the development of cartilaginous grafts engineered using osteoarthritic human infrapatellar fat pad-derived stem cells. Tissue Eng Part A.18:1531-41. 2012.
22. Khan WS, Adesida AB, Tew SR, Andrew JG, Hardingham TE. The epitope characterisation and the osteogenic differentiation potential of human fat pad-derived stem cells is maintained with ageing in later life. Injury.40:150-7. 2009.
23. Lopez-Ruiz E, Peran M, Cobo-Molinos J, Jimenez G, Picon M, Bustamante M, Arrebola F, Hernandez-Lamas MC, Delgado-Martinez AD, Montanez E, Marchal JA. Chondrocytes extract from patients with osteoarthritis induces chondrogenesis in infrapatellar fat pad-derived stem cells. Osteoarthritis Cartilage.21:246-58. 2013.
24. Wickham MQ, Erickson GR, Gimble JM, Vail TP, Guilak F. Multipotent stromal cells derived from the infrapatellar fat pad of the knee. Clin Orthop Relat Res.196-212. 2003.
25. Pires de Carvalho P, Hamel KM, Duarte R, King AG, Haque M, Dietrich MA, Wu X, Shah F, Burk D, Reis RL, Rood J, Zhang P, Lopez M, Gimble JM, Dasa V. Comparison of infrapatellar and subcutaneous adipose tissue stromal vascular fraction and stromal/stem cells in osteoarthritic subjects. J Tissue Eng Regen Med. 2012.
26. Alegre-Aguaron E, Desportes P, Garcia-Alvarez F, Castiella T, Larrad L, Martinez-Lorenzo MJ. Differences in surface marker expression and chondrogenic potential among various tissue-derived mesenchymal cells from elderly patients with osteoarthritis. Cells Tissues Organs.196:231-40. 2012.
27. Mochizuki T, Muneta T, Sakaguchi Y, Nimura A, Yokoyama A, Koga H, Sekiya I. Higher chondrogenic potential of fibrous synovium- and adipose synovium-derived cells compared with subcutaneous fat-derived cells: distinguishing properties of mesenchymal stem cells in humans. Arthritis Rheum.54:843-53. 2006.
28. Lopa S, Colombini A, de Girolamo L, Sansone V, Moretti M. New Strategies in Cartilage Tissue Engineering for Osteoarthritic Patients: Infrapatellar Fat Pad as an Alternative Source of Progenitor Cells. J Biomater Tissue Eng.1:40-8. 2011.
29. Staszkiewicz J, Frazier TP, Rowan BG, Bunnell BA, Chiu ES, Gimble JM, Gawronska-Kozak B. Cell growth characteristics, differentiation frequency, and immunophenotype of adult ear mesenchymal stem cells. Stem Cells Dev.19:83-92. 2010.
30. de Girolamo L, Lopa S, Arrigoni E, Sartori MF, Baruffaldi Preis FW, Brini AT. Human adipose-derived stem cells isolated from young and elderly women: their differentiation potential and scaffold interaction during in vitro osteoblastic differentiation. Cytotherapy.11:793-803. 2009.
31. Bodo M, Lilli C, Bellucci C, Carinci P, Calvitti M, Pezzetti F, Stabellini G, Bellocchio S, Balducci C, Carinci F, Baroni T. Basic fibroblast growth factor autocrine loop controls human osteosarcoma phenotyping and differentiation. Mol Med.8:393-404. 2002.
32. Barbero A, Grogan S, Schafer D, Heberer M, Mainil-Varlet P, Martin I. Age related changes in human articular chondrocyte yield, proliferation and post-expansion chondrogenic capacity. Osteoarthritis Cartilage.12:476-84. 2004.
33. Ranstam J. Repeated measurements, bilateral observations and pseudoreplicates, why does it matter? Osteoarthritis Cartilage.20:473-5. 2012.
34. Gronthos S, Franklin DM, Leddy HA, Robey PG, Storms RW, Gimble JM. Surface protein characterization of human adipose tissue-derived stromal cells. J Cell Physiol.189:54-63. 2001.
35. Lee RH, Kim B, Choi I, Kim H, Choi HS, Suh K, Bae YC, Jung JS. Characterization and expression analysis of mesenchymal stem cells from human bone marrow and adipose tissue. Cell Physiol Biochem.14:311-24. 2004.
36. Fain JN. Release of interleukins and other inflammatory cytokines by human adipose tissue is enhanced in obesity and primarily due to the nonfat cells. Vitam Horm.74:443-77. 2006.

37. Dumond H, Presle N, Terlain B, Mainard D, Loeuille D, Netter P, Pottie P. Evidence for a key role of leptin in osteoarthritis. Arthritis Rheum.48:3118-29. 2003.
38. Vuolteenaho K, Koskinen A, Kukkonen M, Nieminen R, Paivarinta U, Moilanen T, Moilanen E. Leptin enhances synthesis of proinflammatory mediators in human osteoarthritic cartilage--mediator role of NO in leptin-induced PGE2, IL-6, and IL-8 production. Mediators Inflamm.2009:345838. 2009.
39. Toussirot E, Streit G, Wendling D. The contribution of adipose tissue and adipokines to inflammation in joint diseases. Curr Med Chem.14:1095-100. 2007.
40. Distel E, Cadoudal T, Durant S, Poignard A, Chevalier X, Benelli C. The infrapatellar fat pad in knee osteoarthritis: an important source of interleukin-6 and its soluble receptor. Arthritis Rheum.60:3374-7. 2009.
41. Zuk PA, Zhu M, Ashjian P, De Ugarte DA, Huang JI, Mizuno H, Alfonso ZC, Fraser JK, Benhaim P, Hedrick MH. Human adipose tissue is a source of multipotent stem cells. Mol Biol Cell.13:4279-95. 2002.
42. Gimble JM, Guilak F. Differentiation potential of adipose derived adult stem (ADAS) cells. Curr Top Dev Biol.58:137-60. 2003.
43. Guilak F, Awad HA, Fermor B, Leddy HA, Gimble JM. Adipose-derived adult stem cells for cartilage tissue engineering. Biorheology.41:389-99. 2004.
44. Ichinose S, Yamagata K, Sekiya I, Muneta T, Tagami M. Detailed examination of cartilage formation and endochondral ossification using human mesenchymal stem cells. Clin Exp Pharmacol Physiol.32:561-70. 2005.
45. Pelttari K, Winter A, Steck E, Goetzke K, Hennig T, Ochs BG, Aigner T, Richter W. Premature induction of hypertrophy during in vitro chondrogenesis of human mesenchymal stem cells correlates with calcification and vascular invasion after ectopic transplantation in SCID mice. Arthritis Rheum.54:3254-66. 2006.
46. Mueller MB, Tuan RS. Functional characterization of hypertrophy in chondrogenesis of human mesenchymal stem cells. Arthritis Rheum.58:1377-88. 2008.
47. Winter A, Breit S, Parsch D, Benz K, Steck E, Hauner H, Weber RM, Ewerbeck V, Richter W. Cartilage-like gene expression in differentiated human stem cell spheroids: a comparison of bone marrow-derived and adipose tissue-derived stromal cells. Arthritis Rheum.48:418-29. 2003.
48. Kim YH, Yoon DS, Kim HO, Lee JW. Characterization of different subpopulations from bone marrow-derived mesenchymal stromal cells by alkaline phosphatase expression. Stem Cells Dev.21:2958-68. 2012.
49. Jiang T, Liu W, Lv X, Sun H, Zhang L, Liu Y, Zhang WJ, Cao Y, Zhou G. Potent in vitro chondrogenesis of CD105 enriched human adipose-derived stem cells. Biomaterials.31:3564-71. 2010.
50. Quirici N, Scavullo C, de Girolamo L, Lopa S, Arrigoni E, Deliliers GL, Brini AT. Anti-L-NGFR and -CD34 monoclonal antibodies identify multipotent mesenchymal stem cells in human adipose tissue. Stem Cells Dev.19:915-25. 2010.

Chapter 5

Influence on chondrogenesis of human osteoarthritic chondrocytes in co-culture with donor-matched mesenchymal stem cells from infrapatellar fat pad and subcutaneous adipose tissue

Abstract

Co-culture of mesenchymal stem cells (MSCs) and articular chondrocytes (ACs) has been proposed for autologous cartilage cell-based therapies, to overcome the issues associated to limited availability of articular chondrocytes (ACs).

To evaluate the potentiality of a co-culture approach in aged osteoarthritic patients, MSCs from infrapatellar fat pad (IFP-MSCs) and knee subcutaneous adipose tissue (ASCs) were co-cultured with donor-matched osteoarthritic, expanded and cryopreserved, ACs in a 75%/25% ratio. Co-cultures were prepared also from nasal chondrocytes (NCs) to evaluate their possible use as an alternative to ACs. Pellets were differentiated for 14 days, using mono-cultures of each cell type as reference.

Chondrogenic genes SOX9, COL2A1, ACAN were less expressed in co-cultures compared to ACs and NCs. Total GAGs content in co-cultures did not differ significantly from values predicted as the sum of each cell type contribution corrected for the co-culture ratio, as confirmed by histology. No significant differences were observed for GAGs/DNA in mono-cultures, demonstrating a reduced chondrogenic potential of ACs and NCs.

In conclusion, a small percentage of expanded and cryopreserved ACs and NCs did not lead to IFP-MSCs and ASCs chondro-induction. Our results suggest that chondrogenic potential and origin of chondrocytes may play a relevant role in the outcome of co-cultures, indicating a need for further investigations to demonstrate their clinical relevance in the treatment of aged osteoarthritic patients.

Introduction

Articular cartilage is a highly specialized tissue with a low self-repair ability due to the lack of vascularization and to its low cellularity. As a consequence, untreated cartilage lesions can easily degenerate and eventually lead to osteoarthritis (OA) and to the loss of joint functionality (1). Different strategies have been developed to treat promptly chondral lesions, comprising cell-based therapies such as autologous chondrocyte implantation (ACI) (2,3). Major issues associated to the clinical use of autologous chondrocytes are the limited number of chondrocytes harvestable from a small biopsy of cartilage and the de-differentiation process occurring during their required expansion (4,5). Furthermore, advanced age and a pathological state of joints have been demonstrated to reduce the chondrogenic potential of articular chondrocytes (ACs) (6-9) and represent important factors that should be considered when treating chondral lesions in particular categories of patients. To overcome these limitations, other cell sources have been considered as an alternative to ACs. Among terminally differentiated cells, nasal chondrocytes (NCs) have been proposed for cartilage tissue engineering (9) since their harvesting is associated with a lower site morbidity, their chondrogenic potential is not dependent on the donor's age (10) and they respond better than ACs to inflammatory stimuli (11). Beside differentiated cells, mesenchymal stem cells (MSCs) that can be isolated from several adult tissues, such as bone marrow and adipose tissue, have been proposed as an alternative to ACs thanks to their demonstrated proliferative and chondrogenic ability (12,13). Adipose-derived stem cells (ASCs) have been successfully used in several in vivo studies for cartilage generation (14-16). Thus, when developing treatments for knee chondral lesions, infrapatellar fat pad and knee subcutaneous adipose tissue, that are easily accessible during orthopaedic surgery, can be considered appealing sources for MSCs harvesting (17-22).

Recently, the co-culture of ACs and MSCs has gained growing interest, with the aim of both investigating the cross-talk between these two cell types and replacing a fraction of ACs with MSCs to reduce the cartilage biopsy size and the time required for chondrocytes expansion, thus limiting their in vitro de-differentiation. Controversial results have been reported on the generation of cartilage-like matrix and on the chondro-inductive action of chondrocytes in co-culture with ASCs (23-25) or BMSCs (25-29). The different origin and de-differentiation state of chondrocytes used in these studies make the comparison of their results difficult. In addition, apoptosis of MSCs occuring in chondrogenic pellet co-cultures and altering the starting percentages of MSCs and chondrocytes (25) complicates data interpretation.

In the present study we evaluated whether the co-culture of MSCs derived from infrapatellar fat pad (IFP-MSCs) and knee subcutaneous adipose tissue (ASCs) with a small fraction of ACs was able to lead to cartilage-like matrix generation and to the expression of chondrogenic markers similar to those of

ACs. To better resemble a possible clinical application of this strategy we performed autologous co-cultures combining FP-MSCs and ASCs with donor-matched ACs and we used cells derived from OA patients so as not to neglect the impact of a probable pathological state of the cell source on the outcome of co-cultures. Furthermore, to test if NCs could be used as an alternative to ACs, co-culture experiments were performed combining IFP-MSCs and ASCs with NCs obtained from rinoplasty surgery.

Materials and Methods

Cell isolation and expansion

Infrapatellar fat pad, knee subcutaneous adipose tissue and articular cartilage were obtained from 5 OA patients (mean age 64±10 years, range 54-75 years) undergoing knee replacement. Nasal cartilage was obtained from 1 patient (36 years) during rinoplasty procedure. All samples were harvested with patients' informed consent after approval from the Institutional Review Board.

IFP-MSCs and ASCs were isolated by enzymatic digestion (37°C, 30 min) using 0.075% type I collagenase (Worthington Biochemical Co) (30). After digestion, cells were plated in control medium consisting of DMEM (4.5 g/l glucose, Gibco) supplemented with 10% fetal bovine serum (FBS, Lonza), 0.029 mg/ml L-glutamine, 100 U/ml penicillin, 100 µg/ml streptomycin, 10 mM hepes, 1 mM sodium pyruvate (all from Gibco) and expanded until passage 4. ACs and NCs were isolated by enzymatic digestion (37°C, 22 h) using 0.15% type II collagenase (Worthington Biochemical Co) and expanded until passage 2 in control medium supplemented with 5 ng/ml fibroblast growth factor-2 (FGF-2, PeproTech) and 1 ng/ml transforming growth factor-β1 (TGF-β1, PeproTech) (6). At passage 2, ACs were frozen and successively thawed since ACs and the donor-matched IFP-MSCs and ASCs required a different expansion time, although they needed to be combined in the same co-culture experiment. NCs were also expanded until passage 2 and frozen before use.

Chondrogenic co-culture of IFP-MSCs and ASCs combined with ACs and NCs

Chondrogenic differentiation was performed by pellet culture technique. Pellets were obtained by centrifuging 4x105 cells (250 g, 5 min) in a 1.5 ml conical tube and cultured for 14 days in chondrogenic medium containing 0.1 µM dexamethasone (Sigma-Aldrich) and 10 ng/ml TGF-β1 (6). Medium was replaced twice a week. Co-cultures were obtained mixing IFP-MSCs and ASCs with donor-matched ACs or NCs (ratio 75%/25%) as follows: IFP-MSCs/ASCs, ASCs/ACs, IFP-MSCs/NCs, ASCs/NCs. IFP-MSCs, ASCs, ACs and NCs mono-cultures were also prepared.

Analysis of cell distribution in co-culture pellets

To analyze cell distribution in co-culture pellets, ACs were stained with the green fluorescent dye Vybrant DiO, while IFP-MSCs and ASCs were stained with the red fluorescent dye Vybrant CM-DiI (both from Invitrogen) according to the manufacturer's instructions. Stained cells were mixed as in co-culture pellets. One day after pellet formation, pellets were embedded in Tissue-Tek OCT (Sakura), sectioned by cryotome (6 µm) and observed through a fluorescence microscope.

Quantification of GAGs and DNA

Pellets were washed with PBS and incubated in 500 µl of PBE buffer (100 mM Na2HPO4, 10 mM NaEDTA, pH 6.8) containing 1.75 mg/ml L-cystein (Sigma-Aldrich) and 14.2 U/ml papain (Worthington) for 16 h at 60°C. The amount of GAGs was spectrophotometrically measured using 16 mg/ml dimethylmethylene blue (Sigma-Aldrich), with chondroitin sulfate as standard, and DNA content was quantified using the CyQUANT Kit (Invitrogen). On the basis of DNA data, the number of cells in each pellet was estimated considering an average content of 11.6 pg DNA/cell (25,31).

Histological analysis

Pellets were fixed for 24 h in 10% neutral buffered formalin, embedded in paraffin and sectioned at 4 µm. Sections were stained with haematoxylin-eosin (Sigma-Aldrich) or Alcian Blue (pH 2.5, Sigma-Aldrich) to evaluate pellet morphology and GAGs content.

Gene expression analysis

Gene expression of chondrogenic markers was evaluated by real time PCR (Rotor Gene RG3000 system, Qiagen). RNA was purified from pellets using RNeasy Mini kit (Qiagen) and reverse-transcribed to cDNA using iScript cDNA Synthesis Kit (Bio-Rad Laboratories). 20 ng of cDNA were incubated with a PCR mixture including TaqMan Universal PCR Master Mix and TaqMan® Assays-on-Demand™ Gene expression probes (Life Technologies) using the following assays: glyceraldehyde-3-phosphate dehydrogenase (GAPDH, Hs99999905_m1), aggrecan (ACAN, Hs00153936_m1), collagen type II alpha I (COL2A1, Hs01060345_m1), cartilage oligomeric matrix protein (COMP, Hs00164359_m1), SRY (Sex determining region Y)-box9 (SOX9, Hs00165814_m1). Expression of chondrogenic markers was normalized on GAPDH.

Statistical analysis

Data are expressed as mean±SEM and statistical analysis was performed by One-Way ANOVA (GraphPad Prism v5.00, GraphPad Software). Significance was set at $p<0.05$.

Results

Quantification of GAGs and DNA content

Autologous co-cultures were performed combining IFP-MSCs and ASCs with donor-matched ACs. Cell distribution within co-culture pellets was evaluated by staining IFP-MSCs and ACs with a fluorescent dye. One day after pellet formation, IFP-MSCs and ACs were homogeneously mixed within the pellet (Fig. 1). The same behavior was observed in ASCs co-culture pellets (data not shown).

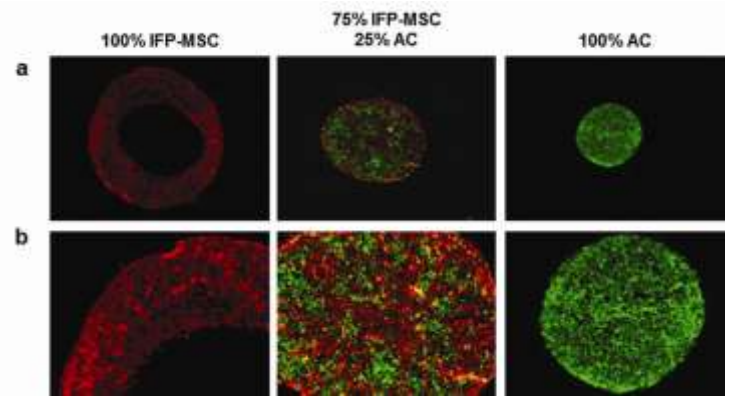

Fig. 1. Representative pictures of macroscopic morphology (a, magnification 4X) and cell distribution (b, magnification 10X) of IFP-MSCs, IFP-MSCs/ACs, and ACs pellets 1 day after their formation. IFP-MSCs are stained red and ACs are stained green.

Pellet cell number evaluation revealed that, starting from $4x10^5$ cells, a significant reduction in cell number occurred in ACs pellets ($2.9x10^5$, $p<0.01$). A more relevant decrease in cell number was observed in IFP-MSCs and ASCs pellets with an average of $1.3x10^5$ and $1.2x10^5$ cells found after 14 days of culture ($p<0.01$ for IFP-MSCs and $p<0.05$ for ASCs), indicating a lower survival of IFP-MSCs and ASCs compared to ACs in pellet culture conditions. A higher number of cells was found in co-culture pellets in comparison with IFP-MSCs and ASCs pellets, even though the differences with respect to ACs pellets remained significant ($p<0.01$) (Fig. 2a). Total GAGs content was 2-fold higher in ACs pellets compared to IFP-MSCs and ASCs pellets ($p<0.001$). In co-culture pellets total GAGs content increased only slightly compared to IFP-MSCs and ASCs pellets and was significantly lower with respect to ACs pellets ($p<0.001$) (Fig. 2b). Given the higher number of cells present in ACs and co-culture pellets, GAGs normalized by DNA was comparable for all the experimental groups (Fig. 2c).

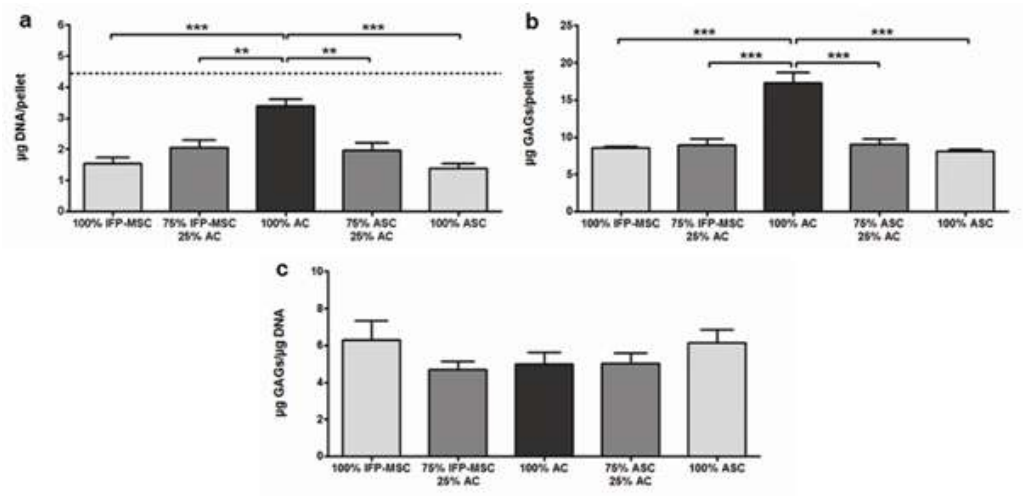

Fig. 2. Quantification of DNA content (a), GAGs content (b) and GAGs content normalized by DNA (c) in ACs co-cultures after 14 days. Dotted line represents average DNA content after 1 day of culture. IFP-MSCs, ACs and ASCs mono-cultures were used as a reference. Data are expressed as mean±SEM.

Similar results were obtained co-culturing IFP-MSCs and ASCs with NCs. After 14 days, a decrease in cell number was observed in NCs pellets ($3.1x10^5$ cells). IFP-MSCs/NCs and ASCs/NCs pellets contained a significantly lower number of cells compared to NCs ($p<0.001$), even though increases were observed with respect to IFP-MSCs and ASCs (Fig. 3a). A small increase in total GAGs content was observed in the co-cultures, but differences with IFP-MSCs and ASCs pellets were not significant (Fig. 3b). GAGs normalized by DNA was similar in all the experimental groups (Fig. 3c).

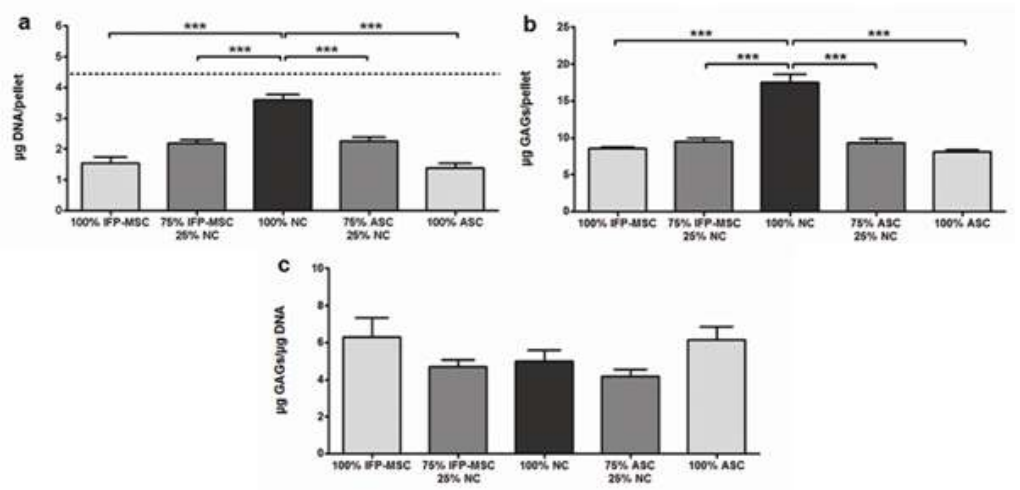

Fig. 3. Quantification of DNA content (a), GAGs content (b) and GAGs content normalized by DNA (c) in NCs co-cultures after 14 days. Dotted line represents average DNA content after 1 day of culture. IFP-MSCs, NCs and ASCs mono-cultures were used as a reference. Data are expressed as mean±SEM.

Histological analysis

Histological evaluation revealed consistent differences in terms of matrix quality when comparing IFP-MSCs and ASCs pellets to ACs and NCs ones. Processing of ASCs pellets revealed their tendency to disaggregate. IFP-MSCs performed better than ASCs, being characterized by a more consistent matrix, however a greater amount of matrix was found in ACs and NCs pellets (Fig. 4a) where GAGs were intensely stained by alcian blue (Fig. 4b). Furthermore, ACs and NCs pellets showed the formation of structures similar to lacunae that were not found in IFP-MSCs and

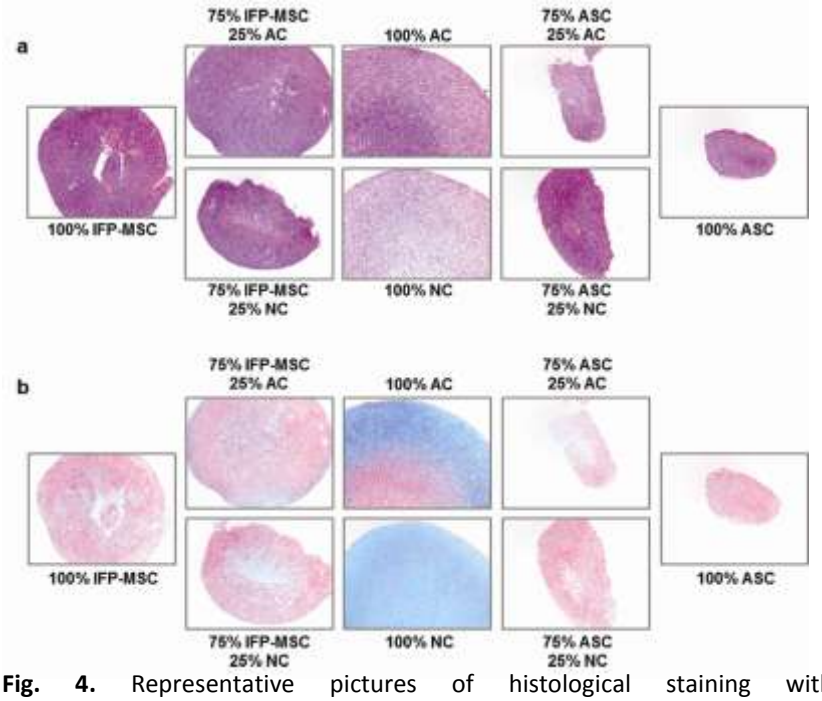

Fig. 4. Representative pictures of histological staining with haematoxylin/eosin (a) and alcian blue (b) of mono-culture and co-culture pellets (magnification 5X) after 14 days. IFP-MSCs, ASCs and ACs represented in these pictures were obtained from the same donor.

ASCs pellets. IFP-MSCs/ACs and IFP-MSCs/NCs co-cultures showed an increased GAGs content compared to IFP-MSCs pellets, increase that was not observed in ASCs co-cultures (Fig. 4b). However, the matrix produced by IFP-MSCs co-cultures had structure and composition that was very distant from that observed in NCs and ACs pellets.

Gene expression analysis

Transcriptional expression of different chondrogenic markers was evaluated considering the global response of both cell types in co-culture. As expected, ACs expressed higher levels of the tested markers in comparison with IFP-MSCs and ASCs and their corresponding co-culture pellets. Increases in COL2A1 and ACAN levels were observed in IFP-MSCs/ACs compared to IFP-MSCs pellets, whereas no up-regulation was observed for SOX9 and COMP. On the other hand, the expression of SOX9, ACAN and COMP was increased in ASCs/ACs compared to ASCs pellets, whereas COL2A1 was almost undetectable (Fig. 5).

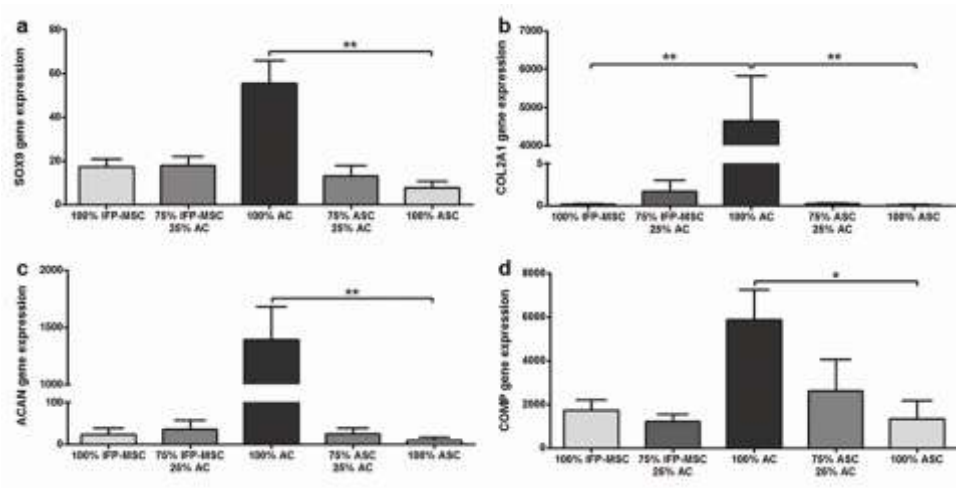

Fig. 5. Gene expression of SOX9 (a), COL2A1 (b), ACAN (c) and COMP (d) in ACs co-cultures after 14 days. IFP-MSCs, ACs and ASCs mono-cultures were used as a reference. Gene levels are normalized to the housekeeping GAPDH and expressed as mean±SEM

IFP-MSCs/NCs and ASCs/NCs co-cultures showed small increases in SOX9, COL2A1 and ACAN expression, but except for the transcriptional factor SOX9, differences in gene levels between NCs and co-culture pellets remained very

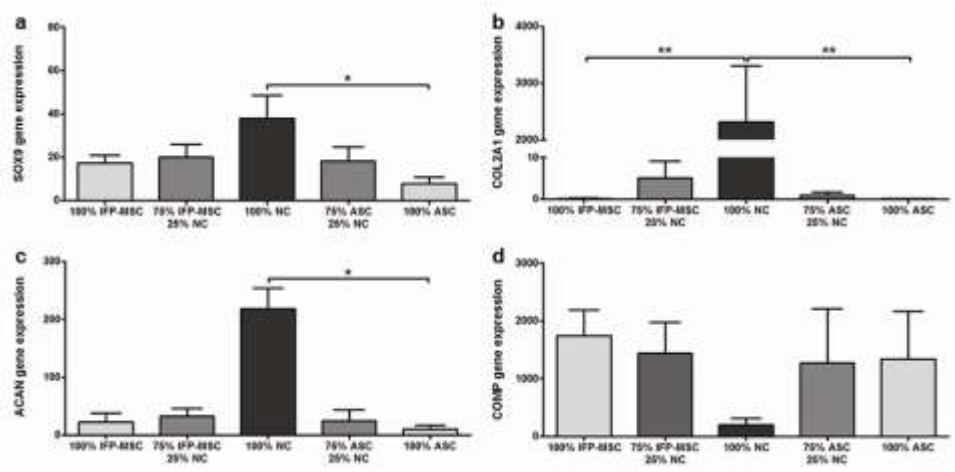

Fig. 6. Gene expression of SOX9 (a), COL2A1 (b), ACAN (c) and COMP (d) in NCs co-cultures after 14 days. IFP-MSCs, NCs and ASCs mono-cultures were used as a reference. Gene levels are normalized to the housekeeping GAPDH and expressed as mean±SEM

consistent (Fig. 6). We found lower levels of COMP in NCs respect to IFP-MSCs and ASCs, which resulted in a reduction of its expression in co-cultures (Fig. 6d).

Discussion

The possibility of replacing a fraction of ACs with MSCs has gained growing interest over the last few years to reduce the number of ACs required for implantation and to limit ACs expansion and de-differentiation. Controversial results about the efficacy of ASCs co-culture with chondrocytes have been reported. Indeed, besides studies showing that ASCs co-culture with ACs or NCs results in chondro-induction, seen as the synergistic action of both cell types to generate cartilagineous matrix (24,25), another study has reported that ASCs contribution is limited to the transcriptional expression of chondrogenic genes (23). Contradictory results have been also reported for co-cultures between BMSCs and ACs (25-29) supporting the idea that cell origin and de-differentiation state of ACs as well as the MSCs/ACs ratio play a fundamental role in determining the outcome.

In this study we evaluated whether the co-culture of IFP-MSCs and ASCs with a small percentage of ACs could lead to the generation of cartilage-like matrix comparable to that obtained from ACs. To better resemble a possible clinical application addressed to treat knee lesion in OA patients, autologous co-cultures were performed through donor-matched IFP-MSCs, ASCs and ACs using cells derived from old OA donors who are known to possess a reduced chondrogenic potential (6-8). Given the growing interest for the use of NCs in cartilage tissue engineering, the same experiments were performed using NCs.

As already reported for BMSCs (25,26), cell death of IFP-MSCs and ASCs occurred during chondrogenic pellet culture, as demonstrated by a significant decrease in cell number after 14 days. Surprisingly, also ACs and NCs underwent cell death, although to a minor extent when compared to IFP-MSCs and ASCs. Evaluation of total GAGs content demonstrated that co-culture with ACs did not lead to IFP-MSCs and ASCs chondro-induction. Indeed, the measured values did not differ significantly from the ones predicted as the sum of the single contribution of ACs and IFP-MSCs or ASCs alone corrected for their ratio in co-culture pellets. A recent study has reported that chondro-induction is observed in co-cultures of ASCs combined with ACs or NCs (25). A major difference between this study and ours can be found in the origin of cells used: while Acharya et al. (25) uniquely used non-expanded healthy chondrocytes, we used ACs from OA donors undergoing a longer expansion phase known to negatively affect ACs chondrogenic phenotype (4). Furthermore, to prepare autologous co-cultures from the same patient we had to cryopreserve ACs because of the different time required for ACs, IFP-MSCs and ASCs expansion. It has been recently shown that ACs cryopreservation can significantly reduce gene expression of SOX9 and COL2 (32), which suggests that the chondrogenic ability of ACs used in our

experiments may have been further impaired by this procedure. Considerations about the impact of cell expansion and cryopreservation on chondrogenic differentiation can also explain the results obtained in NCs co-cultures, in contrast with recently published data (25). Indeed, the low chondrogenic ability of ACs and NCs used in our study was confirmed by GAGs normalized by DNA, which revealed that the amount of GAGs produced by a single cell by ACs and NCs was similar to that observed for IFP-MSCs and ASCs. On the other hand, in accordance with our observations, Giovannini et al. (26) have reported that ACs failed to induce BMSCs to chondrogenesis, although BMSCs/ACs co-culture resulted in significant cartilaginous matrix formation. However, the higher chondrogenic potential of BMSCs in comparison with ASCs (33,34), together with a longer period of chondrogenic differentiation and healthy origin of ACs (26), could explain why in our experiments only in IFP-MSCs/ACs and IFP-MSCs/NCs a small increase in GAGs deposition was observed through histological evaluation.

Performing co-culture only between human cells, it was not possible to distinguish the response of each single cell type, differently from other studies where animal ACs have been co-cultured with human MSCs and specific probes have been used to distinguish the human and bovine genes expression (25,29). Thus, we evaluated the global response in terms of gene expression levels comparing mono-culture and co-culture pellets. We did not observe a significant up-regulation of chondrogenic markers in IFP-MSCs/ACs and ASCs/ACs compared to IFP-MSCs and ASCs pellets and their levels remained notably lower compared to those observed in ACs. Our results differ significantly from those published by Lee et al. (24) where a significant difference in SOX9 and COL2A1 expression was observed between ASCs and ASCs/ACs pellets and levels of these genes were comparable to those of ACs. Despite similarities with our study can be found in ACs expansion and cryopreservation, differences with our results could be related to the higher percentage of ACs (50% ACs/50% ASCs) and to the absence of TGF-β1 during culture (24). Furthermore, in their study ACs were isolated from cartilage showing only minimal OA changes and retained a higher ability to produce GAGs, as demonstrated by values of GAGs/DNA 2-fold higher than ours even in absence of TGF-β1. These dissimilarities could also explain why they obtained the formation of cartilage-like matrix with comparable collagen II deposition in ASCs/ACs and ACs pellets, whereas in our study the co-culture of IFP-MSCs and ASCs with either ACs or NCs did not lead to cartilagineous matrix generation (24). In another study, Hildner et al. (23) analyzed gene expression only in co-cultures performed in a 3D matrix (Tisseel or Tissue Fleece). It must be highlighted that in their study ASCs contribution to the expression of chondrogenic genes was significant only when small percentages of ACs were used (5% or 10%) (23). In our study, results from gene expression analysis of NCs co-cultures were similar to those obtained from ACs co-cultures, despite lower levels of SOX9, COL2A1 and ACAN were found in NCs. Surprisingly,

COMP expression was lower in NCs than in IFP-MSCs and ASCs which resulted in diminished expression of this gene in IFP-MSCs/NCs and ASCs/NCs pellets. In this study we used NCs from a single donor and given inter-donor differences the differential expression of COMP in NCs and ACs would need further investigations to be confirmed. To our knowledge, no study reporting gene analysis in co-culture of ASCs and NCs has been published, which does not permit comparison with our results.

In conclusion, in our study a small percentage of expanded and cryopreserved ACs and NCs failed to induce chondrogenesis in MSCs from infrapatellar fat pad and knee subcutaneous adipose tissue and did not lead to the generation of cartilage-like matrix similar to that produced by ACs and NCs. This result may depend on several combined factors such as the percentage of chondrocytes used, their de-differentiation state related to prolonged expansion and cryopreservation as well as the advanced donors' age and the pathological origin of ACs. These considerations suggest that specific attention must be given to chondrogenic potential and origin of chondrocytes used in co-culture studies and to the experimental design of each study (e.g. MSCs/ACs ratio, use of differentiative factors, differentiation time) to better understand their results. However, clinical applicability of the co-culture approach still deserves further investigation to extend it also to patients characterized by advanced age or degenerative pathologies.

Acknowledgements

I would like to thank all the co-authors: Colombini A., Sansone V., Baruffaldi Preis F.W., Moretti M. Furthermore, I would like to thank all Turner L.J., Bonora C. and Bergamaschi G.B. for their contribution in experiments and in sample harvesting. This work was supported by Italian Ministry of Health and Cariplo Foundation.

References

1. Gelber AC, Hochberg MC, Mead LA, Wang NY, Wigley FM, Klag MJ. Joint injury in young adults and risk for subsequent knee and hip osteoarthritis. Ann Intern Med. 133:321-8. 2000.
2. Farr J, Cole B, Dhawan A, Kercher J, Sherman S. Clinical cartilage restoration: evolution and overview. Clin Orthop Relat Res. 469:2696-705. 2011.
3. Brittberg M, Lindahl A, Nilsson A, Ohlsson C, Isaksson O, Peterson L. Treatment of deep cartilage defects in the knee with autologous chondrocyte transplantation. N Engl J Med.331:889-95. 1994.
4. Schnabel M, Marlovits S, Eckhoff G, Fichtel I, Gotzen L, Vécsei V, Schlegel J. Dedifferentiation-associated changes in morphology and gene expression in primary human articular chondrocytes in cell culture. Osteoarthritis Cartilage. 10:62-70. 2002.
5. Gikas PD, Bayliss L, Bentley G, Briggs TW. An overview of autologous chondrocyte implantation. J Bone Joint Surg Br. 91:997-1006. 2009.
6. Barbero A, Grogan S, Schäfer D, Heberer M, Mainil-Varlet P, Martin I. Age related changes in human articular chondrocyte yield, proliferation and post-expansion chondrogenic capacity. Osteoarthritis Cartilage. 12:476-84. 2004.
7. Tallheden T, Bengtsson C, Brantsing C, Sjögren-Jansson E, Carlsson L, Peterson L, Brittberg M, Lindahl A. Proliferation and differentiation potential of chondrocytes from osteoarthritic patients. Arthritis Res Ther. 7:R560-8. 2005.
8. Eid K, Thornhill TS, Glowacki J. Chondrocyte gene expression in osteoarthritis: Correlation with disease severity. J Orthop Res. 24:1062-8. 2006.
9. Kafienah W, Jakob M, Demarteau O, Frazer A, Barker MD, Martin I, Hollander AP. Three-dimensional tissue engineering of hyaline

cartilage: comparison of adult nasal and articular chondrocytes. Tissue Eng. 8:817-26. 2002.

10. Rotter N, Bonassar LJ, Tobias G, Lebl M, Roy AK, Vacanti CA. Age dependence of biochemical and biomechanical properties of tissue-engineered human septal cartilage. Biomaterials. 23:3087-94. 2002.
11. Scotti C, Osmokrovic A, Wolf F, Miot S, Peretti GM, Barbero A, Martin I. Response of human engineered cartilage based on articular or nasal chondrocytes to interleukin-1β and low oxygen. Tissue Eng Part A. 18:362-72. 2012.
12. Zuk PA, Zhu M, Mizuno H, Huang J, Futrell JW, Katz AJ, Benhaim P, Lorenz HP, Hedrick MH. Multilineage cells from human adipose tissue: implications for cell-based therapies. Tissue Eng. 7:211-28. 2001.
13. Lee RH, Kim B, Choi I, Kim H, Choi HS, Suh K, Bae YC, Jung JS. Characterization and expression analysis of mesenchymal stem cells from human bone marrow and adipose tissue. Cell Physiol Biochem. 14:311-24. 2004
14. Jung SN, Rhie JW, Kwon H, Jun YJ, Seo JW, Yoo G, Oh DY, Ahn ST, Woo J, Oh J. In vivo cartilage formation using chondrogenic-differentiated human adipose-derived mesenchymal stem cells mixed with fibrin glue. J Craniofac Surg. 21:468-72. 2010
15. Yoon HH, Bhang SH, Shin JY, Shin J, Kim BS. Enhanced cartilage formation via three-dimensional cell engineering of human adipose-derived stem cells. Tissue Eng Part A. 18:1949-56. 2012.
16. Kang H, Peng J, Lu S, Liu S, Zhang L, Huang J, Sui X, Zhao B, Wang A, Xu W, Luo Z, Guo Q. In vivo cartilage repair using adipose-derived stem cell-loaded decellularized cartilage ECM scaffolds. J Tissue Eng Regen Med. doi: 10.1002/term.1538. 2012.
17. Wickham MQ, Erickson GR, Gimble JM, Vail TP, Guilak F. Multipotent stromal cells derived from the infrapatellar fat pad of the knee. Clin Orthop Relat Res. 412:196-212. 2003.
18. Dragoo JL, Samimi B, Zhu M, Hame SL, Thomas BJ, Lieberman JR, Hedrick MH, Benhaim P. Tissue-engineered cartilage and bone using stem cells from human infrapatellar fat pads. J Bone Joint Surg Br. 85:740-7. 2003.
19. English A, Jones E, Corscadden D, Henshaw K, Chapman T, Emery P, McGonagle D. A comparative assessment of cartilage and joint fat pad as a potential source of cells for autologous therapy development in knee osteoarthritis. Rheumatology (Oxford). 46:1676-83. 2007.
20. Pires de Carvalho P, Hamel KM, Duarte R, King AG, Haque M, Dietrich MA, Wu X, Shah F, Burk D, Reis RL, Rood J, Zhang P, Lopez M, Gimble JM, Dasa V. Comparison of infrapatellar and subcutaneous adipose tissue stromal vascular fraction and stromal/stem cells in osteoarthritic subjects. J Tissue Eng Regen Med. doi: 10.1002/term.1565. 2012.
21. Alegre-Aguarón E, Desportes P, García-Álvarez F, Castiella T, Larrad L, Martínez-Lorenzo MJ. Differences in surface marker expression and chondrogenic potential among various tissue-derived mesenchymal cells from elderly patients with osteoarthritis. Cells Tissues Organs. 196:231-40. 2012.
22. Mochizuki T, Muneta T, Sakaguchi Y, Nimura A, Yokoyama A, Koga H and Sekiya I. Higher chondrogenic potential of fibrous synovium- and adipose synovium-derived cells compared with subcutaneous fat-derived cells: distinguishing properties of mesenchymal stem cells in humans. Arthritis Rheum. 54:843-53. 2006.
23. Hildner F, Concaro S, Peterbauer A, Wolbank S, Danzer M, Lindahl A, Gatenholm P, Redl H, van Griensven M. Human adipose derived stem cells contribute to chondrogenesis in co-culture with human articular chondrocytes. Tissue Eng Part A. 15:3961-9. 2009.
24. Lee JS, Im GI. Influence of chondrocytes on the chondrogenic differentiation of adipose stem cells. Tissue Eng Part A. 16:3569-77. 2010.
25. Acharya C, Adesida A, Zajac P, Mumme M, Riesle J, Martin I, Barbero A. Enhanced chondrocyte proliferation and mesenchymal stromal cells chondrogenesis in coculture pellets mediate improved cartilage formation. J Cell Physiol. 227:88-97. 2012.
26. Giovannini S, Diaz-Romero J, Aigner T, Heini P, Mainil-Varlet P, Nesic D. Micromass co-culture of human articular chondrocytes and human bone marrow mesenchymal stem cells to investigate stable neocartilage tissue formation in vitro. Eur Cell Mater. 20:245-59. 2010.
27. Sabatino MA, Santoro R, Gueven S, Jaquiery C, Wendt DJ, Martin I, Moretti M, Barbero A. Cartilage graft engineering by co-culturing primary human articular chondrocytes with human bone marrow stromal cells. J Tissue Eng Regen Med. doi: 10.1002/term.1661. 2012.
28. Xu L, Wang Q, Xu F, Ye Z, Zhou Y, Tan WS. Mesenchymal Stem Cells Downregulate Articular chondrocyte differentiation in non-contact coculture systems: implications in cartilage tissue regeneration. Stem Cells Dev. 22:1657-69. 2013.
29. Tsuchiya K, Gouping C, Ushida T, Matsuno T, Tateishi T. The effect of coculture of chondrocytes with mesenchymal stem cells on their cartilaginous phenotype in vitro. Mater Sci Eng C. 24:391-6. 2004.
30. Lopa S, Colombini A, de Girolamo L, Sansone V, Moretti M. New strategies in cartilage tissue engineering for osteoarthritic patients: infrapatellar fat pad as an alternative source of progenitor cells. J Biomater Tissue Eng. 1:40-8. 2011.
31. Jakob M, Demarteau O, SchaferD, Stumm M, Heberer M, Martin I. Enzymatic digestion of adult human articular cartilage yields a small fraction of the total available cells. Connect Tissue Res 2003. 44:173-80.
32. Muiños-López E, Rendal-Vázquez ME, Hermida-Gómez T, Fuentes-Boquete I, Díaz-Prado S, Blanco FJ. Cryopreservation effect on proliferative and chondrogenic potential of human chondrocytes isolated from superficial and deep cartilage. Open Orthop J. 6:150-9. 2012.
33. Huang JI, Kazmi N, Durbhakula MM, Hering TM, Yoo JU, Johnstone B. Chondrogenic potential of progenitor cells derived from human bone marrow and adipose tissue: a patient-matched comparison. J Orthop Res. 23:1383-9. 2005.
34. Im GI, Shin YW, Lee KB. Do adipose tissue-derived mesenchymal stem cells have the same osteogenic and chondrogenic potential as bone marrow-derived cells? Osteoarthritis Cartilage. 13:845-53. 2005.

Chapter 6

Rapid prototyping of multi-well devices for pellet culture and biofabrication of patterned scaffolds

Abstract

Three-dimensional (3D) cultures are widely used as in vitro models for cell culture in basic and translational research. Pellet culture is used in cartilage tissue engineering area to promote *in vitro* chondrogenic differentiation. Unfortunately, handling a high number of experimental replicates in 3D pellet culture experiments is extremely time consuming. To overcome this limitation, we exploited low-cost rapid prototyping techniques, such as laser ablation and replica molding, to generate multi-well chips in polydimethylsiloxane (PDMS) able to support the formation and culture of multiple cell aggregates. The use of PDMS chips significantly reduced the time required for pellet seeding and medium refresh. We found that chondocytes pellets generated with this approach were comparable to pellets obtained by standard culture in polypropylene tubes, in terms of proliferation and metabolic activity. Type II collagen deposition was increased in pellets cultured in PDMS chips, showing that chondrocyte differentiation was improved. The same biofabrication approach was applied to generate a patterned fibrin glue scaffold. As a proof of concept, we biofabricated an implantable multi-well constructs using clinically approved fibrin glue. We demonstrated that regions with different cell densities can be generated within the construct and that cells can be distributed in a spatially controlled way. These multi-well implantable scaffolds can be seeded with multiple cell types allowing the precise distribution of different cell populations, thus representing a useful tool to investigate *in vitro* and *in vivo* cell interactions in a 3D environment.

Introduction

Three-dimensional (3D) cultures are widely used as *in vitro* models for cell culture. Compared with a 2D monolayer culture, a 3D model better mimics the *in vivo* tissue features providing a physiologically relevant environment. Multi-well devices have become a viable alternative to standard methods to generate and culture multiple cell aggregates, having a broad range of applications in the basic research and drug screening on tumor spheroids (1,2) and in tissue engineering basic and translational studies (3,4). Rapid prototyping technologies represent an exceptional tool to generate easy-handling platforms for 3D cell culture. However, existing lithography-based approaches are often expensive and time consuming (5). Indeed, current approaches based on lithographic fabrication require cleanroom facilities and minor changes in the design involve an increase in the cost of fabrication and materials. Laser fabrication, involving material ablation via beams of infrared light, offers an alternative to lithography-based approaches for rapid prototyping (6). Recent studies using 3D laser printing (7) or carbon dioxide laser (CO_2 laser) ablation (8,9) to generate microwells attempted to minimize fabrication complexity.

In this work we present a rapid, low-cost prototyping method which can be readily available for any laboratory to create patterned polydimethylsiloxane (PDMS) chips using polymethylmethacrylate (PMMA) CO_2 laser ablation for the generation of the master template. Multi-well PDMS chips generated with this approach can be used as easy-handling devices for the formation and culture cell aggregates or as molds to biofabricate scaffolds with a controlled architecture.

Articular chondrocytes (ACs) are a widely investigated cell source in the field of cartilage tissue engineering (10,11). Their chondrogenic re-differentiation, necessary to re-acquire the original phenotype after the *in vitro* expansion phase (10-12), is performed inducing the cell to form 3D aggregates by centrifugation in polypropylene conical tubes (13-16). This type of culture is traditionally used in in vitro studies aiming at the characterization of specific cell populations and for the optimization of chondrogenic differentiation protocols. This type of studies normally require to prepare replicates using cells from different donors, leading to a consistent number of samples. Unfortunately, handling a high number of pellets makes routine operations, such as medium refresh, extremely time-consuming. Furthermore, the simultaneous culture of hundreds of pellets requires a consistent fraction of the space available in a standard CO_2 incubator and is related to a high risk of contamination.

Based on the need of user-friendly platforms to implement 3D pellet culture, in the first part of this study we applied the laser ablation and replica molding techniques to generate PDMS chips for the simultaneous culture of several cell aggregates, comparing the viability and differentiation of ACs pellets cultured in the PDMS chips with the one of standard pellets in polypropylene tubes.

Another major demand in the tissue engineering research is the possibility to generate scaffold with a control architecture that allow the control of cell distribution and/or cell orientation by topographical

cues (17). A very recent study has shown that implantable multi-well scaffolds can be used to screen *in vivo* the influence of different extracellular matrix components on the chondrogenic differentiation of cells seeded within the wells (18), demonstrating the potentiality of this approach.

In the present study, we applied laser ablation and replica molding techniques to generate multi-well implantable constructs where different cell types can be embedded both into the scaffold structure and into the wells. Such a scaffold can be used to evaluate the effect of differential cell density areas within the scaffold, a parameter that is known to affect specific biological processes such as cartilagineous matrix deposition (19,20), and the interaction between multiple cell types distributed into the scaffold with a controlled spatial disposition. We used a clinically approved fibrin glue (21-23) to validate our biofabrication process. As a proof of concept, we generated a construct with different cell density regions and we performed a subcutaneous implantation in nude mice to determine the *in vivo* behavior of the multi-well construct.

Materials and Methods

Fabrication of PMMA molds

Drawings of master molds were made by AutoCAD® software (©Autodesk, Inc.) and processed by Corel® DRAWTM software (©Corel Corporation, 2002) (Figure 1). Wells were patterned by laser ablation of a PMMA substrate, following a protocol described elsewhere (8,9), in order to yield an array of 2 and 3.4 mm wells with a conical cross-section. After an optimization phase to identify the best combination of work parameters, selected settings were: of 22.5 W, write speed of 0.08 mm/s and focal distance z of 17.2 mm.

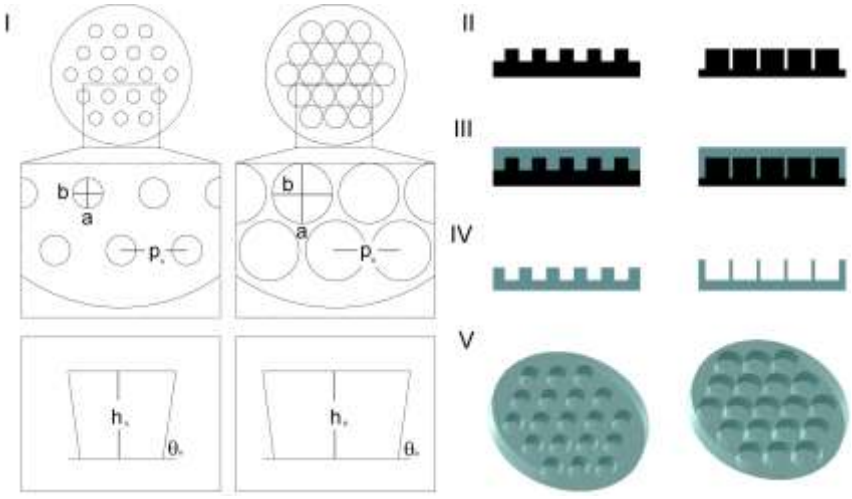

Fig. 1. Schematic of the PDMS chips fabrication process. A drawing is generated in a CAD program (top view with insets showing pitch, diameter in x and y direction, taper angles and height of the wells; I) and used as a pattern for laser ablation of the PMMA (side view; II). PDMS is poured on the patterned PMMA (side view; III). PDMS is peeled off the PMMA after polymerization (side view; IV). Rendering of the PDMS devices (IV).

Fabrication of PDMS chips and molds

For PDMS chips and molds, a PDMS mixture (Dow Corning) was prepared at a 10:1 ratio (prepolymer/curing agent), degassed, poured on a PMMA mold and baked at 70°C for 2h. Once polymerized, the PDMS was carefully peeled off the master template and cleaned with 70% EtOH. After rinsing with ddH_2O, the PDMS devices were sterilized by autoclave.

To evaluate the fidelity to the drawing, geometrical characteristics of PDMS devices (A and B) have been analyzed using the software *Image J* (eccentricity; pitch; taper angles, α and β) (Fig. 1). Well diameter was 2.0 mm for device A and 3.4 mm for device B. The height of the wells (P_A and P_B) was 2 mm, The fabrication steps and the final devices are shown in Fig. 2. PDMS molds to be used in the biofabrication of multi-well scaffolds were plasma treated (Harrick Plasma Instruments, USA) for 8 minutes to increase surface hydrophilicity immediately prior to use.

Cell isolation and expansion

Samples of articular cartilage were harvested from patients affected by osteoarthritis undergoing total hip replacement, with patients informed written consent and with the approval of the Institutional Review Board. Articular chondrocytes were isolated from cartilage by enzymatic digestion using 0.15% type II collagenase (Worthington Biochemical Co) for 22 h at 37°C, according to a previously established protocol (15). The cells were plated at a density of 10^4 cells/cm^2 and cultured in expansion medium. Expansion medium was composed as follows: High Glucose Dulbecco's Modified Eagle's Medium (HG-DMEM, Gibco) supplemented with 10% Fetal Bovine Serum (FBS, Lonza), 1% HEPES (Gibco), 1% Sodium pyruvate (Gibco), 1% Penicillin/Streptomycin/Glutamine (Gibco), 1 ng/mL Transforming Growth Factor ß-1 (TGF-ß1, Peprotech) and 5 ng/mL Fibroblast Growth Factor 2 (FGF-2, Peprotech). At subconfluence, cells were detached by 0.05% trypsin/0.53 mM EDTA (Gibco) and plated at 5×10^3 cells/cm^2 for further expansion. At passage 2 cells were frozen and stored in liquid nitrogen. When needed, cells were thawed and expanded for one passage more. To limit the expansion phase required to obtain a suitable number of cells, cells from different donors were pooled together to perform the experiments.

Fluorescent cell staining

To analyze cell distribution in the fibrin glue constructs, cells were stained either with the green fluorescent dye Vybrant DiO or with the red fluorescent dye Vybrant CM-Dil (both from Invitrogen) according to the manufacturer's instructions. Briefly, after trypsinization cells were suspended at a density of $1x10^6$ cells/mL in serum-free culture medium. Vybrant DiO or Vybrant CM-Dil was added to the cell suspension (5 µL/mL). Cells were incubated for 10 min at 37°C and then centrifuged (1500 rpm, 5 min). Supernatant was removed and the cells were washed twice in expansion medium prior to use.

Pellet formation and culture

Sterile PDMS chips were inserted into the wells of a 12-well multiplate. PDMS chips were then seeded with a total number of $2.85x10^6$ cells in order to generate aggregates containing $1.5x10^5$ cells (19 wells/PDMS chip). Cell seeding was performed by pipetting a volume of cell suspension corresponding to $1x10^5$ cells in each single well. The multi-well was then centrifuged 5 min at 230*g* to favor pellet formation and after 4 h, 2.85 ml of chondrogenic medium were added to the multiplate wells. Control pellets were prepared in 1.5 ml screw-cap tubes. Briefly, $1.5x10^5$ cells were suspended in 150 µL of chondrogenic medium, transferred to 1.5 ml screw-cap tubes and centrifuged 5 min at 230*g*. Chondrogenic medium was composed as follows: HG-DMEM supplemented with 0.029 mg/ml L-glutamine, 100 U/ml penicillin, 100 µg/ml streptomycin, 10 mM Hepes, 1 mM sodium pyruvate, 1.25 mg/ml Human Serum Albumin (HSA, Sigma-Aldrich), 1% ITS+1 (containing 1.0 mg/ml insulin from bovine pancreas, 0.55 mg/ml human transferrin, 0.5 µg/ml sodium selenite, 50 mg/ml bovine serum albumin and 470 µg/ml linoleic acid, Sigma-Aldrich), 0.1 µM dexamethasone, 0.1 mM L-ascorbic acid-2-phosphate and 10 ng/ml TGF-β1. Samples were cultured for 21 days (37°C, 5% CO_2). Medium was replaced twice a week during culture.

Generation of multi-well fibrin glue constructs

The two-component fibrin sealant Tisseel® (Baxter Biosurgery) was used to generate the fibrin glue constructs. The kit contained 110,5 mg/ml clottable protein of which 91 mg human fibrinogen and 3000 KIU/ml aprotinin solution. Thrombin was diluted to 5 U/mL in 40 mM of $CaCl_2$ at pH 7.0.

In the first phase of the study three different configurations of the bottom layer were tested: (1) 19 wells, $Ø_{well}$ 1 mm, h_{well} 1.5 mm; (2) 10 wells, $Ø_{well}$ 1.5 mm, h_{well} 1.5 mm; (3) 7 wells, $Ø_{well}$ 2 mm, h_{well} 1.5 mm. For each construct, $1.15x10^6$ green-stained cells were mixed with fibrinogen and thrombin components (1:1). The mixture was poured into the PDMS mold and let polymerize for 1 h at 37°C.

For cell seeding into the wells, red-stained chondrocytes were suspended at a concentration of $1x10^5$ cells/µL in chondrogenic medium. In the different configurations a different number of cells was seeded in the wells: (1) $1x10^5$ cells in $Ø_{well}$ 1 mm; (2) $2x10^5$ cells in $Ø_{well}$ 1.5 mm; (3) $4x10^5$ cells in $Ø_{well}$ 2 mm. After 15 min, 3 ml of chondrogenic medium were added.

In the second phase of the study, experiments with either unstained or stained cells were performed using the configuration (2) for the bottom layer ($Ø_{well}$ 1.5 mm, h_{well} 1.5 mm). Two types of fibrin glue constructs (Ø 8 mm, h 3 mm) were prepared, each containing a total number of $4x10^6$ cells: (a) multi-well fibrin glue constructs ($Ø_{well}$ 1.5 mm, h_{well} 1.5 mm) with $2x10^6$ cells dispersed in the fibrin glue (bottom layer + top layer) and $2x10^6$ cells seeded into the multi-wells as high density centers; (b) fibrin glue scaffold with $4x10^6$ cells homogeneously distributed as control group.

The multi-well bottom layer was generated as aforementioned. After polymerization, the fibrin glue layer was gently removed from the PDMS mold and transferred into a 12-well multiplate. Custom made PDMS rings ($Ø_{out}$ 10 mm, $Ø_{in}$ 8 mm, h 3 mm) were placed around the bottom layer. Then, $2x10^5$ cells were seeded in each wells and let adhere for 15 min at 37°C. Finally, a top of fibrin glue was generated to ultimate the scaffold. In this phase, the PDMS ring was used to match the bottom layer shape and to avoid fibrin glue leaking. For the top (Ø 8 mm, h 1 mm), $8.5x10^5$ cells were mixed with fibrinogen and thrombin components (1:1). This mixture was poured on top of the multi-well bottom layer and let polymerize for 1 h at 37°C before removing the PDMS ring.

To prepare fibrin glue scaffolds without wells, the custom-made PDMS rings were placed into a 12-well multiplate. Then, $4x10^6$ cells were mixed with fibrinogen and thrombin components (1:1). The mixture was poured into the PDMS ring and let polymerize for 1 h at 37°C.

After complete polymerization, samples were cultured in 3 mL of chondrogenic medium for 1 or 7 days.

In vivo implantation in nude mice of fibrin glue constructs

To evaluate the maintenance of the scaffold structure *in vivo*, the fibrin glue constructs seeded with green-stained and red-stained cells were subcutaneously implanted in nude mice. The *in vivo* study was approved by the Mario Negri Institute for Pharmacological Research (IRFMN) Animal Care and Use Committee (IACUC). Animals and their care were handled in compliance with institutional guidelines as defined in national (Law 116/92, Authorization n.19/2008-A issued March 6, 2008, Italian Ministry of Health) and international laws and policies (EEC Council Directive 86/609, OJ L 358. 1, December 12, 1987; Standards for the Care and Use of Laboratory Animals - UCLA, U.S. National Research Council, Statement of Compliance A5023-01, November 6, 1998).

Three 6-weeks-old female athymic mice were obtained from Harlan® and maintained in the Animal Care Facilities of the IRFMN, under specific pathogen-free conditions with food and water provided *ad libitum*. Animals were anesthetized by intraperitoneal injection of ketamine chloride (80 mg/kg, Imalgene, Merial) and medetomidine hydrochloride (1 mg/kg, Domitor, Pfizer). Surgical procedures were performed in sterile conditions under a laminar flow hood. Four subcutaneous pockets were created on the dorsum of each mouse by blunt dissection through cranial and caudal skin incisions. One fibrin glue scaffold was inserted in each pocket, then the skin was sutured with #4-0 Monocryl thread (Ethicon). After 28 days, the mice were euthanized by CO_2 inhalation and constructs were harvested. After the removal of the fibrotic tissue around the explants, stained cells were visualized with a fluorescence microscope.

Sample analyses

Measurement of time required for pellet seeding and medium refresh

For standard pellet culture and culture in PDMS devices, we measured the time required to perform cell seeding and medium refresh operations. Independent measures were obtained testing 3 operators with different level of skills in cell culture techniques.

Cell viability assay and DNA quantification

After 21 days of pellet culture in chondrogenic medium, cell viability was evaluated by Alamar Blue assay. Briefly, pellets were randomly harvested from different PDMS chips and from the tubes (control group) and transferred to a 96-well multiplate. Then, each pellet was incubated with 100 µL HG-DMEM supplemented with 10% Alamar Blue (4 h, 37°C). After incubation, the supernatant was harvested and fluorescence was measured (540 nm-580 nm) using a Victor X3 Plate Reader (Perkin Elmer).

The same pellets were lysed for DNA quantification. After washing with Phosphate Buffered Saline (PBS), pellets were digested (16 h, 60°C) in 500 µl of PBE buffer (100 mM Na_2HPO_4, 10 mM NaEDTA, pH 6.8) containing 1.75 mg/ml L-cystein (Sigma-Aldrich) and 14.2 U/ml papain (Worthington). DNA quantification was performed by CyQUANT Kit (Invitrogen), according to the manufacturer's instructions.

Histological and immunohistochemical evaluation

For histological analysis, pellets and fibrin glue constructs were fixed for 24 h in 10% neutral buffered formalin, embedded in paraffin and sectioned at 3 µm.

Pellet sections were stained with alcian blue (pH 2.5, Sigma-Aldrich) to visualize glycosaminoglycans (GAGs) deposition. For immunohistochemistry, sections were deparaffinized, rehydrated and treated with 3% hydrogen peroxide in distilled water for 15 minutes. Mouse monoclonal anti-Collagen II (SPM239) (prediluted, Abcam, ab54236) antibody was applied at room temperature for 1 h. The sections were labelled by the avidin-biotin-peroxidase (ABC) procedure (24) with a commercial immunoperoxidase kit (Vectastain Standard Elite; Vector Laboratories).

The immunohistochemical reaction was developed with 3.3' diaminobenzidine (DAB) for 5 min and sections were counterstained for 2 min with Mayer's haematoxylin. For morphological evaluation of fibrin glue scaffolds, sections were stained with hematoxylin and eosin (HE).

Analysis of structure and cell distribution in fibrin glue constructs

The macroscopic features of the different bottom layers were evaluated by stereomicroscope (Olympus SXZ10). Cell distribution into the scaffold and feasibility of cell seeding into the wells were evaluated by

fluorescence microscopy (Olympus IX71) using green- or red-stained cells.

Statistical analysis

Cell viability, DNA content, and metabolic activity data are presented as mean±SD. Comparison among the different experimental groups was performed by One-Way ANOVA with Dunnett's post-test (GraphPad Prism version 5.00 for Windows, GraphPad Software).

Results

Multi-well PDMS chips support the generation and culture of chondrocyte pellets

To determine the optimal laser engraving conditions to achieve the three desired well diameters, an array of lines was printed on PMMA by varying the laser power and write speed. The following settings resulted in uniform wells of the desired sizes. The laser power was set at 22.5 W, the write speed at 0.08 mm/s, and z = 17.2 mm.

Optical images of the fabricated wells can be seen in Fig. 2. PMMA microwells exhibited an irregular edge and debris distributed over the edges (Fig. 2a).

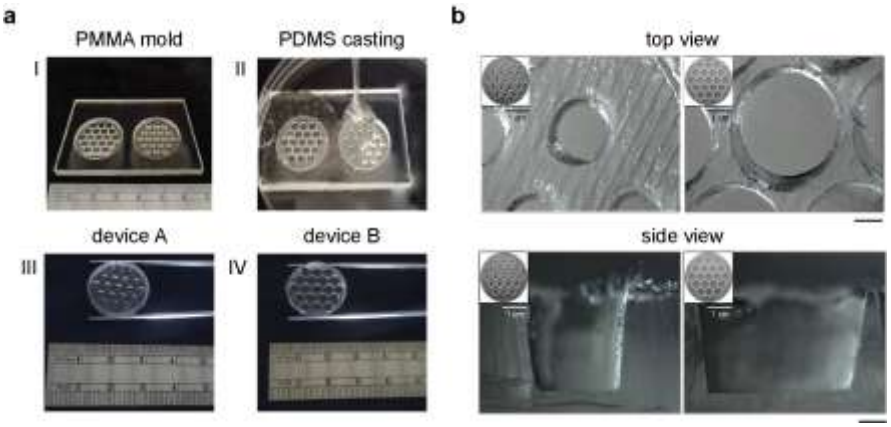

Fig. 2. PDMS chips fabrication process. (a) Ablated PMMA molds (I). PDMS casting for replica molding (II). Device A ($Ø_{well}$ 2 mm) (III). Device B ($Ø_{well}$ 3.4 mm) (IV). (b) Optical images of device A (right) and B (left). Scale bars: 1 mm except where noted.

PDMS multi-well arrays demonstrated fidelity to the original design. The pitch in the well array (center to-center distance) was 2 mm. The inner surface revealed cone-shaped walls (Fig. 2b). Articular chondrocytes were used to test the multi-well PDMS chips in order to evaluate their ability to support the formation of cell pellets.The PDMS chips were designed to fit the wells of a 12 multi-plate, allowing the simultaneous culture of a high number of samples and of different experimental conditions in the same plate,as shown in Figure 3a where PDMS chips immediately after cell seeding are depicted.. The use of these devices significantly reduced the time required for cell seeding and medium refresh operations compared to standard pellet culture, representing a technical amelioration in terms of work efficiency (Fig. 3b). The PDMS chips, thanks to the transparency of the material, also allowed to monitor the samples through microscopy throughout the entire period of culture and to measure basic parameter such as pellet area.

As shown in Fig. 3c, cell aggregates started to form already 24 hours after cell seeding and, after 21 days of culture, pellets were well-formed in both types of PDMS chips. Pellets area increased from 7 to 21 days of chondrogenic culture due to matrix deposition (Fig. 3b). At the end of culture, we compared the

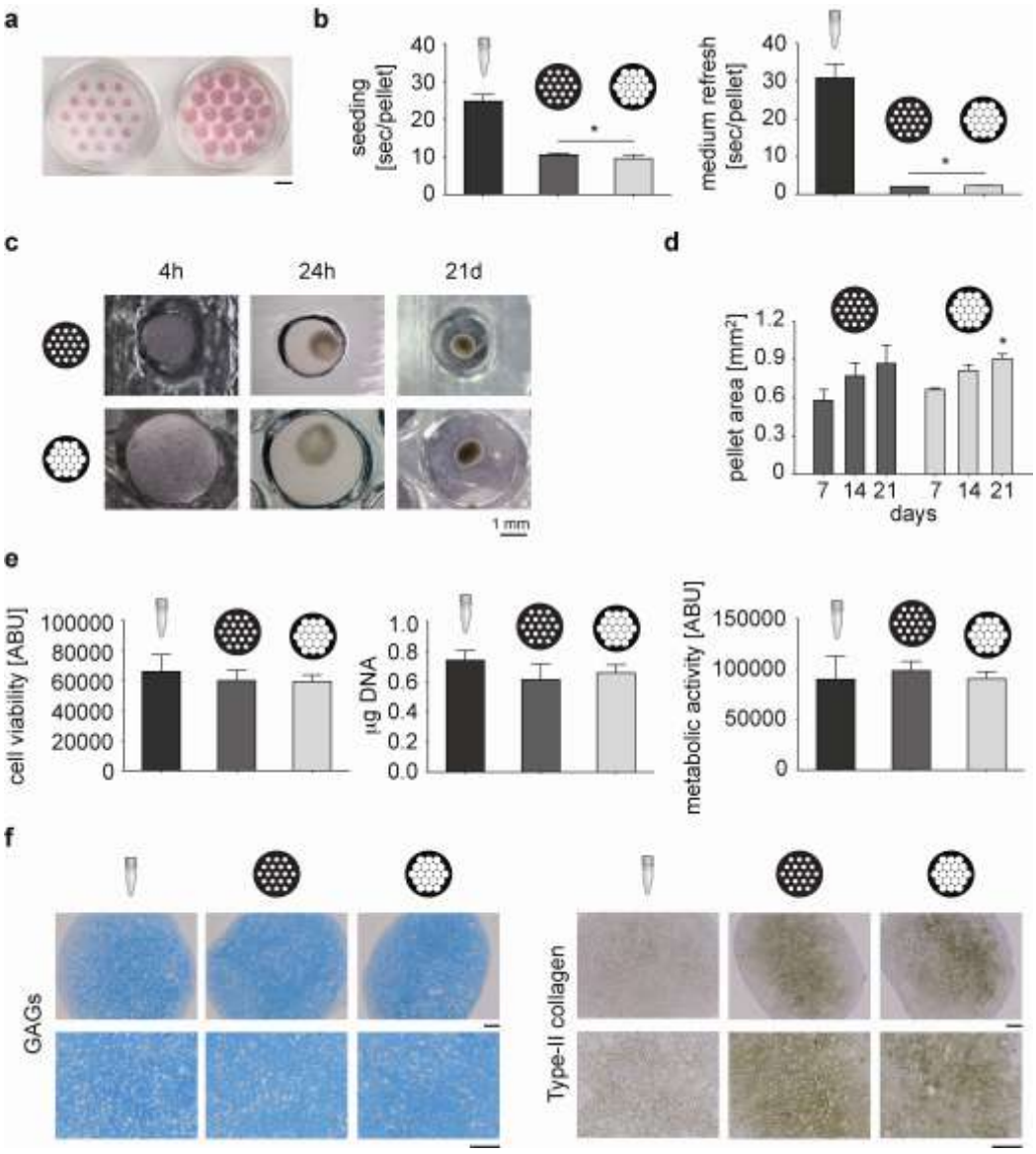

Fig. 3. Validation of PDMS chips for seeding and culture of chondrocyte pellets. (a) Picture of the two PDMS chips positioned in a 12- multiplate immediately after cell seeding. (b) Measurements of the time required to perform cell seeding and medium refresh (* $p<0.001$, PDMS chips vs standard pellet culture). (c) Micrographs of a representative well of the two PDMS chips seeded with chondrocytes at different time points. (d) Average area of pellets cultured in the PDMS chips over time (* $p<0.05$, 21 days vs 7 days). (e) DNA content and cell viability measured in pellets cultured in 1.5 ml tubes (control group, Ctrl) or in PDMS chips after 21 days of culture. Metabolic activity calculated as the ratio between cell viability and DNA content of each single pellets. (f) Histological evaluation of GAGs and type II collagen deposition in control pellets and in pellets cultured in PDMS chips after 21 days of culture.

cell viability of pellets cultured by standard technique and pellets cultured in PDMS chips (Fig. 3d). No significant difference in cell viability was observed among the different experimental groups. In the same way, the DNA content and the metabolic activity of pellets cultured in tubes and in PDMS chips did not differ, showing that pellets cultured in PDMS chips were viable and active as standard pellets. Histological evaluation revealed that GAGs deposition, which is a key marker of chondrogenic differentiation, was comparable in Ctrl pellets and in pellets cultured in multi-well PDMS chips (Fig. 3e). Lacunar structures, similar to those found in native hyaline cartilage, were observed in all the experimental groups. Analysis of type II collagen deposition by immunohistochemistry revealed a more intense staining in pellets cultured in PDMS chips compared to standard pellets, indicating the production of highly specialized extracellular matrix in these samples (Fig. 3f).

PDMS molding allows the generation of multi-well fibrin glue scaffold with differential cell density regions

Multi-well fibrin glue constructs were prepared according to the scheme depicted in Fig. 4a. The easiness of the biofabrication process allowed us to prepare a maximum of 65 samples simultaneously.

PMMA and PDMS molds with the three different tested configurations are shown in Fig. 4b. The PDMS molding was used to produce fibrin glue constructs with different multi-well pattern as shown in Fig. 5a. We noticed that the configuration with 10 wells ($Ø_{well}$ 1.5 mm) was the easiest to produce and manipulate. Indeed, the configuration with larger wells ($Ø_{well}$ 2 mm) had a very thin outer border that did not allow the easy removal of the scaffold from the PDMS mold. The peripheral border of these constructs tended to break during this operation, resulting in lateral leaking of the cells seeded into the wells. On the other hand, the configuration with smaller wells ($Ø_{well}$ 1 mm) was quite easy to manipulate since stiffer, but small imperfections in the fibrin glue bottom layer resulted in a dramatic reduction of the volume of the wells, making the cell seeding not reproducible.

Cell embedding in the bottom layer resulted in a

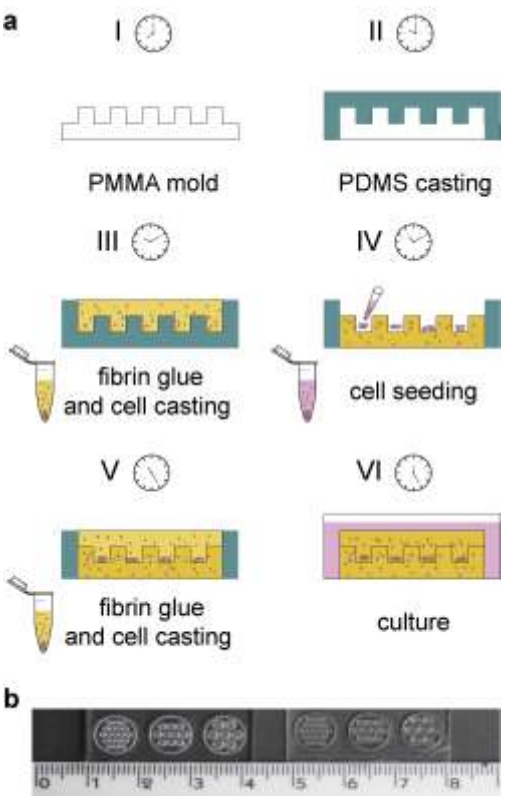

Fig. 4. Schematic of the multi-well fibrin glue construct biofabrication. (a) PMMA molds and PDMS counter-molds were generated. Cell-loaded fibrin glue was poured into the PDMS mold to generate the multi-well bottom layer. After polymerization, the wells were seeded cells. Cell-loaded fibrin glue was then poured on the the bottom layer. (b) Picture of PMMA molds (left) and PDMS counter-molds (right).

homogeneous distribution of cells throughout the scaffold (Fig. 5b, upper row, green-stained cells). The

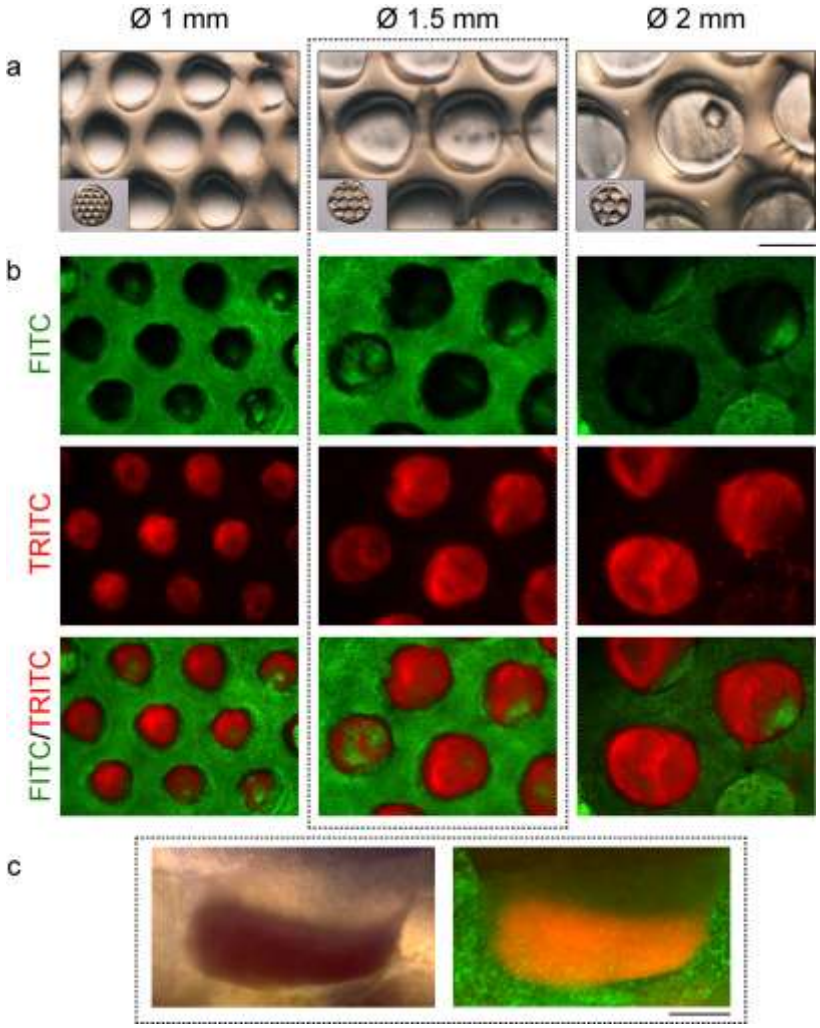

Fig. 5. Biofabrication of multi-well fibrin glue constructs. (a) Micrographs showing the different configurations designed for the fibrin glue bottom layer (scale bar 1 mm). Insets represent the entire bottom layer. (b) Cell distribution in the multi-well constructs. The upper row shows green-stained cells in the bottom layer, the middle row shows red-stained cells in the wells, and the lower row shows the merged picture of the bottom layer with the cell-seeded wells (scale bar 1 mm). (c) Side view of the fibrin glue scaffold section ($Ø_{well}$ 1.5 mm, h 1.5 mm, scale bar 1 mm).

seeding of cells in the multi-wells proved also to be effective (Fig. 5b, middle and lower row). As aforementioned, the incomplete formation of the outer border in the scaffold with $Ø_{well}$ 2 mm, was associated to inefficient cell retention into the wells as shown in Fig. 5b (lower row), where the well in the right corner in the image does not contain any red cell after 24 h of culture.

Thus, we selected the configuration with $Ø_{well}$ 1.5 mm for the prosecution of the study. The central section of the bottom layer shows the cell deposition on the bottom side of each well (Fig. 5c), demonstrating that in this configuration red-stained cells were confined into the wells and that differential cell density regions were generated within the scaffold.

Using the selected configuration of bottom layer (10 wells, $Ø_{well}$ 1.5 mm, h_{well} 1.5 mm) the construct was completed by adding the top layer. In Fig. 6a macroscopic pictures of fibrin glue scaffolds without wells and with wells immediately after complete polymerization are shown. The pattern of multi-wells was still visible under the top layer (Fig. 6a, right image). Morphological evaluation by HE staining showed that the multi-well structure was maintained after 7 days of *in vitro* culture (Fig. 6b). In control scaffolds

cells were homogeneously dispersed into the fibrin glue (left column), whereas the borders of single wells were clearly visible in multi-well scaffolds (right column). Indeed, in multi-well constructs a multi-layer of cells was visible inside the wells demonstrating that differential cell density areas were present into the scaffold. Finally, we evaluated the behavior of multi-well constructs after *in vivo* subcutaneous implantation in nude mice. After 5 weeks of implantation the dimensions of the scaffolds were dramatically reduced. The pictures reported in Fig. 7 represent the same scaffolds photographed prior and after implantation with the same microscope magnification and show the reduction of the diameter from 8 mm to 1.5-2 mm. Surprisingly, despite the reduction in the construct dimensions, the multi-well structure was maintained, as shown in the post-implantation pictures where the high density seeding areas in the wells are still clearly visible.

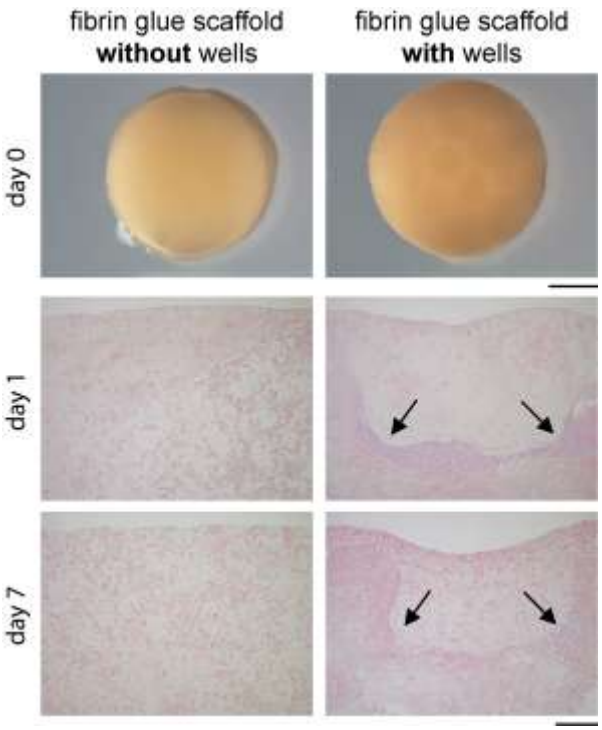

Fig. 6. Histological evaluation after 1 and 7 days of culture. (a) Representative pictures of fibrin glue scaffold. (b) Histological pictures of scaffold stained by H/E showing the borders of a single well and the distribution of cells on the bottom side of the well.

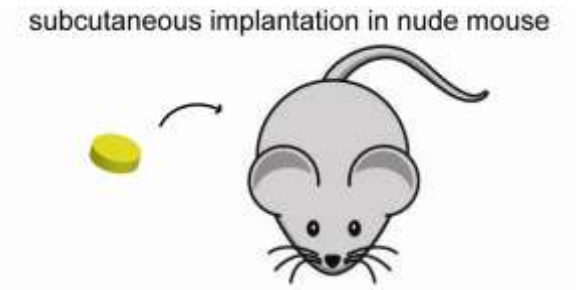

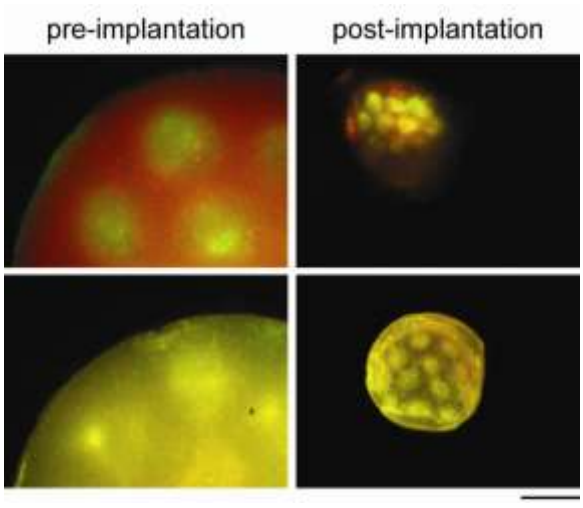

Fig. 7. Evaluation of scaffold structure maintenance after *in vivo* implantation in nude mice. Micrographs showing the dramatic shrinking of the scaffold and the maintenance of the multi-well structure after *in vivo* implantation (upper row: top and bottom layers seeded with red-stained cells, wells seeded with green-stained cells; top layer, bottom layer and wells seeded with a mix of red- and green-stained cells) (fluorescence microscopy, scale bar 1 mm).

Discussion

The primary purpose of this study was to exploit low-cost rapid prototyping techniques to generate multi-well devices for pellet culture and to biofabricate patterned fibrin glue scaffolds.

The use of the PDMS devices significantly reduced the time required for pellet seeding and medium exchange operations, which are highly time-consuming factors when handling several replicates and experimental groups. Furthermore, the possibility to culture simultaneously a maximum of 228 pellets in a single 12-multiplate allowed to reduce significantly the space required for samples culture in the CO_2 incubator. The high hydrophobicity of PDMS (25), related to the low cell adhesion on this material, led to the formation of well-defined chondrocyte pellets and the optical transparency of the PDMS chips allowed to monitor the process of pellet formation and the changes occurring during culture. The comparison between pellets generated and cultured in PDMS chips with pellets in polypropylene tubes did not reveal any significant difference in terms of DNA content, cell viability, and metabolic activity. Deposition of GAGs was similar in the different experimental groups, whereas type-II collagen was more present in pellets cultured in the PDMS chips compared to standard pellets. These results indicate that the generated system was able to support very well both cell viability and chondrogenic differentiation, thus representing an appealing option for 3D cell culture. A similar approach has been used in a very recent study to generate and culture chondrocyte micro-pellets (166 cells each) (4). In this study, the PDMS insert surface required a chemical surface treatment to avoid cell spreading all over the well. Differently, in our PDMS devices we did not need to perform any surface treatment since, probably due to the higher ratio between the number of cells and the surface available for cell adhesion, centrifugation was sufficient to trigger the formation of pellet in the wells. The generated PDMS chips can be also exploited to perform the indirect co-culture of cell aggregates obtained from different cell types. Indeed, thanks to the possibility to precisely seed each single well with a specific cell population and to retrieve pellets from selected wells this system would allow to evaluate the effect of paracrine factors in each cell type, representing a complementary alternative to the trans-well system.

In the second part of the study we applied the same rapid prototyping approach to produce an implantable multi-well fibrin glue scaffold. It has been shown that cell density affects the capability of chondrocyte to generate specific cartilagineous matrix. In particular, several studies have shown that a high cell density in a 3D scaffold improves cartilagineous matrix deposition (19,20). However, this consideration needs to take in account the limitations related to the great number of chondrocytes required to seed the scaffolds with such a high cell density. This requirement is particularly critical considering the limited size of the harvestable biopsy of autologous cartilage that is related to the need to expand *in vitro* articular chondrocytes to achieve a relevant number of cells, implying major drawbacks such as chondrocytes de-differentiation (10-12,26). The generation of high cell density areas

within a scaffold may represent a successful approach to overcome this issue, leading to the formation of "chondrogenic centers" that drive the differentiation process and positively influence the differentiation of regions with lower cell density. Similar approaches have been proposed by other groups that have used chondrocytes aggregates of different dimensions to seed 3D scaffolds (3,27). Here, we did not generate the chondrocyte aggregate before scaffold seeding, but thanks to the ability of cells to adhere to the fibrin glue, regions with high cell density were created by seeding a confluent cell multilayer within the wells. However, the proposed scaffold configurations could be seeded with pre-formed aggregates, being the dimensions of the wells compatible with the dimensions of chondrocyte pellets obtained through standard techniques ($1.5x10^5$ - $5x10^5$ cells/pellet).

As hypothesized for the PDMS chips, a multi-well scaffold like the one generated in this study can be used to evaluate the effects of the co-culture between different cell types, such as chondrocytes and mesenchymal stem cells that are usually investigated through standard 3D culture models which do not allow the spatially controlled distribution of cells, such as pellet culture (28-30) and scaffolds (31,32). The controlled distribution of mesenchymal stem cells and bovine chondrocytes has been performed in a very recent study demonstrating that implantable multi-well scaffolds can be used to screen simultaneously the effect of several extracellular matrix components on the chondrogenic ability of MSCs in co-culture with bovine articular chondrocytes (18). Differently from this screening platform where cells are seeded uniquely into the wells, in our multi-well construct cells can be seeded both into the scaffold structure and inside the wells, allowing to evaluate the interaction among multiple cell population distributed in different regions of the scaffold.

The implantation in nude mice revealed that the architecture of the construct was very stable. Indeed, after 5 weeks of *in vivo* subcutaneous implantation, despite the dramatic shrinking of fibrin glue that has been reported also by other groups (33,34), we found that the multi-well structure was maintained, indicating that our fibrin scaffolds underwent poor remodeling over time. However, since lower concentrations of fibrinogen are compatible with the biofabrication of fibrin glue scaffolds with a controlled architecture (35), this parameter can be modulated in order to increase or decrease the stability of the constructs, depending on the desired application.

Conclusions

We have presented a simple and economical method, employing technologies and instruments accessible at most of the tissue engineering labs, for the generation of devices for the culture of multiple cell aggregates and for scaffold prototyping, which could have a broad range of applications in several research fields.

Acknowledgements

I would like to acknowledge all the co-authors: Piraino F., Kemp R.J., Di Caro C., Lovati A.B., Di Giancamillo A., Moroni L., Rasponi M., Moretti M.

References

1. Burdett E, Kasper FK, Mikos AG, Ludwig JA. Engineering tumors: a tissue engineering perspective in cancer biology. Tissue Eng Part B Rev.16:351-9. 2010.
2. de Ridder L, Cornelissen M, de Ridder D. Autologous spheroid culture: a screening tool for human brain tumour invasion. Crit Rev Oncol Hematol.36:107-22. 2000.
3. Moreira Teixeira LS, Leijten JC, Sobral J, Jin R, van Apeldoorn AA, Feijen J, van Blitterswijk C, Dijkstra PJ, Karperien M. High throughput generated micro-aggregates of chondrocytes stimulate cartilage formation in vitro and in vivo. Eur Cell Mater.23:387-99. 2012.
4. Babur BK, Ghanavi P, Levett P, Lott WB, Klein T, Cooper-White JJ, Crawford R, Doran MR. The interplay between chondrocyte redifferentiation pellet size and oxygen concentration. PLoS One.8:e58865. 2013.
5. Whitesides GM, Ostuni E, Takayama S, Jiang X, Ingber DE. Soft lithography in biology and biochemistry. Annu Rev Biomed Eng.3:335-73. 2001.
6. Becker H, Gartner C. Polymer microfabrication technologies for microfluidic systems. Anal Bioanal Chem.390:89-111. 2008.
7. Napolitano AP, Chai P, Dean DM, Morgan JR. Dynamics of the self-assembly of complex cellular aggregates on micromolded nonadhesive hydrogels. Tissue Eng.13:2087-94. 2007.
8. Selimovic S, Piraino F, Bae H, Rasponi M, Redaelli A, Khademhosseini A. Microfabricated polyester conical microwells for cell culture applications. Lab Chip.11:2325-32. 2011.
9. Piraino F, Selimovic S, Adamo M, Pero A, Manoucheri S, Bok Kim S, Demarchi D, Khademhosseini A. Polyester -assay chip for stem cell studies. Biomicrofluidics.6:44109. 2012.
10. Schulze-Tanzil G. Activation and dedifferentiation of chondrocytes: implications in cartilage injury and repair. Ann Anat.191:325-38. 2009.
11. Giannoni P, Cancedda R. Articular chondrocyte culturing for cell-based cartilage repair: needs and perspectives. Cells Tissues Organs.184:1-15. 2006.
12. Giannoni P, Pagano A, Maggi E, Arbico R, Randazzo N, Grandizio M, Cancedda R, Dozin B. Autologous chondrocyte implantation (ACI) for aged patients: development of the proper cell expansion conditions for possible therapeutic applications. Osteoarthritis Cartilage.13:589-600. 2005.
13. Dehne T, Schenk R, Perka C, Morawietz L, Pruss A, Sittinger M, Kaps C, Ringe J. Gene expression profiling of primary human articular chondrocytes in high-density micromasses reveals patterns of recovery, maintenance, re- and dedifferentiation. Gene.462:8-17. 2010.
14. Zhang Z, McCaffery JM, Spencer RG, Francomano CA. Hyaline cartilage engineered by chondrocytes in pellet culture: histological, immunohistochemical and ultrastructural analysis in comparison with cartilage explants. J Anat.205:229-37. 2004.
15. Jakob M, Demarteau O, Schafer D, Hintermann B, Dick W, Heberer M, Martin I. Specific growth factors during the expansion and redifferentiation of adult human articular chondrocytes enhance chondrogenesis and cartilaginous tissue formation in vitro. J Cell Biochem.81:368-77. 2001.
16. Bernstein P, Dong M, Corbeil D, Gelinsky M, Gunther KP, Fickert S. Pellet culture elicits superior chondrogenic redifferentiation than alginate-based systems. Biotechnol Prog.25:1146-52. 2009.
17. Gerberich BG, Bhatia SK. Tissue scaffold surface patterning for clinical applications. Biotechnol J.8:73-84. 2013.
18. Higuera GA, Hendriks JA, van Dalum J, Wu L, Schotel R, Moreira-Teixeira L, van den Doel M, Leijten JC, Riesle J, Karperien M, van Blitterswijk CA, Moroni L. In vivo screening of extracellular matrix components produced under multiple experimental conditions implanted in one animal. Integr Biol (Camb).5:889-98. 2013.
19. Mauck RL, Wang CC, Oswald ES, Ateshian GA, Hung CT. The role of cell seeding density and nutrient supply for articular cartilage tissue engineering with deformational loading. Osteoarthritis Cartilage.11:879-90. 2003.
20. Talukdar S, Nguyen QT, Chen AC, Sah RL, Kundu SC. Effect of initial cell seeding density on 3D-engineered silk fibroin scaffolds for articular cartilage tissue engineering. Biomaterials.32:8927-37. 2011.
21. Scotti C, Mangiavini L, Boschetti F, Vitari F, Domeneghini C, Fraschini G, Peretti GM. Effect of in vitro culture on a chondrocyte-fibrin glue hydrogel for cartilage repair. Knee Surg Sports Traumatol Arthrosc.18:1400-6. 2010.
22. Ahmed TA, Dare EV, Hincke M. Fibrin: a versatile scaffold for tissue engineering applications. Tissue Eng Part B Rev.14:199-215. 2008.
23. Ahmed TA, Hincke MT. Strategies for articular cartilage lesion repair and functional restoration. Tissue Eng Part B Rev.16:305-29. 2010.
24. Hsu SM, Raine L, Fanger H. Use of avidin-biotin-peroxidase complex (ABC) in immunoperoxidase techniques: a comparison between ABC and unlabeled antibody (PAP) procedures. J Histochem Cytochem.29:577-80. 1981.
25. Berthier E, Young EW, Beebe D. Engineers are from PDMS-land, Biologists are from Polystyrenia. Lab Chip.12:1224-37. 2012.
26. Steinert AF, Ghivizzani SC, Rethwilm A, Tuan RS, Evans CH, Noth U. Major biological obstacles for persistent cell-based regeneration of articular cartilage. Arthritis Res Ther.9:213. 2007.
27. Wolf F, Candrian C, Wendt D, Farhadi J, Heberer M, Martin I, Barbero A. Cartilage tissue engineering using pre-aggregated human articular chondrocytes. Eur Cell Mater.16:92-9. 2008.
28. Giovannini S, Diaz-Romero J, Aigner T, Heini P, Mainil-Varlet P, Nesic D. Micromass co-culture of human articular chondrocytes and

human bone marrow mesenchymal stem cells to investigate stable neocartilage tissue formation in vitro. Eur Cell Mater.20:245-59. 2010.

29. Wu L, Prins HJ, Helder MN, van Blitterswijk CA, Karperien M. Trophic effects of mesenchymal stem cells in chondrocyte co-cultures are independent of culture conditions and cell sources. Tissue Eng Part A.18:1542-51. 2012.
30. Lopa S, Colombini A, Sansone V, Preis FW, Moretti M. Influence on chondrogenesis of human osteoarthritic chondrocytes in co-culture with donor-matched mesenchymal stem cells from infrapatellar fat pad and subcutaneous adipose tissue. Int J Immunopathol Pharmacol.26:23-31. 2013.
31. Sabatino MA, Santoro R, Gueven S, Jaquiery C, Wendt DJ, Martin I, Moretti M, Barbero A. Cartilage graft engineering by co-culturing primary human articular chondrocytes with human bone marrow stromal cells. J Tissue Eng Regen Med. 2012.
32. Hildner F, Concaro S, Peterbauer A, Wolbank S, Danzer M, Lindahl A, Gatenholm P, Redl H, van Griensven M. Human adipose-derived stem cells contribute to chondrogenesis in coculture with human articular chondrocytes. Tissue Eng Part A.15:3961-9. 2009.
33. Silverman RP, Passaretti D, Huang W, Randolph MA, Yaremchuk MJ. Injectable tissue-engineered cartilage using a fibrin glue polymer. Plast Reconstr Surg.103:1809-18. 1999.
34. Peretti GM, Randolph MA, Villa MT, Buragas MS, Yaremchuk MJ. Cell-based tissue-engineered allogeneic implant for cartilage repair. Tissue Eng.6:567-76. 2000.
35. Koroleva A, Gittard S, Schlie S, Deiwick A, Jockenhoevel S, Chichkov B. Fabrication of fibrin scaffolds with controlled microscale architecture by a two-photon polymerization-micromolding technique. Biofabrication.4:015001. 2012.

Chapter 7

The use of a bi-directional perfusion bioreactor for cartilage engineering promotes the reconstruction of hyaline cartilage rather than fibrotic cartilage

Abstract

We previously reported that a cocktail of bone morphogenetic protein (BMP)-2, insulin and triiodothyronine (BIT) could trigger re-differentiation of human chondrocytes after their amplification on plastic, with cartilage-characteristic matrix reconstruction when the chondrocytes were seeded in collagen sponges. However, this matrix was not homogenously distributed in the scaffolds, most likely because the collagen sponges were cultivated in static conditions. With the aim of enhancing cellular access to nutrients and the soluble factors, bi-directional flow was tested to perfuse the scaffolds during cartilage reconstruction.

After 3 weeks of amplification on plastic, ACs were seeded then cultivated for 21 days in collagen sponges under bi-directional flow, by using a prototype of OPB (Oscillating Perfusion Bioreactor). We established a program of perfusion including phases of high and low perfusion speeds to alternate sequences of cell stimulation and matrix deposition. For comparison, cultures of ACs in collagen sponges were performed in static conditions. The status of the chondrocyte phenotype and the nature of the matrix synthesized in collagen sponges were evaluated by real time PCR, Western Blotting and immunohistochemistry analyses. The viability and cell proliferation were also monitored.

The results clearly indicate that perfusion improved cartilage matrix deposition within the sponges, in comparison with static conditions. More precisely, in the sponges cultured in the bioreactor, redifferentiated and metabolically active ACs produced a cartilaginous matrix rich in type II and type IX collagens and in glycosaminoglycans, with no sign of hypertrophy. Interestingly, a much lower amount of type I collagen was produced in the sponges cultivated in dynamic conditions, indicating therefore that bi-directional perfusion limits the risk of fibrocartilage formation.

The combination of ACs, collagen sponges, and the BIT cocktail with the bi-directional perfusion bioreactor favors the reconstruction of hyaline cartilage. Importantly, bi-directional perfusion abolishes the spatial concentration gradients routinely observed in scaffolds in static culture. This study also demonstrates the value of a multi-factorial approach for the design of cell-based grafts for cartilage repair.

Introduction

Population aging leads to an increasing number of symptoms related to degenerative lesions in articular cartilage. Among the younger population, traumatic cartilage lesions also have an increasing incidence given the importance of intensive sport practice in our society. Articular cartilage is an avascular tissue that has poor intrinsic healing capacities. Consequently, cartilage focal lesions are irreversible and often lead to osteoarthritis (OA), causing pain and disabilities for the patients. Several surgical approaches such as mosaicplasty or microfracture have been developed to repair damaged cartilage and avoid total joint replacement. However, these treatments remain unsatisfactory with the formation of a fibrocartilage rich in type I collagen which has different biomechanical properties from the hyaline cartilage, rich in type II collagen.

Consequently, articular cartilage is a good candidate for cell therapy and tissue engineering approaches. The first cell therapy used in orthopaedic surgery was the Autologous Chondrocyte Implantation (ACI) developed by Brittberg *et al.* (1). ACI is now performed worldwide for the treatment of articular cartilage focal lesions. Briefly, chondrocytes are collected from a small biopsy of non-bearing healthy cartilage and amplified *in vitro*. The cell suspension is then implanted in the focal lesion of the same patient under a periosteal flap for the first generation of ACI or under a collagen membrane for the second.

During chondrocyte expansion *in vitro*, it is well known that a dedifferentiation process occurs (2). This dedifferentiation is characterized by the loss of type II collagen expression in favor of fibrotic type I collagen expression (2,3). Thus, several studies demonstrated that the tissue produced during ACI was a fibrocartilage rich in type I collagen. Despite improvement in the quality of life of the patients, health agencies that survey ACI now agree that the method should be improved by the use of biomaterials and growth factors in order to deliver well differentiated chondrocytes and to broaden ACI clinical application to larger defects and developing OA lesions.

In the context of matrix associated ACI (MACI), we previously demonstrated the reconstruction of a cartilage-characteristic matrix in collagen sponges by sequential addition of soluble factor cocktails during chondrocyte amplification (FGF-2 and Insulin, FI) and their culture in collagen scaffolds (BMP-2, Insulin and T3, BIT) (4). The FI-BIT combination allows a strong increase of cell reservoir, the chondrocyte redifferentiation and an enhanced matrix synthesis in collagen sponges. However, matrix deposition occurred only on the periphery of the scaffold, suggesting that nutrients and growth factors did not access the core of the sponge.

Perfusion bioreactors are known to improve the homogeneity of the matrix produced in biomaterials (5) (6). In this study, a bidirectional interstitial perfusion bioreactor prototype, the Oscillating Perfusion Bioreactor (OPB) (7), was selected to perfuse the collagen sponges, with the view of improving cellular

access to nutrients and growth factors. The OPB was first used to enhance the formation of tissue engineered cardiac grafts independently and interactively with insulin-like growth factor (8). In another study, Valonen *et al.* used the OPB to engineer cartilage constructs in polycaprolactone scaffolds (9). They demonstrated that the culture of human mesenchymal stem cells in polycaprolatone scaffolds in the OPB prototype led to higher total collagen content and more homogenous matrix deposition in a chondrogenic medium. These exciting results prompted us to investigate the effects of bidirectional perfusion to stimulate human articular chondrocytes in collagen sponges, in combination with the BIT cocktail, in the context of MACI procedure. Special attention was given to the newly synthesized matrix in the collagen sponges through a careful analysis of its deposition and its protein composition.

Materials and Methods

Cell amplification

Primary cultures of human chondrocytes were prepared from macroscopically healthy zones of osteoarthritic hip joints obtained from 12 donors (age range: 33-74) undergoing total hip replacement. The study was carried out in full accordance with local ethics guidelines and cartilage samples were collected after obtaining written informed consent of the donors and with the approval of the Institute Review Board. Chondrocytes were extracted as previously described (10). Briefly, small slices of cartilage were sequentially digested in culture medium consisting of DMEM/Ham's F12 (Gibco-Invitrogen) with 0.2 % trypsin (Sigma) for 30 min at 37°C, followed by 0.15 % bacterial collagenase A (Roche Applied Science) overnight. The cells were then seeded at a density of 0.8×10^4 cells/cm^2 in culture medium supplemented with 10 % Newborn Calf Serum (NCS) (Hyclone), 50 µg/ml streptomycin (Panpharma) and 2 µg/ml amphotericin B (Bristol Myers Squibb). At this stage, cells were designated P0. 36 h after seeding (P0-36h), medium was changed and was supplemented with 5 ng/ml FGF-2 (R&D Systems) and 5 µg/ml insulin (Umuline rapide, Lilly). The cocktail of FGF-2 and insulin was designated FI. The culture medium was replaced 3 times a week until cells reached confluence. The cells were then trypsinized and replated at the same density for another passage (P1). After each trypsinization, cells were stained with Trypan blue and the ones excluding the dye were counted with a hemocytometer.

The Oscillating Perfusion Bioreactor (OPB)

The Oscillating Perfusion Bioreactor was used as previously described (8). In brief, each scaffold was press-fitted into the base of a specimen holder. Then, the specimen holder was closed, resulting in a collagen sponge immobilized in a 6.35-mm-diameter by 8-mm-long chamber within a loop of gas-permeable silicone rubber tubing (1/32 inch wall thickness, Cole Parmer Vernon Hills, IL). Each loop was

mounted on a 12.5-cm-diameter supporting disc (Fig. 1). 18 closed-loop chambers were mounted on an incubator-compatible motorized frame that slowly oscillated the chambers around their central axis (Fig. 1). Interstitial fluid flow was ensured by fixing the construct within the specimen chamber to avoid fluid flow around the construct.

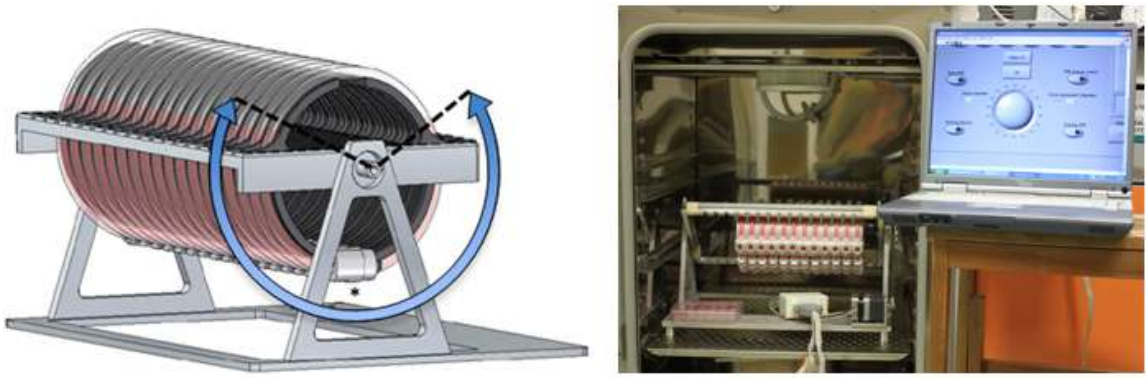

Fig. 1. Oscillating Perfusion Bioreactor (OPB). The scaffold is fixed into a sample holder (asterisk) which is connected to a silicon tube forming the culture chamber. The chamber rotates around the central axis following an oscillatory movement, allowing the bi-directional interstitial perfusion through the scaffold full-thickness. A maximum of 18 independent chambers can be simultaneously positioned in the OPB frame. The left picture shows the OPB in the incubator with the PC-based control.

Cell culture in collagen sponges

Collagen sponges composed of native (90-95%) type I collagen and (5-10%) type III collagen were prepared from calf skin by Symatese Biomatériaux (Chaponost, France). They were crosslinked to increase their stability by using glutaraldehyde and sterilized by 25 kGy β-radiation. They were sized with a skin biopsy punch (Laboratoires Stiefel, France) as discs with 8 mm diameter and 2 mm thickness, which corresponds to a volume of 0.1 cm^3. Their pore size was around 100 nm.

Static conditions

Passaged P1 chondrocytes contained in 15 ml of culture medium were seeded onto the sponges with 13×10^6 cells/cm^3 (750 000 cells per sponge) and the sponges were placed in 6-well culture plates and incubated at 37°C for 2 h. Ten milliliters of culture medium containing 10 % NCS and supplemented with 50 µg/ml 2-Phospho-L-ascorbic acid (trisodium salt, Fluka) was then added to the wells. After 48h, medium was replaced by culture medium containing 10 % NCS and supplemented with 50 µg/ml 2-Phospho-L-ascorbic acid in the absence or presence of 200 ng/ml of recombinant human BMP-2 (Dibotermine-alpha, drug form of BMP-2 contained in the kit InductOs, Wyeth), 5 mg/ml insulin (Umulin, Lilly) and 100 nM thyroxin T3 (Sigma). The cocktail of BMP-2, insulin and T3 was designated BIT. The medium containing 10 % NCS and ascorbate was referred as control medium for the culture in scaffold. Medium was replaced twice a week over a culture period of 21 days.

Dynamic conditions

Passaged P1 chondrocytes were dynamically seeded onto the sponges with 13×10^6 cells/cm^3. More precisely, three milliliters of cell suspension were added to 7 ml of culture medium in each OPB chambers. The OPB worked at 1000 µm/s for 24h and was slowed down at 300 µm/s for the following 24 h.

After 48 h, medium was replaced by six milliliters of culture medium containing 10 % NCS, 50 µg/ml streptomycin (Panpharma) and 2 µg/ml amphotericin B (Bristol Myers Squibb) and supplemented with 50 µg/ml 2-Phospho-L-ascorbic acid (trisodium salt, Fluka), in the absence or presence of 200 ng/ml of recombinant human BMP-2 (Dibotermine-alpha, drug form of BMP-2 contained in the kit InductOs, Wyeth), 5 mg/ml insulin (Umulin, Lilly) and 100 nM thyroxin T3 (Sigma). The cocktail of BMP-2, insulin and T3 was designated BIT. The culture medium containing 10 % NCS and ascorbate was referred as control medium for the dynamic culture in scaffold. Medium was replaced twice a week over a culture period of 21 days.

Program 1: After the seeding phase, and during the whole culture period, the OPB worked at a constant speed of 100 µm/s.

Program 2: After the seeding phase, during 72 h, the OPB worked at a constant speed of 5 µm/s. Then, a progressive increase of perfusion speed from 5 µm/s to 20 µm/s was applied in 7 days. During the last 9 days, cycles with variations of perfusion flow rate were planned as followed: 8 h at 5 µm/s followed by a quick increase to 20 µm/s in 16 h.

The programs of dynamic culture are indicated as prog 1 and prog 2 in the text.

In vivo subcutaneous implantation

The *in vivo* study was approved by the Mario Negri Institute for Pharmacological Research (IRFMN) Animal Care and Use Committee (IACUC). Animals and their care were handled in compliance with institutional guidelines as defined in national (Law 116/92, Authorization n.19/2008-A issued March 6, 2008, by the Italian Ministry of Health) and international laws and policies (EEC Council Directive 86/609, OJ L 358. 1, December 12, 1987; Standards for the Care and Use of Laboratory Animals - UCLA, U.S. National Research Council, Statement of Compliance A5023-01, November 6, 1998).

6-weeks-old female athymic mice were obtained from Harlan® and maintained in the Animal Care Facilities of IRFMN, under specific pathogen-free conditions with food and water provided *ad libitum*. Animals were anesthetized by intraperitoneal injection of ketamine chloride (80 mg/kg, Imalgene, Merial) and medetomidine hydrochloride (1 mg/kg, Domitor, Pfizer) and surgeries were performed under a laminar flow hood, in sterile conditions. Unconnected subcutaneous pockets were created on the dorsum of each mouse by blunt dissection through cranial and caudal skin incisions. After *in vitro* culture for 21 days, one collagen sponge was inserted per pocket, then the skin was sutured with #4-0

Monocryl thread (Ethicon).

After 6 weeks, the mice were euthanized by CO_2 inhalation. At explantation, all constructs were dissected free from the nude mice, weighed and processed for histological analysis.

Gene expression analysis by reverse transcription-polymerase chain reaction (RT-PCR)

Total RNA was isolated from the chondrocytes cultured in monolayer or in collagen sponges after 21 days of culture by using the NucleoSpin RNA II kit (Macherey-Nagel), according to manufacturer's instructions. Total RNA was then reverse transcribed as previously described (11).

Real-time PCR amplifications were performed in a 20 µl reaction mix containing 10 µl Fast Start Universal SYBR green master (Roche), 4 µl RT aliquot diluted at 1:5 in sterilized water, 300 nM each primer and 4 µl water. Amplification was performed in a Rotorgene (Qiagen). Thermal cycling conditions consisted of an initial denaturation step of 95°C for 2 min, 40 cycles of 95°C for 15s and annealing and extension at 60°C for 30s. The sequences of the primers used in this study have been previously described (12). Fluorescence thresholds (C_t) were determined automatically by the software with efficiencies of amplification for the studied genes ranging between 90% and 110%. *GAPDH* C_t value was substracted from the target sequence C_t value to obtain ΔC_t. The level of expression was then calculated as $2^{-\Delta Ct}$ and expressed as the mean of duplicate samples.

Antibodies

Polyclonal rabbit antibodies to human type II collagen (Ref 20211) were kindly provided by D. J. Hartmann (13). Polyclonal rabbit antibodies to type I collagen were from Novotec (Ref 20111) and to actin from Sigma (Ref A5060). Monoclonal antibody to type IX collagen (23-5D1) was kindly provided by B. R. Olsen (14). Secondary antibodies were: alkaline phosphatase-conjugated anti-rabbit or anti-mouse IgG (Bio-Rad) and horseradish peroxidase (HRP)-conjugated anti-rabbit IgG (Cell signaling for Western blotting assays and Vector kit Immpress for immunohistochemistry experiments).

Western-blot analysis

After 21 days of *in vitro* culture, collagen sponges were frozen in liquid nitrogen. After thawing, they were rinsed with phosphate-buffered saline containing 2 mM EDTA and 0.2 mM PMSF, refrozen, then ground with a mortar and pestle into a fine powder finally resuspended and boiled in Laemmli buffer.

For Western-blot analysis, equivalent amounts of proteins were separated by SDS-polyacrylamide gel electrophoresis on 4-12 % gradient gels for sponge samples, and on 6 % gels for culture medium samples. After transfer, membranes were probed with primary antibodies, washed and incubated with alkaline phosphatase-conjugated IgG for types I, II and IX collagens or with HRP-conjugated IgG for actin

detection. After multiple washes, bound antibodies were detected on X-ray films using an Immun-star AP or HRP chemiluminescent substrate (Bio-Rad). Membranes were re-probed with antibodies after striping (Re-Blot Plus Strong, Chemicon).

Densitometry analyses were performed for type I and type II collagen on the western blotting data from every experiment with the ImageJ software. The values were calculated as the total of each collagen forms, namely the mature collagen chains, the unprocessed chains (pro) and the processing intermediates of the procollagen containing the aminopropetide (pN) or the carboxypropetide (pC), and normalized to the actin.

Histological and immunohistochemical analysis

Histological examinations of the collagen sponges seeded with chondrocytes were performed after 21 days of *in vitro* culture and after subsequent 6 weeks of *in vivo* implantation in nude mice. The collagen sponges were rinsed in phosphate-buffered saline and fixed for 24 hours with 4 % neutral-buffered formalin. After dehydration in a graded series of ethanol baths, samples were embedded in paraffin, sectioned at 5 µm and stained with Mayer's hematoxylin. For histochemical detection of sulfated proteoglycans, sections were stained with 0.5% safranin-O in 0.1 M sodium acetate at pH 7.4 for 10 min. Safranin-O is a cationic dye that binds GAGs and stains orange in an aqueous mounting medium (15).

Hematoxylin-eosin counterstaining and immunohistochemical analysis were performed on 4-5 µm sections. Incubation with type II collagen antibodies was followed by incubation with HRP-conjugated secondary antibodies. Sections were revealed with diaminobenzidine and observed with a DM 750 microscope (Leica) with an integrated color camera (ICC50 HD). Image acquisition was achieved with Las Ez software (Leica).

Statistical analysis

Differences in relative gene expression between experimental groups were analyzed using the Mann-Whitney *U*-test for non-parametric analysis. A p-value < 0.05 was considered as significant. The number of experiments carried out is noted in the figure legends.

Results

Topography of the neosynthesized matrix in the collagen sponges

Chondrocytes were amplified in monolayer and then seeded on collagen sponges for a three-week culture period in static or in dynamic conditions. The metabolic activity of the chondrocytes was verified during monolayer expansion and at the end of the culture in collagen sponges (data not shown).

Haematoxylin eosin stainings were realized to assess the repartition of the matrix synthesized by chondrocytes in collagen sponges. The proteoglycan content was evaluated by safranin O staining. In static culture conditions, as expected, a peripheral deposition of matrix rich in proteoglycans was evidenced (Fig. 2).

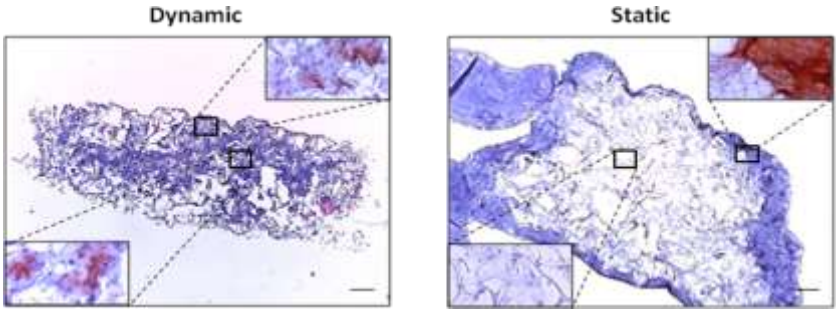

Fig. 2. Deposition of cartilage-characteristic matrix under static and dynamic conditions**.** Human articular chondrocytes were cultured in collagen sponges for 21 days in static or dynamic conditions (prog 1), in the presence of BIT cocktail. Haematoxylin Eosin staining shows the matrix distribution in the sponges (Scale bars 100µm). Inserts show the Safranin O staining of the scaffold periphery (top right) and core (bottom left) at higher magnification. Images shown are representative of the experimental results (n=6).

No matrix production was detected in the core of the collagen sponges. On the contrary, under bi-directional perfusion, we observed a homogenous deposition of matrix within the scaffold. The produced matrix was characteristic of cartilage with the presence of proteoglycans both in the core and at the periphery of the scaffold.

Characterization of the matrix synthesized by chondrocytes in the collagen sponges

To further characterize the matrix produced by chondrocytes in the collagen sponges, we realized immunohistochemical analyses for type II and type I collagens that are markers of hyaline cartilage and fibrocartilage respectively.

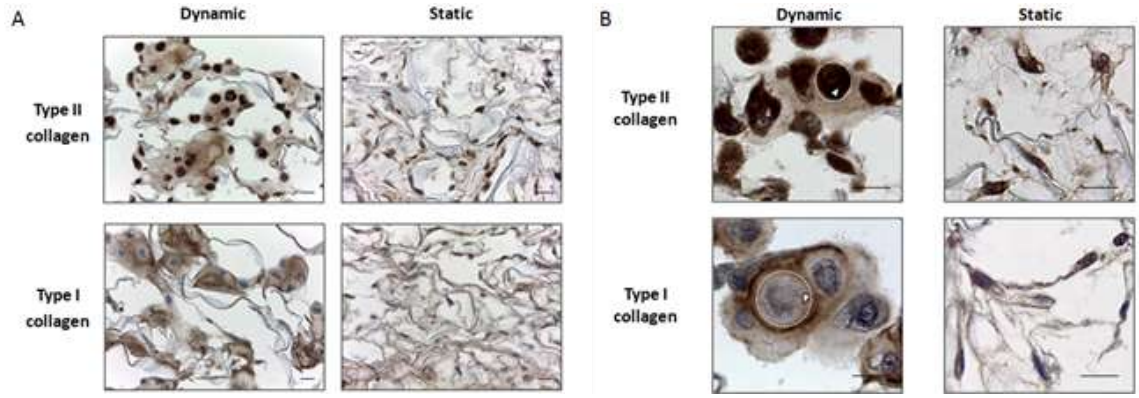

Fig. 3. Immunostaining of type II and type I collagen neo-synthesized by chondrocytes in collagen sponges in static or dynamic conditions. The chondrocytes were cultured for 21 days in collagen sponges in presence of the BIT cocktail in static or dynamic conditions (prog 2). The pictures show the scaffold core and are representative of experiments performed with cells isolated from six donors. (A) Dynamic culture conditions led to the formation of matrix production units rich in collagens (Scale bar: 10µm) (B) At the cellular level (dotted line), under dynamic culture conditions, the chondrocyte cytoplasm (white arrow head) is stained for type II but not for type I collagen (Scale bar: 10µm).

In static culture conditions, in the scaffold core, chondrocytes were isolated and had a fibroblastic-like

shape characteristic of dedifferentiated chondrocytes (Fig. 3A). Regarding the collagen sponges cultured under bidirectional perfusion, well-defined matrix production units were homogeneously distributed in the scaffolds. Those units were constituted of several chondrocytes surrounded by newly synthesized matrix. Dynamic culture conditions also promoted a round morphology of the chondrocytes, typical of differentiated chondrocytes, whether the perfusion flow was constant (supplementary data S1) or not (Fig. 3A).

At the cellular level, in static culture conditions, chondrocyte cytoplasms were stained for both type I and type II collagens, indicating an active production of those collagens after 21 days of culture (Fig. 3B). Very interestingly, under bidirectional perfusion, close examination revealed that type II collagen, but not type I collagen, was present in the cytoplasm, suggesting that, after three weeks of culture, the production of type II collagen was still active whereas type I collagen was no more synthesized.

Dynamic culture conditions promote selectively type II collagen content over type I collagen

To determine the biochemical composition of the newly synthesized matrix in the collagen sponges, western blotting analyses were performed on the hyaline cartilage markers, type II and type IX collagen, and on the fibrocartilage matrix marker, type I collagen. Type II and type IX collagen were detected in both static and dynamic culture conditions (Fig. 4).

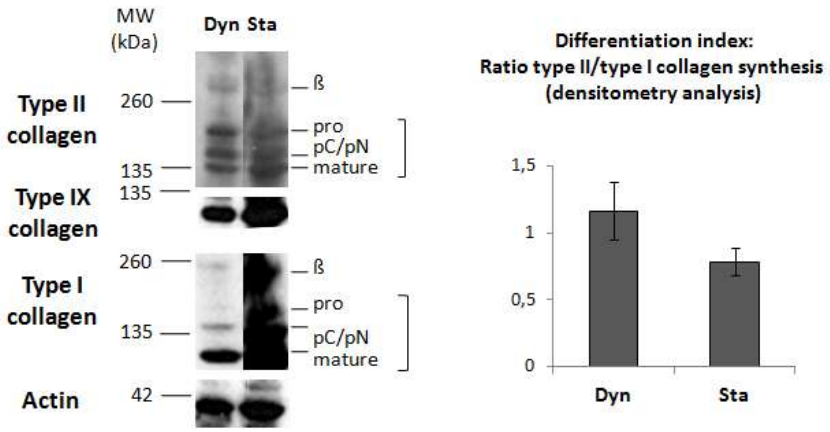

Fig. 4. Analysis of type I and type II collagen production by western blot analysis. A representative western blot analysis of the type II, type IX and type I collagen after 21 day of culture in collagen sponges in static (Sta) or dynamic conditions (Dyn) (prog 2) is shown in the left panel. The mature collagen chains, the unprocessed chains (pro) and the processing intermediates of the procollagen containing the aminopropetide (pN) or the carboxypropetide (pC) are indicated for type II and type I collagen. The upper band represents the dimers of collagen molecules (β). The immunoblotting for actin is shown as a loading control. These results are representative of six different experiments. The right panel shows the ratio of type II and type I collagen at the protein level after 21 days of culture. Densitometry analysis was performed on the western blotting data from all the experiments. The values were calculated as the total of each form, and normalized to the actin. The results are indicated as mean±SD (n=6).

Covalently cross-linked dimers of type II collagen were also evidenced suggesting the presence of a fibrillar network. Very strikingly, a lower production of type I collagen was evidenced in dynamic culture conditions. This results was observed in the two dynamic culture conditions tested in this study, whether the perfusion velocity was constant (supplementary data S2) or not (Fig. 4). Therefore, the ratio

of type II / type I collagen production is favored in dynamic culture conditions (Fig. 4). The health agencies commonly use the ratio of type II/type I collagen gene expression as an index of chondrocyte differentiation and of tissue engineering construct quality. In our study, at the mRNA level, this differentiation index was increased by dynamic culture conditions (supplementary data S3). Considering that tissue engineering requires protein level evaluation, we went further in assessing the quality of the synthesized matrix by measuring this ratio at the protein level via a densitometry analysis of the western blotting data (Fig. 4). It showed that dynamic culture conditions favored hyaline cartilage matrix production over fibrocartilage matrix synthesis. Besides, at the end of the *in vitro* culture, a more detailed analysis of the different forms of type I and type II collagens corresponding to the different steps of collagen maturation indicated that equivalent amounts of procollagen and mature form of type II collagen were synthesized in both static and dynamic culture conditions, whereas equivalent amounts of procollagen and mature forms of type I collagen were produced only in static conditions. Indeed, dynamic culture conditions led to a very low amount of type I procollagen, suggesting that type I collagen was no longer synthesized.

This result was further supported by the analysis of the engineered constructs at different time-points of culture. We monitored the expression and deposition of type I and type II collagens in the scaffolds, at 7, 14 and 21 days of culture. After 7 days of culture, chondrocytes still showed a fibroblastic-like shape, characteristic of dedifferentiated chondrocytes, whereas, from day 14, a round morphology, typical of fully differentiated chondrocytes, was observed. Immunohistochemical analyses showed that pericellular matrix rich in type II collagen was detected from 14 days of culture and the matrix production units were defined only after 21 days of culture (Fig 5). A strong type II collagen staining was observed in chondrocyte cytoplasms at every time-point, whereas, for type I collagen, it was observed only at 7 days of dynamic culture (Fig. 5). This suggests that the type I collagen was produced early in the culture period, which is in accordance with the previous results.

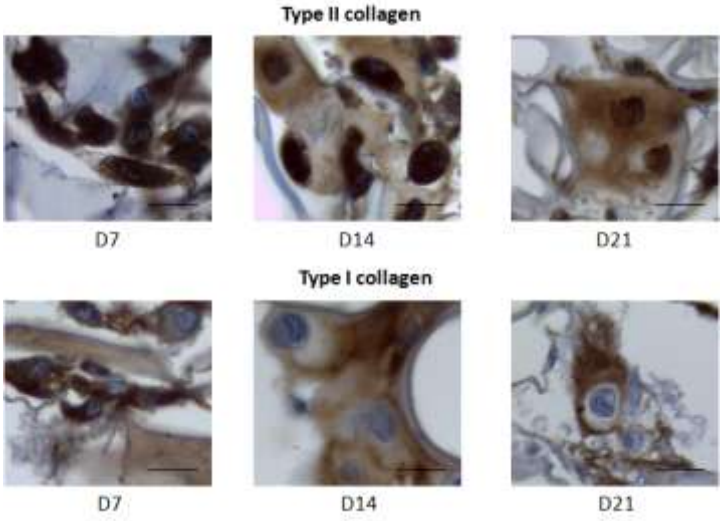

Fig. 5. Analysis of the type II and type I collagen deposition in the collagen sponges at different time points. Collagen sponges seeded with chondrocytes were cultured in static or dynamic (prog 1). Samples were analyzed after 7 days (D7), 14 days (D14) or at the end of the culture (D21) by immunohistochemical analyses to evaluate the type II and type I collagen deposition. The pictures shown are representative of the experimental results (n=2). Scale bar: 10µm.

At the gene expression level, *COL2A1* mRNA steady-state levels in collagen sponges gradually increased over 21 days of culture both in static and dynamic conditions (Fig. 6). These results were coherent with the western blotting analysis showing an active production of type II collagen during the whole culture. On the other hand, *COL1A1* mRNA level was lower at each time point in dynamic culture conditions, which is consistent with the western blotting results at the end of the culture. Type I collagen expression remained steady during the whole static culture. On the contrary, after 7 days of dynamic culture, a strong decrease of *COL1A1* mRNA level was observed, confirming the arrest of type I collagen expression during the 3D culture. Yet, the ratio of type II/type I collagen synthesis was enhanced in dynamic culture conditions as soon as 14 days of culture (Fig. S4).

This highlights that the combination of the BIT cocktail and bidirectional perfusion allowed the deposition of a hyaline cartilage matrix in collagen sponges by promoting type II collagen production over type I collagen. Interestingly, this reconstructed cartilage appeared stable after 6 weeks of in vivo implantation (Fig. S5).

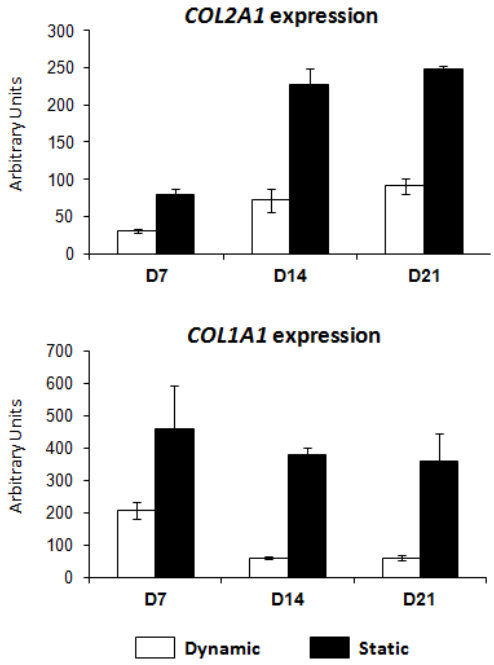

Fig. 6. Analysis of the type II and type I collagen gene expression in dynamic and static conditions. Collagen sponges seeded with chondrocytes were cultured in static or dynamic (prog 1) conditions. After 7 (D7), 14 (D14), and 21 (D21) days, samples were analyzed by real time PCT to evaluate the transcriptional expression of type II and type I collagen Data were normalized on *GAPDH*. The values are presented as mean±SD.

Discussion

The present study was performed to develop a tissue engineering strategy for the reconstruction of articular cartilage using human chondrocytes, a collagen scaffold and a bidirectional bioreactor prototype. This bioreactor system considered features of significance not only to tissue culture, but also to clinical translation (asepsis, scale-up, automation, and ease of use) (16). Previous studies have shown the potential of perfusion bioreactor to allow a homogenous matrix deposition in biomaterials (17-19). In accordance with these results, in our study bidirectional perfusion of collagen sponges seeded with human articular chondrocytes led to the deposition of an homogenous cartilaginous matrix within the scaffolds in the presence of the BIT cocktail.

After chondrocyte monolayer expansion and seeding in collagen sponges, two different perfusion programs were performed in this study. A constant perfusion with a flow speed of 5 µm/s was selected for program 1. Wendt *et al.* (17) have demonstrated that similar perfusion speed allows to obtain a

defined oxygen tension and a homogeneous matrix deposition. Flow speeds used in program 2 were selected according to previous studies on perfusion bioreactors (20-22). Davisson *et al.* (20) and Shahin and Doran (21) demonstrated that a slow perfusion speed during the first days of culture, respectively 10 µm/s and 7 µm/s, was required to protect the early matrix deposition in porous scaffolds in comparison with high perfusion speed, respectively 170 µm/s and 19 µm/s. Shahin and Doran (21) also proved that type II collagen and proteoglycan synthesis was enhanced with a slow increase of perfusion flow speed from 7 to 19 µm/s. In the present study, the lowest flow speed was applied at 5 µm/s on the basis of a previous study showing that a similar flow speed increased matrix synthesis and deposition (22). No major differences were detected between the two programs in terms of matrix deposition, suggesting that the advantages of the bidirectional perfusion were more important than the variations induced by the different flow speeds.

Special attention was given to the nature of the extracellular matrix synthesized by chondrocytes, with a view of cartilage matrix reconstruction. Our results demonstrated that hyaline cartilage markers were produced both in static or dynamic conditions. Besides, in dynamic culture conditions, the typical round morphology of chondrocytes was restored. The role of cell shape was demonstrated to be a key factor in the re-expression of the chondrocyte phenotype (23,24). More precisely, the actin cytoskeleton organization influences the expression of the chondrogenic transcription factor Sox9 (25,26) that promotes especially type II collagen expression. After monolayer amplification, chondrocytes showed a fibroblastic-like shape that was maintained until 7 days post-seeding. After 21 days of dynamic culture in collagen sponges, we observed a restoration of the round morphology typical of differentiated chondrocytes. In this study, the chondrocyte morphological changes from fibroblastic-like to round shape was observed after 14 days of dynamic culture, simultaneously with the decrease in type I collagen expression. Perfusion without the BIT cocktail was not sufficient to promote the change of cell shape after 21 days of culture (data not shown). On the other hand, in static culture conditions, BIT cocktail treatment was not sufficient to induce changes in cell morphology within the sponge core, but round chondrocytes were found in the matrix produced at the periphery of the scaffold, as shown in a previous study (4). These results suggest that the combination of perfusion with the BIT cocktail induces the cell rounding and the deposition of cartilage characteristic matrix in the core of the collagen sponges and allows an homogeneous distribution of engineered cartilage.

Other studies using perfusion have shown an increase in the collagen content (9,21). In our study, no dramatic increase in collagen content was noticed between dynamic and static culture conditions. Type II collagen expression was even favored in static culture conditions. This result is consistent with the ones of Mizuno *et al.* that showed that perfusion leads to a decrease in the synthesis of hyaline cartilage markers by calf' chondrocytes in collagen sponges (27). Yet, in the present study, the combination of the

perfusion in the OPB with the BIT cocktail treatment improved the chondrocyte phenotype as it favored the ratio of type II/type I collagens both at the gene expression and the protein synthesis levels. Thus, even though the quantity of the engineered cartilage was not increased, its quality was improved by the combined use of the OPB bioreactor and the BIT cockatil.

Our data showed that type I collagen was produced after 7 days of dynamic culture, but decreased dramatically for the rest of the culture period. This is an important result since we seeded the collagen sponges with fully dedifferentiated chondrocytes. Indeed, chondrocytes after monolayer amplification are known to undergo dedifferentiation (2) which is characterized by a loss of type II collagen expression in favor of type I collagen. This phenomenon is enhanced by the FI cocktail treatment (4, 28). Therefore, the chondrocytes seeded in the collagen sponges had a strong *COL1A1* expression explaining the type I collagen production at early stage of culture in both dynamic and static conditions. Thus, the combination of the BIT cocktail and the bioreactor culture led to an arrest of type I collagen expression and synthesis. It is consistent with the study of Raimondi *et al.* that showed that perfusion of human chondrocytes cultured in pellets inhibits the type I collagen expression observed when the pellets are cultured in static conditions (29). The same type I collagen synthesis inhibition was made in perfused human articular cartilage explants in comparison with explants cultivated in static conditions by Strehl *et al.* (19, 30).

The type II/type I collagen ratio was favored not only at the gene but also at the protein level in dynamic culture conditions. It evidences the specific expression of the differentiated phenotype of chondrocytes especially since, in other cell types like osteoblastic cell lines (31) or gingival cells (32), culture under perfusion triggers an induction of type I collagen production. So, the decrease in type I collagen production observed in dynamic culture conditions is part of the redifferentiation process triggered by the combination of the perfusion culture and the BIT cocktail treatment. Therefore, our data suggest a specific differential control of type I and type II collagens in chondrocytes under perfusion. The exact nature of molecular mechanisms are still to be determined, but it is known that perfusion exert mechanical forces such as fluid shear stress (18) and that chondrocyte phenotype and especially cartilage matrix proteins expression are sensitive to mechanical forces (33).

In our model, culture of chondrocytes under perfusion in the presence of 10% of serum only was not sufficient to induce the matrix production and the chondrocyte redifferentiation (data not shown). Thus, the combination of the BIT cocktail with the perfusion culture triggered a synergistic response in favor of chondrocyte differentiation. Therefore, we can hypothesize that signaling cross talks between soluble and biomechanical factors enhanced cell differentiation. In human osteoblasts seeded in collagen scaffolds, Kopf *et al.* demonstrated that a direct cross talk between BMP-2 and mechanotransduction signaling occurred (34). Such cooperative regulation of the BMP pathway can be partially responsible of

the synergistic response of chondrocytes to the fluid shear stress and BIT cocktail in our study.

Other molecular mechanisms triggered by perfusion have been identified such as the activation of the mitogen-activated pathway kinase (MAPK) pathway, as reviewed by Chiquet *et al.* (35). Interestingly, the cytoskeleton organization has also been found to be under the influence of perfusion (36) and this could also contribute to the rounding of cell shape observed in our study.

Acknowledgements

I would like to thank all the co-authors: Mayer N, Talò G, Lovati A, Riboldi S, Moretti M, Mallein-Gerin F.

References

1. Brittberg M, Lindahl A, Nilsson A, Ohlsson C, Isaksson O, Peterson L. Treatment of deep cartilage defects in the knee with autologous chondrocyte transplantation. N Engl J Med.331:889-95. 1994.
2. Schnabel M, Marlovits S, Eckhoff G, Fichtel I, Gotzen L, Vecsei V, Schlegel J. Dedifferentiation-associated changes in morphology and gene expression in primary human articular chondrocytes in cell culture. Osteoarthritis Cartilage.10:62-70. 2002.
3. Marlovits S, Hombauer M, Truppe M, Vecsei V, Schlegel W. Changes in the ratio of type-I and type-II collagen expression during monolayer culture of human chondrocytes. J Bone Joint Surg Br.86:286-95. 2004.
4. Claus S, Mayer N, Aubert-Foucher E, Chajra H, Perrier-Groult E, Lafont J, Piperno M, Damour O, Mallein-Gerin F. Cartilage-characteristic matrix reconstruction by sequential addition of soluble factors during expansion of human articular chondrocytes and their cultivation in collagen sponges. Tissue Eng Part C Methods.18:104-12. 2012.
5. Darling EM, Athanasiou KA. Articular cartilage bioreactors and bioprocesses. Tissue Eng.9:9-26. 2003.
6. Concaro S, Gustavson F, Gatenholm P. Bioreactors for tissue engineering of cartilage. Adv Biochem Eng Biotechnol.112:125-43. 2009.
7. Moretti MG, Freed, L.E., Langer R. Oscillating Cell Culture Bioreactor, Pub. No.: US2010/0297233 A1. Nov. 25, 2010.
8. Cheng M, Moretti M, Engelmayr GC, Freed LE. Insulin-like growth factor-I and slow, bi-directional perfusion enhance the formation of tissue-engineered cardiac grafts. Tissue Eng Part A.15:645-53. 2009.
9. Valonen PK, Moutos FT, Kusanagi A, Moretti MG, Diekman BO, Welter JF, Caplan AI, Guilak F, Freed LE. In vitro generation of mechanically functional cartilage grafts based on adult human stem cells and 3D-woven poly(epsilon-caprolactone) scaffolds. Biomaterials.31:2193-200. 2010.
10. Hautier A, Salentey V, Aubert-Foucher E, Bougault C, Beauchef G, Ronziere MC, De Sobarnitsky S, Paumier A, Galera P, Piperno M, Damour O, Mallein-Gerin F. Bone morphogenetic protein-2 stimulates chondrogenic expression in human nasal chondrocytes expanded in vitro. Growth Factors.26:201-11. 2008.
11. Valcourt U, Gouttenoire J, Moustakas A, Herbage D, Mallein-Gerin F. Functions of transforming growth factor-beta family type I receptors and Smad proteins in the hypertrophic maturation and osteoblastic differentiation of chondrocytes. J Biol Chem.277:33545-58. 2002.
12. Martin I, Jakob M, Schafer D, Dick W, Spagnoli G, Heberer M. Quantitative analysis of gene expression in human articular cartilage from normal and osteoarthritic joints. Osteoarthritis Cartilage.9:112-8. 2001.
13. Le Guellec D, Mallein-Gerin F, Treilleux I, Bonaventure J, Peysson P, Herbage D. Localization of the expression of type I, II and III collagen genes in human normal and hypochondrogenesis cartilage canals. Histochem J.26:695-704. 1994.
14. Warman M, Kimura T, Muragaki Y, Castagnola P, Tamei H, Iwata K, Olsen BR. Monoclonal antibodies against two epitopes in the human alpha 1 (IX) collagen chain. Matrix.13:149-56. 1993.
15. Rosenberg L. Chemical basis for the histological use of safranin O in the study of articular cartilage. J Bone Joint Surg Am.53:69-82. 1971.
16. Moretti MG, Cheng, M.Y., Nichol, J.W., Freed, L.E. An oscillatory perfused bioreactor for cell and tissue culture. 2nd Annual Conference on Methods in Bioengineering, Cambridge, MA. 2007.
17. Wendt D, Stroebel S, Jakob M, John GT, Martin I. Uniform tissues engineered by seeding and culturing cells in 3D scaffolds under perfusion at defined oxygen tensions. Biorheology.43:481-8. 2006.
18. Moretti M, Freed LE, Padera RF, Lagana K, Boschetti F, Raimondi MT. An integrated experimental-computational approach for the study of engineered cartilage constructs subjected to combined regimens of hydrostatic pressure and interstitial perfusion. Biomed Mater Eng.18:273-8. 2008.
19. Pei M, Solchaga LA, Seidel J, Zeng L, Vunjak-Novakovic G, Caplan AI, Freed LE. Bioreactors mediate the effectiveness of tissue engineering scaffolds. FASEB J.16:1691-4. 2002.
20. Davisson T, Sah RL, Ratcliffe A. Perfusion increases cell content and matrix synthesis in chondrocyte three-dimensional cultures. Tissue Eng.8:807-16. 2002.
21. Shahin K, Doran PM. Strategies for enhancing the accumulation and retention of extracellular matrix in tissue-engineered cartilage cultured in bioreactors. PLoS One.6:e23119. 2011.

22. Pazzano D, Mercier KA, Moran JM, Fong SS, DiBiasio DD, Rulfs JX, Kohles SS, Bonassar LJ. Comparison of chondrogensis in static and perfused bioreactor culture. Biotechnol Prog.16:893-6. 2000.
23. Benya PD, Shaffer JD. Dedifferentiated chondrocytes reexpress the differentiated collagen phenotype when cultured in agarose gels. Cell.30:215-24. 1982.
24. Zhang J, Yang Z, Li C, Dou Y, Li Y, Thote T, Wang DA, Ge Z. Cells behave distinctly within sponges and hydrogels due to differences of internal structure. Tissue Eng Part A.19:2166-75. 2013.
25. Kumar D, Lassar AB. The transcriptional activity of Sox9 in chondrocytes is regulated by RhoA signaling and actin polymerization. Mol Cell Biol.29:4262-73. 2009.
26. Woods A, Wang G, Beier F. Regulation of chondrocyte differentiation by the actin cytoskeleton and adhesive interactions. J Cell Physiol.213:1-8. 2007.
27. Mizuno S, Allemann F, Glowacki J. Effects of medium perfusion on matrix production by bovine chondrocytes in three-dimensional collagen sponges. J Biomed Mater Res.56:368-75. 2001.
28. Liu G, Kawaguchi H, Ogasawara T, Asawa Y, Kishimoto J, Takahashi T, Chung UI, Yamaoka H, Asato H, Nakamura K, Takato T, Hoshi K. Optimal combination of soluble factors for tissue engineering of permanent cartilage from cultured human chondrocytes. J Biol Chem.282:20407-15. 2007.
29. Raimondi MT, Bonacina E, Candiani G, Lagana M, Rolando E, Talo G, Pezzoli D, D'Anchise R, Pietrabissa R, Moretti M. Comparative chondrogenesis of human cells in a 3D integrated experimental-computational mechanobiology model. Biomech Model Mechanobiol.10:259-68. 2011.
30. Strehl R, Tallheden T, Sjogren-Jansson E, Minuth WW, Lindahl A. Long-term maintenance of human articular cartilage in culture for biomaterial testing. Biomaterials.26:4540-9. 2005.
31. Mai Z, Peng Z, Wu S, Zhang J, Chen L, Liang H, Bai D, Yan G, Ai H. Single bout short duration fluid shear stress induces osteogenic differentiation of MC3T3-E1 cells via integrin beta1 and BMP2 signaling cross-talk. PLoS One.8:e61600. 2013.
32. Mathes SH, Wohlwend L, Uebersax L, von Mentlen R, Thoma DS, Jung RE, Gorlach C, Graf-Hausner U. A bioreactor test system to mimic the biological and mechanical environment of oral soft tissues and to evaluate substitutes for connective tissue grafts. Biotechnol Bioeng.107:1029-39. 2010.
33. Grodzinsky AJ, Levenston ME, Jin M, Frank EH. Cartilage tissue remodeling in response to mechanical forces. Annu Rev Biomed Eng.2:691-713. 2000.
34. Kopf J, Petersen A, Duda GN, Knaus P. BMP2 and mechanical loading cooperatively regulate immediate early signalling events in the BMP pathway. BMC Biol.10:37. 2012.
35. Chiquet M, Tunc-Civelek V, Sarasa-Renedo A. Gene regulation by mechanotransduction in fibroblasts. Appl Physiol Nutr Metab.32:967-73. 2007.
36. Chiquet M, Gelman L, Lutz R, Maier S. From mechanotransduction to extracellular matrix gene expression in fibroblasts. Biochim Biophys Acta.1793:911-20. 2009.

Supplementary Figures

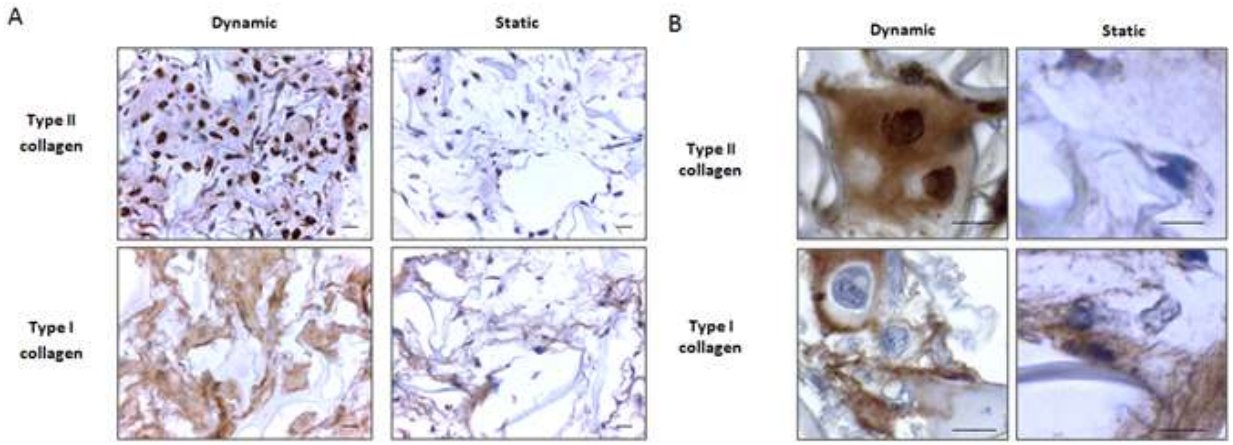

Fig. S1. Immunostaining of type II and type I collagens neo-synthesized by chondrocytes in collagen sponges in static or dynamic culture conditions. Chondrocyte-seeded collagen sponges were cultured for 21 days in presence of the BIT cocktail in static or dynamic conditions (prog 1). The pictures are taken in the scaffold core and are representative of chondrocytes isolated from six donors. (A) Dynamic culture conditions led to the formation of matrix production units rich in collagens (Scale bars 10µm). (B) At the cellular level, under dynamic culture, the chondrocyte cytoplasm is stained for type II but not for type I collagen (Scale bars 10µm).

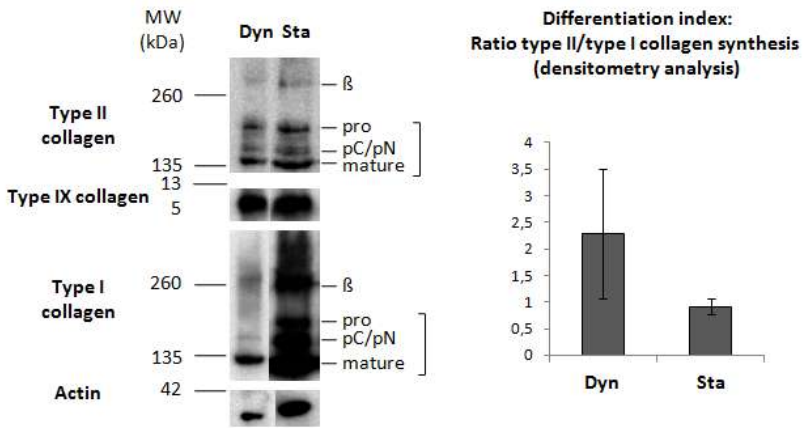

Fig. S2. Bi-directional perfusion favors the differentiation index at the protein level. A representative western blotting analysis of the type II, type IX and type I collagen after 21 day of culture in collagen sponges in static (Sta) or dynamic conditions (Dyn) (prog 2) is shown in the left panel. The mature collagen chains, the unprocessed chains (pro) and the processing intermediates of the procollagen containing the aminopropetide (pN) or the carboxypropetide (pC) are indicated for type II and type I collagen. The upper band represents the dimers of collagen molecules (β). The immunoblotting for actin is shown as a loading control. These results are representative of six different experiments. The right panel shows the ratio of type II and type I collagen at the protein level after 21 days of culture. Densitometry analysis was performed on the western blotting data from all the experiments. The values were calculated as the total of each form, and normalized to the actin. The results are indicated as mean±SD (n=6).

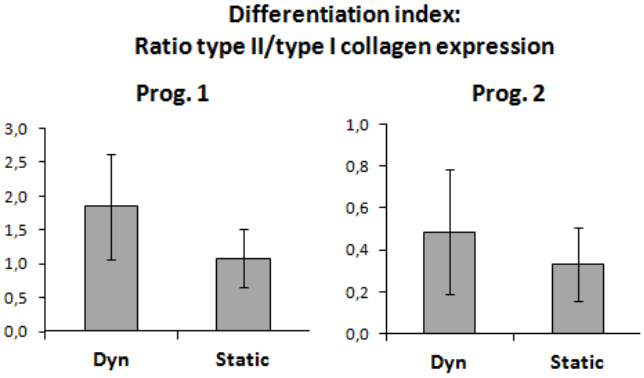

Fig. S3. Ratio of type II and type I collagen transcriptional expression in different conditions of dynamic culture. Chondrocyte-seeded collagen sponges were cultured in static or dynamic culture conditions using two different perfusion programs for the dynamic culture (prog. 1, n=6; prog. 2, n=4) The transcriptional expression of *COL2A1* and *COL1A1* was evaluated by real time PCR. Data were normalized on *GAPDH* The ratio values are indicated as mean±SD.

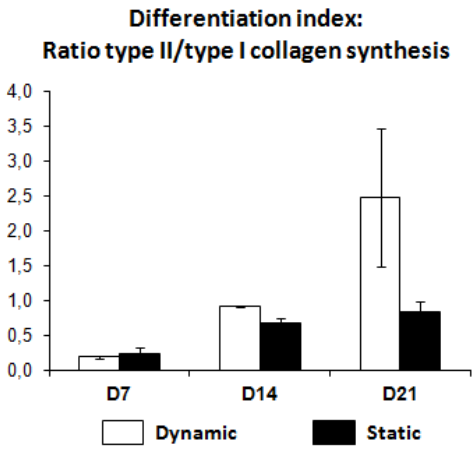

Fig. S4. Ratio of type II and type I collagen expression at different time points during culture. Collagen sponges seeded with chondrocytes were cultured in static or dynamic (prog. 1) conditions. After 7 (D7), 14 (D14), and 21 (D21) days, samples were analyzed by real time PCT to evaluate the transcriptional expression of type II and type I collagen Data were normalized on *GAPDH*. The ratio of type II/type I collagen gene expression was determined using the values measured in the experiments reported in Fig. 5. The values are presented as mean±SD.

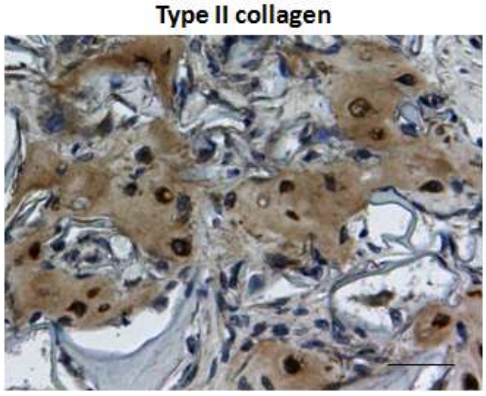

Fig. S5. Immunohistochemistry of type II collagen in the collagen sponge after 6 weeks of subcutaneous implantation in nude mice Chondrocyte-seeded sponges were cultured for 21 days in static or dynamic (prog 2) conditions and then implanted into the subcutaneous pockets of nude mice. The picture shows the immunostaining of type II collagen in the core of a scaffold cultured for 21 days in dynamic conditions prior to implantation in nude mice (Scale bar 10µm).

Chapter 8

Orthopedic bioactive implants: hydrogel enrichment of macroporous titanium for the delivery of mesenchymal stem cells and strontium

Abstract

Insufficient implant stability is an important determinant in the failure of cementless prostheses. To improve osseointegration, we aim at generating a bioactive implant combining a macroporous titanium (TT) with a biocompatible hydrogel to encapsulate osteoinductive factors and osteoprogenitor cells.

Amidation and cross-linking degree of an amidated carboxymethylcellulose hydrogel (CMCA) were characterized by FT-IR spectrometry and mechanical testing. Bone marrow mesenchymal stem cells (BMSCs) from osteoarthritic patients were cultured on CMCA hydrogels, TT and TT loaded with CMCA (TT+CMCA) with an optimized concentration of $SrCl_2$ to evaluate cell viability and osteo-differentiation.

Amidation and cross-linking degree were homogeneous among independent CMCA batches. $SrCl_2$ at 5 µg/ml significantly improved BMSCs osteo-differentiation increasing calcified matrix ($p<0.01$), type I collagen expression ($p<0.05$) and Alkaline Phosphatase activity. TT+CMCA samples better retained cells into the TT mesh, significantly improving cell seeding efficiency respect to TT ($p<0.05$). BMSCs on TT+CMCA underwent a more efficient osteo-differentiation with higher Alkaline Phosphatase ($p<0.05$) and calcium levels compared to cells on TT.

Based on these in vitro results, we envision the association of TT with strontium-enriched CMCA and BMSCs as a promising strategy to generate bioactive implants promoting bone neoformation at the implant site.

Introduction

Joint replacement is widely used to recover articular functionality in joints compromised by degenerative pathologies or severe traumas. The integration between bone and implant is crucial in cementless prostheses where bone ingrowth is required to grant fixation. The achievement of an optimal osseointegration can lead to a reduction in the risk of implant mobilization and, consequently, in the number of revision procedures (1-3), which have major drawbacks such as patients' morbidity and relevant costs for National Health Systems. With this aim, cementless implant technology has evolved with the introduction of porous metallic materials to maximize bone ingrowth and bone-to-implant contact (4-7). Among the different types of porous titanium, Trabecular Titanium™ (TT) is currently clinically used in acetabular cups and to fill cavitary and segmental bone defects. This macroporous titanium is characterized by multiple layers of hexagonal pores with a 640 μm diameter (8), macroporosity that facilitates cell migration and bone deposition (9). It has been shown that porous titanium implants can be enriched, either directly (10-12) or by association with biocompatible hydrogels (13-16), with antibiotics (14) , VEGF (15) and FGF-2 (16). To improve implant osseointegration, osteogenic factors can used for implant enrichment. Strontium is a low cost ion and is easier to handle compared to osteoinductive proteins, such as BMP-2, being therefore an ideal candidate to enrich off-the-shelf materials for bone tissue engineering, as proposed for hydroxyapatite (17,18) and, more recently, for titanium (19,20). Indeed, strontium ranelate is a drug used for the treatment of osteoporosis thanks to its ability to increase bone neoformation and to reduce bone resorption (21-23). Furthermore, strontium has a positive effect on osteogenic differentiation of bone marrow mesenchymal stem cells (BMSCs) (24-28) which are resident at the implant site and are characterized by an intrinsic osteogenic potential (29-31). It has been demonstrated that the use of autologous bone marrow concentrate, obtained by an intra-operative approach, improves bone healing (32). Thus, loading BMSCs into the implant may represent a promising approach to increase the population of osteogenic progenitor cells (33,34) at the implant site, especially when aging and age-related diseases negatively affect bone deposition (35).

We envision that autologous BMSCs can be isolated and seeded into a titanium prosthesis pre-loaded with a strontium-enriched hydrogel with a completely intra-operative approach. The implantation of a bioactive prosthesis, delivering cells and osteogenic signals, could result in higher implant stability and faster osseointegration, reducing recovery time and improving patients' quality of life. In this study we combined TT with an amidated carboxymethylcellulose hydrogel (CMCA), previously used for chondrocyte culture (36). We evaluated if cell seeding efficiency and osteogenic differentiation were improved when TT was enriched with CMCA (TT+CMCA) as compared to normal TT that represents a clinical standard reference. To better resemble a possible clinical application, BMSCs were obtained

from OA patients.

Materials and Methods

Substrates preparation

CMCA polymer synthesis

A water-based synthesis was developed to obtain amidated carboxymethylcellulose (CMCA) from carboxymethylcellulose (CMC, CEKOL® 30000, CP Kelko), in alternative to organic synthesis (37). CMC was solubilized in ddH2O (1.5% W/V) with N-hydroxysuccinimide (Fluka) at a molar ratio 1:1. Methylamine (Merk) was added to CMC solution, at a molar ratio 1:1 with CMC. pH was adjusted to 4.7 with HCl (Sigma-Aldrich) and finally, amidation of CMC was obtained by adding 1-ethyl-3-(3-dimethyl-aminopropyl)-carbodiimide (EDC, Ubichem) at a molar ratio 1:1 with CMC. After 3 h at r.t., purification was performed by ultrafiltration (Millipore Cogent M1, 100 kDa membrane). Purity was controlled by FT-IR spectrometry (Spectrum 400 FT-IR FT-NIR, Perkin-Elmer). Purified CMCA was freeze-dried for storage.

Validation of CMCA polymer functionalization by FT-IR spectrometry

FT-IR spectrometry was used for a semi-quantitative evaluation of amidation degree. Since bands for COO^- (1590 cm^{-1}) and amidic group (1640 cm^{-1}) were too near to allow a clear distinction between them, an acidification step with Dowex resin (Sigma-Aldrich) was performed to convert COO^- groups into COOH groups. As a result, the absorption peaks of amidic groups (1640 cm^{-1}) were clearly distinguished from those of the groups that did not react (1730 cm^{-1}) and the percentage of amidic moieties introduced was calculated.

CMCA hydrogel cross-linking

Freeze-dried CMCA polymer was solubilized (1.7% W/V) in ddH_2O together with N-hydroxysuccinimide at molar ratio 1:1 with CMCA. 1,3-diaminopropane (Merk) was added in a ratio of 1:2 with CMCA and pH was adjusted to 4.7 with HCl. Finally, the activator EDC was added at a molar ratio 1:1 with CMCA. Cross-linking reaction took 3 h and hydrogel purification was performed by washing in ddH_2O. To verify cross-linking reproducibility, 5 min after the addition of EDC 6 ml of reaction blend were sampled with a 10 ml syringe without needle and kept at r.t. to let the cross-linking reaction end. Since cross-linking degree affects hydrogel mechanical properties, LFPlus digital testing tensile machine (Amestek) was used to measure the injection force needed to extrude the hydrogel from the syringe.

CMCA hydrogel loading into Trabecular Titanium™ mesh

Trabecular Titanium™ (Ti6Al4V, Ø 8 mm, h 3 mm, pore Ø 640 µm) was obtained by electron beam melting (8). Hydrated CMCA was injected into TT mesh through a syringe. The amount of hydrated

CMCA loaded was determined by weighing (analytical balance Ohaus, Adventurer Pro AV2101C). Constructs were oven-dried at 50°C and sterilized by EtO.

BMSCs culture and osteogenic differentiation

BMSCs isolation and expansion

Bone marrow was harvested from the femoral compartment of 9 OA patients (mean age 59±4 years) undergoing total hip replacement, after written consent. Bone marrow was centrifuged and plated in control medium consisting of HG-DMEM (High Glucose, Gibco) with 10% Fetal Bovine Serum (FBS, Lonza), 0.029 mg/ml L-glutamine, 100 U/ml penicillin, 100 µg/ml streptomycin, 10 mM hepes, 1 mM sodium pyruvate (all from Gibco) supplemented with 5 ng/ml FGF-2 (Peprotech). BMSCs were selected for plastic adherence and expanded. Cells were frozen at passage 2 and, at need, thawed and expanded until passage 4.

Selection of $SrCl_2$ concentration to improve BMSCs osteogenic differentiation

Cells were seeded at $3x10^3$ cells/cm^2 and cultured for 14 days in osteogenic medium consisting of control medium supplemented with 10 nM dexamethasone, 10 mM glycerol-2-phosphate, 150 µM L-ascorbic acid-2-phosphate and 10 nM cholecalciferol (all from Sigma-Aldrich) (38) in the presence of 0, 1, 5, 10 and 20 µg/ml $SrCl_2$ (Sigma-Aldrich).

Culture of BMSCs on CMCA hydrogel

Hydrated CMCA was dispensed a 24-multiplate (0.75 ml/well), and then oven-dried at 50°C and sterilized in EtO. 24 h before cell seeding, CMCA samples were hydrated with 0.75 ml of medium. $7.5x10^5$ BMSCs were suspended in 1 ml of medium, seeded on CMCA and cultured up to 21 days in different media: control, osteogenic or osteogenic with 5 µg/ml SrCl2.

Osteogenic differentiation of BMSCs on TT and TT+CMCA

$7.5x10^5$ BMSCs were suspended in 75 µl of medium and seeded on normal TT or on TT+CMCA samples. After 3 h, 1 ml of medium was added. TT and TT+CMCA samples were cultured up to 21 days in osteogenic medium with 5 µg/ml SrCl2.

Evaluation of cell behavior on biomaterials

Cell seeding efficiency

Seeding efficiency on TT and TT+CMCA was determined by DNA quantification 24 h after seeding (CyQuant kit, Invitrogen) and calculated as percentage of the number of seeded cells.

Cell viability

Cell viability was determined by Alamar Blue assay (Invitrogen). 800 µl of 10% Alamar Blue in HG-DMEM

w/o phenol red were added to each sample and incubated for 4 h at 37°C. Fluorescence (540 nm-580 nm) was read using a Victor X3 Plate Reader (Perkin Elmer).

Calcified matrix deposition

Calcified matrix was quantified by Alizarin Red-S (AR-S, pH 4.1, Fluka) staining. After washing, each sample was unstained with 10% cetylpyridinium chloride monohydrate (CPC, Sigma-Aldrich) in 0.1 M phosphate buffer (pH 7.0) and absorbance was read at 570 nm (39).

Gene expression of type I collagen

Expression of type I collagen (COL1A1) was evaluated by real time PCR (Rotor Gene RG3000 system, Qiagen). RNA was purified with RNeasy Mini kit (Qiagen)and reverse-transcribed to cDNA with iScript cDNA Synthesis Kit (Bio-Rad Laboratories) (5 min at 25°C, 30 min at 42°C, 5 min at 85°C). 20 ng of cDNA were incubated with a PCR mixture including TaqMan Universal PCR Master Mix and TaqMan® Assays-on-Demand™ Gene expression probes (Life Technologies) (2 min at 50°C, 10 min at 95°C, 40 cycles of 15 sec at 95°C, 1 min at 60°C). COL1A1 expression was normalized on glyceraldehyde 3-phosphate dehydrogenase (GAPDH).

Alkaline Phosphatase activity

Alkaline Phosphatase (ALP) activity was determined by enzymatic assay incubating cell lysates at 37°C with 1 mM p-nitrophenylphosphate in 100 mM diethanolamine and 0.5 mM MgCl2 (pH 10.5, Sigma-Aldrich) (40). Absorbance was read at 405 nm. ALP was normalized on protein content, determined by BCA Protein Assay Kit (Pierce Biotechnology).

Calcium quantification

Calcium quantification was performed by Randox assay (Randox Laboratories Ltd). Samples were incubated with 0.5 M HCl for 6 h at 4°C on a rotating plate. Supernatants were incubated with the Randox working solution. Absorbance was read at 570 nm.

Scanning Electron Microscopy analysis

BMSCs adhesion and matrix production were evaluated by SEM. Samples were fixed for 1 h in glutaraldehyde (1.2% in 0.1 M sodium cacodylate buffer), washed with 0.1 M sodium cacodylate buffer and fixed for 1 h in OsO_4 (1% in 0.1 M sodium cacodylate buffer). Samples were dehydrated through graded EtOH, submitted to critical point drying with CO_2, sputter-coated with gold and analyzed with Sigma Scanning Electron Microscope (Zeiss, 10 kEV).

Statistical Analysis

Data are expressed as mean±SEM, unless differently specified. Statistical analyses were performed using Student's t-test to compare two groups and Two-Way ANOVA to compare groups at different time

points (Graph Pad Prism, v 5.0). Significance was set at $p<0.05$.

Results and Discussion

Substrates preparation

Validation of CMCA hydrogel amidation and cross-linking

Hydrophilicity of CMC was increased introducing amidic groups in the polymer backbone. To avoid the use of dimethylformamide, a very toxic reagent (41-43) used for the organic synthesis of CMCA (37), a water-based synthesis was developed. FT-IR spectra (Fig. 1a) allowed the quantification of amidic groups introduced and, as shown in Fig. 1b, we observed that the amidation degree was homogeneous among independent samples (39.4±2.3%). Different CMCA batches were homogeneous for cross-linking degree as demonstrated by similar values of injection force (258.5±12.8 N) measured by a mechanical extrusion test (Fig. 1c). To demonstrate the reliability of this method, cross-linking was performed starting from different CMCA concentrations. When CMCA concentration was lower (1.6% W/V) injection force was reduced, whereas when it was higher (1.8% W/V) we observed an increase in this parameter. This method, easier and less expensive compared to titration and NMR (37,44), can be used as a routine quality control to evaluate the homogeneity of cross-linking among different batches of production and can reveal small differences in the starting conditions of the cross-linking reaction. Nevertheless, quality controls should include further analyses to grant the spatial homogeneity of hydrogel cross-linking.

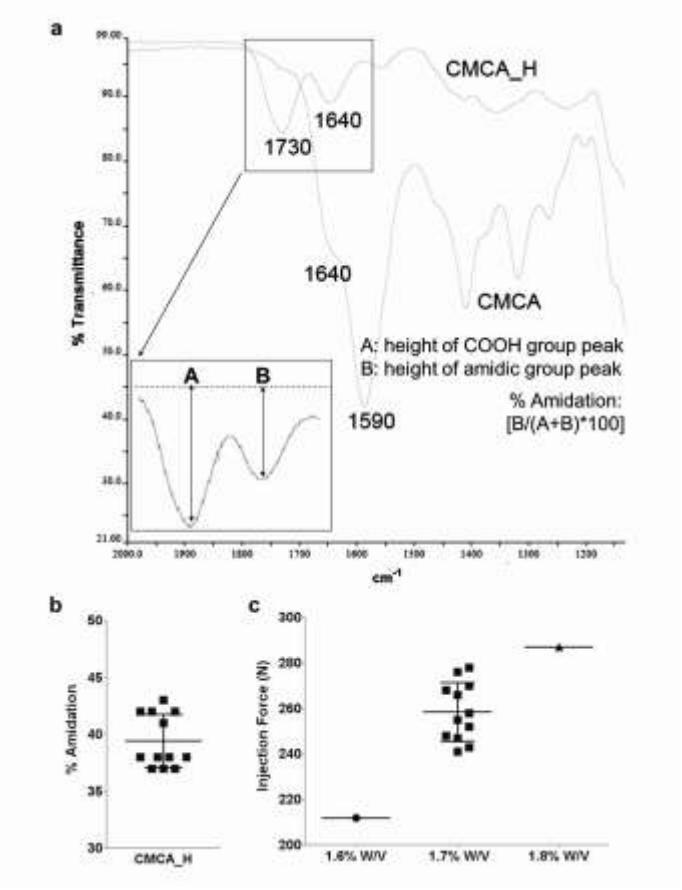

Fig. 1. CMCA amidation and cross-linking degree. (a) FT-IR spectra of CMCA before and after the acidification step (CMCA_H). Inset represents COOH and amidic group peaks. (b) Amidation degree calculated on the basis of FT-IR spectra (mean±SD, n=12). (c) Cross-linking validation by mechanical testing starting from 1.7% CMCA (W/V, mean±SD, n=12). Control samples were prepared starting from 1.6% and 1.8% CMCA (W/V).

CMCA hydrogel loading into TT mesh

CMCA loaded within the TT mesh through a syringe was homogeneously distributed in TT pores (Fig. 2a). CMCA loading was reproducible as demonstrated by the low variability in the amount of hydrogel loaded among different samples (Fig. 2b). In our approach the interaction between CMCA and TT was granted by the increase of volume of CMCA that, once rehydrated with the cell suspension, remained entrapped within TT structure without any loss of hydrogel during culture. As an alternative, phosphonate derivatives of CMC can be developed to generate a chemical bound between titanium and hydrogel (45).

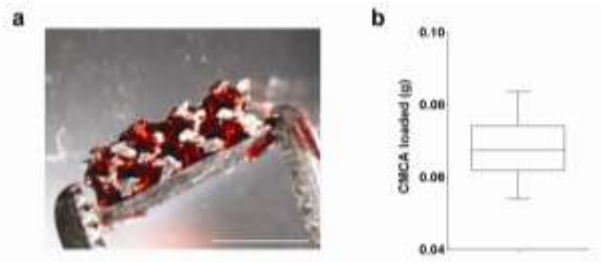

Fig. 2. CMCA loading into TT. (a) Section of TT+CMCA (scale bar 5 mm, CMCA stained red). (b) Weight of hydrated CMCA loaded into TT mesh (mean±SD, n=47).

Selection of $SrCl_2$ concentration to improve BMSCs osteogenic differentiation

Aiming at the future incorporation of $SrCl_2$ within CMCA hydrogel, BMSCs were cultured in the presence of different amounts of $SrCl_2$ to select a suitable concentration for the improvement of their osteogenic differentiation. Since these in vitro tests are oriented towards our aim to implant a bioactive device made from TT and CMCA directly into the bone, all the experiments were performed in osteogenic medium, mimicking the differentiative signals that in vivo would be provided by the adjacent bone.

The evaluation of osteogenic markers in BMSCs cultured with different concentrations of $SrCl_2$ revealed that the best one to improve BMSCs osteogenic differentiation was 5 µg/ml (Fig. 3).

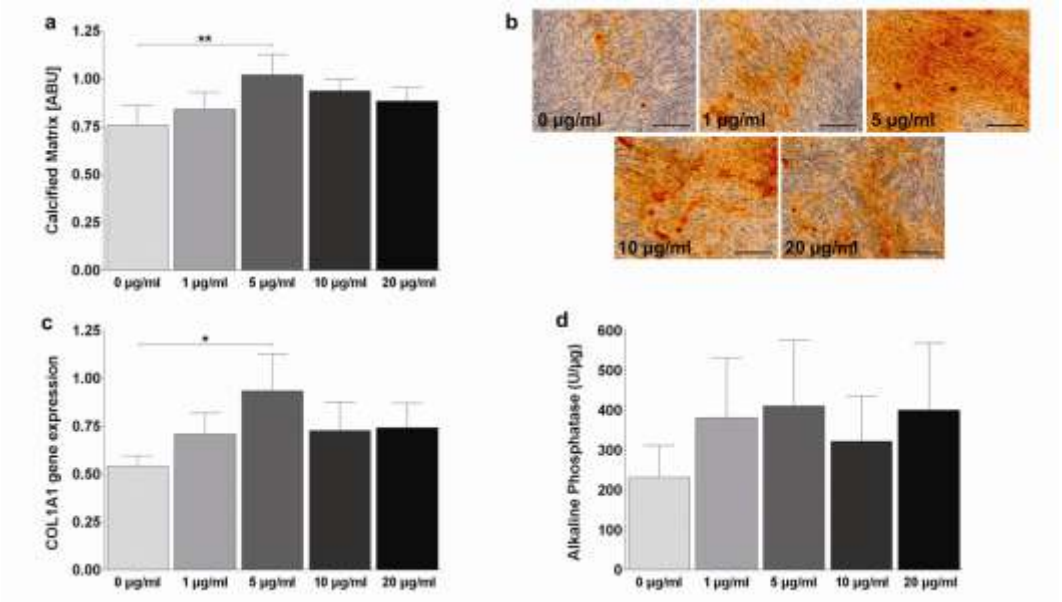

Fig. 3. Selection of $SrCl_2$ concentration to improve BMSCs osteogenic differentiation. (a) Quantification of calcified matrix after AR-S staining (ABU, arbitrary units; n=6, ** p<0.01). (b) Micrographs of BMSCs stained with AR-S. (c) Type I collagen (COL1A1) expression normalized to GAPDH (n=3, * p<0.05). (d) ALP activity (ALP Units/µg of proteins, n=6).

Indeed, a statistically significant increase in calcified matrix deposition was observed in cells in osteogenic medium with 5 µg/ml $SrCl_2$, compared to osteogenic medium without $SrCl_2$ ($p<0.01$, Fig. 3a). Representative micrographs showing calcified matrix stained by AR-S are reported in Fig. 3b. The osteoinductive effect of $SrCl_2$ was evident also on type I collagen gene expression, with cells cultured in osteogenic medium with 5 µg/ml $SrCl_2$ showing the highest expression of this marker ($p<0.05$, Fig. 3c). Even ALP activity was increased by the presence of $SrCl_2$, but differences were not significant (Fig. 3d). Our results demonstrated that a low concentration of $SrCl_2$ (5 µg/ml) improved BMSCs osteogenic differentiation, accordingly with data by Sila-Asna et al. (24). Strontium has a positive effect on bone metabolism (21) and on MSCs osteogenic differentiation (26,28). Furthermore, it has been demonstrated to improve osseointegration when delivered at the implant site by direct incorporation within titanium (19), or inclusion in a hydroxyapatite coating (20) and in bone graft extenders (46). Since the in vivo effect of strontium on bone metabolism is associated with increased BMSCs osteogenesis (27), we believe that the simultaneous inclusion of BMSCs and strontium in a hydrogel loaded into titanium may promote bone ingrowth by a dual action on host progenitor cells resident at the implant site and on cells encapsulated into the hydrogel.

BMSCs culture and osteogenic differentiation in CMCA hydrogel

BMSCs viability in CMCA without titanium was determined during culture in the presence of different media: control, osteogenic and osteogenic supplemented with 5 µg/ml SrCl2. BMSCs viability was maintained during culture in all the tested conditions (Fig. 4a). ALP activity was quantified after 14 and 21 days as marker of osteogenic differentiation (Fig. 4b). To confirm our data on the osteoinductive effect of $SrCl_2$, BMSCs were cultured in CMCA and differentiated either in normal osteogenic medium or in osteogenic medium with 5 µg/ml $SrCl_2$. Cells cultured in CMCA maintained their osteogenic potential. Indeed, at 14 days a significant increase in ALP was observed in cells cultured in osteogenic medium with $SrCl_2$ compared to cells in control and osteogenic medium (+274% and +62% respectively, $p<0.05$). The difference between this group and control cells remained statistically significant even at 21 days (+80%, $p<0.05$). The same trend was observed in calcium levels but increases were not significant due to the

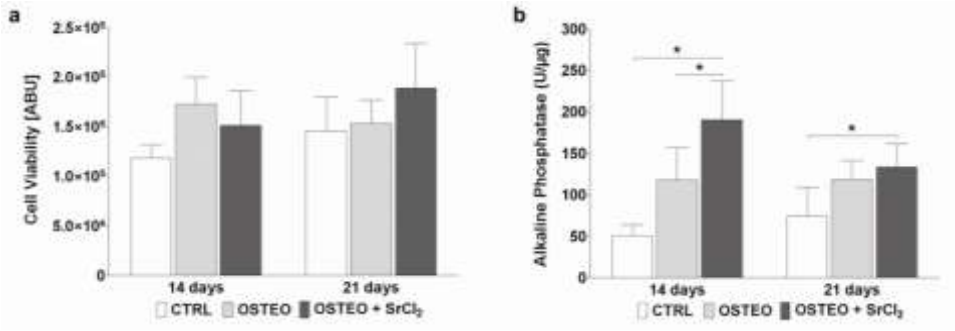

Fig. 4. Viability and osteogenic differentiation of BMSCs on CMCA hydrogel. (a) BMSCs viability in different culture media (ABU, arbitrary units, n=6, * $p<0.05$). (b) ALP activity (ALP Units/µg of proteins, n=4, * $p<0.05$).

great inter-donor variability (data not shown).

Accordingly with data by Leone *et al.* (36), who used CMCA for chondrocyte differentiation, we did not observe any cytotoxic effect of CMCA. Culture on CMCA did not impair the ability of BMSCs to respond to the osteogenic stimuli provided by culture medium. These results, together with the already demonstrated lack of inflammatory response in rabbits treated with CMCA (36), support the potential clinical use of this hydrogel in bone applications.

Improvement of TT-BMSCs interaction by enrichment with CMCA hydrogel

Cell seeding efficiency and cell adhesion

The presence of CMCA inside TT pores significantly increased cell seeding efficiency (+21% compared to TT without CMCA, $p<0.05$, Fig. 5a). This increase was probably due to the ability of CMCA to immobilize cells inside TT. In view of a clinical application, it should be highlighted that the difference in cell retention between TT and TT+CMCA would be even more crucial since cells would not be allowed to adhere to TT for 3 hours before being in contact with body fluids, as we let them in our experiments before adding culture medium.

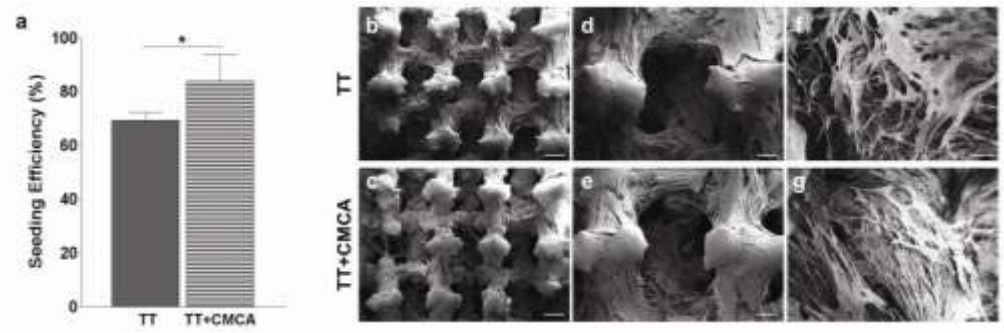

Fig. 4. Cell seeding efficiency and cell adhesion on TT and TT+CMCA. (a) Seeding efficiency expressed as percentage with respect to the initial number of seeded cells (n=5, * $p<0.05$). (b-g) SEM analysis after 21 days of culture. BMSCs adhesion on TT and TT+CMCA outer surface (b-c, scale bar 500 µm). Magnification of a titanium pore covered by cells and extracellular matrix (d-e, scale bar 200 µm). Adherent cells inside the inner surface of titanium pores (f-g, scale bar 50 µm).

We believe that prostheses made of Trabecular Titanium™ pre-loaded with dry CMCA could be easy-to-handle devices for the orthopedic clinical practice. CMCA loaded in these devices could be hydrated intra-operatively with a suspension of autologous BMSCs obtained by bone marrow and directly implanted. After 21 days of culture, SEM showed that BMSCs colonized both TT and TT+CMCA samples, covering the surface of titanium samples (Fig. 5b-c) and the inner surface of pores (Fig. 5d-e) and displaying cell attachment to TT and TT+CMCA through the formation of cell protrusions (Fig. 5 f-g). These observations are coherent with recent results proving the ability of TT to support the growth of human adipose derived stem cells (47,48). No difference was observed between TT and TT+CMCA demonstrating that CMCA did not impair the ability of cells to colonize and fill with matrix TT pores.

BMSCs viability and osteogenic differentiation

Viability and osteogenic differentiation of BMSCs on TT and TT+CMCA were assessed to compare their osteoconductivity. As shown in Fig. 6a, no difference in cell viability was observed between TT and TT+CMCA. After 14 days, ALP activity was significantly increased in TT+CMCA samples (+91%, $p<0.05$, Fig. 6b) supporting the idea that TT combined with CMCA is more osteoconductive than TT. The same trend was observed in calcium quantification, with higher values for BMSCs cultured on TT+CMCA with respect to TT (Fig. 6c).

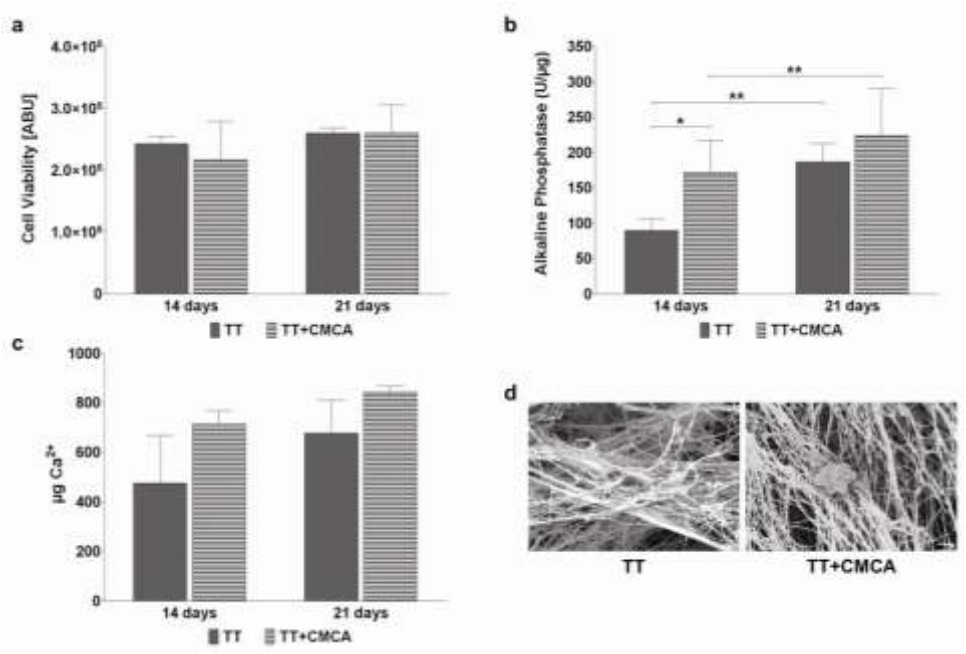

Fig. 6. BMSCs behavior on TT and TT+CMCA. (a) Cell viability of BMSCs (ABU, arbitrary units, n=8). (b-c) ALP activity (b) and calcium quantification (c) (n=4, * $p<0.05$, ** $p<0.01$). (d) Fibrillar structure of extracellular matrix produced by BMSCs after 21 days of culture (SEM analysis, scale bar 1 µm).

Matrix characterized by a fibrillar structure was found to be deposited by cells inside titanium pores in both TT and TT+CMCA (Fig. 6d). The observed increases in osteogenic markers demonstrated that the association of TT and CMCA lead to a construct with improved osteoconductivity compared to TT. Further improvement of this feature by the association of TT with a hydrogel enriched with an osteoinductive factor appears a very promising strategy to improve implant osseointegration that grants prosthetic stability (1-3). Recently, factors such as VEGF and FGF-2 have been incorporated in hydrogel coatings to obtain bioactive titanium (15,16). Preliminary experiments demonstrated that $SrCl_2$ can be included in the CMCA hydrogel and subsequently released (data not shown). In this study we found that $SrCl_2$ at 5 µg/ml is able to improve osteogenic differentiation of BMSCs. This data will guide us in the selection of the initial amount of $SrCl_2$ that should be incorporated into CMCA to obtain a similar final concentration released to the cells in the implant, at least in the initial phase of healing process. It is possible to speculate that, in vivo, strontium will be gradually eluted from CMCA included in a TT mesh creating a gradient of strontium concentrations that may vary with time and distance from the implant. Nevertheless, the presence of an optimal

concentration of strontium within implant will provide BMSCs seeded into TT with signals triggering their initial osteogenic differentiation. In view of a future clinical application, CMCA would be enriched with $SrCl_2$, loaded within TT mesh and oven-dried to generate off-the-shelf devices that can be easily seeded with autologous cells during surgery. In these bioactive implants, the hydrogel would play a key role retaining of progenitor cells at the bone-implant interface and delivering an osteogenic signal in addition to physiological signals from bone.

Conclusions

Faster and improved bone ingrowth into a porous titanium implant may confer better stability during the healing process. Our results demonstrate that the association of a biocompatible hydrogel, such as CMCA, with a macroporous titanium may represent a suitable approach to effectively immobilize autologous BMSCs within the implant. The enrichment with strontium and osteoprogenitor cells would convert the prosthesis from inert to bioactive, promoting osseointegration and consequently reducing the risk of mobilization and the number of revision procedures. This strategy could be exploited also in revision surgery, where macroporous titanium can be used to fill void bone spaces and to provide an anchorage point for revision components, helping the surgeon to manage bone loss at implant interface. Based on these considerations, we envision that the generation of bioactive implants that can deliver to the implant site both progenitor cells and osteogenic signals would represent a significant step forward respect to the current clinical practice.

Acknowledgements

I would like to thank all the co-authors: Mercuri D, Colombini A, De Conti G, Segatti F, Zagra L, Moretti M. Furthermore, I would like to thank Pedroli S., Tavola M., Sadr N., and Fusi S. for their precious help. This study was funded by Italian Ministry of Health (RF-IOG-2007-647233).

References

1. Bobyn JD. Fixation and bearing surfaces for the next millennium. Orthopedics.22:810-2. 1999.
2. Albrektsson T, Branemark PI, Hansson HA, Lindstrom J. Osseointegrated titanium implants. Requirements for ensuring a long-lasting, direct bone-to-implant anchorage in man. Acta Orthop Scand.52:155-70. 1981.
3. Ochsner PE. Osteointegration of orthopaedic devices. Semin Immunopathol.33:245-56. 2011.
4. Chaudhari A, Braem A, Vleugels J, Martens JA, Naert I, Cardoso MV, Duyck J. Bone tissue response to porous and functionalized titanium and silica based coatings. PLoS One.6:e24186. 2011.
5. Shannon FJ, Cottrell JM, Deng XH, Crowder KN, Doty SB, Avaltroni MJ, Warren RF, Wright TM, Schwartz J. A novel surface treatment for porous metallic implants that improves the rate of bony ongrowth. J Biomed Mater Res A.86:857-64. 2008.
6. Spoerke ED, Murray NG, Li H, Brinson LC, Dunand DC, Stupp SI. Titanium with aligned, elongated pores for orthopedic tissue engineering applications. J Biomed Mater Res A.84:402-12. 2008.
7. Heinl P, Muller L, Korner C, Singer RF, Muller FA. Cellular Ti-6Al-4V structures with interconnected macro porosity for bone implants fabricated by selective electron beam melting. Acta Biomater.4:1536-44. 2008.

8. Marin E, Fusi S, Pressacco M, Paussa L, Fedrizzi L. Characterization of cellular solids in Ti6Al4V for orthopaedic implant applications: Trabecular titanium. J Mech Behav Biomed Mater.3:373-81. 2010.
9. Karageorgiou V, Kaplan D. Porosity of 3D biomaterial scaffolds and osteogenesis. Biomaterials.26:5474-91. 2005.
10. Daugaard H, Elmengaard B, Andreassen T, Bechtold J, Lamberg A, Soballe K. Parathyroid hormone treatment increases fixation of orthopedic implants with gap healing: a biomechanical and histomorphometric canine study of porous coated titanium alloy implants in cancellous bone. Calcif Tissue Int.88:294-303. 2011.
11. Petrie TA, Raynor JE, Reyes CD, Burns KL, Collard DM, Garcia AJ. The effect of integrin-specific bioactive coatings on tissue healing and implant osseointegration. Biomaterials.29:2849-57. 2008.
12. Clark PA, Moioli EK, Sumner DR, Mao JJ. Porous implants as drug delivery vehicles to augment host tissue integration. FASEB J.22:1684-93. 2008.
13. Vrana NE, Dupret-Bories A, Bach C, Chaubaroux C, Coraux C, Vautier D, Boulmedais F, Haikel Y, Debry C, Metz-Boutigue MH, Lavalle P. Modification of macroporous titanium tracheal implants with biodegradable structures: tracking in vivo integration for determination of optimal in situ epithelialization conditions. Biotechnol Bioeng.109:2134-46. 2012.
14. De Giglio E, Cometa S, Ricci MA, Cafagna D, Savino AM, Sabbatini L, Orciani M, Ceci E, Novello L, Tantillo GM, Mattioli-Belmonte M. Ciprofloxacin-modified electrosynthesized hydrogel coatings to prevent titanium-implant-associated infections. Acta Biomater.7:882-91. 2011.
15. De Giglio E, Cometa S, Ricci MA, Zizzi A, Cafagna D, Manzotti S, Sabbatini L, Mattioli-Belmonte M. Development and characterization of rhVEGF-loaded poly(HEMA-MOEP) coatings electrosynthesized on titanium to enhance bone mineralization and angiogenesis. Acta Biomater.6:282-90. 2010.
16. Ichinohe N, Kuboki Y, Tabata Y. Bone regeneration using titanium nonwoven fabrics combined with fgf-2 release from gelatin hydrogel microspheres in rabbit skull defects. Tissue Eng Part A.14:1663-71. 2008.
17. Capuccini C, Torricelli P, Sima F, Boanini E, Ristoscu C, Bracci B, Socol G, Fini M, Mihailescu IN, Bigi A. Strontium-substituted hydroxyapatite coatings synthesized by pulsed-laser deposition: in vitro osteoblast and osteoclast response. Acta Biomater.4:1885-93. 2008.
18. Ni GX, Chiu KY, Lu WW, Wang Y, Zhang YG, Hao LB, Li ZY, Lam WM, Lu SB, Luk KD. Strontium-containing hydroxyapatite bioactive bone cement in revision hip arthroplasty. Biomaterials.27:4348-55. 2006.
19. Park JW, Kim HK, Kim YJ, Jang JH, Song H, Hanawa T. Osteoblast response and osseointegration of a Ti-6Al-4V alloy implant incorporating strontium. Acta Biomater.6:2843-51. 2010.
20. Li Y, Li Q, Zhu S, Luo E, Li J, Feng G, Liao Y, Hu J. The effect of strontium-substituted hydroxyapatite coating on implant fixation in ovariectomized rats. Biomaterials.31:9006-14. 2010.
21. Marie PJ, Felsenberg D, Brandi ML. How strontium ranelate, via opposite effects on bone resorption and formation, prevents osteoporosis. Osteoporos Int.22:1659-67. 2011.
22. Bonnelye E, Chabadel A, Saltel F, Jurdic P. Dual effect of strontium ranelate: stimulation of osteoblast differentiation and inhibition of osteoclast formation and resorption in vitro. Bone.42:129-38. 2008.
23. Meunier PJ, Roux C, Seeman E, Ortolani S, Badurski JE, Spector TD, Cannata J, Balogh A, Lemmel EM, Pors-Nielsen S, Rizzoli R, Genant HK, Reginster JY. The effects of strontium ranelate on the risk of vertebral fracture in women with postmenopausal osteoporosis. N Engl J Med.350:459-68. 2004.
24. Sila-Asna M, Bunyaratvej A, Maeda S, Kitaguchi H, Bunyaratavej N. Osteoblast differentiation and bone formation gene expression in strontium-inducing bone marrow mesenchymal stem cell. Kobe J Med Sci.53:25-35. 2007.
25. Choudhary S, Halbout P, Alander C, Raisz L, Pilbeam C. Strontium ranelate promotes osteoblastic differentiation and mineralization of murine bone marrow stromal cells: involvement of prostaglandins. J Bone Miner Res.22:1002-10. 2007.
26. Peng S, Zhou G, Luk KD, Cheung KM, Li Z, Lam WM, Zhou Z, Lu WW. Strontium promotes osteogenic differentiation of mesenchymal stem cells through the Ras/MAPK signaling pathway. Cell Physiol Biochem.23:165-74. 2009.
27. Peng S, Liu XS, Wang T, Li Z, Zhou G, Luk KD, Guo XE, Lu WW. In vivo anabolic effect of strontium on trabecular bone was associated with increased osteoblastogenesis of bone marrow stromal cells. J Orthop Res.28:1208-14. 2010.
28. Yang F, Yang D, Tu J, Zheng Q, Cai L, Wang L. Strontium enhances osteogenic differentiation of mesenchymal stem cells and in vivo bone formation by activating Wnt/catenin signaling. Stem Cells.29:981-91. 2011.
29. Caplan AI. Mesenchymal stem cells. J Orthop Res.9:641-50. 1991.
30. Pittenger MF, Mackay AM, Beck SC, Jaiswal RK, Douglas R, Mosca JD, Moorman MA, Simonetti DW, Craig S, Marshak DR. Multilineage potential of adult human mesenchymal stem cells. Science.284:143-7. 1999.
31. Barry FP, Murphy JM. Mesenchymal stem cells: clinical applications and biological characterization. Int J Biochem Cell Biol.36:568-84. 2004.
32. Jager M, Herten M, Fochtmann U, Fischer J, Hernigou P, Zilkens C, Hendrich C, Krauspe R. Bridging the gap: bone marrow aspiration concentrate reduces autologous bone grafting in osseous defects. J Orthop Res.29:173-80. 2011.
33. Kalia P, Coathup MJ, Oussedik S, Konan S, Dodd M, Haddad FS, Blunn GW. Augmentation of bone growth onto the acetabular cup surface using bone marrow stromal cells in total hip replacement surgery. Tissue Eng Part A.15:3689-96. 2009.
34. van den Dolder J, Farber E, Spauwen PH, Jansen JA. Bone tissue reconstruction using titanium fiber mesh combined with rat bone marrow stromal cells. Biomaterials.24:1745-50. 2003.
35. Mehta M, Strube P, Peters A, Perka C, Hutmacher D, Fratzl P, Duda GN. Influences of age and mechanical stability on volume, microstructure, and mineralization of the fracture callus during bone healing: is osteoclast activity the key to age-related impaired healing? Bone.47:219-28. 2010.
36. Leone G, Fini M, Torricelli P, Giardino R, Barbucci R. An amidated carboxymethylcellulose hydrogel for cartilage regeneration. J Mater Sci

Mater Med.19:2873-80. 2008.

37. Barbucci R, Leone G, Monici M, Pantalone D, Fini M, Giardino R. The effect of amidic moieties on polysaccharides: evaluation of the physicochemical and biological properties of amidic Carboxymethylcellulose (CMCA) in the form of linear polymer and hydrogel. J Mater Chem.15:2234-41. 2005.
38. de Girolamo L, Lopa S, Arrigoni E, Sartori MF, Baruffaldi Preis FW, Brini AT. Human adipose-derived stem cells isolated from young and elderly women: their differentiation potential and scaffold interaction during in vitro osteoblastic differentiation. Cytotherapy.11:793-803. 2009.
39. Halvorsen YD, Franklin D, Bond AL, Hitt DC, Auchter C, Boskey AL, Paschalis EP, Wilkison WO, Gimble JM. Extracellular matrix mineralization and osteoblast gene expression by human adipose tissue-derived stromal cells. Tissue Eng.7:729-41. 2001.
40. Bodo M, Lilli C, Bellucci C, Carinci P, Calvitti M, Pezzetti F, Stabellini G, Bellocchio S, Balducci C, Carinci F, Baroni T. Basic fibroblast growth factor autocrine loop controls human osteosarcoma phenotyping and differentiation. Mol Med.8:393-404. 2002.
41. Hurtt ME, Placke ME, Killinger JM, Singer AW, Kennedy GL, Jr. 13-week inhalation toxicity study of dimethylformamide (DMF) in cynomolgus monkeys. Fundam Appl Toxicol.18:596-601. 1992.
42. Senoh H, Aiso S, Arito H, Nishizawa T, Nagano K, Yamamoto S, Matsushima T. Carcinogenicity and chronic toxicity after inhalation exposure of rats and mice to N,N-dimethylformamide. J Occup Health.46:429-39. 2004.
43. Ohbayashi H, Yamazaki K, Aiso S, Nagano K, Fukushima S, Ohta H. Enhanced proliferative response of hepatocytes to combined inhalation and oral exposures to N,N-dimethylformamide in male rats. J Toxicol Sci.33:327-38. 2008.
44. Lenzia F, Sannino A, Borriello A, Porro F, Capitani D, Mensitieri G. Probing the degree of crosslinking of a cellulose based superabsorbing hydrogel through traditional and NMR techniques. Polymer.44:1577-88. 2003.
45. Barbucci R, Arturoni E, Panariello G, Di Canio C, Lamponi S. A new amido phosphonate derivative of carboxymethylcellulose with an osteogenic activity and which is capable of interacting with any Ti surface. J Biomed Mater Res A.95:58-67. 2010.
46. Vestermark MT, Hauge EM, Soballe K, Bechtold JE, Jakobsen T, Baas J. Strontium doping of bone graft extender. Acta Orthop.82:614-21. 2011.
47. Gastaldi G, Asti A, Scaffino MF, Visai L, Saino E, Cometa AM, Benazzo F. Human adipose-derived stem cells (hASCs) proliferate and differentiate in osteoblast-like cells on trabecular titanium scaffolds. J Biomed Mater Res A.94:790-9. 2010.
48. Asti A, Gastaldi G, Dorati R, Saino E, Conti B, Visai L, Benazzo F. Stem Cells Grown in Osteogenic Medium on PLGA, PLGA/HA, and Titanium Scaffolds for Surgical Applications. Bioinorg Chem Appl.831031. 2010.

Chapter 9

In vivo evaluation of bone deposition in macroporous titanium implants loaded with mesenchymal stem cells and strontium-enriched hydrogel

Abstract

Bone-implant integration represents a major requirement to grant implant stability and reduce the risk of implant loosening. This study investigates the effect of progenitor cells and strontium-enriched hydrogel on the osseointegration of titanium implants. To mimic implant-bone interaction, an ectopic model was developed grafting Trabecular Titanium™ (TT) implants into decellularized bone seeded with human bone marrow mesenchymal stem cells (hBMSCs). TT was loaded or not with strontium-enriched amidated carboxymethylcellulose hydrogel (CMCA) and/or hBMSCs. Constructs were implanted subcutaneously in athymic mice and osteodeposition was investigated with micro-CT, SEM, and pull-out at 4, 8 and 12 weeks. Fluorescence imaging was performed at 8 and 12 weeks, histology at 4 and 8 weeks. Micro-CT demonstrated the homogeneity of the engineered bone in all groups, supporting the reproducibility of the ectopic model. Fluorescence imaging, histology, SEM and pull-out mechanical testing showed superior tissue ingrowth in TT implants loaded with both strontium-enriched CMCA and hBMSCs. In our model, the synergic action of the bioactive hydrogel and hBMSCs increased both the bone deposition and TT integration. Thus, we suggest that using prostheses pre-loaded with strontium-enriched CMCA and seeded with BMSCs could represent a valid single-step surgical strategy to improve implant osseointegration.

Introduction

Titanium is widely used to produce prosthetic implants because of its biocompatibility, high strength-to-weight ratio and low elastic modulus (1,2). In cementless prosthesis, primary implant stability is achieved by passive mechanical fixation within the bone, then secondary stability is achieved through osseointegration (3). Osseointegration and implant stability are essential to reduce the risk of implant loosening (4,5) and consequently the revision surgeries. Since the bone-implant interface is the weakest point during the initial healing (6), porous metal materials have been developed for cementless implants to maximize bone-to-implant contact and bone ingrowth (7-9). Furthermore, surface coatings have been developed to activate the bio-inert surface of metallic implants, as the combination of titanium with hydrogels (10,11). Strontium (Sr) is a promising candidate for implant enrichment, as recently proposed for bone scaffolds (12) and titanium (13,14). Indeed, the anabolic and anticatabolic effects of strontium on bone (15), together with its ability to promote osteogenic differentiation of bone marrow mesenchymal stem cells (BMSCs) (16,17) are believed to support implant bone ingrowth. It has been shown that BMSCs seeded into titanium implants or transplanted in the peri-implant site are able to improve osseointegration (18-20). This approach could be particularly useful in elderly patients, where age and age-related pathologies can deplete the population of BMSCs or impair their osteogenic ability (21). Among porous metals developed for prosthetic implants, Trabecular Titanium™ (TT) is clinically used for acetabular cup and revision components. This macroporous titanium has a structure resembling the trabecular bone that has been optimized to improve bone ingrowth (22). Previously, we have demonstrated that a low concentration of strontium can induce hBMSCs osteogenic differentiation and that the association of TT with an amidated carboxymethylcellulose (CMCA) hydrogel significantly improves cell retention and hBMSCs differentiation (23). Based on these promising results, we suggest that TT implants preloaded with a Sr-enriched CMCA hydrogel could be loaded with autologous BMSCs and implanted in a one-step approach to improve osseointegration. Ectopic models have been used to evaluate bone formation and to highlight the pristine effects of bioactive factors and transplanted heterologous/xenogenic cells, avoiding the complex interactions of native bone environment (24). However, only a recent study has proposed a subcutaneous ectopic model of osseointegration, using titanium screws and ceramic scaffolds (25).

In our *in vivo* study, to evaluate if the association of TT with Sr-enriched CMCA and hBMSCs could ameliorate bone deposition, we developed an ectopic model of osseointegration, where athymic mice acted as “living bioreactors” and a bone scaffold seeded with osteogenic pre-differentiated hBMSCs and cultured prior to implantation was used to mimic bone.

Materials and Methods

Experimental design

This study used a full factorial design testing the association of TT with two factors (Sr-enriched CMCA, here on called CMCA, and hBMSCs), resulting in four groups: TT (absence of CMCA and hBMSCs); TT+CMCA (presence of CMCA, absence of hBMSCs); TT+BMSCs (absence of CMCA, presence of hBMSCs) and TT+CMCA+BMSCs (presence of CMCA and hBMSCs) (Fig. 1A). TT group was used as control for data normalization, since it represents the current clinical practice. Samples from each group were analyzed as follows: fluorescence imaging (n=3, 8 and 12 weeks); micro-CT (n=3, 4, 8 and 12 weeks); histology and histomorphometry (n=2, 4 and 8 weeks); SEM at (n=1, 4, 8 and 12 weeks); pull-out at (n=3, 4 and 8 weeks; n=4, 12 weeks).

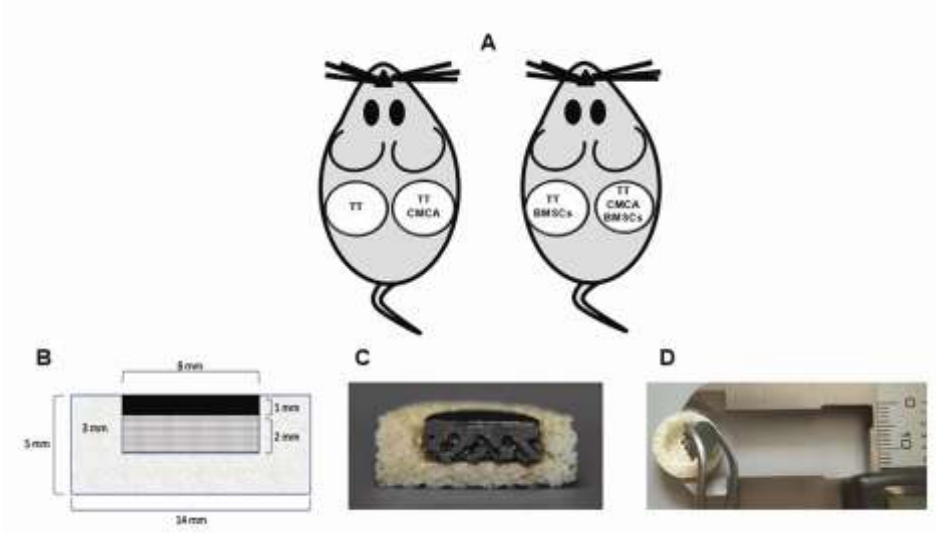

Fig. 1. Experimental design. (a) Implantation scheme (12 mice per time point): 6 animals received TT and TT+CMCA, 6 animals received TT+BMSCs and TT+CMCA+BMSCs. (b) Construct scheme: grey structure represents engineered bone (Ø 14 mm x h 5 mm), black structure represents the TT compact head (Ø 8 mm x h 1 mm), and the grid structure represents the trabecular structure of TT disk (Ø 8 mm x h 2 mm). (c) Side-view picture of the assembled construct. (d) Construct assembling by press-fit.

Materials description

Trabecular Titanium™ was provided as disks (Ø 8mm, h 3mm, Ti6Al4V, Limacorporate s.p.a.) with a compact head (Ø 8mm, h 1mm) and a trabecular structure (22) (Ø 8mm, h 2mm) CMCA was synthetized(23) and enriched with $SrCl_2$ (Sigma-Aldrich) prior to loading into TT. TT+CMCA samples consisted in TT disks loaded with CMCA (wet weight 0.07g/sample.).

Cell culture and osteogenic pre-differentiation

Human BMSCs were isolated from 5 osteoarthritic patients undergoing total hip replacement (mean age 57±6 years) under informed written consent and approval of the Institutional Review Board. Bone marrow was centrifuged (400g, 10 min) and plated in complete medium: high glucose Dulbecco's

Modified Eagle Medium (Gibco), 10% fetal bovine serum (Lonza), 1mM sodium pyruvate, 100mM hepes, 2mM L-glutamine, 100µg/mL streptomycin, 100U/mL penicillin (all from Gibco), 5ng/mL bFGF (Peprotech). Cells were expanded until passage 2 and frozen. When needed, cells were thawed and differentiated in osteogenic medium (26): complete medium with 0.15mM L-ascorbic acid, 10nM dexamethasone, 10nM cholecalciferol, and 10mM β-glycerophosphate (all from Sigma-Aldrich).

Construct model assembling

The constructs were composed of TT or TT+CMCA, unseeded or seeded with hBMSCs, grafted in cell-seeded bone scaffolds [Figure 1(B)]. Decellularized bovine cancellous bone (Tutobone®, Tutogen Medical GmbH) was cut in cylinders (Ø 14mm, h 5mm) and centrally holed (Ø 8mm, h 3mm) to insert TT or TT+CMCA. After 3 weeks of differentiation, $8.5x10^5$ hBMSCs were seeded on bone scaffold and cultured for 1 week in osteogenic medium. The day before implantation, $7.5x10^5$ hBMSCs pre-differentiated for 4 weeks were seeded on TT and TT+CMCA. On the implantation day, TT and TT+CMCA, unseeded or seeded with hBMSCs, were grafted in the bone scaffold [Figure 1(C)].

In vivo subcutaneous implantation

Animals were handled under the approval of the Institutional Animal Care and Use Committee of Mario Negri Institute for Pharmacological Research. Procedures and animal care were conducted in conformity with institutional guidelines in compliance with national (Law 116/92, Authorization n.19/2008-A issued March 6, 2008, by the Italian Ministry of Health) and international laws and policies (EEC Council Directive 86/609, OJ L 358. 1, December 12, 1987; Standards for the Care and Use of Laboratory Animals - UCLA, United States National Research Council, Statement of Compliance A5023-01, November 6, 1998).

Thirty-six 6-weeks-old female athymic mice (from Harlan®) were maintained under specific pathogen-free conditions with food and water provided *ad libitum*. Twelve animals per time point (4, 8, 12 weeks) received two implants/each inserted subcutaneously in dorsal pockets with the compact head of TT facing the skin. Surgeries were conducted under general anesthesia by intraperitoneal injection of ketamine chloride (80 mg/kg, Imalgene, Merial) and medetomidine hydrochloride (1 mg/kg, Domitor, Pfizer). A blunt dissection was conducted to create a pocket between the aponeurosis and the subcutaneous tissue for construct placement, then the skin was sutured with #4-0 Monocryl thread (Ethicon). After 4, 8 and 12 weeks mice were euthanized by CO_2 inhalation and implants were removed for investigations.

Bone deposition analysis by fluorescence imaging

Imaging of bone deposition within the constructs was performed using the fluorescent bisphosphonate agent OsteoSense™750 (VisEN Medical) (27,28). This analysis was performed at 8 and 12 weeks, because at 4 weeks there was an high risk of inflammatory response and poor uptake of the fluorescent agent in the construct area. Mice were intravenously injected with 2 nmol/subject OsteoSense™750. After 24 hours, optical scans were acquired on living mice and *ex vivo* on explanted constructs. For the *in vivo* scan, animals were anesthetized with a continuous flow of 2% isoflurane. The fluorescent signal was detected using the Explore Optix System equipped with a fixed pulsed laser diode as illumination source (734nm excitation - 770nm emission, ART Advanced Research Technologies). Fluorescence was recorded as pseudo-color images showing the distribution of detected photon counts. Overlay of the grey-scale (body reference photograph) and pseudo-color images allowed the localization of fluorescent signal in the animal. *Ex vivo* imaging was performed on explants on both dorsal and ventral side defining a region of interest (ROI). Optiview software (version 2.02.00; ART Advanced Research Technologies) elaborated the data and the intensity of the Fluorescence Lifetime Imaging (FLI) signal was shown as pseudo-color scale bars. In explanted constructs, the photon counts emitted from each ROI-related pixel of dorsal side were coupled with those of ventral side. Values were normalized respect to TT.

Micro-CT analysis

At 4, 8 and 12 weeks, explanted constructs were scanned with an Explore Locus micro-CT scanner (GE Healthcare) using 80 kV voltage, 450 µA current with 400 msec exposure time per projection and 400 projections over 360°. The isotropic resolution was 27µm and the reconstructed 3D images were analyzed using MicroView software (version 2.1.2; GE Healthcare). A volume of interest (VOI) comprising the whole construct was designed and a histogram, depicting the distribution of voxel along the scale of density expressed in Hounsfield units, was computed. Based on the histogram, the different regions of each construct were separated using a global thresholding procedure. Isosurface volume rendering function was applied to determine the volume of each region.

Histological analysis and histomorphometry

Samples were histologically investigated at 4 and 8 weeks. The death of one mouse of the 12-weeks group reduced the number of samples designed for histology, thus the remaining samples were investigated by pull-out test. Explants were fixed in 10% formalin, dehydrated in a graded series of ethanol and embedded in methyl-metacrylate (Technovit®7200). Middle cross-sections were ground to about 60-90µm (Exakt Apparatebau) and stained with toluidine blue. The software ImageJ1.45s® was used to detect the various components of the construct (titanium, bone scaffold, newly formed tissue)

and to perform the histomorphometric analysis. Tissue ingrowth was calculated as the percentage of the space available for tissue ingrowth occupied by newly formed tissue and represented as relative increase respect to TT.

Scanning electron microscopy (SEM)

After 4, 8, and 12 weeks, explants were fixed in 2.5% paraformaldehyde and 2.5% glutaraldehyde in 0.1 M Na-Cacodylate buffer (pH 7.4), then rinsed with Na-Cacodylate buffer and fixed for 1 h in OsO_4 (1% in Na-Cacodylate buffer). Samples were dehydrated in ethanol and hexamethyldisilazane (Sigma-Aldrich), mounted on aluminum stubs and sputter-coated with gold (E5100 Polaron Instruments). Observations were performed with Sigma Scanning Electron Microscope (Zeiss) fitted with secondary (SE) and backscattered electrons (BSE) detectors, and images were acquired at 10 kV at working distance of 7mm.

Mechanical pull-out tests

Pull-out tests were performed to determine the interfacial shear strength of the implanted constructs after 4, 8, and 12 weeks. Tests were performed on a mechanical testing bench (servo-hydraulic universal MTS MiniBionix 858, load range 25 KN Load cell class 0.5 - Calibration certified 2010_002) using a custom-made pull-out system and support jigs. Samples were centered over the support jig and a screw was glued on the titanium compact head. Samples were then placed on a flat surface and secured onto a vise. The pull-out test was performed applying a constant crosshead speed of 0.5 mm/min on the constructs and recording the resulting pull-out force trend. Peak force values were normalized respect to the average value measured in TT after 4 weeks and expressed as relative increase.

Statistical Analysis

Statistical analysis was performed using the One-Way ANOVA with Bonferroni's post-hoc test (Graph Pad Prism v5.00, Graph Pad software) to compare the experimental groups within the same time point. Data are presented as mean$\pm$standard error (SE) unless differently specified. Level of significance was set at $p<0.05$.

Results

Gross appearance

All animals survived the surgery and post-operative period without complications, with the exception of one mouse, which showed local infection and skin ulceration after 8 weeks and was removed from the

study. The implanted constructs evoked an initial inflammatory response, which receded during time. At the time of sample harvesting, no signs of infection and/or foreign body reaction were observed and the implants were easily dissected from subcutaneous tissue. Gross appearance of the explants revealed the formation of a vascular network throughout the constructs already after 4 weeks (Fig. 2A).

Bone deposition analysis by fluorescence imaging

Osteosense™750-related signal, visualized by *in vivo* imaging, was clearly detectable in regions subjected to active bone turnover (skull, scapula, spine, hind limbs) (Fig. 2B). The signal in the implanted constructs was partially masked by the stronger signal coming from active bone remodeling regions of mice. To overcome this limitation, we analyzed *ex vivo* the distribution of Osteosense™750 scanning the samples with the TT compact head upward (dorsal) or downward (ventral) (Fig. 2C). At 8 weeks, TT+BMSCs and TT+CMCA+BMSCs signals were higher compared to TT and TT+CMCA samples, that displayed comparable FLI photon counts. After 12 weeks, FLI photon counts in TT+CMCA and TT+BMSCs samples were 1.5-fold higher compared to TT. More interestingly, the signal of TT+CMCA+BMSCs constructs was higher compared to all the other groups [Figure 2(D)].

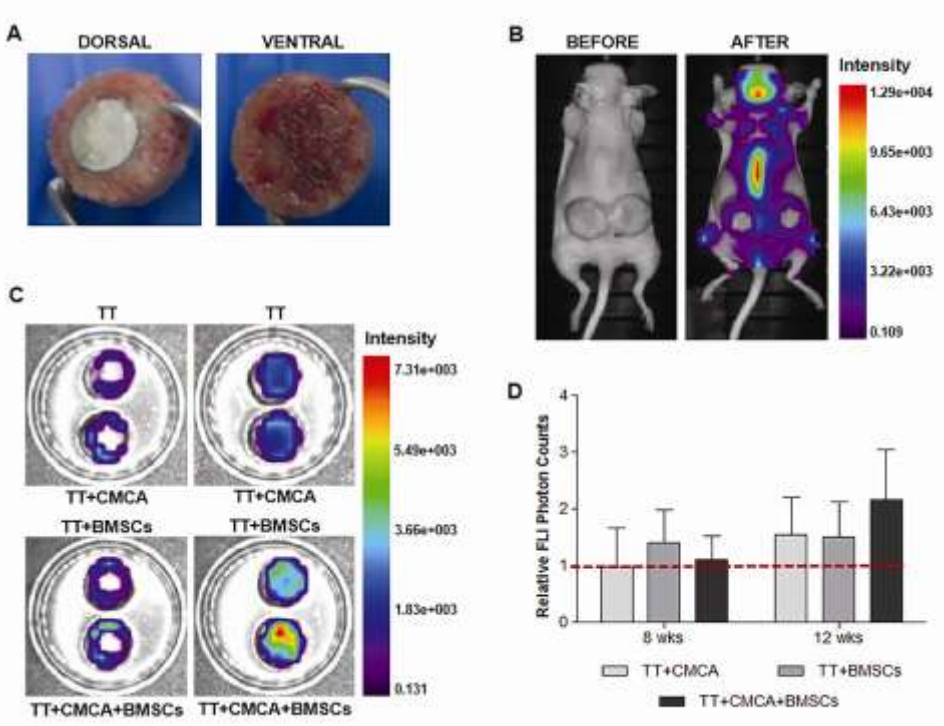

Fig. 2. *In vivo* and *ex vivo* fluorescence imaging of osteodeposition (a) Gross appearance of explanted constructs in dorsal and ventral view. (b) Representative FLI images before and 24h after injection of Osteosense™750 in a living mouse. (c) Representative images FLI images of Osteosense™750 uptake in explanted constructs in dorsal (left column) and ventral (right column) view. (d) Quantification of Osteosense™750-related FLI signal. Photon counts emitted from dorsal and ventral side of each construct were coupled and normalized respect to TT value at the corresponding time point (TT=1, red line).

Micro-CT analysis

Micro-CT was performed to obtain information on volumetric appearance of the constructs and to

analyze the matrix deposition. The 3D rendering of the implanted construct is shown in Fig. 3(A). Within each assembled construct we identified different regions on the basis of their different ability to attenuate X-rays. Fig. 3(B) shows the different attenuation peaks associated with void space (A), matrix deposited within bone (B), bone trabeculae (C), matrix deposited within titanium (D), and titanium structure (E) and the spatial distribution of voxel with the same attenuation coefficient. For all the groups, the volume of engineered bone, corresponding to the sum of bone matrix and bone trabeculae (B+C), was homogeneous after 4 weeks from implantation (Fig. 3C).

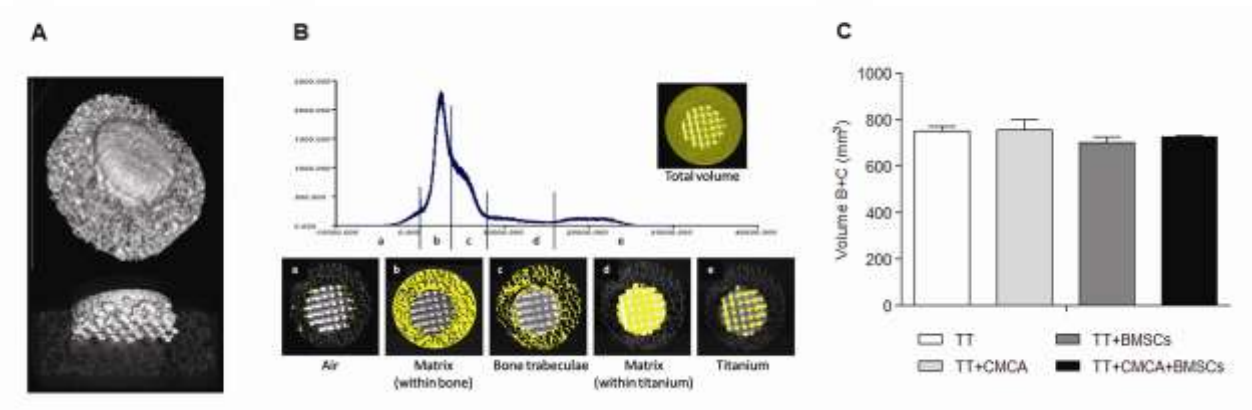

Fig. 3. Micro-CT analysis. (a) 3D rendering of the implanted construct (top image) and 3D rendering of the TT disk within the bone scaffold displayed in the background as 2D shaded image (bottom image) (b) Representative intensity histogram of tomogram data. The vertical lines indicate the threshold-based phase separation of air (A), matrix within bone (B), bone trabeculae (C), matrix within titanium (D) and titanium trabecular structure (E). Below, the resultant 2D ROIs (yellow) of the different construct compartments (A-E) superimposed on micro-CT sections. (c) Volume of engineered bone comprising matrix and bone trabeculae (B+C) in the different groups at 4 weeks. Volume measures (mm^3) are graphed as mean±SD.

The same result was obtained comparing the volume of engineered bone in the different groups after 8 and 12 weeks (data not shown). For each implant, we tried to determine the bone mineral density (BMD) to evaluate the ongoing mineralization process (data not shown). Despite our efforts, we were not able to precisely quantify the density of newly formed bone matrix, since titanium caused a high scattering of x-rays both in the TT disk and in the surrounding bone region.

Histological analysis and histomorphometry

After 8 weeks, Toluidine Blue staining of explanted constructs revealed that poor integration occurred between TT and engineered bone in TT and TT+CMCA groups (Fig. 4A,B). A more consistent amount of newly formed tissue was found at the bone-TT interface in TT+BMSCs and TT+CMCA+BMSCs groups (Fig. 4C,D). Upon close inspection at higher magnification, fibrovascular tissue was observed in TT+BMSCs group (Fig. 4E). Only in TT+CMCA+BMSCs samples, we observed areas with concentric whorls of spindle shaped cells with matrix deposition reminiscent of early bone formation (Fig. 4F). Representative histomorphometric analysis of tissue ingrowth within the constructs is shown in Fig. 4G.

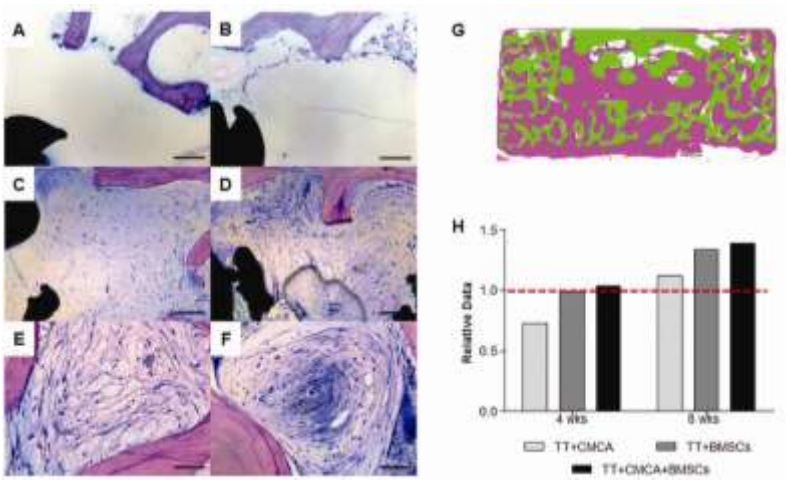

Fig. 4. Histological and histomorphometric analysis of the constructs. Histology at 8 weeks after implantation: (a-d) interface between titanium and engineered bone in TT (a), TT+CMCA (b), TT+BMSCs (c), and TT+CMCA+BMSCs (d) (Scale bars 200 µm); (e) bundles of fibrovascular tissue at bone-TT interface in TT+BMSCs (Scale bar 100 µm); (f) concentric layers of spindle cells interspersed with ECM in TT+CMCA+BMSCs (Scale bar 100 µm). Titanium (T) and engineered bone (B) are specified in the images. (g) Representative image used for histomorphometric analysis. TT and bone trabeculae are represented in green and newly formed tissue is represented in pink. (h) Quantification of tissue ingrowth at 4 and 8 weeks after implantation. Data were normalized respect to TT value at the same time point and expressed as fold increase (TT=1, red line).

At 4 weeks, tissue ingrowth in TT, TT+BMSCs, and TT+CMCA+BMSCs samples was similar, whereas at 8 weeks TT+BMSCs and TT+CMCA+BMSCs showed a greater tissue ingrowth compared to TT and TT+CMCA samples (Fig. 4H).

Scanning electron microscopy (SEM)

After 4 weeks, SEM analysis highlighted striking differences between experimental groups where TT was enriched with hBMSCs in comparison with groups where TT was unseeded. Indeed, matrix filled the space at the bone-implant interface in TT+BMSCs and TT+CMCA+BMSCs, whereas empty space was clearly visible in TT and TT+CMCA samples (Fig. 5A).

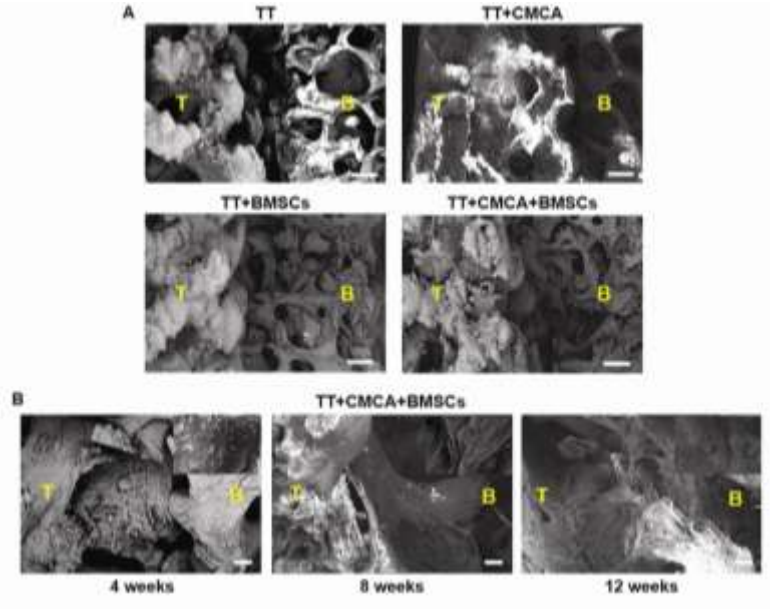

Fig. 5. SEM evaluation of new matrix deposition. (a) SEM images of the bone-TT interface (yellow arrows) 4 weeks after implantation. Titanium (T) and engineered bone (B) are respectively on the left and right side of pictures (Scale bars 500 µm). (b) SEM images of TT+CMCA+BMSCs at 4, 8 and 12 weeks after implantation showing the progressive increase in matrix organization (Scale bars 100 µm). Insets represent the same areas at a higher magnification (Scale bars 5 µm).

At all the tested time-points, TT+CMCA+BMSCs showed a superior matrix content at the bone-TT interface. A clear increase in quantity and organization of newly formed matrix was observed in this experimental group over time (Fig. 5B).

Mechanical pull-out tests

Pull-out test was carried out by means of a customized apparatus (Fig. 6A,B). A representative curve of pull-out force is shown in Fig. 6C, where the maximum value corresponds to the maximum load achieved before failure following a mixed fracture mode (cohesive and adhesive). After 4 weeks, pull-out peak force in all the experimental groups was comparable to that measured for TT alone. At later time points, the association of TT with Sr-enriched CMCA and hBMSCs resulted in higher pull-out peak force values compared to all the other experimental groups. Furthermore, in TT+BMSCs and TT+CMCA+BMSCs groups, pull-out peak force increased from 4 to 12 weeks, whereas values measured in TT+CMCA group remained more stable during time (Fig. 6D).

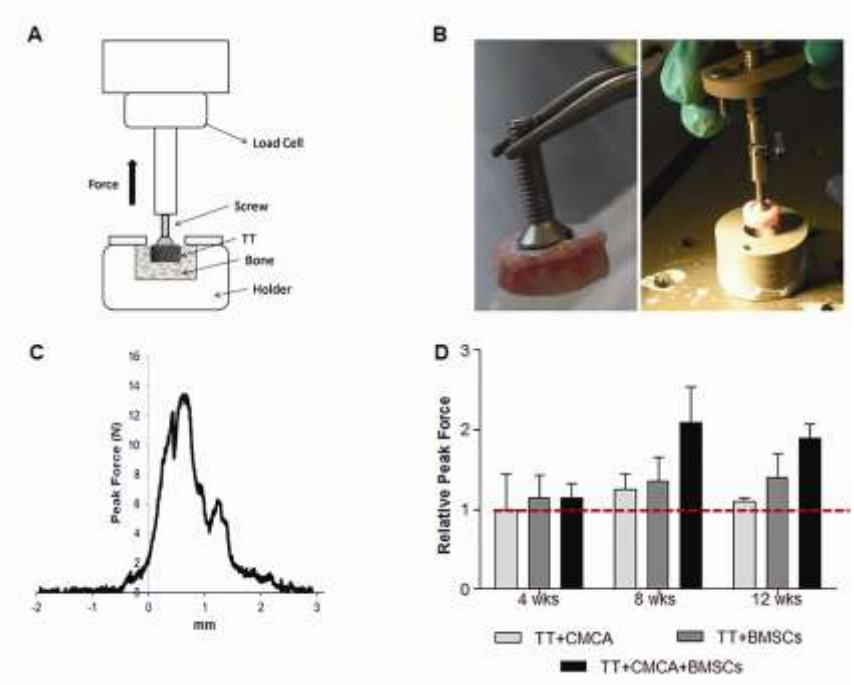

Fig. 6. Evaluation of bone-TT integration through pull-out biomechanical testing. (a) Pull-out servo-hydraulic machine scheme. (b) Custom made construct holder. (c) Representative curve of pull-out peak force. (d) Quantification of pull-out peak force. For each group, the mean values of peak force (N) were normalized respect to the value of TT at 4 weeks, used as baseline (TT=1, red line).

Discussion

Osseointegration, achieved through the matrix deposition at the bone-implant interface, significantly contributes to the success of implanted devices (3,5). In our previous *in vitro* study (23), we demonstrated that the association of TT and CMCA significantly increases cell retention within TT and hBMSCs osteogenic differentiation in the presence of strontium, suggesting that hBMSCs and Sr-enriched CMCA could be combined to generate bioactive TT implants.

In this *in vivo* study, we generated an ectopic model of osseointegration in athymic mice by subcutaneous implantation of constructs composed of engineered bone and TT, loaded or not with Sr-enriched CMCA and hBMSCs. To evaluate the influence of these factors on implant integration, we used a multimodal approach combining imaging techniques, mechanical testing and histological analysis. A recent study by Park *et al.* (25) employed a subcutaneous model of osseointegration. In this proof-of-concept study, a synthetic scaffold was loaded with BMP-2 to induce bone differentiation of the rat host

cells and coupled with a compact titanium dental implant. Differently, we firstly engineered *in vitro* a construct using a decellularized bone scaffold enriched by osteogenic pre-differentiated hBMSCs, then we inserted a porous TT disk loaded or not with a bioactive hydrogel and human cells. In our subcutaneous model of osseointegration, engineered bone scaffolds were filled with high-density connective tissue, in accordance with results from Park *et al.* (25). The formation of a vascular network throughout the constructs after 4 weeks suggests that, although other ectopic implant sites provide more efficient vascularization (24), in our model vascularization was achieved even at an early time point. Bone deposition was monitored by *in vivo* and *ex vivo* imaging using a fluorescent bisphosphonate agent (27,28). The higher signal observed in TT+CMCA+BMSCs constructs suggests that the association of TT with Sr-enriched CMCA and hBMSCs stimulates bone remodeling, as confirmed by the high near-infrared fluorescence signal measured in this experimental group. Micro-CT technology is a non-destructive technique used for the evaluation of bone regeneration and bone-implant bonding (29,30). In our study, micro-CT was used to verify the homogeneity of the engineered bone. We found that the engineered bone was homogeneous in all the experimental groups, indicating that dissimilarities among groups were not a consequence of differences in the surrounding engineered bone. Given the impossibility to evaluate the bone deposition within TT by micro-CT due to the high scattering of x-rays induced by titanium (29,31), we performed histological and histomorphometric analyses obtaining results coherent with the ones of fluorescence imaging. These data were sustained by SEM results that showed a superior matrix deposition in TT+CMCA+BMSCs constructs, supporting, once again, the hypothesis that hBMSCs and Sr cooperate in generating a stable interaction between TT and bone. Pull-out tests were used to evaluate osseointegration (31-34). The lack of data from histological analysis at 12 weeks did not allow us to correlate the pull-out data with the bone deposition occurring at the implant interface. In our experiments, pull-out peak force for TT achieved values of 15 N, being comparable to values reported in literature for titanium implants inserted in rat tibiae (32,33) and demonstrating the validity of our model. Thus, an immediate outcome of this study is the development of an ectopic model which could be used to analyse the effects on implant osseointegration of surface treatments or bioactive factors loading, as well as the influence of implanted cells, avoiding the complex interaction of host cells and endogenous factors that act as incontrollable variables in orthotopic models (24). Noticeably, the use of athymic mice is useful to test the effect of heterologous cell sources, allowing the use of human cells as we did here, where only cells from aged osteoarthritic patients were used to resemble the possible clinical application of TT implants. However, the ectopic model has limitations related to the absence of a native bone response and, since our results were achieved with a limited number of animals, a further evaluation in an orthotopic model will be performed.

In this *in vivo* study, we showed that the synergic effect of osteogenic progenitor cells and Sr-enriched

CMCA loaded into TT enhanced matrix deposition at the bone-implant interface. Other studies have demonstrated that the strontium-enrichment of titanium increases bone apposition on implant surface and leads to greater osseointegration in orthotopic animal models (13,14). In our study, where an ectopic model was used, the enrichment of implant with the cellular component was crucial to achieve a better bone-implant integration. Indeed, the most striking differences in terms of osteodeposition and integration were observed between unseeded groups (TT and TT+CMCA) and groups where TT and TT+CMCA were enriched with hBMSCs, demonstrating the key role of osteogenic progenitor cells. Considering that prostheses are usually applied in aged patients, where the number and osteogenic potential of resident BMSCs can be diminished (21), we believe that loading the implant with autologous progenitor cells can be a good strategy to increase the population of bone-forming cells at the implant site, as reported in recent studies (18-20). In our previous *in vitro* study (23), we demonstrated that the enrichment of TT with CMCA results in significantly higher cell retention . This would ensure the maintenance of hBMSCs in implanted TT+CMCA prostheses, preventing cells from being washed away by body fluids. Autologous BMSCs have been proved safe even in the long-term period (34). We believe that the enrichment of TT implants with Sr-enriched CMCA and autologous BMSCs obtained with an intra-operative approach, would improve osseointegration with a dual action. Firstly, the enrichment of the osteogenic progenitor cell population would increase matrix deposition at the implant interface. Secondly, strontium would promote osteogenic differentiation of hBMSCs loaded into TT and resident at the peri-implant site.

In conclusion, we found a positive trend in matrix deposition and implant integration when titanium was simultaneously enriched with strontium and hBMSCs. This positive effect could be relevant in the clinical practice to reduce the risk of implant mobilization, with important benefits both for patients and for National Health Systems. We believe that, if these outcomes will be further confirmed in an orthotopic model, this approach may have a considerable clinical potential, representing a step forward in respect to the current clinical practice.

Acknowledgements

I would like to thank all the co-authors: Lovati A.B., Lopa S., Talò G., Previdi S., Recordati C., Mercuri D., Segatti F., Zagra L., Moretti M. I would also like to thank De Conti G. for chemical and mechanical assistance and Fusi S., Facchini A. for scientific support. Additionally, Marchesi D. and Benigni M. for support in SEM and histological analyses, respectively. This study was funded by the Italian Ministry of Health (RF-IOG-2007-647233). Previdi S. is recipient of a Monzino Foundation fellowship.

References

1. Head WC, Bauk DJ, Emerson RH, Jr. Titanium as the material of choice for cementless femoral components in total hip arthroplasty. Clin Orthop Relat Res.85-90. 1995.
2. Wang K. The use of titanium for medical applications in the USA. Materials Science and Engineering: A.213:4. 1996.
3. Park JB. Orthopedic prosthesis fixation. Ann Biomed Eng.20:583-94. 1992.
4. Albrektsson T, Branemark PI, Hansson HA, Lindstrom J. Osseointegrated titanium implants. Requirements for ensuring a long-lasting, direct bone-to-implant anchorage in man. Acta Orthop Scand.52:155-70. 1981.
5. Bobyn JD. Fixation and bearing surfaces for the next millennium. Orthopedics.22:810-2. 1999.
6. Johansson CB, Hansson HA, Albrektsson T. Qualitative interfacial study between bone and tantalum, niobium or commercially pure titanium. Biomaterials.11:277-80. 1990.
7. Shannon FJ, Cottrell JM, Deng XH, Crowder KN, Doty SB, Avaltroni MJ, Warren RF, Wright TM, Schwartz J. A novel surface treatment for porous metallic implants that improves the rate of bony ongrowth. J Biomed Mater Res A.86:857-64. 2008.
8. Spoerke ED, Murray NG, Li H, Brinson LC, Dunand DC, Stupp SI. Titanium with aligned, elongated pores for orthopedic tissue engineering applications. J Biomed Mater Res A.84:402-12. 2008.
9. Heinl P, Muller L, Korner C, Singer RF, Muller FA. Cellular Ti-6Al-4V structures with interconnected macro porosity for bone implants fabricated by selective electron beam melting. Acta Biomater.4:1536-44. 2008.
10. De Giglio E, Cometa S, Ricci MA, Zizzi A, Cafagna D, Manzotti S, Sabbatini L, Mattioli-Belmonte M. Development and characterization of rhVEGF-loaded poly(HEMA-MOEP) coatings electrosynthesized on titanium to enhance bone mineralization and angiogenesis. Acta Biomater.6:282-90. 2010.
11. Ichinohe N, Kuboki Y, Tabata Y. Bone regeneration using titanium nonwoven fabrics combined with fgf-2 release from gelatin hydrogel microspheres in rabbit skull defects. Tissue Eng Part A.14:1663-71. 2008.
12. Tian M, Chen F, Song W, Song Y, Chen Y, Wan C, Yu X, Zhang X. In vivo study of porous strontium-doped calcium polyphosphate scaffolds for bone substitute applications. J Mater Sci Mater Med.20:1505-12. 2009.
13. Park JW, Kim HK, Kim YJ, Jang JH, Song H, Hanawa T. Osteoblast response and osseointegration of a Ti-6Al-4V alloy implant incorporating strontium. Acta Biomater.6:2843-51. 2010.
14. Li Y, Li Q, Zhu S, Luo E, Li J, Feng G, Liao Y, Hu J. The effect of strontium-substituted hydroxyapatite coating on implant fixation in ovariectomized rats. Biomaterials.31:9006-14. 2010.
15. Marie PJ, Felsenberg D, Brandi ML. How strontium ranelate, via opposite effects on bone resorption and formation, prevents osteoporosis. Osteoporos Int.22:1659-67. 2011.
16. Peng S, Liu XS, Wang T, Li Z, Zhou G, Luk KD, Guo XE, Lu WW. In vivo anabolic effect of strontium on trabecular bone was associated with increased osteoblastogenesis of bone marrow stromal cells. J Orthop Res.28:1208-14. 2010.
17. Yang F, Yang D, Tu J, Zheng Q, Cai L, Wang L. Strontium enhances osteogenic differentiation of mesenchymal stem cells and in vivo bone formation by activating Wnt/catenin signaling. Stem Cells.29:981-91. 2011.
18. Kalia P, Coathup MJ, Oussedik S, Konan S, Dodd M, Haddad FS, Blunn GW. Augmentation of bone growth onto the acetabular cup surface using bone marrow stromal cells in total hip replacement surgery. Tissue Eng Part A.15:3689-96. 2009.
19. Gao C, Seuntjens J, Kaufman GN, Tran-Khanh N, Butler A, Li A, Wang H, Buschmann MD, Harvey EJ, Henderson JE. Mesenchymal stem cell transplantation to promote bone healing. J Orthop Res.30:1183-9. 2012.
20. Dozza B, Di Bella C, Lucarelli E, Giavaresi G, Fini M, Tazzari PL, Giannini S, Donati D. Mesenchymal stem cells and platelet lysate in fibrin or collagen scaffold promote non-cemented hip prosthesis integration. J Orthop Res.29:961-8. 2011.
21. Duque G. Bone and fat connection in aging bone. Curr Opin Rheumatol.20:429-34. 2008.
22. Marin E, Fusi S, Pressacco M, Paussa L, Fedrizzi L. Characterization of cellular solids in Ti6Al4V for orthopaedic implant applications: Trabecular titanium. J Mech Behav Biomed Mater.3:373-81. 2010.
23. Lopa S, Mercuri D, Colombini A, De Conti G, Segatti F, Zagra L, Moretti M. Orthopedic bioactive implants: Hydrogel enrichment of macroporous titanium for the delivery of mesenchymal stem cells and strontium. J Biomed Mater Res A. 2013.
24. Scott MA, Levi B, Askarinam A, Nguyen A, Rackohn T, Ting K, Soo C, James AW. Brief review of models of ectopic bone formation. Stem Cells Dev.21:655-67. 2012.
25. Park JC, Lee JB, Daculsi G, Oh SY, Cho KS, Im GI, Kim BS, Kim CS. Novel analysis model for implant osseointegration using ectopic bone formation via the recombinant human bone morphogenetic protein-2/macroporous biphasic calcium phosphate block system in rats: a proof-of-concept study. J Periodontal Implant Sci.42:136-43. 2012.
26. Lopa S, Colombini A, de Girolamo L, Sansone V, Moretti M. New Strategies in Cartilage Tissue Engineering for Osteoarthritic Patients: Infrapatellar Fat Pad as an Alternative Source of Progenitor Cells. J Biomater Tissue Eng.1:40-8. 2011.
27. Zilberman Y, Kallai I, Gafni Y, Pelled G, Kossodo S, Yared W, Gazit D. Fluorescence molecular tomography enables in vivo visualization and quantification of nonunion fracture repair induced by genetically engineered mesenchymal stem cells. J Orthop Res.26:522-30. 2008.
28. Hoff BA, Chughtai K, Jeon YH, Kozloff K, Galban S, Rehemtulla A, Ross BD, Galban CJ. Multimodality imaging of tumor and bone response in a mouse model of bony metastasis. Transl Oncol.5:415-21. 2012.
29. Jones AC, Milthorpe B, Averdunk H, Limaye A, Senden TJ, Sakellariou A, Sheppard AP, Sok RM, Knackstedt MA, Brandwood A, Rohner D, Hutmacher DW. Analysis of 3D bone ingrowth into polymer scaffolds via micro-computed tomography imaging. Biomaterials.25:4947-54. 2004.
30. Perilli E, Parkinson IH, Reynolds KJ. Micro-CT examination of human bone: from biopsies towards the entire organ. Ann Ist Super Sanita.48:75-82. 2012.

31. Branemark R, Ohrnell LO, Nilsson P, Thomsen P. Biomechanical characterization of osseointegration during healing: an experimental in vivo study in the rat. Biomaterials.18:969-78. 1997.
32. Petrie TA, Raynor JE, Reyes CD, Burns KL, Collard DM, Garcia AJ. The effect of integrin-specific bioactive coatings on tissue healing and implant osseointegration. Biomaterials.29:2849-57. 2008.
33. Reyes CD, Petrie TA, Burns KL, Schwartz Z, Garcia AJ. Biomolecular surface coating to enhance orthopaedic tissue healing and integration. Biomaterials.28:3228-35. 2007.
34. Wakitani S, Okabe T, Horibe S, Mitsuoka T, Saito M, Koyama T, Nawata M, Tensho K, Kato H, Uematsu K, Kuroda R, Kurosaka M, Yoshiya S, Hattori K, Ohgushi H. Safety of autologous bone marrow-derived mesenchymal stem cell transplantation for cartilage repair in 41 patients with 45 joints followed for up to 11 years and 5 months. J Tissue Eng Regen Med.5:146-50. 2011.

Chapter 10

Arthritic synovial fluid modulates the expression of pro- and anti-inflammatory mediators in macrophages

Abstract

Synovitis is a common trait of osteoarthritis (OA) and rheumatoid arthritis (RA), with synovium showing an increased presence of macrophages. Given the key role of macrophages in arthritic pathologies, we investigated the effect of the stimulation with OA and RA synovial fluid (SF) on the transcriptional expression of pro- and anti-inflammatory mediators in different macrophage subsets.

Adherent macrophages were cultured in non-activating conditions (M0), stimulated with IFNγ and TNFα towards a pro-inflammatory phenotype (M1), or with IL4 towards an anti-inflammatory phenotype (M2). After pre-activation, macrophages were treated for 12 hours with SF from 6 donors with no joint disease (Ctrl SF), 10 OA donors (OA SF) and 10 RA donors (RA SF). The transcriptional expression of *IL6*, *TNFα*, *IL1β*, *IL10*, *CCL18*, *CD206* and *IL1Ra* was then analyzed.

Compared to Ctrl SF, *IL10* was decreased in response to RA SF in M0 and M2 macrophages. OA SF also decreased *IL10*, but only in M2 macrophages. The treatment with OA SF increased *IL1ra* expression in all macrophages subsets compared to Ctrl SF. RA SF also increased *IL1ra* but only in M0 macrophages. *IL6* and *CCL18* expression was decreased by RA SF in M2 macrophages, whereas the other genes were not affected by any type of SF in any macrophage subsets.

Since *IL10* was up-regulated in response to the pro-inflammatory M1 stimulation, probably as a feedback mechanism, the down-regulation of *IL10* and the up-regulation of *IL1Ra* in macrophages treated with arthritic SF suggest that SF from OA and RA joints is a less pro-inflammatory stimulus for macrophages than non-arthritic SF. This may mimic the macrophage situation in the joint, where feedback mechanisms are induced to counteract the ongoing pro-inflammatory processes.

Introduction

Osteoarthritis (OA) and rheumatoid arthritis (RA) are widespread pathologies which severely affect patients quality of life. Despite specific clinical features that allow a clear distinction between OA and RA, synovial inflammation is a common trait (1,2). Indeed, synovitis, which causes joint swelling and exudation in RA patients, is observed in various degrees also in OA patients, with OA synovium showing a mixed inflammatory infiltrate mainly consisting of macrophages (1).

The increased number of macrophages in the synovium of OA and RA patients, together with the positive effect of drugs that counteract TNFα in RA patients (3) and with the promising results of treatments inhibiting monocyte migration in rats (4), suggests that these cells are key players in triggering and maintaining the inflammatory state that eventually leads to cartilage and bone disruption. The central role of macrophages in arthritic pathologies supports the interest in investigating their phenotype in response to the stimulation with pathological signals, such as the synovial fluid (SF) of OA and RA patients. Indeed, it is well-known that the synovial fluid from diseased joints contains increased levels of pro-inflammatory and chemotactic mediators (3,5,6) and it has been previously shown that SF from OA and RA patients affects the immunomodulatory potential of mesenchymal stem cells (5).

Based on these considerations, the aim of the present study was to investigate the effect of synovial fluid obtained from OA and RA patients on the transcriptional expression of anti-inflammatory and pro-inflammatory mediators on macrophages isolated from peripheral blood. We hypothesized that *in vivo* OA and RA synovial fluids are able to influence the phenotype of macrophages recruited to the joint, modulating the transcriptional expression of genes involved in the inflammatory process. We investigated this by testing the effect of OA and RA SF, using SF obtained from donors without any joint pathology as control, on non-activated macrophages and on macrophages activated by the treatment with IFNγ and TNFα (M1 activation) or IL4 (M2 activation).

Materials and Methods

Monocyte isolation

Three buffy coats of healthy donors were obtained from the blood bank (Sanquin Bloodbank, Rotterdam, the Netherlands). Monocytes were isolated by Ficoll density gradient (Ficoll-Paque™ PLUS, GE Healthcare). Briefly, 30 mL of buffy coat diluted with 0.1% PBS/BSA (1:5 ratio) were layered on the top of 15 mL of Ficoll. After centrifugation (15 min, 1000g), the interphase containing peripheral blood mononuclear cells was collected, washed in running buffer (0.5% PBS/BSA, 2 mM EDTA), labeled with 100 µL of anti-CD14 magnetic beads (CD14 microbeads human, MACS Separation columns LS and MidiMACS™ Separator; all Miltenyi Biotec), and isolated according to the manufacturer's guidelines.

After selection, CD14--positive viable cells were counted by Trypan Blue exclusion.

CD14-positive cells culture and stimulation

Immediately after counting, monocytes from 3 different donors were pooled together using $2x10^7$ cells from each single donor. Monocytes were seeded in 48-well plates in a concentration of $5x10^5$ cells/cm^2 and in X-vivo 15 medium (Lonza) with 20% FCS (Lonza), 0.6% fungizone (Gibco) and 0.1% gentamycine (Gibco), either without any further supplement (M0), or stimulated with 10 ng/mL IFNγ (recombinant human interferon-γ, PeproTech) and 50 ng/ml TNFα (recombinant human tumor necrosis factor-α, PeproTech) to obtain an M1 phenotype or with 10 ng/mL IL-4 (recombinant human interleukin 4, PeproTech) to obtain an M2 phenotype. After 12h of culture (37°C, 5% CO_2), triplicates from each condition were harvested for RNA isolation and gene expression analysis.

Treatment of non-stimulated and stimulated macrophages with synovial fluid from control and pathological donors

Control synovial fluid samples were obtained from donors without any joint disease (Ctrl SF, n=6). Arthritic synovial fluid was obtained from end-stage osteoarthritic patients (OA SF, n=10) and from patients affected by rheumatoid arthritis (RA SF, n=10). After 12 hours of culture under M0, M1, or M2 conditions, medium was removed and macrophages were treated with the different types of SF. Final concentration of SF in each well was 50%. M0, M1, and M2 stimulating conditions were maintained during culture with SF to evaluate the effect of each sample of synovial fluid on non-stimulated and stimulated macrophages. Baseline samples were prepared by culturing macrophages in M0, M1 and M2 conditions without adding synovial fluid. All the samples were cultured for 12 hours and then harvested for RNA isolation and gene expression analysis.

RNA isolation and qPCR

Samples were harvested in 350 µL RLT-buffer (Qiagen) and RNA isolation was performed using the RNeasy Microkit (Qiagen) according to the manufacturer's instructions. RNA concentration was measured using a spectrophotometer (NanoDrop ND1000 UV–VIS, Isogen Life Science B.V.,). cDNA was prepared using RevertAid First Strand cDNA Synthesis Kit (MBI Fermentas) according to the manufacturer's instructions. qPCR was performed by Bio-Rad CFX96 Touch™Applied Biosystems) using either Taqman Universal PCR mastermix (ABI, Branchburg) or qPCR™Mastermix Plus for SYBR® Green I (Eurogentec). Glyceraldehyde-3-phosphate dehydrogenase was used as housekeeper gene (*GAPDH*, Fw: GTCAACGGATTTGGTCGTATTGGG; Rev: TGCCATGGGTGGAATCATATTGG; probe: Fam-TGGCGCCCCAACCAGCC-Tamra). For gene expression analysis, the following genes were chosen: *IL6 (*Fw:

TCGAGCCCACCGGGAACGAA, Rev: GCAGGGAAGGCAGCAGGCAA)*, TNFα* (Fw: GCCGCATCGCCGTCTCCTAC, Rev: AGCGCTGAGTCGGTCACCCT)*, IL1β (Fw CCCTAAACAGATGAAGTGCTCCTT, Rev GTAGTCGGATGCCGCCAT), IL10 (Fw: ACCTGCCTAACATGCTTCGAG, Rev: CCAGCTGATCCTTCATTTGAAAG), CCL18 (*Fw: GCACCATGGCCCTCTGCTCC, Rev: GGGCACTGGGGGCTGGTTTC), *CD206 (*Fw: TGGCCGTATGCCGGTCACTGTTA, Rev: ACTTGTGAGGTCACCGCCTTCCT)*, IL1ra (Fw: AACAGAAAGCAGGACAAGCG, Rev: CCTTCGTCAGGCATATTGGT)* (all from Eurogentec, SybrGreen). Relative gene expression was calculated using the $2^{-\Delta CT}$ method (7).

Statistical analysis

Comparison among the different types of SF was performed by One-Way ANOVA for non-parametric data (Kruskal-Wallis test) with Dunnett's multiple comparison post-hoc test. Comparison between baseline samples (non-treated with SF) and each experimental group was performed by unpaired T-test with Welch's correction (samples with non-homogeneous variance).

Results

Stimulation of macrophages for 24 hours with IFNγ and TNFα prior to treatment with synovial fluid resulted in the up-regulation of *IL6*, *TNFα*, and *IL1β*, and in the down-regulation of *CD206* demonstrating the effective induction of the M1 phenotype was induced. *IL10* was also upregulated in M1-stimulated cells, probably as a feedback reaction to the pro-inflammatory stimulation. On the other hand, stimulation of macrophages with IL4 induced the expression of *CCL18*, *CD206* and *IL1ra* confirming the

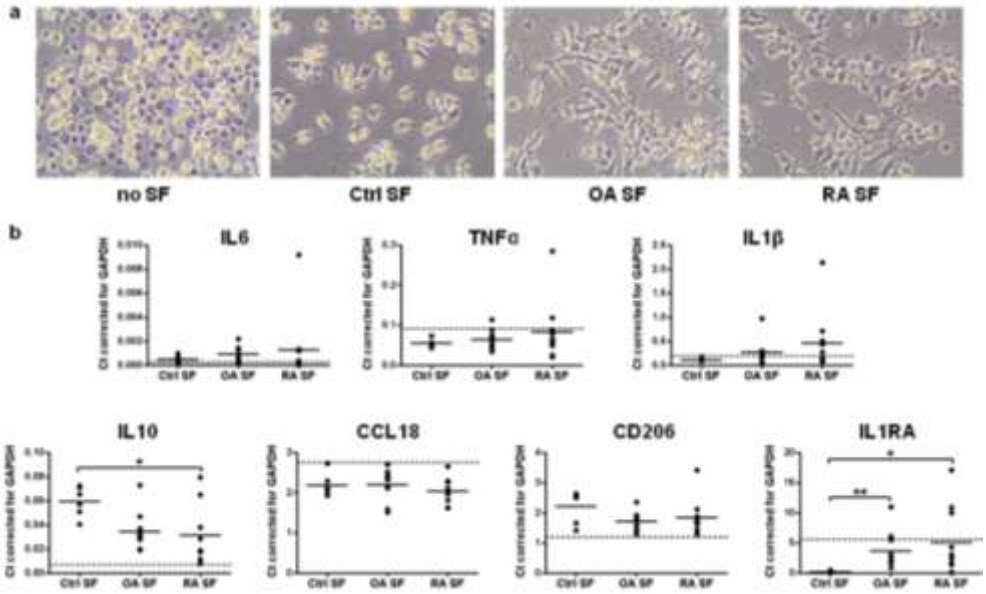

Fig. 1. Effect of different synovial fluids on non-activated macrophages (M0). (a) Representative pictures of macrophages cultured without SF or with Ctrl, OA, and RA SF (magnification 10X). (b) Gene expression data represented as aligned dot plot with mean; each dot represents an independent data corresponding to a different SF donor. Dotted lines indicate the average gene expression in samples cultured without SF (* *P<0.05;* ** *P<0.01*).

induction of an M2 phenotype (dotted lines in each graph, Fig. 1-3).

Cell morphology changes by the treatment with SF. In particular, in the presence of OA and RA SF a more elongated morphology and a higher number of clusters was seen than with macrophages cultured in the absence of SF (Fig. 1-3). In the macrophages without M1 or M2 stimuli (Fig. 1b), *TNFα* expression was significantly down-regulated by Ctrl SF (*P<0.01*) and OA SF (*P<0.05*), whereas no effect was observed for RA SF. *IL10* and *CD206* were up-regulated in all the types of SF (*P<0.01*) compared to the baseline, whereas *IL1ra* was significantly down-regulated by Ctrl SF (*P<0.001*) but not by OA and RA SF.

Comparing the effect of Ctrl SF to arthritic SF, we found that (Fig. 1b, lower row) *IL10* expression was down-regulated by the treatment with RA SF (*P<0.05*), while *IL1ra* expression was increased by OA SF (*P<0.01*) and RA SF (*P<0.05*). No other statistically significant differences among the SF types were observed for the analyzed genes.

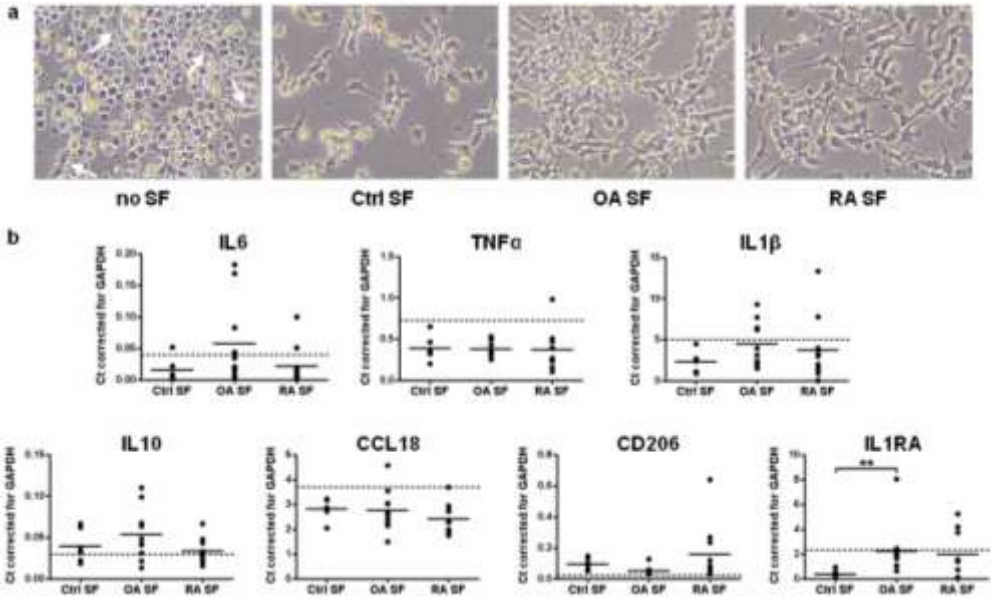

Fig. 2. Effect of different synovial fluids on M1-activated macrophages. (a) Representative pictures of macrophages cultured in the presence of IFNγ and TNFα without SF or with Ctrl, OA, and RA SF (magnification 10X). (b) Gene expression data represented as aligned dot plot with mean; each dot represents an independent data corresponding to a different SF donor. Dotted lines indicate the average gene expression in samples cultured without SF (** *P<0.01*).

In M1-stimulated macrophages (Fig. 2b), the treatment with all the different types of SF induced a significant down-regulation of *TNFα* (*P<0.01*) and up-regulation of *CD206* (*P<0.05*) compared to macrophages cultured in the absence of SF. A significant increase in *IL10* levels was also observed in macrophages treated with OA SF compared to baseline samples (*P<0.001*). As already observed for M0 macrophages, the treatment with Ctrl SF reduced the expression of *IL1ra* compared to macrophages cultured in the absence of SF (*P<0.01*).

Comparing the effect of Ctrl SF and arthritic SF on M1-stimulated macrophages, we found that macrophages treated with OA SF expressed significantly higher levels of *IL1ra* compared to cells treated with Ctrl SF (*P<0.001*, Fig. 2b). No significant difference among the experimental groups was observed

for the other analyzed markers.

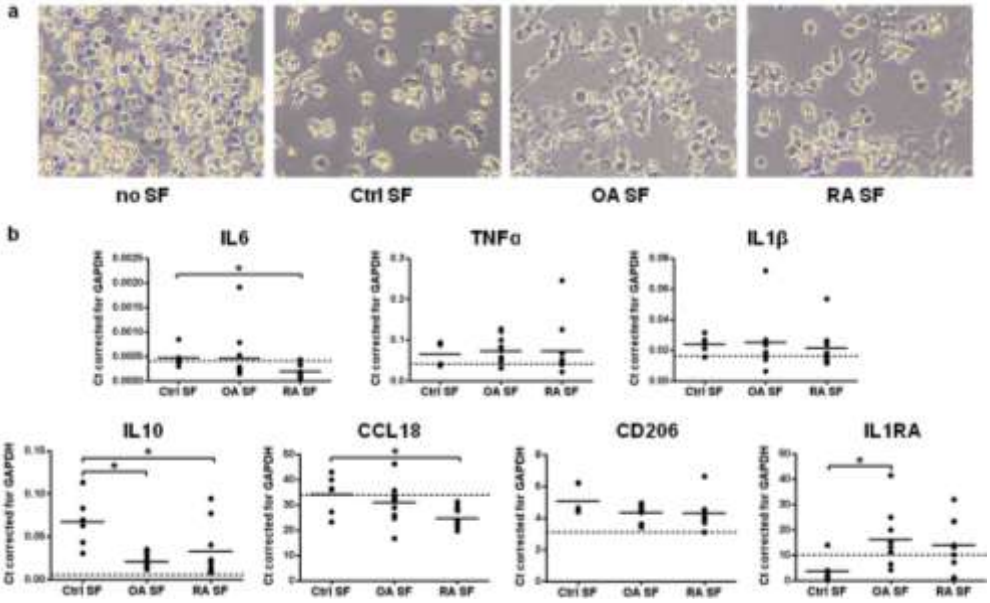

Fig. 3. Effect of different synovial fluids on M2-activated macrophages. (a) Representative pictures of macrophages cultured in the presence of IL4 without SF or with Ctrl, OA, and RA SF (magnification 10X). (b) Gene expression data represented as aligned dot plot with mean; each dot represents an independent data corresponding to a different SF donor. Dotted lines indicate the average gene expression in samples cultured without SF (* *P<0.05*).

In M2-stimulated macrophages (Fig. 3b) we observed the significant upregulation of *IL10* and down-regulation of *IL1ra* in samples treated with Ctrl SF. The treatment with OA SF and RA SF significantly reduced the expression of *IL10* (*P<0.05*) in comparison with Ctrl SF. Furthermore, macrophages treated with OA SF expressed higher levels of *IL1ra* than with Ctrl SF (*P<0.05*), whereas *IL6* and *CCL18* were significantly lower in cells treated with RA SF than when treated with Ctrl SF (*P<0.005*). For the other tested genes we did not observe any significant difference between Ctrl SF and arthritic SF.

Discussion

Synovitis and an increased number of macrophages residing in the synovium are common features of OA and RA (1,2). The key role of this cell type in the maintenance of the inflammatory state has been suggested by the positive effect of drugs that counteract TNFα in RA patients (3), a pro-inflammatory cytokine which is tipically secreted by macrophages, and with the promising results of treatments inhibiting monocyte migration in rats (4). It is known that SF of OA and RA patients is enriched with cytokines and chemokines involved in inflammatory processes and cell recruitment (3,5,6), thus here we evaluated the effect of SF from OA and RA patients on the transcriptional expression of different subset of macrophages (M0, M1, M2).

Among the tested genes, we found that *IL10* and *IL1ra* were the ones mostly affected by the treatment with SF. IL10 is a well-recognized anti-inflammatory cytokine that we found to be induced in response to

stimulation with IFNγ and TNFα as a feedback mechanism to counteract the pro-inflammatory stimulation. A similar effect was observed in M0 and M2 macrophages cultured in the presence of Ctrl SF that expressed levels of *IL10* similar to those of M1 macrophages without SF. On the other hand in M0 and M2-stimulated macrophages, the levels of *IL10* were significantly decreased by OA and RA SF compared to Ctrl SF. Thus, unexpectedly, in our experiments the macrophages sensed the OA and RA SF as less pro-inflammatory than Ctrl SF. It has been shown that IL-10 protein is produced by RA and OA synovial membrane cultures and that it can be detected in synovial membrane biopsies from OA and RA patients, whereas IL-10 is not found in normal synovial membrane (8). The presence of IL-10 in OA and RA SF could thus explain why in our experimental set up *IL10* expression was decreased in macrophages treated with arthritic SF compared to macrophages treated with Ctrl SF. This interpretation may appear in contrast with previously published results showing that IL-10 induces the transcriptional expression of *IL10* in a dose-dependent manner in monocyte-derived macrophages (9). However, this study also demonstrated that in the presence of pro-inflammatory stimuli such as LPS, the treatment with IL10 reduced the expression of its own gene. Thus, the simultaneous presence of IL10 and pro-inflammatory mediators in OA and RA SF could explain our results. The differences in *IL10* expression observed when treating M0 and M2 macrophages with OA and RA SF, were lost in M1 conditions. This is probably due to the strong upregulation of *IL10* transcription induced by the treatment with IFNγ and TNFα. Concerning the expression of *IL1ra*, we found that this gene was down-regulated by pro-inflammatory stimulation with IFNγ and TNFα and up-regulated by anti-inflammatory stimulation with IL4. Accordingly with data on *IL10* expression, Ctrl SF was recognized as a pro-inflammatory environment, leading to a significant reduction in *IL1ra* transcription in unstimulated macrophages (M0) as well as in macrophages stimulated towards M1 and M2 phenotype. The results from macrophages treated with OA and RA SF support the idea that arthritic SF represents for macrophages a less pro-inflammatory environment than Ctrl SF. Indeed, macrophages treated with OA SF showed significantly increased levels of *IL1ra* in all the different macrophage phenotypes, even in the macrophages stimulated towards the pro-inflammatory M1 phenotype. In addition *IL1ra* levels were significantly increased in M0 macrophages treated with RA SF.

In conclusion, SF from diseased OA and RA joints is a less pro-inflammatory stimulus for macrophages than non-arthritic SF. This may mimic the macrophage situation in the joint, where feedback mechanisms are induced to counteract the ongoing pro-inflammatory processes .

Acknowledgements

I would like to acknowledge all the co-authors: Leijs M.J.C., Moretti M., Lubberts E., van Osch G.J.V.M., Bastiaansen-Jenniskens Y.M.

References

1. Sellam J, Berenbaum F. The role of synovitis in pathophysiology and clinical symptoms of osteoarthritis. Nat Rev Rheumatol.6:625-35. 2010.
2. Boissier MC, Semerano L, Challal S, Saidenberg-Kermanac'h N, Falgarone G. Rheumatoid arthritis: from autoimmunity to synovitis and joint destruction. J Autoimmun.39:222-8. 2012.
3. Brennan FM, McInnes IB. Evidence that cytokines play a role in rheumatoid arthritis. J Clin Invest.118:3537-45. 2008.
4. Shahrara S, Proudfoot AE, Park CC, Volin MV, Haines GK, Woods JM, Aikens CH, Handel TM, Pope RM. Inhibition of monocyte chemoattractant protein-1 ameliorates rat adjuvant-induced arthritis. J Immunol.180:3447-56. 2008.
5. Leijs MJ, van Buul GM, Lubberts E, Bos PK, Verhaar JA, Hoogduijn MJ, van Osch GJ. Effect of Arthritic Synovial Fluids on the Expression of Immunomodulatory Factors by Mesenchymal Stem Cells: An Explorative in vitro Study. Front Immunol.3:231. 2012.
6. Beekhuizen M, Gierman LM, van Spil WE, Van Osch GJ, Huizinga TW, Saris DB, Creemers LB, Zuurmond AM. An explorative study comparing levels of soluble mediators in control and osteoarthritic synovial fluid. Osteoarthritis Cartilage.21:918-22. 2013.
7. Livak KJ, Schmittgen TD. Analysis of relative gene expression data using real-time quantitative PCR and the 2(-Delta Delta C(T)) Method. Methods.25:402-8. 2001.
8. Katsikis PD, Chu CQ, Brennan FM, Maini RN, Feldmann M. Immunoregulatory role of interleukin 10 in rheumatoid arthritis. J Exp Med.179:1517-27. 1994.
9. Staples KJ, Smallie T, Williams LM, Foey A, Burke B, Foxwell BM, Ziegler-Heitbrock L. IL-10 induces IL-10 in primary human monocyte-derived macrophages via the transcription factor Stat3. J Immunol.178:4779-85. 2007.

Chapter 11

General discussion and conclusions

General discussion and conclusions

Osteoarthritis (OA) is a widespread invalidating disease that implies articular cartilage and subchondral bone damage as well as a chronic inflammatory state of joint, eventually leading to the complete loss of joint functionality (1-4). With the aim of investigating basic and translational aspects related to the development of cell-based approaches for early and late stage OA patients, in this thesis we characterized different cell sources for cartilage treatment and we applied multi-disciplinary approaches for the development of three-dimensional constructs and for the generation of bioactive implants. Furthermore, to better characterize the OA environment, we investigated the effect of stimuli typical of OA joint on macrophage phenotype.

To extend cell-based therapies involving the use of articular chondrocytes (ACs) to early OA patients, the impact of donor age and pathological state of cartilage on cell phenotype needs to be accurately evaluated. We isolated ACs from a large number of aged OA patients (***Chapter 3***) and we found that donor age was negatively correlated with the proliferation rate of ACs. The sampling of the donors included in the study (75% patients older than 63 years) can explain the lack of correlation between age and cellular yield. In fact, according to a previous study, the most relevant reduction in cellular yield is observed between patients younger than 40 years and older patients, whereas this feature is not affected by the increasing age in older patients (5). No significant correlation was observed between the level of cartilage degeneration and cellular yield and proliferation rates. However, in samples with the highest degree of cartilage degeneration the cellular yield was reduced. These findings together with recent data showing that the ability of OA chondrocytes to participate to tissue homeostasis and cartilagineous matrix production is impaired by senescence and epigenetic modifications (6,7), suggests that further investigations are needed to assess the clinical relevance of autologous OA chondrocytes in aged OA patients, especially considering that the application of cell-based therapies to extended lesions would require a longer expansion phase to retrieve a sufficient number of cells, which may greatly affect the ability of ACs to recover a differentiated phenotype.

In order to overcome the limitations of articular chondrocytes, mesenchymal stem cells have been proposed as an alternative cell source for the development of cell-based chondral treatments. In particular, adipose-derived MSCs have been proposed as candidates for musculo-skeletal applications (8-12), thanks to their multi-differentiative potential and to the simplicity of adipose tissue harvesting procedure. In particular, considering the development of cell-based therapies for knee chondral lesions, MSCs resident in the infrapatellar fat pad (IFP-MSCs) and in the knee subcutaneous adipose tissue (ASCs) can be considered as promising candidates thanks to their multi-differentiative potential and to the high accessibility of these adipose depots during knee surgery (13-15). In order to compare these cell sources, we performed a donor-matched evaluation of the multi-lineage potential of MSCs derived from infrapatellar fat pad (IFP-MSCs) and knee subcutaneous adipose tissue (ASCs) (***Chapter 4***). Our results highlighted a differential commitment of IFP-MSCs and ASCs In particular, ASCs showed a superior osteogenic potential, whereas IFP-MSCs were characterized by a superior chondrogenic ability. In our study both cell populations were isolated from the same patient, eliminating the bias of inter-donor variability. Furthermore, in view of a future clinical application in OA patients, cells were obtained from middle-aged and aged OA donors. The

immunophenotype was coherent with the one reported in previous studies for IFP-MSCs and ASCs (13,14,16-18) and, in accordance with literature, no difference was observed between the two cell populations (13,14). Significantly higher levels of osteogenic markers were observed in ASCs compared to IFP-MSCs. These results were different from other studies reporting a similar or higher osteogenic potential of IFP-MSCs, determined on the basis of qualitative stainings (14,15). The use of quantitative analyses, the inclusion of a more appropriate number of donors, and a more careful selection of the adipose fraction of infrapatellar fat pad may explain the different result obtained in our study. We also demonstrated that IFP-MSCs display a superior chondrogenic commitment compared to ASCs, being able to extend the findings of previous studies (13,14) to a large population of OA donors and providing an effective demonstration of the superior chondrogenic commitment of IFP-MSCs in this category of patients. Hence, despite similar surface markers expression at the undifferentiated state, we found that different populations of MSCs display significantly different commitment towards specific cell lineages. This suggests that more predictive markers should be used to identify which population of MSCs is more suitable for a specific clinical application, as recently proposed by studies characterizing the features of specific subsets of MSCs (19-21).

Since both ACs and MSCs are promising cell candidates for chondral applications, in the last decade several groups have focused on the co-culture of these cell types (22). The rationale of this approach relies on the intrisinc chondrogenic potential of ACs and MSCs, as well as on the hypothesis that co-cultured chondrocytes may exert a positive influence on MSCs chondrogenesis. Results from studies investigating the co-culture of ACs with bone marrow-derived (23-28) and adipose-derived MSCs (23,24,29,30) suggest that the outcome of the co-culture approach is strongly dependent on the origin and de-differentiation state of articular chondrocytes. Considering the application of a co-culture approach to aged OA patients, it is evident that the impact of origin and pathological features of chondrocytes may be particularly relevant. To resemble a possible clinical treatment for knee lesion in OA patients, we performed autologous co-cultures using donor-matched IFP-MSCs, ASCs and ACs obtained from aged OA donors ***(Chapter 5)***. In our experiments, co-cultured ACs did not exert a chondroinductive influence on IFP-MSCs and ASCs. A major difference between our study and others reporting MSCs chondroinduction was the origin of the articular chondrocytes. Indeed, the studies demonstrating a chondroinductive effect of ACs on MSCs employ either animal chondrocytes (26,27,30) or non expanded healthy chondrocytes (24,25), that have a superior chondrogenic potential compared to expanded human ACs from aged OA patients. Furthermore, to prepare autologous co-cultures we had to cryopreserve ACs because of the different time required to expand ACs, IFP-MSCs and ASCs derived from the same donor. The cryopreservation of ACs is known to reduce the expression of chondrogenic genes (31) and may have further impaired the chondrogenic ability of ACs used in our experiments. Performing autologous co-culture, it was not possible to distinguish the response of each cell type, differently from studies where animal ACs are co-cultured with human MSCs and specific probes are used (24). Comparing the global transcriptional levels of chondrogenic genes in mono-cultures and co-cultures, we did not observe a significant up-regulation of chondrogenic markers in IFP-MSCs/ACs and ASCs/ACs. This result differs from literature

data reporting a significant up-regulation of chondogenic genes in ASCs/ACs co-culture (23). In this case, the discrepancy can be explained both by the different origin of ACs and by the different ASCs/ACs ratio (50:50), supporting the idea that several factors are involved in determining the outcome of ACs and MSCs co-culture. In our experiments, prolonged expansion and cryopreservation as well the origin from OA aged donors had a dramatic effect on the chondrogenic potential of ACs, indicating that the clinical applicability of the co-culture approach deserves further investigation to be extended to aged patients affected by degenerative pathologies.

Basic and translational research in the field of cartilage tissue engineering requires the use of 3D culture models, as pellet cultures (32-36) and scaffolds (37,38). In the last years, low-cost rapid prototyping techniques have been used to produce devices for the formation and culture of cell aggregates (39-43). These technologies can also be exploited to generate implantable multi-well scaffolds that can be used as *in vitro* and *in vivo* screening platforms (44). We used laser ablation and replica molding to generate multi-well devices for pellet culture and patterned fibrin glue scaffold (***Chapter 6***). The use of multi-well devices in polydimethylsiloxane (PDMS) significantly reduced the time required for routinary cell culture operations, which are highly time-consuming factors when handling several replicates in different experimental conditions. The intrinsic features of PDMS, such as high hydrophobicity and optical transparency (45), allowed the formation of well-defined cell aggregates and sample monitoring by optical microscopy during culture. The PDMS multi-well chips well supported cell viability and differentiation of ACs in pellets, demonstrating their suitability for chondrogenic pellet culture. Given the possibility to seed each well with a specific cell population and to harvest pellets from selected wells, this system presents also a great potential for the indirect co-culture of multiple cell types, representing a possible alternative complementary to the trans-well system. Exploiting the same rapid prototyping techniques, we biofabricated a multi-well implantable fibrin glue construct, where regions with differential cell density can be easily generated. Since cell density is known to affect cartilagineous matrix deposition (46,47), this scaffold can be used to evaluate if high cell density regions work as “chondrogenic centers”, as previously proposed by other groups that have used chondrocytes aggregates for scaffold seeding (48,49). Furthermore, in this scaffold different cell types can be seeded within the scaffold structure and in the wells, suggesting that it can used for the spatially controlled co-culture of different cell types in alternative to standard scaffolds (25,29).

To develop a clinically relevant strategy for the *in vitro* engineering of cartilagineous tissue, different factors need to be combined. The use of clinically approved growth factors and scaffolds is a fundamental step to get the clinical translability of lab research, according to the “bench to bedside” approach. Additionally, automated systems for the generation and culture of 3D constructs can be implemented to satisfy the high standard safety and quality requirements necessary to bring tissue engineering products into the clinical practice (50). Following these principles, in collaboration with the group supervised by Prof. Frédéric Mallein-Gerin (Institut de Biologie et Chimie des Proteines, Lyon, France), we used a perfusion bioreactor to improve the quality and distribution of matrix produced by articular chondrocytes cultured within a 3D scaffold. A collagen sponge approved for clinical use was used as scaffold and expansion and re-differentiation of ACs was performed using a specific cocktail of clinically

approved growth factors (***Chapter 7***). The perfusion bioreactor used in our experiments (OPB, Oscillating Perfusion Bioreactor) allowed the simultaneous culture of up to 18 samples in independent chambers, providing a promising platform to generate in parallel several constructs. We found that cell distribution and matrix homogeneity were increased by perfusion culture. In particular, only samples cultured in dynamic conditions showed matrix deposition into the scaffold core, whereas in the inner region of sponges cultured in dynamic conditions we observed poor presence of cells and matrix. In dynamic conditions, the rounded morphology typical of native chondrocytes was restored, indicating the re-differentiation of ACs (51-54), as also suggested by the reduced expression of type I collagen and by the superior type II/type I collagen ratio. Both dynamic culture and the re-differentiation cocktail were needed to induce cell rounding and the deposition of cartilagineous matrix throughout the collagen sponges, suggesting a synergistic action of soluble factors and culture regimen. Differently from other studies (55,56), we did not observe an increase in the amount of total matrix in dynamically cultured scaffolds. In our experimental set-up perfusion culture improved the homogeneity and quality, but not the overall quantity, of extracellular matrix. We tested two different perfusion protocols, shifting from a program working at costant speed to a program applying a slow perfusion speed in the first days of culture and repeated cycles of increasing speed in the following days (56-58), but we did not observe major differences between them in terms of matrix deposition. In this study we implemented some of the requirements for clinical translability of engineered tissue, such as the use of clinically approved reagents and scaffolds and the use of automated culture systems. Given the observed increase in the quality and homogeneity of extracellular matrix, the use of perfusion bioreactors in combination with optimized culture protocols holds great promises for the *in vitro* generation of clinically relevant engineered grafts, overcoming the limitations of static culture that directly correlate with the increasing size of the engineered tissues and providing a tool to improve automation and reproducibility of tissue engineering processes.

Despite their great potential for the treatment of articular cartilage defects, cell-based approaches aiming at cartilage restoration are not clinically relevant when considering late stage OA joints with extensive lesions to cartilage and exposure of subchondral bone. In these patients, joint replacement is currently the only available clinical option and cell-based therapies can be used to overcome limitations of implant technology. In cementless implants the improvement of implant osseointegration is a key requirement to grant implant stability. In order to generate a bioactive implant with improved osseointegration we combined a macroporous titanium (Trabecular Titanium™, TT) with a strontium enriched hydrogel (CMCA) and bone marrow-derived MSCs (BMSCs) (***Chapter 8, Chapter 9***). Strontium was chosen as osteoinductive factors due to its positive effect on osteodeposition and for its intrinsic features, such as low price and high stability. BMSCs were chosen as osteoprogenitor cells, since they can participate to the bone healing process and can be isolated with an intra-operative approach (59,60). We found that the association of macroporous titanium with a biocompatible hydrogel significantly increased cell retention within titanium, which could be critical during and immediately after surgery whereby cells can be washed away by body fluids. Strontium proved to be effective in improving BMSCs osteogenic differentiation, being suitable for the generation of enriched osteoinductive titanium implants. We tested the performance of this composite bioactive

implant in an *in vivo* ectopic model of osseointegration. To do that, we engineered *in vitro* a cell-seeded bone scaffold in order to mimic the bone and we grafted the titanium implant either unloaded or loaded with BMSCs and/or Sr-enriched CMCA. The use of athymic mice in our *in vivo* model allowed us to use a clinically relevant cell source (i.e. BMSCs obtained from aged OA patients) and to clearly distinguish the effect of implanted cells and strontium. However, the ectopic model has limitations related to the absence of a native bone response which in *in vivo* orthotopic implants plays a key role in promoting bone deposition. In accordance with previous study demonstrating that the enrichment of implants with progenitor cells (59,61,62) or strontium (63,64) leads to an improved osseointegration, we found a positive trend in matrix deposition and implant integration when titanium was simultaneously enriched with BMSCs and strontium. Considering that prostheses are usually applied in aged patients, where the number and osteogenic potential of resident BMSCs can be reduced (65), loading the implant with autologous progenitor cells may represent a successful strategy to increase the population of bone-forming cells at the implant site. We believe that the use of bioactive implants loaded with Sr-enriched CMCA and autologous BMSCs obtained with an intra-operative approach would improve osseointegration with a dual action. Firstly, the enrichment of the osteogenic progenitor cell population would increase matrix deposition at the implant interface. Secondly, strontium would promote osteogenic differentiation of BMSCs loaded into TT and resident at the peri-implant site. The synergic action of these factors can be relevant in the clinical practice to reduce the risk of implant mobilization, with possible benefits for patients and for National Health Systems. If these outcomes will be further confirmed in an orthotopic model, this approach may have a considerable clinical potential, representing a step forward respect to the current clinical practice.

Cell-based approaches have a great potential and can be exploited in different ways for the treatment of OA patients (66,67). However, the impact of the inflammatory state of OA joints on re-implanted cells cannot be neglected and deserves further investigation. The newly accepted role of cytokines and immune cells in OA progression (4,68,69) involves the recognition that implanted cells and/or constructs may be subjected to the same inflammatory stimuli that contributed to joint damage, which may negatively affect the outcome of cell-based approaches (70-74). In order to better evaluate the impact of OA environment on re-implanted cells or constructs, *in vitro* models mimicking the OA joint are needed. These models should comprise soluble factors present in the OA joint and key cell types, such as macrophages that drive the pro-inflammatory and catabolic processes in OA (75-77). In collaboration with the Connective Tissue Cells and Repair group supervised by Prof. Gerjo J.V.M. van Osch (Erasmus MC, Rotterdam, The Netherlands), we investigated the effect of OA stimuli (i.e. soluble factors contained in the synovial fluids of OA patients) on the phenotype of different subsets of macrophages (M0, M1, M2) (***Chapter 10***). The transcriptional expression of several pro- and anti-inflammatory mediators was analyzed in the presence of synovial fluid obtained from donors without any joint disease and from OA donors. We found that the expression of specific genes (*IL10* and *IL1ra*) was affected by the treatment with arthritic synovial fluid, demonstrating that pathological environment is able to influence the phenotype of macrophages. Further investigations are needed to determine if the observed transcriptional changes correspond to alterations in the

release of soluble factors that, in the joint, may influence the tissues in direct contact with the synovial fluid and the fate of implanted cells or engineered grafts. On the other hand, the immunomodulatory properties of MSCs may also play a role in determining the outcome of cell-based approach employing MSCs as cell source. Indeed, MSCs potential resides not only in their multi-differentiative potential, but also in their ability to suppress pro-inflammatory processes (78,79), as shown by the promising results obtained through local delivery of MSCs in preclinical models of joint disease, indicating that MSCs paracrine signalling might be more even more relevant than their differentiative potential in stimulating tissue repair. The immunomodulatory function of MSCs is able to influence also macrophage phenotype, inducing them to shift from a pro-inflammatory to an anti-inflammatory phenotype (80,81), an ability that may be particularly relevant when treating OA patients with MSCs-based approaches. Thus, the assessment of the therapeutic potency of specific subsets of MSCs should include the evaluation of the ability to secrete immunomodulatory paracrine factors in addition to the traditional assays based on the expression of specific cell-surface markers and the characterization of multi-lineage potential.

Altogether these findings indicate the need for basic and translational studies better resembling the multi-factorial complexity that is found in OA joints. This complexity is reflected in the impaired phenotype of OA chondrocytes as well as in the inflammatory environment of joint, that may negatively affect the outcome of cell-based approaches. Thus, the suitability of OA articular chondrocytes for the treatment of extensive lesions in OA patients still deserves further investigation. Basic and translational studies should face practical issues such as the optimization of clinically approved protocols for *in vitro* expansion and re-differentiation of OA chondrocytes, which represent a key step towards the clinical applicability of this cell source to OA lesions given the higher number of cells required and the reduced chondrogenic potential of ACs from aged OA donors. In the same way, the evaluation of the clinical relevance of the co-culture approach should not neglect the impact of these negative features on the chondroinductive potential of ACs. In this field, further investigation is needed to verify whether it is possible to extend the promising results obtained using non-expanded healthy articular chondrocytes to co-cultures involving the use of expanded OA chondrocytes from aged patients. Besides articular chondrocytes, MSCs can be considered a promising tool for the development of novel cell-based approaches. Here, the identification of specific subsets of MSCs displaying a peculiar commitment should drive the selection of the most suitable cell candidate for a specific application. Indeed, despite common features that allow the identification of MSCs (i.e. expression of typical cell surface markers, multi-differentiative potential), specific populations of MSCs harvested from different anatomical sytes have intrinsic features that make them more or less suitable for a specific application. Hence, more predictive markers for the evaluation of the therapeutic potency of different populations of MSCs should be identified and this analysis should include the evaluation of their paracrine immunomodulatory function in a novel view of MSCs as potential “anti-inflammatory drugs”. The implementation of 3D culture models and automated devices for the production and culture of engineered grafts is also a key step in the process bringing the results obtained in tissue engineering labs into the clinical practice. In particular, the optimization of high-throughput 3D culture systems is fundamental in the basic research for the optimization of chondrogenic differentiation protocols and for the study

of the cross-talk between different cell types, whereas automated dynamic culture systems can be exploited to engineer clinically relevant grafts, overcoming the limitations of static culture and granting high quality and safety standards. This multidisciplinary approach can be also exploited for the cell-based improvement of existing therapeutic options, as we suggested for the improvement of implant osseointegration through the association of multiple elements comprising mesenchymal stem cells, osteoinductive factors, biocompatible hydrogels and macroporous titanium. Finally, the investigation of pro-inflammatory processes ongoing in the OA joints can drive the development of novel *in vitro* models to evaluate the fate of cell and engineered constructs implanted in a diseased environment.

References

1. Wenham CY, Conaghan PG. New horizons in osteoarthritis. Age Ageing.42:272-8. 2013.
2. Aigner T, Rose J, Martin J, Buckwalter J. Aging theories of primary osteoarthritis: from epidemiology to molecular biology. Rejuvenation Res.7:134-45. 2004.
3. van der Kraan PM, van den Berg WB. Osteoarthritis in the context of ageing and evolution. Loss of chondrocyte differentiation block during ageing. Ageing Res Rev.7:106-13. 2008.
4. Sellam J, Berenbaum F. The role of synovitis in pathophysiology and clinical symptoms of osteoarthritis. Nat Rev Rheumatol.6:625-35. 2010.
5. Barbero A, Grogan S, Schafer D, Heberer M, Mainil-Varlet P, Martin I. Age related changes in human articular chondrocyte yield, proliferation and post-expansion chondrogenic capacity. Osteoarthritis Cartilage.12:476-84. 2004.
6. Rose J, Soder S, Skhirtladze C, Schmitz N, Gebhard PM, Sesselmann S, Aigner T. DNA damage, discoordinated gene expression and cellular senescence in osteoarthritic chondrocytes. Osteoarthritis Cartilage.20:1020-8. 2012.
7. Kim KI, Park YS, Im GI. Changes in the epigenetic status of the SOX-9 promoter in human osteoarthritic cartilage. J Bone Miner Res.28:1050-60. 2013.
8. Rada T, Reis RL, Gomes ME. Adipose tissue-derived stem cells and their application in bone and cartilage tissue engineering. Tissue Eng Part B Rev.15:113-25. 2009.
9. Rhee SC, Ji YH, Gharibjanian NA, Dhong ES, Park SH, Yoon ES. In vivo evaluation of mixtures of uncultured freshly isolated adipose-derived stem cells and demineralized bone matrix for bone regeneration in a rat critically sized calvarial defect model. Stem Cells Dev.20:233-42. 2011.
10. Choi JW, Park EJ, Shin HS, Shin IS, Ra JC, Koh KS. In Vivo Differentiation of Undifferentiated Human Adipose Tissue-Derived Mesenchymal Stem Cells in Critical-Sized Calvarial Bone Defects. Ann Plast Surg. 2012.
11. Kang H, Peng J, Lu S, Liu S, Zhang L, Huang J, Sui X, Zhao B, Wang A, Xu W, Luo Z, Guo Q. In vivo cartilage repair using adipose-derived stem cell-loaded decellularized cartilage ECM scaffolds. J Tissue Eng Regen Med. 2012.
12. Jung SN, Rhie JW, Kwon H, Jun YJ, Seo JW, Yoo G, Oh DY, Ahn ST, Woo J, Oh J. In vivo cartilage formation using chondrogenic-differentiated human adipose-derived mesenchymal stem cells mixed with fibrin glue. J Craniofac Surg.21:468-72. 2010.
13. Alegre-Aguaron E, Desportes P, Garcia-Alvarez F, Castiella T, Larrad L, Martinez-Lorenzo MJ. Differences in surface marker expression and chondrogenic potential among various tissue-derived mesenchymal cells from elderly patients with osteoarthritis. Cells Tissues Organs.196:231-40. 2012.
14. Mochizuki T, Muneta T, Sakaguchi Y, Nimura A, Yokoyama A, Koga H, Sekiya I. Higher chondrogenic potential of fibrous synovium- and adipose synovium-derived cells compared with subcutaneous fat-derived cells: distinguishing properties of mesenchymal stem cells in humans. Arthritis Rheum.54:843-53. 2006.
15. Pires de Carvalho P, Hamel KM, Duarte R, King AG, Haque M, Dietrich MA, Wu X, Shah F, Burk D, Reis RL, Rood J, Zhang P, Lopez M, Gimble JM, Dasa V. Comparison of infrapatellar and subcutaneous adipose tissue stromal vascular fraction and stromal/stem cells in osteoarthritic subjects. J Tissue Eng Regen Med. 2012.
16. English A, Jones EA, Corscadden D, Henshaw K, Chapman T, Emery P, McGonagle D. A comparative assessment of cartilage and joint fat pad as a potential source of cells for autologous therapy development in knee osteoarthritis. Rheumatology (Oxford).46:1676-83. 2007.
17. Gronthos S, Franklin DM, Leddy HA, Robey PG, Storms RW, Gimble JM. Surface protein characterization of human adipose tissue-derived stromal cells. J Cell Physiol.189:54-63. 2001.
18. Lee RH, Kim B, Choi I, Kim H, Choi HS, Suh K, Bae YC, Jung JS. Characterization and expression analysis of mesenchymal stem cells from human bone marrow and adipose tissue. Cell Physiol Biochem.14:311-24. 2004.
19. Kim YH, Yoon DS, Kim HO, Lee JW. Characterization of different subpopulations from bone marrow-derived mesenchymal stromal cells by alkaline phosphatase expression. Stem Cells Dev.21:2958-68. 2012.
20. Jiang T, Liu W, Lv X, Sun H, Zhang L, Liu Y, Zhang WJ, Cao Y, Zhou G. Potent in vitro chondrogenesis of CD105 enriched human adipose-derived stem cells. Biomaterials.31:3564-71. 2010.
21. Quirici N, Scavullo C, de Girolamo L, Lopa S, Arrigoni E, Deliliers GL, Brini AT. Anti-L-NGFR and -CD34 monoclonal antibodies identify multipotent mesenchymal stem cells in human adipose tissue. Stem Cells Dev.19:915-25. 2010.
22. Leijten JC, Georgi N, Wu L, van Blitterswijk CA, Karperien M. Cell sources for articular cartilage repair strategies: shifting from monocultures to cocultures. Tissue Eng Part B Rev.19:31-40. 2013.
23. Lee JS, Im GI. Influence of chondrocytes on the chondrogenic differentiation of adipose stem cells. Tissue Eng Part A.16:3569-77. 2010.

24. Acharya C, Adesida A, Zajac P, Mumme M, Riesle J, Martin I, Barbero A. Enhanced chondrocyte proliferation and mesenchymal stromal cells chondrogenesis in coculture pellets mediate improved cartilage formation. J Cell Physiol.227:88-97. 2012.
25. Sabatino MA, Santoro R, Gueven S, Jaquiery C, Wendt DJ, Martin I, Moretti M, Barbero A. Cartilage graft engineering by co-culturing primary human articular chondrocytes with human bone marrow stromal cells. J Tissue Eng Regen Med. 2012.
26. Meretoja VV, Dahlin RL, Kasper FK, Mikos AG. Enhanced chondrogenesis in co-cultures with articular chondrocytes and mesenchymal stem cells. Biomaterials.33:6362-9. 2012.
27. Meretoja VV, Dahlin RL, Wright S, Kasper FK, Mikos AG. Articular Chondrocyte Redifferentiation in 3D Co-cultures with Mesenchymal Stem Cells. Tissue Eng Part C Methods. 2014.
28. Giovannini S, Diaz-Romero J, Aigner T, Heini P, Mainil-Varlet P, Nesic D. Micromass co-culture of human articular chondrocytes and human bone marrow mesenchymal stem cells to investigate stable neocartilage tissue formation in vitro. Eur Cell Mater.20:245-59. 2010.
29. Hildner F, Concaro S, Peterbauer A, Wolbank S, Danzer M, Lindahl A, Gatenholm P, Redl H, van Griensven M. Human adipose-derived stem cells contribute to chondrogenesis in coculture with human articular chondrocytes. Tissue Eng Part A.15:3961-9. 2009.
30. Hwang NS, Im SG, Wu PB, Bichara DA, Zhao X, Randolph MA, Langer R, Anderson DG. Chondrogenic priming adipose-mesenchymal stem cells for cartilage tissue regeneration. Pharm Res.28:1395-405. 2011.
31. Muinos-Lopez E, Rendal-Vazquez ME, Hermida-Gomez T, Fuentes-Boquete I, Diaz-Prado S, Blanco FJ. Cryopreservation effect on proliferative and chondrogenic potential of human chondrocytes isolated from superficial and deep cartilage. Open Orthop J.6:150-9. 2012.
32. Dehne T, Schenk R, Perka C, Morawietz L, Pruss A, Sittinger M, Kaps C, Ringe J. Gene expression profiling of primary human articular chondrocytes in high-density micromasses reveals patterns of recovery, maintenance, re- and dedifferentiation. Gene.462:8-17. 2010.
33. Zhang Z, McCaffery JM, Spencer RG, Francomano CA. Hyaline cartilage engineered by chondrocytes in pellet culture: histological, immunohistochemical and ultrastructural analysis in comparison with cartilage explants. J Anat.205:229-37. 2004.
34. Jakob M, Demarteau O, Schafer D, Hintermann B, Dick W, Heberer M, Martin I. Specific growth factors during the expansion and redifferentiation of adult human articular chondrocytes enhance chondrogenesis and cartilaginous tissue formation in vitro. J Cell Biochem.81:368-77. 2001.
35. Bernstein P, Dong M, Corbeil D, Gelinsky M, Gunther KP, Fickert S. Pellet culture elicits superior chondrogenic redifferentiation than alginate-based systems. Biotechnol Prog.25:1146-52. 2009.
36. Pelttari K, Steck E, Richter W. The use of mesenchymal stem cells for chondrogenesis. Injury.39 Suppl 1:S58-65. 2008.
37. Kosuge D, Khan WS, Haddad B, Marsh D. Biomaterials and scaffolds in bone and musculoskeletal engineering. Curr Stem Cell Res Ther.8:185-91. 2013.
38. Filardo G, Kon E, Roffi A, Di Martino A, Marcacci M. Scaffold-based repair for cartilage healing: a systematic review and technical note. Arthroscopy.29:174-86. 2013.
39. Mohammed MI, Desmulliez MP. Planar lens integrated capillary action microfluidic immunoassay device for the optical detection of troponin I. Biomicrofluidics.7:64112. 2013.
40. Yap YC, Guijt RM, Dickson TC, King AE, Breadmore MC. Stainless steel pinholes for fast fabrication of high-performance microchip electrophoresis devices by CO2 laser ablation. Anal Chem.85:10051-6. 2013.
41. Khan Malek CG. Laser processing for bio-microfluidics applications (part I). Anal Bioanal Chem.385:1351-61. 2006.
42. Khan Malek CG. Laser processing for bio-microfluidics applications (part II). Anal Bioanal Chem.385:1362-9. 2006.
43. Fiorini GS, Chiu DT. Disposable microfluidic devices: fabrication, function, and application. Biotechniques.38:429-46. 2005.
44. Higuera GA, Hendriks JA, van Dalum J, Wu L, Schotel R, Moreira-Teixeira L, van den Doel M, Leijten JC, Riesle J, Karperien M, van Blitterswijk CA, Moroni L. In vivo screening of extracellular matrix components produced under multiple experimental conditions implanted in one animal. Integr Biol (Camb).5:889-98. 2013.
45. Berthier E, Young EW, Beebe D. Engineers are from PDMS-land, Biologists are from Polystyrenia. Lab Chip.12:1224-37. 2012.
46. Talukdar S, Nguyen QT, Chen AC, Sah RL, Kundu SC. Effect of initial cell seeding density on 3D-engineered silk fibroin scaffolds for articular cartilage tissue engineering. Biomaterials.32:8927-37. 2011.
47. Mauck RL, Wang CC, Oswald ES, Ateshian GA, Hung CT. The role of cell seeding density and nutrient supply for articular cartilage tissue engineering with deformational loading. Osteoarthritis Cartilage.11:879-90. 2003.
48. Wolf F, Candrian C, Wendt D, Farhadi J, Heberer M, Martin I, Barbero A. Cartilage tissue engineering using pre-aggregated human articular chondrocytes. Eur Cell Mater.16:92-9. 2008.
49. Moreira Teixeira LS, Leijten JC, Sobral J, Jin R, van Apeldoorn AA, Feijen J, van Blitterswijk C, Dijkstra PJ, Karperien M. High throughput generated micro-aggregates of chondrocytes stimulate cartilage formation in vitro and in vivo. Eur Cell Mater.23:387-99. 2012.
50. Martin I, Smith T, Wendt D. Bioreactor-based roadmap for the translation of tissue engineering strategies into clinical products. Trends Biotechnol.27:495-502. 2009.
51. Benya PD, Shaffer JD. Dedifferentiated chondrocytes reexpress the differentiated collagen phenotype when cultured in agarose gels. Cell.30:215-24. 1982.
52. Zhang J, Yang Z, Li C, Dou Y, Li Y, Thote T, Wang DA, Ge Z. Cells behave distinctly within sponges and hydrogels due to differences of internal structure. Tissue Eng Part A.19:2166-75. 2013.
53. Kumar D, Lassar AB. The transcriptional activity of Sox9 in chondrocytes is regulated by RhoA signaling and actin polymerization. Mol Cell Biol.29:4262-73. 2009.
54. Woods A, Wang G, Beier F. Regulation of chondrocyte differentiation by the actin cytoskeleton and adhesive interactions. J Cell Physiol.213:1-8. 2007.
55. Valonen PK, Moutos FT, Kusanagi A, Moretti MG, Diekman BO, Welter JF, Caplan AI, Guilak F, Freed LE. In vitro generation of mechanically functional cartilage grafts based on adult human stem cells and 3D-woven poly(epsilon-caprolactone) scaffolds. Biomaterials.31:2193-200. 2010.
56. Shahin K, Doran PM. Strategies for enhancing the accumulation and retention of extracellular matrix in tissue-engineered cartilage cultured in bioreactors. PLoS One.6:e23119. 2011.
57. Davisson T, Sah RL, Ratcliffe A. Perfusion increases cell content and matrix synthesis in chondrocyte three-dimensional cultures. Tissue Eng.8:807-16. 2002.
58. Pazzano D, Mercier KA, Moran JM, Fong SS, DiBiasio DD, Rulfs JX, Kohles SS, Bonassar LJ. Comparison of chondrogensis in static and perfused bioreactor

culture. Biotechnol Prog.16:893-6. 2000.
59. Kalia P, Coathup MJ, Oussedik S, Konan S, Dodd M, Haddad FS, Blunn GW. Augmentation of bone growth onto the acetabular cup surface using bone marrow stromal cells in total hip replacement surgery. Tissue Eng Part A.15:3689-96. 2009.
60. van den Dolder J, Farber E, Spauwen PH, Jansen JA. Bone tissue reconstruction using titanium fiber mesh combined with rat bone marrow stromal cells. Biomaterials.24:1745-50. 2003.
61. Gao C, Seuntjens J, Kaufman GN, Tran-Khanh N, Butler A, Li A, Wang H, Buschmann MD, Harvey EJ, Henderson JE. Mesenchymal stem cell transplantation to promote bone healing. J Orthop Res.30:1183-9. 2012.
62. Dozza B, Di Bella C, Lucarelli E, Giavaresi G, Fini M, Tazzari PL, Giannini S, Donati D. Mesenchymal stem cells and platelet lysate in fibrin or collagen scaffold promote non-cemented hip prosthesis integration. J Orthop Res.29:961-8. 2011.
63. Park JW, Kim HK, Kim YJ, Jang JH, Song H, Hanawa T. Osteoblast response and osseointegration of a Ti-6Al-4V alloy implant incorporating strontium. Acta Biomater.6:2843-51. 2010.
64. Li Y, Li Q, Zhu S, Luo E, Li J, Feng G, Liao Y, Hu J. The effect of strontium-substituted hydroxyapatite coating on implant fixation in ovariectomized rats. Biomaterials.31:9006-14. 2010.
65. Duque G. Bone and fat connection in aging bone. Curr Opin Rheumatol.20:429-34. 2008.
66. Diekman BO, Guilak F. Stem cell-based therapies for osteoarthritis: challenges and opportunities. Curr Opin Rheumatol.25:119-26. 2013.
67. O'Connell GD, Lima EG, Bian L, Chahine NO, Albro MB, Cook JL, Ateshian GA, Hung CT. Toward engineering a biological joint replacement. J Knee Surg.25:187-96. 2012.
68. Beekhuizen M, Gierman LM, van Spil WE, Van Osch GJ, Huizinga TW, Saris DB, Creemers LB, Zuurmond AM. An explorative study comparing levels of soluble mediators in control and osteoarthritic synovial fluid. Osteoarthritis Cartilage.21:918-22. 2013.
69. Scanzello CR, Goldring SR. The role of synovitis in osteoarthritis pathogenesis. Bone.51:249-57. 2012.
70. Heldens GT, Blaney Davidson EN, Vitters EL, Schreurs BW, Piek E, van den Berg WB, van der Kraan PM. Catabolic factors and osteoarthritis-conditioned medium inhibit chondrogenesis of human mesenchymal stem cells. Tissue Eng Part A.18:45-54. 2012.
71. Kruger JP, Endres M, Neumann K, Stuhlmuller B, Morawietz L, Haupl T, Kaps C. Chondrogenic differentiation of human subchondral progenitor cells is affected by synovial fluid from donors with osteoarthritis or rheumatoid arthritis. J Orthop Surg Res.7:10. 2012.
72. Boeuf S, Graf F, Fischer J, Moradi B, Little CB, Richter W. Regulation of aggrecanases from the ADAMTS family and aggrecan neoepitope formation during in vitro chondrogenesis of human mesenchymal stem cells. Eur Cell Mater.23:320-32. 2012.
73. Rohner E, Matziolis G, Perka C, Fuchtmeier B, Gaber T, Burmester GR, Buttgereit F, Hoff P. Inflammatory synovial fluid microenvironment drives primary human chondrocytes to actively take part in inflammatory joint diseases. Immunol Res.52:169-75. 2012.
74. Hoff P, Buttgereit F, Burmester GR, Jakstadt M, Gaber T, Andreas K, Matziolis G, Perka C, Rohner E. Osteoarthritis synovial fluid activates pro-inflammatory cytokines in primary human chondrocytes. Int Orthop.37:145-51. 2013.
75. Benito MJ, Veale DJ, FitzGerald O, van den Berg WB, Bresnihan B. Synovial tissue inflammation in early and late osteoarthritis. Ann Rheum Dis.64:1263-7. 2005.
76. Blom AB, van Lent PL, Libregts S, Holthuysen AE, van der Kraan PM, van Rooijen N, van den Berg WB. Crucial role of macrophages in matrix metalloproteinase-mediated cartilage destruction during experimental osteoarthritis: involvement of matrix metalloproteinase 3. Arthritis Rheum.56:147-57. 2007.
77. Smeets TJ, Barg EC, Kraan MC, Smith MD, Breedveld FC, Tak PP. Analysis of the cell infiltrate and expression of proinflammatory cytokines and matrix metalloproteinases in arthroscopic synovial biopsies: comparison with synovial samples from patients with end stage, destructive rheumatoid arthritis. Ann Rheum Dis.62:635-8. 2003.
78. Frank MH, Sayegh MH. Immunomodulatory functions of mesenchymal stem cells. Lancet.363:1411-2. 2004.
79. Barry F, Murphy M. Mesenchymal stem cells in joint disease and repair. Nat Rev Rheumatol.9:584-94. 2013.
80. Kim J, Hematti P. Mesenchymal stem cell-educated macrophages: a novel type of alternatively activated macrophages. Exp Hematol.37:1445-53. 2009.
81. Eggenhofer E, Hoogduijn MJ. Mesenchymal stem cell-educated macrophages. Transplant Res.1:12. 2012.

Appendix

Scientific pubblications

Scientific pubblications

Lopa S, Madry H. Bioinspired scaffolds for osteochondral regeneration. Review. Tissue Eng. (2014) [In press]

Lopa S, Colombini A, Sansone V, Preis FW, Moretti M. Influence on chondrogenesis of human osteoarthritic chondrocytes in co-culture with donor-matched mesenchymal stem cells from infrapatellar fat pad and subcutaneous adipose tissue. Int J Immunopathol Pharmacol. (2013) 26 (1 Suppl):23-31

Laganà M, Arrigoni C, Lopa S, Sansone V, Zagra L, Moretti M, Raimondi MT. Characterization of articular chondrocytes isolated from 211 osteoarthritic patients. Cell Tissue Bank. (2013) [Epub ahead of print]

Lopa S, Mercuri D, Colombini A, De Conti G, Segatti F, Zagra L, Moretti M. Orthopedic bioactive implants: hydrogel enrichment of macroporous titanium for the delivery of mesenchymal stem cells and osteoinductive factors. J Biomed Mater Res A. (2013) 101(12):3396-403

Lopa S, Colombini A, de Girolamo L, Sansone V, Moretti M. New strategies in cartilage tissue engineering for osteoarthritic patients: infrapatellar fat pad as an alternative source of progenitor cells. J. Biomater. Tissue Eng. (2011) 1:40-48

de Girolamo L, Arrigoni E, Stanco D, Lopa S, Di Giancamillo A, Addis A, Borgonovo S, Dellavia C, Domeneghini C, Brini AT. Role of autologous rabbit adipose-derived stem cells in the early phases of the repairing process of critical bone defects.J Orthop Res. (2011) 29(1):100-8

Lopa S, De Girolamo L, Arrigoni E, Stanco D, Rimondini L, Baruffaldi Preis FW, Lanfranchi L, Ghigo M, Chiesa R, Brini AT. Enhanced biological performance of human adipose-derived stem cells cultured on titanium-based biomaterials and silicon carbide sheets for orthopaedic applications. J Biol Regul Homeost Agents. (2011) 25(2 Suppl):S35-42

Conforti E, Arrigoni E, Piccoli M, Lopa S, de Girolamo L, Ibatici A, Di Matteo A, Tettamanti G, Brini AT, Anastasia L. Reversine increases multipotent human mesenchymal cells differentiation potential. J Biol Regul Homeost Agents. (2011) 25(2 Suppl):S25-33

Quirici N, Scavullo C, de Girolamo L, Lopa S, Arrigoni E, Deliliers GL, Brini AT. Anti-L-NGFR and -CD34 monoclonal antibodies identify multipotent mesenchymal stem cells in human adipose tissue. Stem Cells Dev. (2010) 19(6):915-25

Arrigoni E, Lopa S, de Girolamo L, Stanco D, Brini AT. Isolation, characterization and osteogenic differentiation of

adipose-derived stem cells: from small to large animal models. Cell Tissue Res. 2009 338(3):401-11

de Girolamo L, Lopa S, Arrigoni E, Sartori MF, Baruffaldi Preis FW, Brini AT. Human adipose-derived stem cells isolated from young and elderly women: their differentiation potential and scaffold interaction during in vitro osteoblastic differentiation. Cytotherapy. 2009;11(6):793-803